

9. SUPPRESSION OF ENGINE NACELLE FIRES

Anthony Hamins, Thomas Cleary, Paul Borthwick, Nickolai Gorchkov,
Kevin McGrattan, Glenn Forney, and William Grosshandler
Building and Fire Research Laboratory

Cary Presser, Chemical Sciences and Technology Laboratory

Lynn Melton, Department of Chemistry, University of Texas, Dallas, Texas

Contents

	Page
9. SUPPRESSION OF ENGINE NACELLE FIRES	1
9.1 Overview	3
9.2 Review of Nacelle Geometry and Fire Protection Systems	3
9.2.1 Development of Agent Requirements	5
9.2.2 Specifications for Aircraft Fire Protection	8
9.3 Measurements Characterizing the Stability Limits of Engine Nacelle Fires	10
9.3.1 Background	10
9.3.2 Suppression of a Baffle Stabilized Spray Flame	12
9.3.2.1 Experimental Method and Apparatus	12
9.3.2.2 Agent Injection	17
9.3.2.3 Experimental Results and Discussion	19
9.3.2.4 Summary of Spray Flame Results	48
9.3.3 Suppression of a Baffle Stabilized Pool Fire	53
9.3.3.1 Experimental Method and Apparatus	55
9.3.3.2 Experimental Results	60
9.3.3.3 Discussion of Experimental Results	61
9.3.4 Suppression of Re-ignition	61
9.3.4.1 Experimental Method and Apparatus	67
9.3.4.2 Experimental Results and Discussion	68
9.3.5 Flammability Limits	76
9.3.5.1 Background	76
9.3.5.2 Experimental Method and Apparatus	76
9.3.5.3 Experimental Results and Discussion	77
9.3.6 Discussion and Summary of Combustion Experiments	77
9.3.6.1 Suppression of Baffle Stabilized Flames	77
9.3.6.2 Mixing in a Baffle Stabilized Flow Field	80
9.3.6.3 System Design Considerations	83
9.4 Flow Field Modeling and Validation in a Mock Nacelle	84
9.4.1 Description of the CFD Model	85
9.4.1.1 Introduction	85

9.4.1.2	Modeling Assumptions	85
9.4.1.3	The Computational Grid	86
9.4.2	Experimental Facility	86
9.4.2.1	Agent Concentration Determination	90
9.4.2.2	Air Flow Measurements	91
9.4.2.3	Characterization of the Flow Tunnel Without Agent Injection.	91
9.4.3	Comparison of Calculations with Experimental Measurements.	94
9.4.4	Numerical Simulations	101
9.4.5	Conclusions	104
9.5	A Simple Model for Agent Delivery Requirements	104
9.5.1	Simple Mixing Models Applied to Engine Nacelle Fire Suppression	104
9.5.2	Agent Requirements for Generic Nacelles	113
9.5.2.1	Minimum Fire Suppressant Requirements	114
9.5.2.2	Comparison of the Model to the Military Specification for Halon 1301	156
9.5.3	Comparison of Predicted Alternative Agent Requirements to Halon 1301 Requirements	161
9.5.4	Comparison of the Model to Full-Scale Test Data	161
9.5.5	Re-ignition Suppression Requirements	169
9.5.6	Impact of Unmodeled Phenomena	176
9.5.7	Conservative Design Allowance	176
9.5.8	Preliminary Agent Mass Guidelines	177
9.5.9	System Performance Criteria	177
9.5.10	Procedure for Determination and Validation of Nacelle Fire Suppression Requirements	190
9.5.11	Summary of the Model	191
9.6	Summary and Recommendations	191
9.7	Acknowledgments	194
9.8	References	194

9.1 Overview

The engine nacelle encases the jet engine compressor, combustors, and turbine. A nacelle fire is typically a turbulent diffusion flame stabilized behind an obstruction in a moderately high speed air flow. The fuel source for a fire in the nacelle are leaking pipes carrying jet fuel or hydraulic fluid, that can feed the fire either as a spray or in the form of a puddle or pool. Extinguishment occurs when a critical amount of agent is transported to the fire. After suppression of the fire, re-ignition can occur as fuel vapor makes contact with a hot metal surface or an electrical spark due to shorted wires.

Because of its many positive attributes, halon 1301, or trifluorobromomethane (CF_3Br), has been used as a fire extinguishing agent for protecting aircraft engine nacelles. Fortunately, in-flight fires are not frequent. In commercial U.S. aircraft during the 18 year period from 1956 to 1974, a total of 56 nacelle fires occurred. In U.S. military aircraft, 80 to 90 noncombat fires occurred annually during that period (Altman *et al.*, 1983). In general, halon systems have been very effective in suppressing nacelle fires (Tedeschi and Leach, 1995). As halon 1301 is replaced with possibly less effective suppressant, continued effective aircraft protection becomes a challenge. For this reason, organized guidance in the determination of the amount of replacement agent required for protection of engine nacelles over a range of operating conditions is needed. In this study, a series of experimental measurements were conducted and simple models were developed in an effort to provide an improved understanding of the influence of various parameters on the processes controlling flame stability in engine nacelles. The knowledge gained is compiled into usable tools which may assist suppression system designers determine the mass and rate of agent injection required for engine nacelle fire suppression.

This section is broken into several subsections. In Section 9.2, a brief description of the range of parameters which characterize the temperature and flow field in engine nacelles is provided in an effort to understand possible fire conditions. The historical development of current halon 1301 fire protection systems in engine nacelles is described and current specifications for design and certification are summarized. In Section 9.3, the results of four distinct experiments are discussed. First, the suppression effectiveness of candidate replacement agents are tested on a turbulent jet spray flame. Second, suppression of a baffle stabilized pool fire is described. Third, the impact of the replacement agents on ignition temperature of fuel/air/agent mixtures flowing over a hot metal surface is discussed. Finally, experiments determining the flammability limits of propane/air/HFC-125 mixtures are discussed. A detailed description of the experimental methods and results are included for each configuration. The experimental studies are summarized in a discussion that emphasizes the importance of agent entrainment into the recirculation/combustion zone of obstacle stabilized flames. In Section 9.4, computational modeling of gaseous agent injection into a mock engine nacelle is described. The calculations are compared to measurements conducted in a wind tunnel in an effort to validate the model. In Section 9.5, a simple model is developed to give guidance on agent concentration requirements for flame suppression in generic nacelle configurations. A step-by-step procedure is proposed as a guideline for fire protection system design and certification. Key findings and recommendations are compiled in Section 9.6, acknowledgments are cited in Section 9.7, and references are listed in Section 9.8.

9.2 Review of Nacelle Geometry and Fire Protection Systems

There is no such thing as a typical engine nacelle. Each aircraft type has a nacelle with a distinct geometry and with varying amounts of clutter in the form of tubes, boxes, and so on. It is possible,

Table 1. Engine nacelle characteristics

Aircraft	Free Volume (m ³)	Max Air Flow (kg/s)	Max T _{air} (°C)	Max T _{wall} (°C)	System
YF-16	1.5 ^b	1.1 ^b	150 ^b	230 ^b	1301 ^b
F-15/F-100	2.4 ^b	0.9 ^b	≈320 ^b	≈300 ^b	1301 ^b
F-111/TF-30	a	1.2 ^b	110 ^b	140 ^b	1202 ^b
S-3A/TF-34	0.60 ^b	1 ^b	210 ^b @sea level	77 ^b @sea level	none ^b
F-22	2.8 ^c	0.2 ^c	a	a	a
727/JT-8D	a	0 ^b	a	a	1301 ^b
F/A-18	1.1 ^d	0.9 ^d	330 ^d	390 ^d	1301 ^d
F-104/J-79	a	12 ^b	180 ^b	660 ^b	none ^b

a data not available.

b McClure *et al.*, (1974)

c Kolley (1993)

d Picard *et al.*, (1993)

however, to idealize a nacelle through characterization of key parameters. An idealization facilitates estimation of the minimum amount of agent required for fire protection.

Current fire protection systems for engine nacelles consist of one or more bottles and pipes leading to the nacelle. The piping that carries the agent into the nacelle is a simple tube. Nozzles are not typically used. In some cases, a tee is used to enhance agent dispersion throughout the nacelle. The diameter of the tube carrying the agent is a means to control the rate of agent injection. For halon 1301, the agent enters the nacelle as a two phase flow which rapidly flash vaporizes. Agent is typically introduced into the nacelle at a single location, although some aircraft such as the B2 have as many as 12 agent injection locations. Unfortunately, very few public documents are available which describe aircraft engine nacelle geometries in detail.

The range of conditions which exist in engine nacelles are of interest, because this information facilitates proper design of fire protection systems. For example, the air temperature in the nacelle impacts flame stability and the ease of extinguishment. The maximum wall surface temperature poses a hazard as it may promote the ignition of a leaking jet fuel or hydraulic fluid line. Maximum wall temperatures in current aircraft nacelles can be as high as 650 °C. Bleed air from the engine, flowing through the nacelle, can also act as an ignition source and can be as high as 600 °C according to Altman *et al.*, (1983), although no specific aircraft types are mentioned. Advanced aircraft may even have higher surface and air temperatures (Altman *et al.*, 1983). Table 1 lists values of the free volume, air flow, and maximum values of the air and wall temperatures in nacelles for a number of different aircraft under typical operating conditions. Table 1 also presents the agent type currently used for aircraft fire protection, which includes halon 1301 (CF₃Br) and halon 1202 (CF₂Br₂). Unfortunately, much of the available information is anecdotal, such as the response to a written survey presented in the Booz-Allen-Hamilton report (Kolley, 1993). Comprehensive, detailed information on

these parameters is reported by McClure *et al.*, (1974) for the F-111 aircraft. That report is an excellent model of determination of key engine nacelle parameters.

Actual values of the maximum nacelle wall temperature, the air flow, and the maximum air temperature in the nacelle vary as a function of aircraft velocity, ambient temperature, and specific location within the nacelle as well as many other parameters. Minimum air temperature in the nacelle can reach values as low as -60 °C, depending on ambient conditions. The pressure inside the nacelle varies with altitude. For a F-111 aircraft, pressures can be sub or super-ambient, varying from 13 to 124 kPa (2 to 18 psia) (McClure *et al.*, 1974). Typical average free stream air velocities in nacelles cover a wide range of values, with maximum velocities as high as 100 m/s in some aircraft (Altman *et al.*, 1983).

9.2.1 Development of Agent Requirements. The history of halon 1301 engine nacelle suppression system requirements provides insight to fire prevention strategies currently employed for engine nacelle fire extinguishment. The following chronology is not meant to be a comprehensive history, but details the development of the technical basis for the current Military Specification and its potential deficiencies, either in terms of under- or over-design. Understanding the current guidelines for halon 1301 systems should assist in the development of new guidelines for alternative agents.

Suppression systems for protected aircraft engine nacelles have primarily relied on halon 1202 and, predominately, halon 1301 since the late 1950s. At present, most U.S. military and civilian aircraft use halon 1301 (McClure, 1974; Kolleck, 1993). In the 1950s, halon 1301 proved to be a most effective fire extinguishing agent in engine nacelle applications given the premiums placed on weight and storage volume inherent in aircraft. A knowledge base of halon systems was built upon the experience and experimental programs of the Civil Aeronautics Administration (CAA) and the military. A large fraction of that knowledge base was utilized in MIL-E 22285, the Military Specification written in 1959, specific to halon 1301 systems for (military) aircraft. Commercial aircraft have similar requirements.

Some aircraft with single engines (F-15) or pylon mounted engines (KC-135) do not have active fire protection for the engine nacelle(s) (McClure, 1974). An engine nacelle fire usually renders the engine inoperable or it is purposely shut-down, thus, in the case of single engine planes there is little reason to suppress a fire since the aircraft would be without power. In the case of pylon-mounted, multi-engine aircraft, an engine fire can continue to burn and not pose a threat to the rest of the aircraft; damage is limited to the engine.

The initial research performed by the CAA (the predecessor to the Federal Aviation Administration) dealing with in-flight aircraft engine fires took place between 1940 and 1943 (Grieme, 1941; Hansberry, 1948). Aircraft engines at that time were all of the piston/propeller type. Interestingly, that work was performed on the grounds of the National Bureau of Standards in Washington, DC prior to CAA's establishment of the Technical Development and Evaluation Center in Indianapolis. Full-scale engine/wing assemblies were tested in front of a wind tunnel to simulate flight conditions. Tests were performed with the engine running and fuel fires initiated in the nacelle to closely match in-flight fire scenarios. Data concerning relative agent efficiencies, required amounts, and design of distribution systems were gathered (Grieme, 1941). With the introduction of jet engine propulsion, more research and development on nacelle fire protection followed. Klein (1950a) reported the results of the Jet Engine Fire Protection Program of the U.S. Air Force. The effect on fire suppression of a number of agents, distribution systems (consisting of perforated piping), and agent injection rates were investigated. The CAA performed a number of tests on the XB-45 aircraft, evaluating methyl bromide and halon 1202 (Hughes, 1953). Perforated piping distribution rings were used to disperse the agent in the annular cross-section of the nacelle.

In the early 1950's, a simpler and more efficient design termed the high-rate-discharge (HRD) system was developed at the CAA (Hughes, 1953; Middlesworth, 1954; Hansberry, 1954; 1956). No distribution rings were employed; agent was injected through an open tube at a rate much higher than previous systems employing perforated piping and/or nozzles. In the high-rate-discharge system, agent dispersion occurs primarily by the turbulent mixing of the agent jet and the nacelle air. It was found that less agent was required to suppress nacelle fires with this technique and the less complicated design saved weight. This technique is described in MIL-E 22285. Hansberry (1956) reported on design features which were empirically found to increase effectiveness of the HRD technique. He reported that agent outlets should be as far forward as possible in zones with high air flow, and the outlets should be positioned to produce a helical spray pattern. Also, discharges parallel or perpendicular to the nacelle centerline were "not effective" (less effective). Agent discharge durations varied between 0.5 and 0.9 s for the initial HRD tests. This was translated into a design discharge duration of less than 1 s. Equations giving the weight of extinguishing agents as required for HRD systems as a function of air flow and net volume of the nacelle, for a "smooth" and "rough" zone in low air flows and for "smooth" zones in high air flow were reported.

The selection of the most suitable agent for nacelle applications was an ongoing task through the 1940's and 1950's and prior to halon 1301, other extinguishing agents were used or considered, most notably carbon tetrachloride, carbon dioxide, methyl bromide, chlorobromomethane, and D-L (a mixture of chlorobromomethane and carbon dioxide developed in Germany). The German Air Ministry sponsored the research leading to chlorobromomethane and D-L systems for aircraft (NFPA Quarterly, 1948; Klein, 1950b). Both full-scale engine fires and small-scale testing were performed in the U.S to evaluate suppression efficiency of various agents. Chlorobromomethane, methyl bromide, carbon dioxide, Freon 12, Freon 22, methyl iodide, and a patented mixture of methyl bromide, ethyl bromide and ethylenechlorobromide were considered by the Air Force for jet engine fire protection (Klein, 1950a). The CAA studied methyl bromide, CO₂, bromochloromethane and halon 1301 (Hansberry, 1956). In the late 1940s, the Air Force Air Material Command began an agent development program for a superior fire extinguishing agent (Klein, 1950b). A superior agent was defined as providing better extinguishing properties than bromochloromethane (BC) over a temperature range from -65 to 160 °F, would be less toxic and less corrosive than BC, suitable for class A,B, and C fires, and have a higher specific gravity than BC.

A comprehensive screening of candidate fire suppression agents was performed by the Purdue Research Foundation (Malcolm, 1950). The bench-scale apparatus used for that study was the Bureau of Mines flammability apparatus (Coward and Jones, 1939) which was found to give repeatable results. The apparatus was used to determine if a mixture of combustible vapor, air and agent could be ignited by an inductive spark generated across a electrode gap. A map of the fuel/air and agent ratios that could be ignited starting from the flammability limits of the fuel in air alone represented the flammable range of the mixture. Peak agent concentrations required to inert n-heptane/air/agent mixtures at room temperature were obtained. The peak value was considered a measure of the relative agent effectiveness. HFC-125 and HFC-227 were not included in that study, but halon 1301 and CF₃I were included. A driving force in the agent selection for HRD systems also included physical characteristics such as agent volatility.

It was recognized that the ability to make temporal concentration measurements would provide a means to evaluate a suppression system without resorting to actual aircraft engine fire testing or merely relying on calculations, visual observations, and discharge duration estimates (New and Middlesworth, 1953). A suitable measurement technique was developed such that concentration measurements could be made during simulated flight conditions or actual aircraft flight (Demaree and Dierdorf, 1959). The suppression system evaluation was based on concentration measurements at various locations in the nacelle to confirm that the desired design concentration was achieved and

maintained during flight or under simulated flight conditions. The design concentration was obtained by measuring concentrations during a number of tests of various aircraft extinguishing systems that were deemed adequate for extinguishing full-scale fires. It was concluded that a concentration of 6 % by volume of halon 1301 over a duration of not less than 0.5 s at all sampling locations in the nacelle was sufficient to extinguish all test fires (Demaree and Dierdorf, 1959). It was not stated what the minimum duration in any single location should be, implying a lower limit of 0.5 s. It turns out that the inerting concentration from the Bureau of Mines flammability apparatus for a n-heptane/air/halon 1301 mixture at ambient temperature and near atmospheric pressure is also approximately the same value, 6.1 % (Malcolm, 1950). This small-scale result, though known at the time of the concentration apparatus development, was not apparently considered during the design concentration identification process. The Military Specification was published in 1959, and except for an addendum in 1960, remained unchanged. The Military Specification calls for a 6 % volumetric concentration and 0.5 s minimum duration for all locations in the protected area. Suppression research after the implementation of the Military Specification (MIL-E 22285) in 1959 continued because of concerns related to the significant changes in the nacelle environment for advanced (supersonic) aircraft.

Concerns relating to nacelle fire protection, as well as other fire safety issues were raised during the early phase of supersonic aircraft development. Supersonic flight presents unique aircraft environments not encountered in subsonic flight. Gerstein and Allen (1964) detail some of the aircraft environmental factors associated with fire hazards during supersonic flight. Those factors directly related to nacelle fires include:

1. Temperature: elevated skin surface temperatures, high stagnation air temperatures and low ambient air temperatures.
2. Pressure: typically low ambient pressure.
3. Air Flow: high air flow.

McClure *et al.*, (1974) reported extensively on the operating environment in the F-111 nacelle, a supersonic aircraft. They listed high temperatures, both surface and ram-air temperatures and high air flow conditions. Recently, (Picard *et al.*, 1993) the U.S. Navy's F/A-18 aircraft was put through extensive testing to examine the possible causes of a high incidence of engine nacelle fires. A large amount of in-flight nacelle temperature (surface and air) and air flow data were gathered.

Studies with the Aircraft Engine Nacelle Fire Test Simulator showed that for many nacelle conditions, the amount of halon 1301 required for suppression was much less than current guidelines, provided that very rapid injection took place, and hot surface re-ignition did not occur (Johnson and Grenich, 1986). In some cases, a factor of ten decrease was observed. In addition, peak agent concentrations lower than the design concentration were found to extinguish nacelle fires. Johnson and Grenich (1986) also reported the effects of simulated battle damage to a particular nacelle configuration. Depending on the exact details of the damage, agent requirements changed and current guidelines were not sufficient.

No changes in the concentration and duration requirements in the Military Specification were promulgated due to changes in nacelle conditions associated with supersonic flight. The performance history of aircraft engine nacelle suppression systems confirms the reliable nature of those systems designed to meet the Military Specification (Botteri *et al.*, 1972; Tedeschi and Leach, 1995) which suggests a conservative design philosophy.

9.2.2 Specifications for Aircraft Fire Protection. Typically, there is air flow through the nacelle to provide cooling of hot surfaces and to sweep out combustible vapors. While serving these important functions, the air flow also dilutes the extinguishing agent after a discharge, and carries it out of the nacelle rapidly. The number of air exchanges per unit time (volumetric air flow/ net volume) depends on the aircraft design and reaches highs of about one per second (Kolleck, 1993). No lower limit can be placed on the number of air exchanges because a ground fire scenario is possible where, for most aircraft, no nacelle air flow is provided. Clearly, the amount of agent required to achieve a specified concentration in the nacelle depends on the air flow and the nacelle volume. Those two variables along with a description of the nacelle geometry are the parameters in the design guidelines of the Military Specification.

Section 3.8.1 of the Navy Specification MIL-E 22285, and Section 3.2.2.3.9b of the Air Force Specification MIL-F-87168, both entitled "Quantity of Agent," detail design guidelines for the minimum quantity of halon 1301 to be discharged into a nacelle. The two Military Specifications are very similar. The design guidelines are given below, presented in English and SI units. The actual specifications are broken into two major categories. The first category includes rough nacelles with low air flows and smooth nacelles. For these cases, the Military Specification calls for the larger value of either of the following two formulas:

$$W(lbs) = 0.05 V(ft^3) , \quad W(kg) = 0.80 V(m^3) \quad (1)$$

$$\begin{aligned} W(lbs) &= 0.02 V(ft^3) + 0.25 \dot{W}_{air} (lbs/s) , \\ W(kg) &= 0.32 V(m^3) + 0.25 \dot{W}_{air} (kg/s) \end{aligned} \quad (2)$$

For a rough nacelle interior with a high air flow:

$$\begin{aligned} W(lbs) &= 3 [0.02 V(ft^3) + 0.25 \dot{W}_{air} (lbs/s)] , \\ W(kg) &= 3 [0.32 V(m^3) + 0.25 \dot{W}_{air} (kg/s)] \end{aligned} \quad (3)$$

For a deep frame nacelle interior with a high air flow:

$$\begin{aligned} W(lbs) &= 0.16 V(ft^3) + 0.56 \dot{W}_{air} (lbs/s) , \\ W(kg) &= 2.57 V(m^3) + 0.56 \dot{W}_{air} (kg/s) \end{aligned} \quad (4)$$

where W is the mass of agent, \dot{W}_{air} is the mass flow of air passing through the zone at normal cruising conditions, and V is the "free" volume of the zone. The nacelle free volume is defined as the total nacelle volume minus the volume due to clutter. Low air flow is defined as less than 0.45 kg/s (1 lb/s) at cruise and high air flow is defined as greater than 0.45 kg/s (1 lb/s) at typical cruise conditions.

By definition, a smooth nacelle has no circumferential ribs protruding into the nacelle; a rough nacelle has circumferential ribs protruding less than 15 cm (6 in.) into the nacelle; a deep frame nacelle has circumferential ribs greater than 15 cm (6 in.) protruding into the nacelle, or a configuration with cavities 15 cm (6 in.) or more in depth (measured transversely). A smooth nacelle may contain clutter such as electronic housings, hydraulic and fuel lines, transducers, and clamps which may create flow disturbances. The ribs are added to a nacelle to provide structural integrity.

Section 3.9 of the Military Specification specifies that the discharge duration of the agent must be less than 1 s, measured from the time the agent exits the delivery tube and begins to enter the nacelle. Section 3.8 of the Military Specification, entitled "Concentration of Agent," details the performance criteria of the extinguishing system. "Actuation of the extinguishing system shall produce a concentration of agent at least 6 % by volume (22 % by weight) in all parts of the affected zone. This condition shall persist in each part of the zone for at least 0.5 s at normal cruising condition."

The Military Specification does not provide references or any discussion pertaining to the design guidelines or performance criteria. It is recommended that the rationale for any revision of the Military Specifications be fully documented. Available documentation, however, points out obvious connections between experimental studies and the Military Specification. Hansberry (1956) reported the agent requirements for smooth nacelles (Equations (1) and (2)). Many reports resort to speculation regarding the derivation of the Military Specifications (Altman *et al.*, 1983; McClure and Springer, 1974; Gerstein and Allen, 1964). Hansberry (1956) did not derive the smooth nacelle equation, but only states that it was empirically derived. Although the air flows investigated ranged from 0 to at least 16 lb/s, the range of nacelle volumes was not reported.

Examination of Equation (2) shows that it is not dimensionally consistent. Without documentation regarding its rationale, several authors have speculated on its derivation. Gerstein and Allen (1964) and McClure *et al.*, (1974) suggested the following:

$$W = X_c \rho_{agent} V + \frac{\rho_{agent} t X_c}{\rho_{air} (1 - X_c)} \dot{W}_{air} \quad (5)$$

This equation gives the mass of agent (W) required to provide the volume (V) and the incoming air flow (\dot{W}_{air}) with the design concentration (X_c) over the discharge time (t). The agent and air densities (ρ_{agent} and ρ_{air}) are evaluated at ambient conditions in the nacelle. Assuming a one second discharge time for the agent and isothermal mixing of air and gaseous agent at 21 °C and atmospheric pressure, the equation reduces to:

$$W (lbs) = 0.023 V (ft^3) + 0.34 \dot{W}_{air} (lbs/s) \quad (6)$$

The coefficients in Equation (6) are consistent with those in Equation (2). This type of analysis (Equations (5) and (6)) began with the early CO₂ systems (Mapes, 1954). The analysis assumed an idealized partition of the agent between the volume and the incoming air flow and lacks any physical basis related to spatial and temporal mixing of agent in the nacelle volume. It is only speculation that the design guidelines for smooth nacelles evolved from such a theoretical basis and were confirmed with full-scale testing. The design equations for rough nacelles and deep-framed nacelles cannot be derived from such a simple argument and probably evolved from testing. For example, the effects of transverse ribs (a rough nacelle design) were reported by the CAA (Hughes, 1953). The fact that the design guidelines for rough nacelles with a high air flow (Equation (3)) are the same as the guidelines

for smooth nacelles (or rough nacelles) with a low air flow (Equation (2)) multiplied by a factor of three, also suggests an empirical foundation.

Interestingly, parameters which may be important in flame stability such as the air temperature, the pressure and hot metal surface temperatures are not explicitly addressed in the design guidelines (Equations (1)-(4)). In addition, the actual dimensions and spacing of the ribs in rough nacelles are not considered, except for the case of very deep nacelles, which are treated separately.

The suppression guidelines will be reconsidered in Section 9.5 in terms of a simple model which endeavors to give guidance on agent mass delivery rate and concentration requirements for flame suppression in a generic nacelle using the replacement agents.

9.3 Measurements Characterizing the Stability Limits of Engine Nacelle Fires

9.3.1 Background. The search for a replacement for halon 1301 has led to testing of alternative agents in the Wright Patterson full-scale Aircraft Engine Nacelle Test Facility as well as in bench scale experiments (Grosshandler *et al.*, 1994). There are, however, many nacelle geometries and operating conditions for which a new suppressant is needed. Because testing cannot be performed for all possible aircraft and conditions, knowledge is needed which will provide guidance in the extension of the full-scale data to untested systems and conditions. For these reasons, experiments are conducted in several experimental configurations, over a range of conditions which are thought to resemble fires which may occur in a nacelle.

The key parameters that affect flame stability and thereby control flame extinction and the prevention of re-ignition are agent effectiveness and flow field dynamics. Flow field dynamics govern the rate of agent entrainment and the concentration of agent in a fire zone. Pitts *et al.*, (1990) outlined current understanding of fire suppression, incorporating a comprehensive review of the relevant literature, in addition to a discussion of agent effectiveness, test methods, and the role of different suppression mechanisms. A large number of studies have been conducted on fire suppression and a great deal is known about the relative efficiencies of various species in laminar flames (Grosshandler *et al.*, 1994). A large number of laminar flame studies have investigated the structure of inhibited flames to learn about mechanisms of flame inhibition (Pitts *et al.*, 1990; Grosshandler *et al.*, 1994). Global measures of the effectiveness of an agent has been quantified through heat capacity considerations (Tucker *et al.*, 1981; Sheinson *et al.*, 1989).

It has been shown that a criterion for reactant ignition and flame extinction involves the Damköhler Number (D) which is the ratio of a characteristic flow time to a characteristic chemical reaction time, *i.e.*, $D \equiv t_{flow}/t_{chem}$. For laminar nonpremixed flames, Liñan (1974) showed that as D decreases, the maximum flame temperature and the fuel burning rate decrease until a critical value of the Damköhler number is obtained, D_c , such that the flame abruptly extinguishes. Liñan (1974) also showed that as the maximum reactant temperature increases, a critical value of the Damköhler number is obtained, D_p , such that the reactants abruptly ignite. The Damköhler number criteria for ignition and extinction suggest a number of strategies for extinguishing fires and preventing re-ignition. These strategies include increasing the flow field strain rate or flame stretch (to decrease t_{flow}), cooling the reactants, reactant removal, or chemical inhibition which increases t_{chem} (Williams, 1974).

Engine nacelle fires can occur either in the form of a spray or a puddle. In either type of fire, flame stability is enhanced by flow field obstacles, which act as flame holders. There is a rich literature base regarding the stability of baffle stabilized flames. If a flame is established behind a flow obstacle or bluff body, a recirculation zone will form. The presence of the recirculation zone enhances

flame stability. In this situation, the obstacle acts as a flame holder. Flame blow-off occurs when air flows past the obstacle at sufficiently high velocities (Zukowski and Marble, 1955; Lefebvre, 1983). A large number of engineering studies have focussed on the stability of baffle stabilized premixed flames with application to turbine engine design. A comprehensive summary of the results is given by Lefebvre (1983). Some investigators indicate the importance of the structure of the recirculation zone in stabilizing flames, and in particular the characteristic time for mass exchange between the free stream and the recirculation zone (Longwell *et al.*, 1953; Bovina, 1958; Winterfeld, 1965). Mestre (1955) found that flame blow-off was related to the characteristic time for entrainment into the recirculation zone. The relative size of the enclosure surrounding the flame holder has also been found to effect flame stability by changing the character of the recirculation zone (Lefebvre, 1983; Winterfeld, 1965). In general, the blow-off velocity increases and flame stability is enhanced by a number of factors including a reduction in velocity, increase in inlet temperature, increase in gas pressure, reduction in turbulence intensity, change in the equivalence ratio towards the flammability peak, increase in the flameholder size, increase in the flameholder drag coefficient (through changes in the shape of the flameholder), reduction in geometric blockage and for liquid fuels increase in fuel volatility, and finer atomization for liquid sprays (*i.e.*, reduction of mean drop size). Several models describing blow-off of baffle stabilized premixed flames have been developed. Beér and Chigier (1983) suggested that

$$\frac{V_{bo}}{p^{n-1} \cdot d} = \text{constant} \quad (7)$$

where V_{bo} is the free stream velocity at blow-off, d is the baffle diameter, p is the pressure, and n is the reaction order which characterizes the global combustion processes. For kerosene, which is nearly identical to JP-8 jet fuel, Lefebvre and Halls (1959) recommended that $n=2.0$. Equation (7) states that an increased velocity or decreased values of d or p , leads to diminished flame stability until a critical value is obtained when flame blow-off occurs.

Flame suppression of baffle stabilized flames by an agent is analogous to the flame blow-off studies by Lefebvre and coworkers. The time required for an agent to entrain into the recirculation zone is a key parameter in understanding suppression of baffle stabilized flames by a suppressant. This characteristic mixing time or residence time is extremely important in developing fire protection strategies, since it influences the free stream agent concentration and duration required to obtain extinction. Agent entrainment into a baffle stabilized combustion zone is influenced by the free stream flow, the baffle size, and the free stream agent concentration/duration. These ideas, related to agent mixing into a baffle stabilized combustion zone, will form the basis of the simple suppression model developed in Section 9.5.

Few studies have investigated the effectiveness of an agent in suppressing bluff body stabilized flames. Hirst and Sutton (1961) measured enhanced stability in obstacle stabilized pool flames. Flame stability was characterized by the air velocity required to blow-off a flame. Flame stability was measured to be a function of the obstacle size. The blow-off velocity increased, obtained a maximum, and then decreased, as the height of the obstacle above the fuel surface increased. In a series of papers, Hirst, Dyer, and coworkers reported interesting results regarding the suppression of obstacle stabilized flames (Hirst *et al.*, 1976; 1977; Dyer *et al.*, 1977a; 1977b). An obstacle stabilized pool fire may occur when liquid jet fuel or hydraulic fluid forms a puddle behind a rib in the nacelle. Interpretation of their results in terms of a simple mixing model, described in detail in Section 9.3.2.3.4, suggests two key points. First, a characteristic mixing time (τ) for the agent to

entrain into the recirculation zone behind a flame holder or obstacle is a principal parameter governing flame suppression. The characteristic entrainment or mixing time is equal to the characteristic residence time in the recirculation zone. This result suggests that the Damköhler number flow time, t_{flow} , is related to the mixing time, τ , in the case of baffle stabilized flames. Second, the minimum agent concentration required to achieve extinction in baffle stabilized pool fires are consistent with the peak flammability limits of a reactive system. The agent concentrations required for suppression of baffle stabilized fires can be a factor of two larger than agent concentrations required to extinguish cup burner flames burning the same fuel. The flammability limits define conditions under which self-sustaining combustion can or cannot exist. Although peak flammability limits have been measured for a large number of halogenated molecules, there are no data available in the literature for HFC-125 (C_2HF_5), the agent selected by the Halon Transition Team for halon replacement (Malcolm, 1950). Section 9.3.5 describes measurements of the flammability limits for HFC-125 in propane/air mixtures.

9.3.2 Suppression of a Baffle Stabilized Spray Flame. Grosshandler and coworkers (1994)

developed a baffle stabilized coaxial turbulent spray burner for testing the effectiveness of gaseous fire suppressants. Experiments were performed using jet fuel and hydraulic fluids with the air at ambient and elevated temperatures. The agents tested were nitrogen, four perfluorinated compounds, C_2F_6 , C_3F_8 , C_4F_{10} , and cyclo- C_4F_8 ; four hydrogen/fluorine compounds, CF_3CHF_2 , $\text{CF}_3\text{CH}_2\text{CF}_3$, C_2HF_5 , and CFH_2CF_3 ; the mixture 60 % CH_2F_2 /40 % C_2HF_5 ; the chlorinated agents CHF_2Cl and CHFClCF_3 ; CF_3Br , and CF_3I . In addition, sodium bicarbonate powder (NaHCO_3) was tested. The measurements rated the relative suppression behavior of the different agents. The research described here extends that study to a broader range of conditions, typical of in-flight engine nacelle environments, and focuses on the performance of the three down-selected agents, namely HFC-125 (C_2HF_5), HFC-227 (C_3HF_7), and CF_3I .

A fuel spray represents a unique combustion situation. A ruptured high pressure fuel, lubricant or hydraulic fluid line can supply a steady flow of fuel for a fire stabilized behind obstacles in the engine nacelle. Small droplets quickly evaporate and the momentum from the spray efficiently entrains the air necessary for combustion. Extinguishment of the burning spray will occur when a critical amount of agent entrains into the combustion zone.

Flame stability is also influenced by parameters other than the rate of agent entrainment. These include the air flow and temperature, the fuel type, the pressure, and the agent type (CF_3I , HFC-125, or HFC-227). The key objective of the studies reported in this subsection was to compare the effectiveness of the candidate agents in suppressing obstacle stabilized spray flames under a variety of conditions typical of nacelle fires. The effectiveness of the agents in suppressing other types of combustion phenomena will be addressed in Sections 9.3.3-9.3.5 where obstacle stabilized pool fires, ignition over a heated plate, and flammability limits will be considered, respectively.

9.3.2.1 Experimental Method and Apparatus. No standard laboratory apparatus exists for evaluating the effectiveness of an agent in extinguishing an in-flight nacelle spray fire. One apparatus used for spray flame suppression measurements is mentioned in the literature, but details of its operation or experimental results are not reported (Hirst, 1963). The experimental facility used here was based upon the earlier NIST study which has been described in detail (Grosshandler *et al.*, 1993; 1994; 1995; Vazquez *et al.*, 1994).

Figure 1 shows a cross-sectional view through the burner. The apparatus incorporated an air delivery system, a fuel delivery system, an agent injection system, and a combustion zone. Air at atmospheric pressure co-flowed around a 1.9 cm diameter fuel tube within a 0.5 m long, 7.3 cm inner diameter stainless steel tube. The fuel was injected along the centerline through a pressure-jet nozzle

(Delevan model 0.5-45-B)¹ that formed a 45° solid-cone spray, typical of a simple oil furnace or gas turbine combustor. The exit of the nozzle extended 0.2 cm beyond the open end of the stainless steel pipe. The flame was stabilized by a steel disk (nominally 3.5 cm diameter and 0.2 cm thick) attached to the body of the nozzle. A pyrex tube with an 8.6 cm inner diameter, supported on a brass ring, contained the flame 6.3 cm beyond the outer steel casing. A black and white photograph of the turbulent jet spray burner was presented in an earlier report (Grosshandler *et al.*, 1994). Figure 2 shows a schematic drawing of the nozzle, the stabilization disk, and the fuel spray. A torroidal vortex of length L was created as the air/agent mixture flowed past the stabilization disk.

A number of modifications to the original burner design (Grosshandler *et al.*, 1994) were introduced to improve performance and experimental control. The diameter was increased from 5.0 to 7.3 cm to diminish fuel spray impingement on the burner walls and thereby minimize the formation of a fuel puddle on the bottom of the pyrex tube. A water jacket surrounding the fuel line was added to prevent heating of the fuel for experiments where the air temperature was increased. Earlier results showed that a heated fuel supply could impact flame stability (Grosshandler *et al.*, 1994).

Measurements showed that the orientation of the nozzle relative to the tube axis affected flame stability. To insure that the cantilevered fuel line-nozzle system was properly aligned, a tri-spoke (each 1 mm diameter) alignment guide was attached to the fuel line approximately 10 cm upstream of the nozzle exit.

The air was supplied through a sonic orifice by a high capacity compressor at 900 kPa. The pressure was monitored upstream of the sonic orifice allowing determination of the air flow. Average velocities across the burner cross-section could obtain values as high as 50 m/s. Temperatures from ambient to approximately 350 °C, measured with a type-K thermocouple positioned 1 m upstream of the combustion zone, were obtained using a 60 kW electric air heater.

JP-8 aviation fuel was stored in an 18 liter tank and delivered to the burner with an electric pump at pressures controllable to 1.1 MPa. The fuel pressure was fixed at 900 ± 10 kPa and the flow was controlled by a needle valve and monitored using a rotameter. The flow was calibrated at the operating temperatures and pressure. An analysis of the JP-8 fuel shows that it contains many components. The measured heat of combustion for JP-8 was 46.52 kJ/g and the elemental (mole based) composition was 34.1 % carbon and 65.9 % hydrogen (Grosshandler *et al.*, 1994). This is consistent with the $C_{12}H_{22}$ molecular structure for JP-8 used by Johnson *et al.*, (1988) with a corresponding molecular weight of 166 g/mole. The measured liquid density at room temperature was 0.81 g/ml. The same JP-8 batch was used for all of the experiments described in this section.

A series of super-ambient pressure experiments were conducted by replacing the pyrex tube shown in Figure 1 by a 40 cm long brass tube fitted with a butterfly valve at the tube end, facilitating control of the pressure which was varied from ambient to 135 kPa (5 psig). Figure 3 shows a schematic drawing of this confined spray apparatus, which allowed steady control of the system pressure. A pyrex observation window and three ports allowed access for ignition, a pressure gage, and an automatic fuel shutoff which was triggered by flame extinction.

The independent parameters which were controlled in the spray burner facility were the air flow, the agent delivery interval or injection duration, the air temperature, the system pressure, the fuel flow, and the agent temperature. Table 2 lists the range of the independent parameters which were investigated. Extinction measurements were performed with three gaseous agents for all conditions. They

¹ Certain trade names and company products are mentioned in the text or identified in an illustration in order to specify adequately the experimental procedure and equipment used. In no case does such identification imply recommendation or endorsement by the National Institute of Standards and Technology, nor does it imply that the products are necessarily the best available for the purpose.

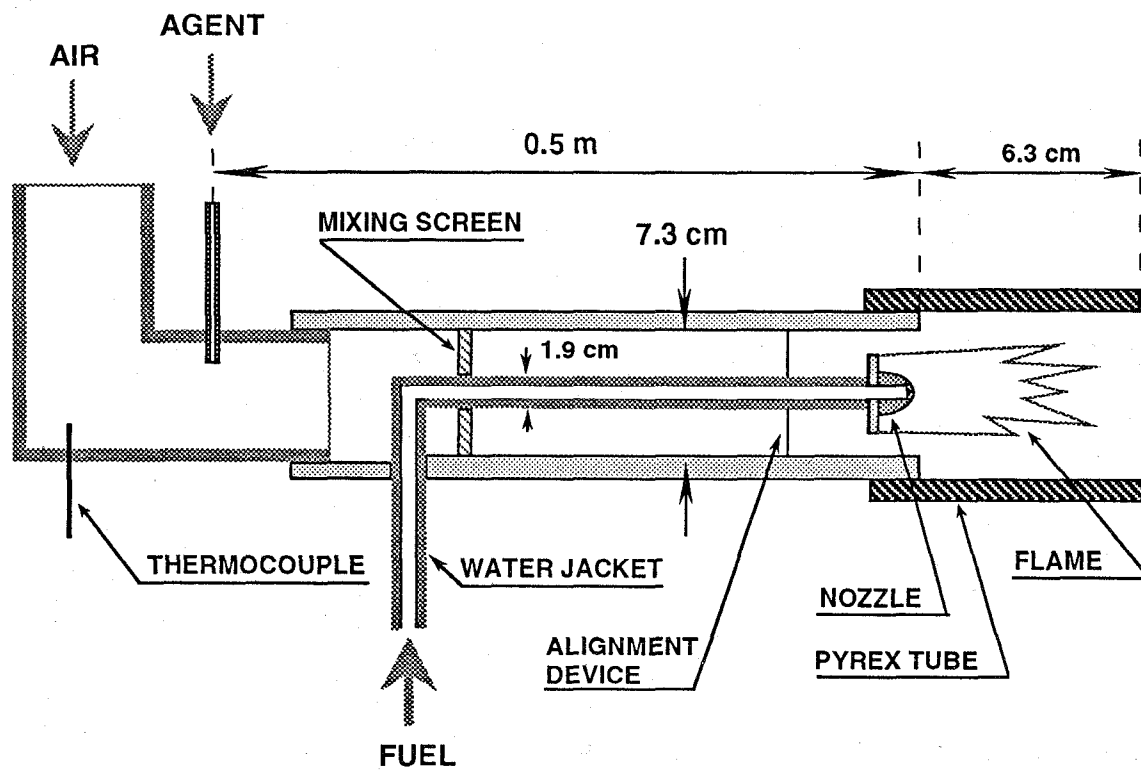


Figure 1. Schematic drawing of the turbulent jet spray burner.

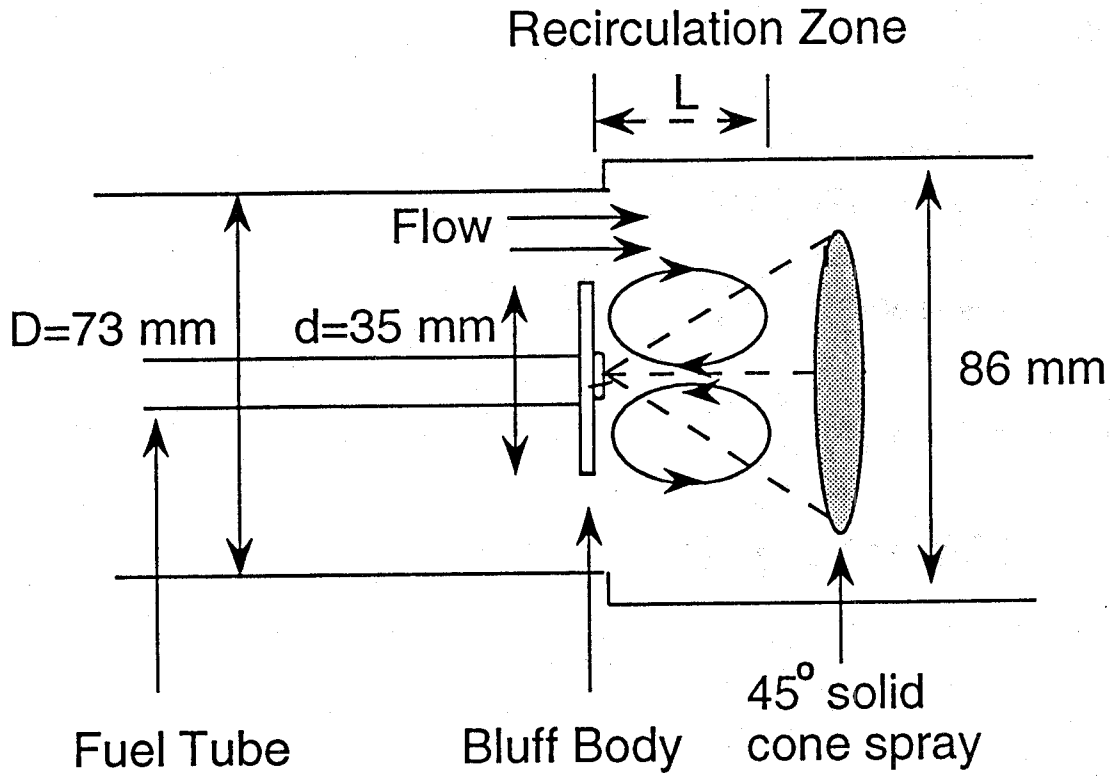


Figure 2. Schematic diagram of the recirculation zone behind the stabilization disk.

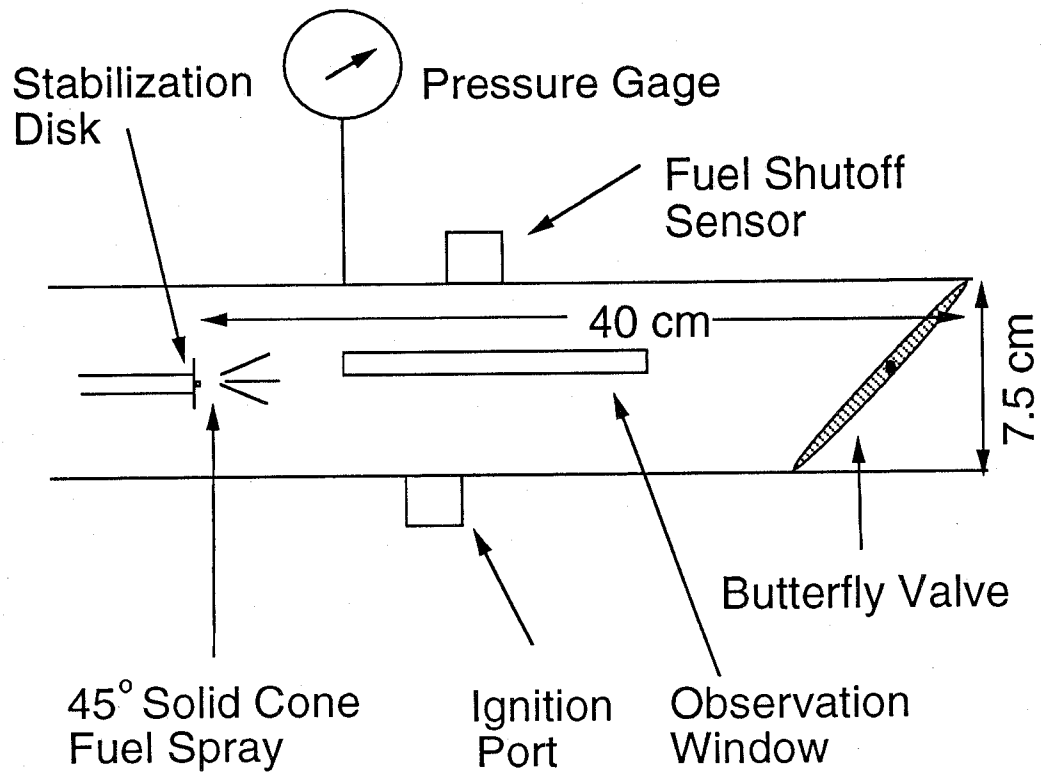


Figure 3. Schematic diagram of the confined spray burner.

Table 2. Operating parameters in the spray burner

Parameter	Range
air velocity	2 - 33 m/s
agent delivery interval	50 - 800 ms
air temperature	20 - 350 °C
system pressure	101-135 kPa (0-5 psig)
fuel flow	
1. air flow constant	14 - 28 ml/min
2. global ϕ constant	
agent temperature	20 - 150 °C

were CF_3I , C_2HF_5 (HFC-125), and C_3HF_7 (HFC-227). Extinction measurements were also performed using CF_3Br to establish a performance reference. In some experiments gaseous N_2 was also tested. The primary dependent experimental parameters were the agent mass and the rate of injection required for suppression.

9.3.2.2 Agent Injection. The injection mechanism, shown in Figure 4, consisted of the agent supply connected to a stainless steel storage vessel through a metering valve, and to the burner through a computer controlled solenoid valve. The storage volume, including a 1.0 or 2.25 liter pressure vessel and associated plumbing, was 1040 or 2290 ± 10 ml, respectively. The agent pressure was adjustable up to 687 kPa. The agent temperature and pressure in the storage vessel were measured with a type-K thermocouple and a pressure transducer located upstream of the solenoid valve. Uniform dispersion across the air stream was enhanced by injecting the gas in a radial direction into a reduced diameter (25 mm) section of the air pipe through two 6 mm diameter tubes. Screens with 50 % open area were placed 40 mm and 80 mm downstream of the injection point to ensure complete mixing between the air and agent prior to encountering the flame zone. For some experiments, the agent was heated to 150 °C by wrapping heating tape over the agent storage vessel. The amount of injected agent was controlled by varying the initial pressure and the time that the solenoid valve was open.

The agent injection system under idealized conditions (incompressible flow, massless valves, no pressure losses) was designed to deliver a square-wave pulse of agent to the burner for the amount of time programmed by the computer controller. The actual flow deviated somewhat from an ideal square wave pulse. Examples of this are seen in Figure 40 of Section 11, where the measured transient agent concentration between the outer wall and the fuel line just upstream of the stabilization disk is shown. The character of the agent pulse varied from a perfect square wave to an upward sloping or a downward sloping concentration trace. A portion of this character was attributed to the mechanics of the solenoid actuation mechanism. The agent concentration was calculated as the average concentration over the injection interval. Measurements showed that small deviations from a square wave pulse had only minimal effect on the agent mass required to obtain flame extinction.

There was a delay between the time when the solenoid was triggered and the time when the flow of agent actually began. When the valve opened, pressure waves were created which reverberated in the injection system at the acoustic velocity, causing the flow rate to modulate. In order to avoid flow

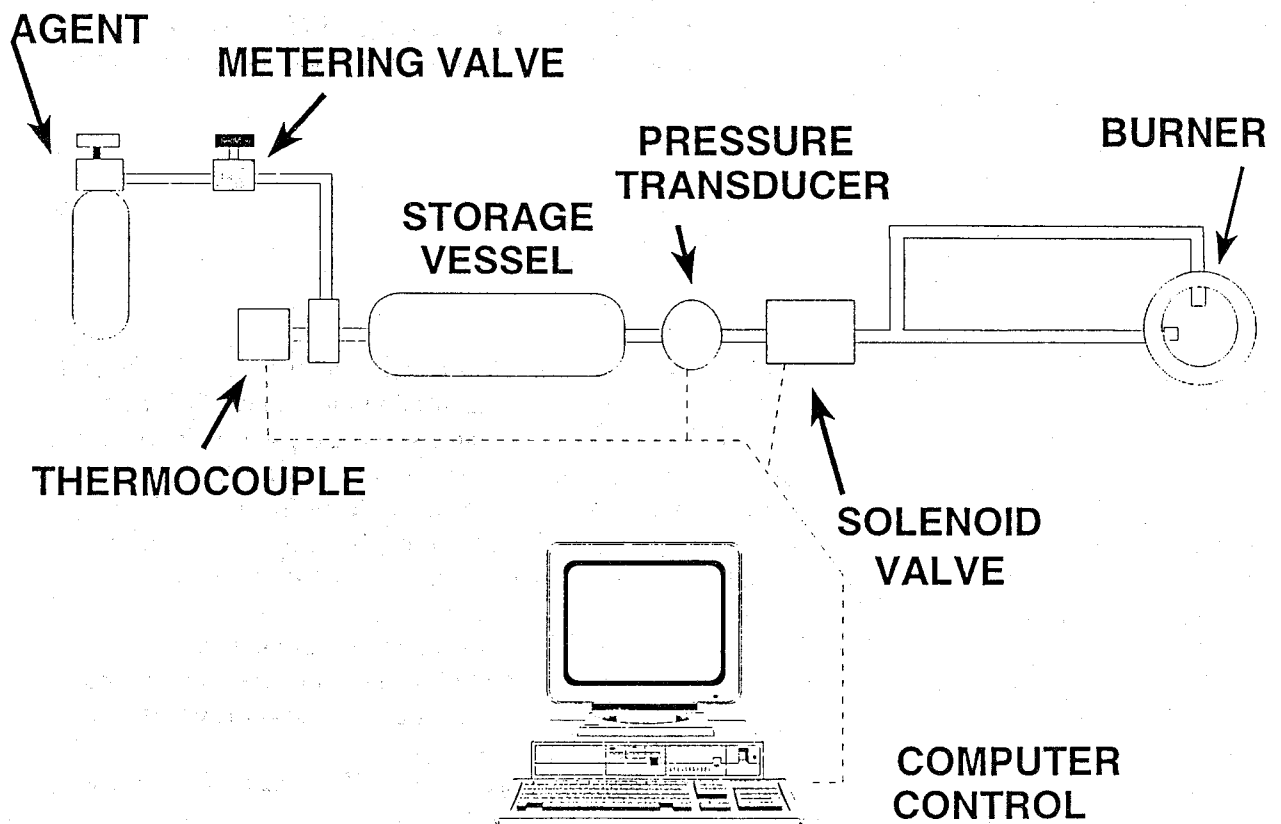


Figure 4. Schematic diagram of the agent injection mechanism.

restrictions, a large solenoid valve was required. Unfortunately, the valve opened and closed at different rates, depending on the agent vessel pressure. The minimum achievable delivery time was approximately 60 ms. Control of the solenoid opening time was limited to ± 16 ms, which was related to the 60 Hz electro-servo control.

The mass of agent delivered to the air stream was determined by measuring the mass loss, m , in the vessel of volume V , at pressure P , and temperature T , using the Redlich-Kwong equation of state:

$$m = \frac{PVM}{RT} \left[\frac{1}{1 - bm/V} - \frac{am/(VRT^{3/2})}{1 + bm/V} \right]^{-1} \quad (8)$$

where M is the molecular weight of the gaseous agent, R is the gas constant, and a and b are constants dependent upon the critical properties of the agent (Van Wylen and Sonntag, 1978). The initial temperature was measured, and the final temperature was determined by assuming that the expansion occurred isentropically following the relation:

$$\frac{T_f}{T_i} = \left(\frac{P_f}{P_i} \right)^{\frac{\gamma-1}{\gamma}} \quad (9)$$

where γ is the ratio of the specific heats of the gas and the subscripts i and f refer to initial and final conditions. By measuring the change in pressure, Equation (8) was used in an iterative fashion to determine the total mass injected into the burner. Equation (9) assumes that the gas was ideal. From Equation (8), the deviation from ideal gas behavior was found to be a maximum of 7 % for the gaseous agents. The pressure data were collected at a rate of 1000 Hz, with the initial and final conditions found from the average of at least 500 points measured one-half second prior to the release of the agent and one-half second after the solenoid valve closed. A mass-time curve has been described in detail (Grosshandler *et al.*, 1994).

The mass of agent added to the flame was determined from Equation (8), and the actual time interval of agent injection into the burner was estimated from the linear portion of the slope in the mass-time curve. The mass flow of agent was determined from the ratio of the mass injected to the time of injection over a linear portion of the slope in the mass-time curve.

The agent mass fraction is denoted as β , which is defined as the ratio of the mass flow of agent, \dot{m}_i , to the total mass flow of agent and air, \dot{m}_{Air} :

$$\beta = \frac{\dot{m}_i}{\dot{m}_i + \dot{m}_{Air}} \quad (10)$$

Discussion of the suppression measurements in terms of the agent mass fraction facilitates comparison of the experimental results with similar measurements under other flame conditions or in different combustion configurations. An effective agent is characterized by a small value of β .

9.3.2.3 Experimental Results and Discussion. The protocol used in the experiments was to ignite the fuel spray with a propane torch and to set the air flow to the desired level. The flame was

allowed to burn for ≈ 20 s to ensure steady operation. If a smaller "pre-burn" or warm-up time was used, the flame was less stable. Experiments were conducted for a single agent over a range of conditions. When the agent was changed, the storage vessel was evacuated and flushed several times with new agent to purge contaminating gases from the system. The pressure in the vessel was adjusted with the solenoid valve closed using the inlet metering valve. Initially, a pressure was chosen which was expected to be insufficient to extinguish the flame. Data acquisition was initiated and the response of the flame to the injection process was observed. If the flame was not extinguished, the pressure in the agent vessel was increased and the experiment repeated immediately. Eventually a pressure was found which was sufficient to suppress the flame. This procedure was repeated at least twice for each condition. Each extinction data point, therefore, represents many experiments. It is estimated that a total of over 1000 suppression experiments were conducted. Uncertainty in the mass of agent required to extinguish the spray flame was estimated as 15 %, based on repeat measurements and a propagation of error analysis.

9.3.2.3.1 Characterization of Facility. A series of experiments were carried out to determine reasonable baseline conditions for the fuel and air flows, the diameter of the stabilization disk, the location of the pyrex tube, and the impact on flame stability of a layer of soot deposited on the stabilization disk.

The air and fuel flows were varied to ascertain how the flame was affected by the operating conditions. Figures 5 and 6 show the average observed flame length as a function of the fuel and air flows respectively. As the air flow increased, the visible flame length decreased, until at very high air flows the flame extinguished. At high air flows, the flame appeared like a rapidly swirling luminous ball. Some amount of blue emission was visible in photographs, but not by visual observation. Little flame luminosity was observed beyond 10 cm downstream of the nozzle. For air velocities less than 2 m/s, the flame appeared as an ignited spray cone, nearly blue for the first 2 cm downstream from the nozzle and then yellow. Under these conditions, a luminous recirculation zone was not observed to exist, and apparently, the inertia associated with the fuel droplets was much greater than the momentum associated with the toroidal vortex behind the stabilization disk. Low air velocity flames were achievable only after ignition at moderate air velocities and careful, slow decrease of the air flow. As the fuel flow increased, the flame length increased and the flame appeared more luminous.

The trajectory of fuel droplets was observed to change with air flow. Under non-combusting conditions with a low air flow, the droplets traveled on near-linear trajectories in the downstream direction, at approximately 45° from the axis. As the air flow increased, a critical value was obtained which caused the droplets to alter their trajectories. Further increases in the air flow, caused the droplets to turn nearly 180° , causing them to be entrained into the toroidal vortex behind the stabilization disk. Apparently the momentum associated with the droplets was overwhelmed by the momentum associated with the toroidal vortex of the recirculation zone. For a fuel flow of 21 ml/min (0.28 g/s), the critical air velocity causing a change in droplet trajectory was approximately 17 m/s. Under combusting conditions, observation of the fuel droplet trajectories was not possible, due to obscuration by flame luminosity as well as a decreasing droplet diameter associated with fuel evaporation. These observations suggest that the flame structure and stability may be influenced by complex droplet dynamics occurring in the flame. In addition, the droplet size distribution is expected to change with fuel flow through the nozzle.

An operating condition of 21 ml/min was selected for the JP-8 flow. An air velocity of 7.5 m/s at ambient temperature and pressure was selected as a reasonable baseline operating condition. These conditions produced a 13 kW flame with an overall equivalence ratio of about 0.1. Under these conditions, a layer of soot formed on the nozzle and stabilization disk surface in a matter of minutes.

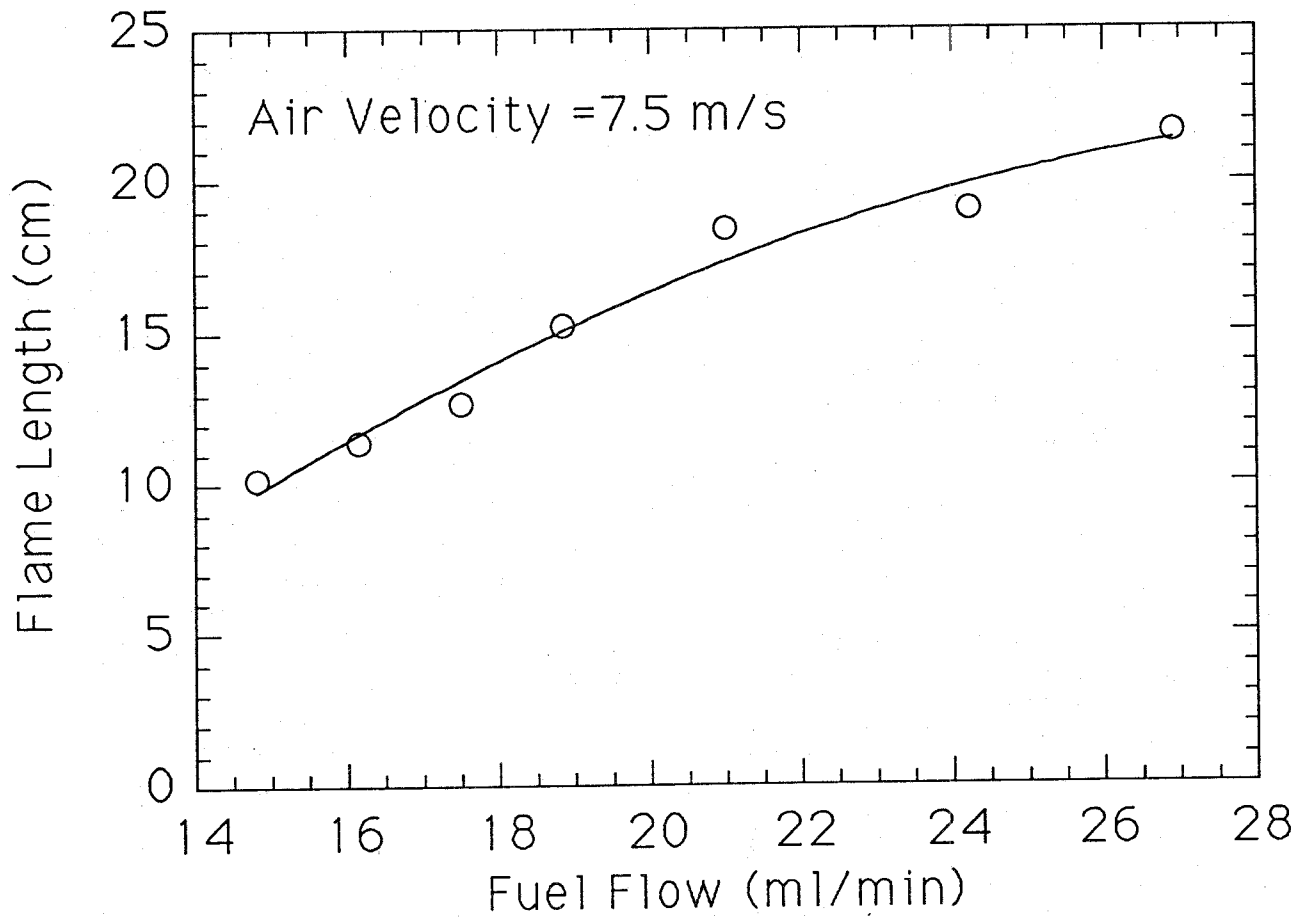


Figure 5. Measured spray flame length as a function of fuel flow.

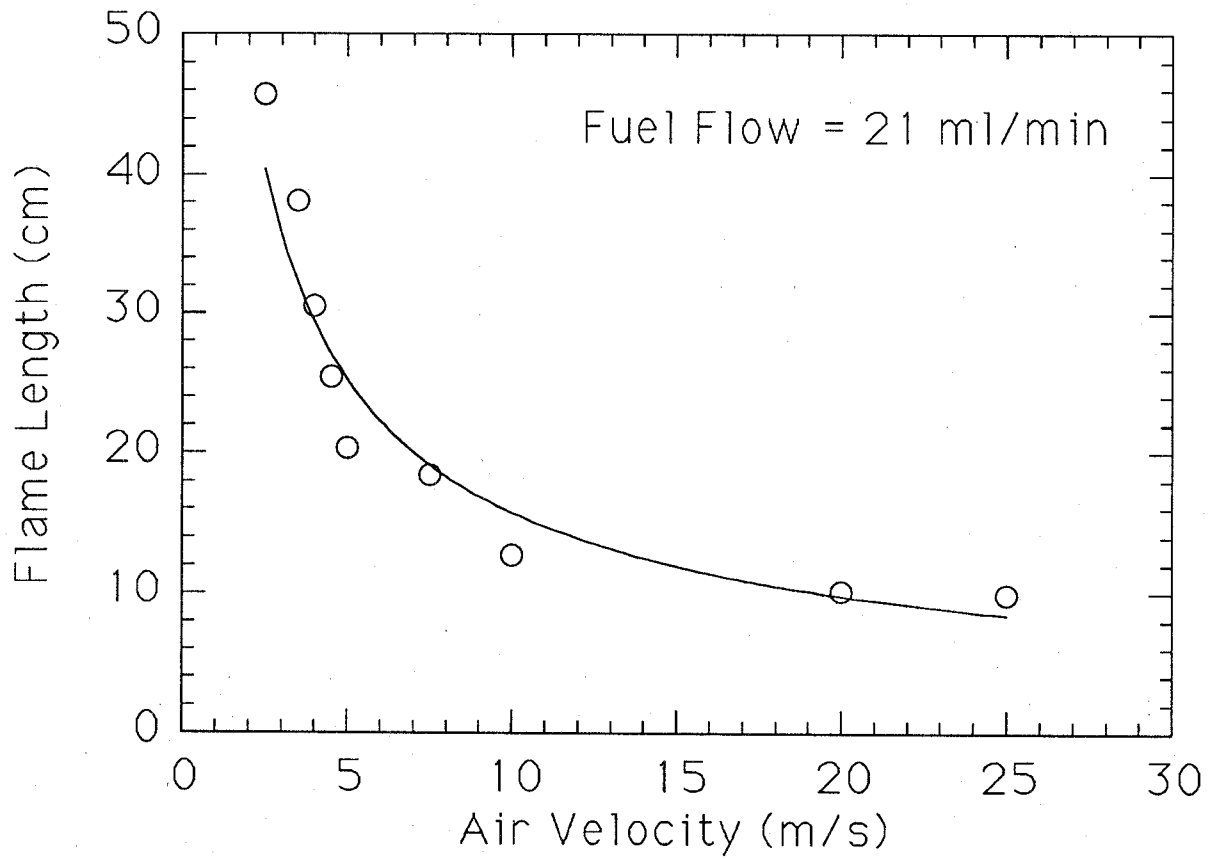


Figure 6. Measured spray flame length as a function of air flow.

Accumulation of a large amount of soot was found to increase flame stability. A possible explanation for this is that the soot acted like a thermal insulator, reducing heat losses to the stabilization disk/flame holder. Thus, the soot was cleaned periodically (every ≈ 3 min). Cleaning necessitated closing the fuel flow and extinguishing the flame.

Measurements showed that the location of the pyrex tube had little impact on the critical agent concentration at extinction for distances greater than 6.3 cm downstream of the nozzle. For shorter distances, the flame was easier to extinguish. Therefore, the pyrex tube was maintained 6.3 cm downstream of the nozzle for all flame extinction experiments.

Experiments were conducted to compare flame extinction measurements in the original burner (Grosshandler *et al.*, 1994) to measurements in the new burner. Figure 7 shows the critical HFC-227 mass fraction (β) required to extinguish JP-8 spray flames as a function of air velocity for short agent injection intervals (65 ms). The critical agent concentrations are similar in the two burners, with the original burner slightly more stable. This is not surprising considering the blow-off results described in Section 9.3.2.3.2 below.

An annular shaped steel disk (4 cm O.D., 1.5 cm I.D.) was placed on axis, downstream of the spray nozzle, to test the impact of a (secondary) flow field obstacle on flame stability. Using the standard configuration, with the primary (3.5 cm diameter) obstacle in place upstream of the nozzle and with fuel flowing, a propane pilot flame was used to ignite the fuel. If the obstacle was more than approximately 6 cm downstream of the nozzle, then it was not possible to stabilize a flame behind the secondary obstacle. The flame would blow-off as soon as the pilot flame was removed. Both a metal and a ceramic stabilizer were tested, yielding the same results. If the obstacle was moved to within approximately 6 cm of the nozzle, the flame jumped back and attached itself to the primary obstacle. Thus, it was not possible to stabilize the (45° solid cone) spray flame unless ignition occurred within the recirculation zone. The recirculation zone downstream of the secondary obstacle apparently did not provide conditions suitable for flame stabilization.

Experiments conducted with air as the extinguishing agent demonstrated that the flame could not be suppressed simply by blowing it out (Grosshandler *et al.*, 1994). When air was injected into the burner, the flame was observed to fluctuate momentarily, but was never extinguished. The flame also fluctuated when agent was injected into the burner. This was probably associated with a rapid change in the overall free stream velocity, which has an effect on the character of the recirculation zone.

In baffle stabilized flames such as the spray burner, the agent concentration in the recirculation zone is the key to flame suppression. Because isothermal flow dynamics upstream of the fire source play an important role in the rate of agent entrainment into the recirculation zone, quantitative measurements of the transient agent concentration were conducted as a function of spatial location under non-combusting conditions. This was accomplished using the aspirated hot film probe described in detail in Section 11 of this report. CF_3Br was injected (250 ms duration) into a moderate air flow (velocity = 5 m/s). Measurements were made 2 cm upstream of the stabilization disk (see Figure 1). The results, which are shown in Figure 8, indicate that agent mixing was fairly uniform across the tube diameter. The agent injection rate and duration were also investigated and are described in detail in Section 11.

9.3.2.3.2 Flame Blow-off. Flame stability in the original (5.3 cm) and the redesigned (7.3 cm) burners was directly compared by measuring the air velocity required to blow-off the JP-8 spray flames. A series of stabilization disks were tested with diameters of 2.22 cm, 2.86 cm, 3.49 cm, and 4.13 cm, all 4 mm thick, and all made from the same steel stock. A 3.49 mm diameter, 2 mm thick disk from a different steel stock was also tested. Figure 9 shows the air blow-off velocity (V_{bo}) as a function of the diameter of the stabilization disk. The same type of nozzle and fuel flow was used in all tests (21 ml/min). Changing the stabilizer diameter had a small effect on flame stability, with the

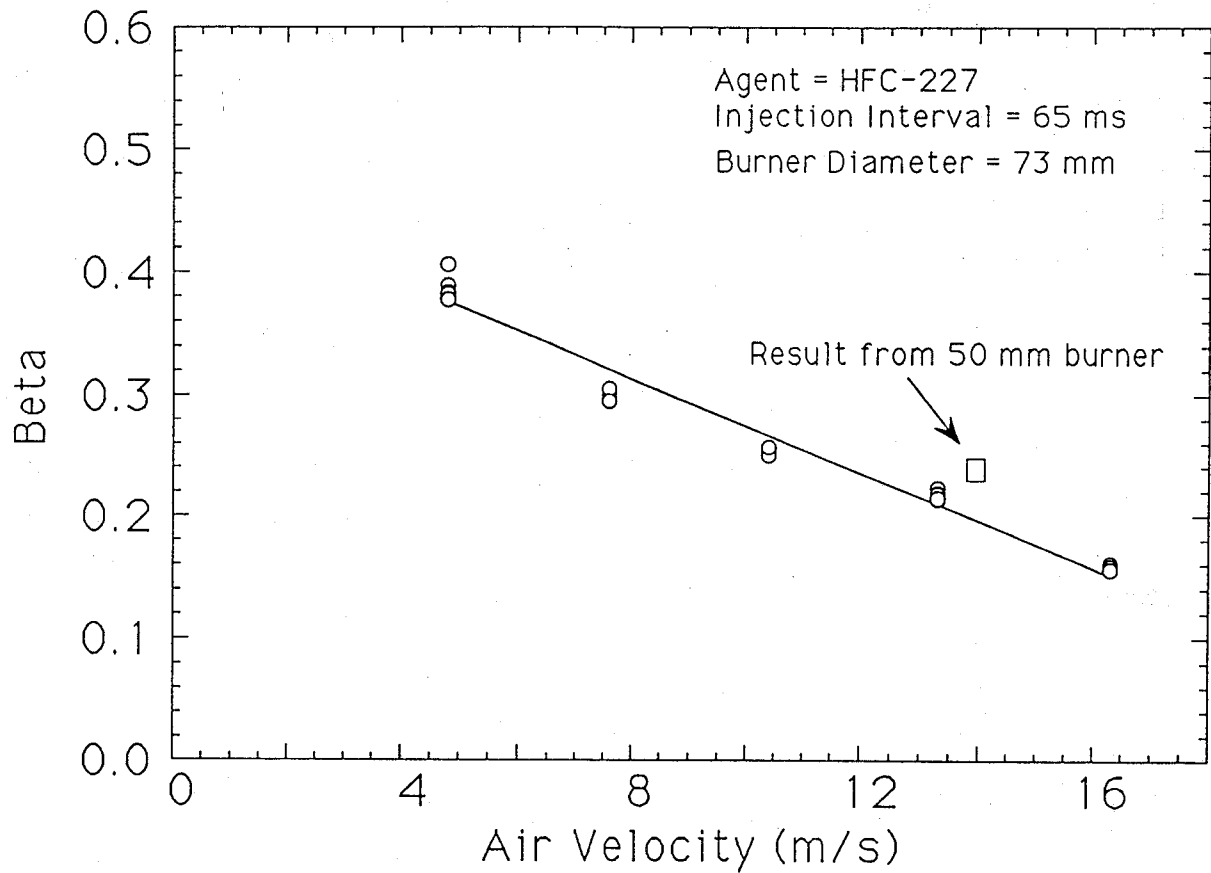


Figure 7. The critical mass fraction of HFC-227 at extinction for the JP-8 spray flame as a function of air velocity for a 65 ms injection interval.

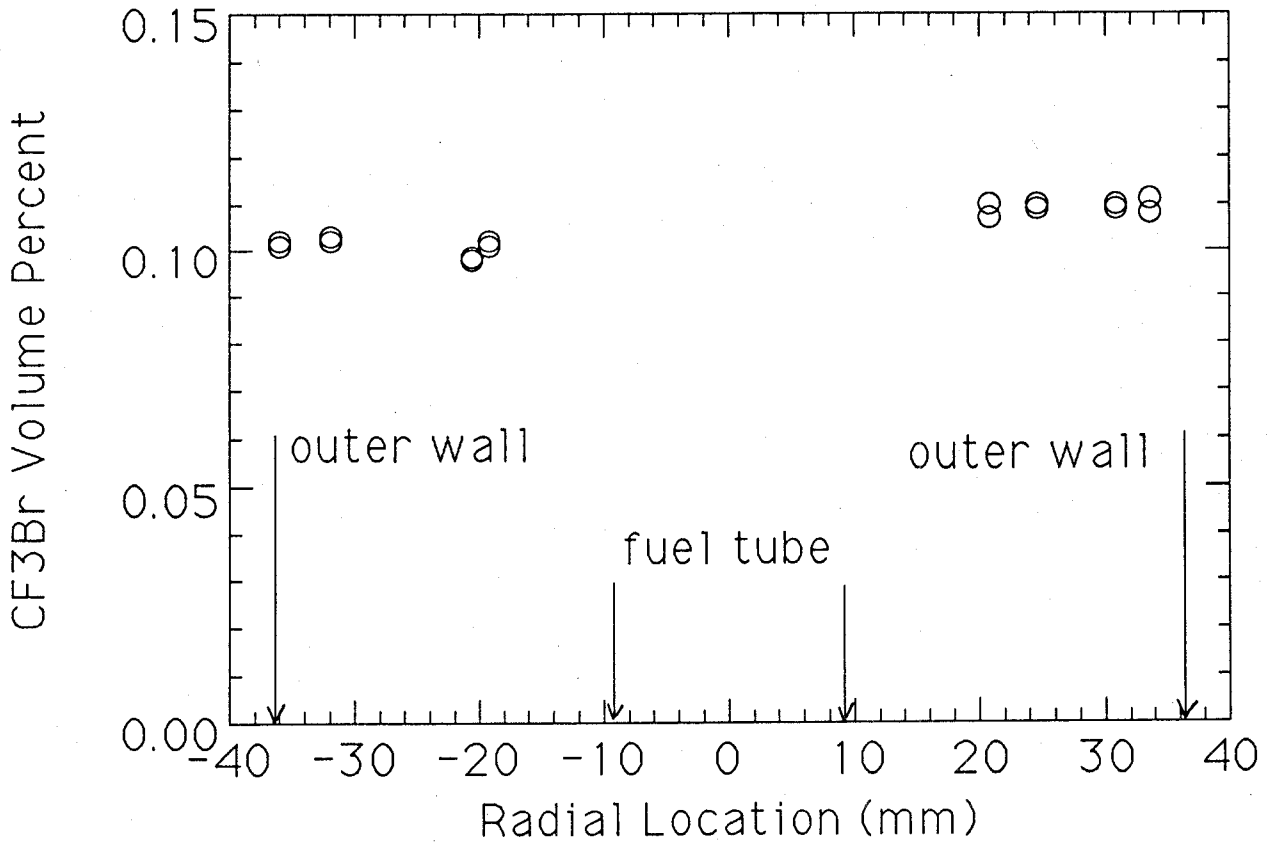


Figure 8. CF₃Br concentration as a function of location in the spray burner.

3.5 cm diameter disks (2 mm and 4 mm thick) yielding the most stable flames in both burners. A stable flame was sustainable until the air velocity across the duct was approximately 33 m/s in the 7.3 cm burner. Flames could not be stabilized with the 2.2 cm disk in either burner, nor with the 4.1 cm disk in the original (5.3 cm) burner. Blow-off velocities in the original burner were approximately 25 % higher than in the modified burner (7.3 cm) for the same disk diameter. This difference was attributed to the stabilizing effect of geometric blockage. The blockage (B) can be quantified as the ratio of the open (or non-blocked) area to the total area:

$$B = \frac{D^2 - d^2}{D^2} = 1 - (d/D)^2 \quad (11)$$

where D is the burner diameter and d is the baffle diameter. The effect of blockage on flame stability has been investigated by Winterfeld (1965) and discussed by Lefebvre (1983). Winterfeld's results will be described in detail in Section 9.3.2.3.4.

9.3.2.3.3 Effect of Air Velocity. A fixed injection time of 700 ms was chosen to test the performance of the three alternative agents in extinguishing the spray flame. The selection of this injection interval facilitates comparison of the results with suppression results from other configurations. Figure 10 shows the critical mass of CF_3Br and the three alternative agents at extinction as a function of air velocity. For conditions below the data points, the flames were not extinguished, whereas for conditions above the data points, the flames were extinguished. A single data point may represent as many as three to ten experiments. The measurements showed that halon 1301 (CF_3Br) required the least amount of mass to extinguish the flames, followed by CF_3I , and the other two agents, HFC-125 (C_2HF_5) and HFC-227 (C_3HF_7), which were measured to have nearly identical effectiveness. CF_3Br required as much as a factor of three less mass than HFC-125 or HFC-227 to extinguish the spray flames. As the air velocity (V) increased, the agent mass required to achieve flame extinction increased, obtained a maximum, and then decreased. At high air velocities, the flames were less stable and easier to extinguish, *i.e.*, less agent was required to extinguish them. At $V=33$ m/s, air with no agent addition caused flame extinction.

Figure 11 shows the critical mass delivery rate of agent at extinction as a function of air velocity for the same data as shown in Figure 10. The rate is determined from the ratio of the mass delivered to the injection period. The injection period is related to the solenoid opening time and is estimated by measuring the depletion of agent from the reservoir. As the air velocity increased, the mass delivery rate increased, obtained a maximum, and then decreased, similar to Figure 10. The data are consistent with Figure 10. CF_3Br required the smallest delivery rate to extinguish the flames, followed by CF_3I , and the other two agents, HFC-125 and HFC-227, which were measured to have nearly identical effectiveness.

Figure 12 shows the critical mass fraction of agent at extinction (β , as defined in Equation (10)) as a function of air velocity for the same data as shown in Figures 10 and 11. As the air velocity increased from 3 m/s, β decreased. For very low air velocities (2 m/s), β decreased or remained nearly the same as the results for $V=3$ m/s. For all agents, the values of β for the low air velocity spray flame results were very similar to agent extinction concentrations measured in cup burner flames and in opposed flow diffusion flames (OFDF) at low (25 s^{-1}) strain rates (Grosshandler *et al.*, 1994). Table 3 documents the correspondence between the flame extinction measurements in the three burners. All tests were conducted with JP-8 fuel. The correspondence between the cup burner results and the low strain rate OFDF results have been previously documented (Grosshandler *et al.*, 1994).

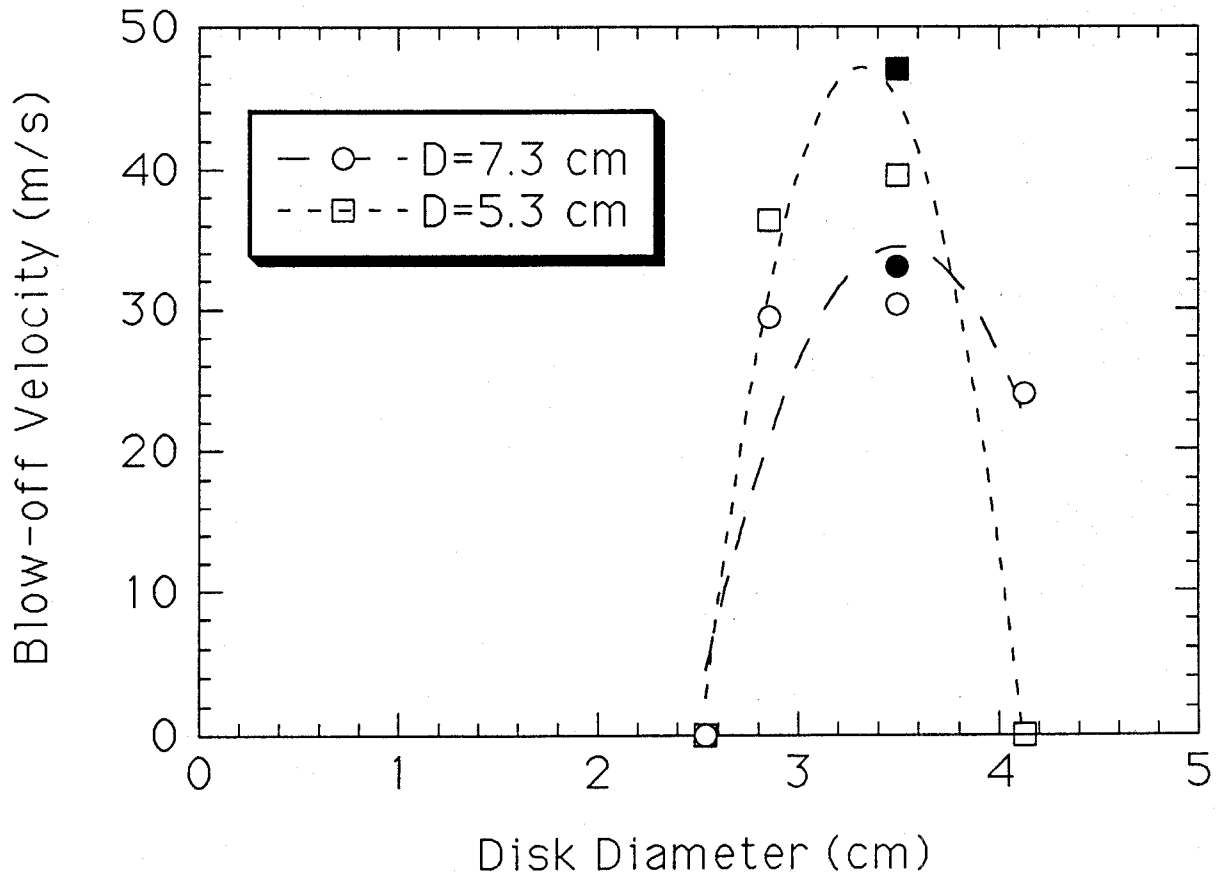


Figure 9. Air blow-off velocity as a function of the diameter of the stabilization disk. The filled and open symbols represent disks with thicknesses of 4 mm and 2 mm, respectively.

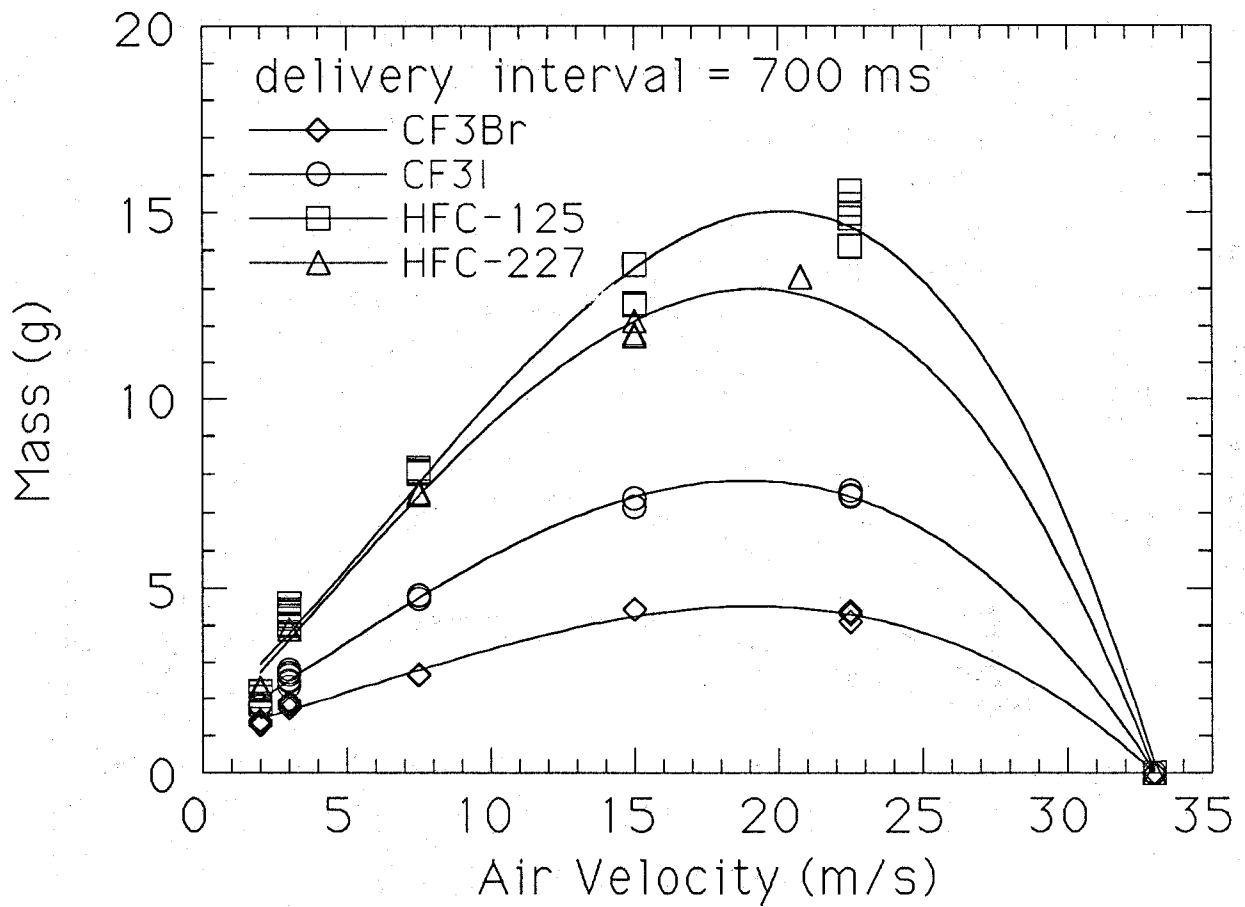


Figure 10. The critical mass of agent at extinction as a function of air velocity.

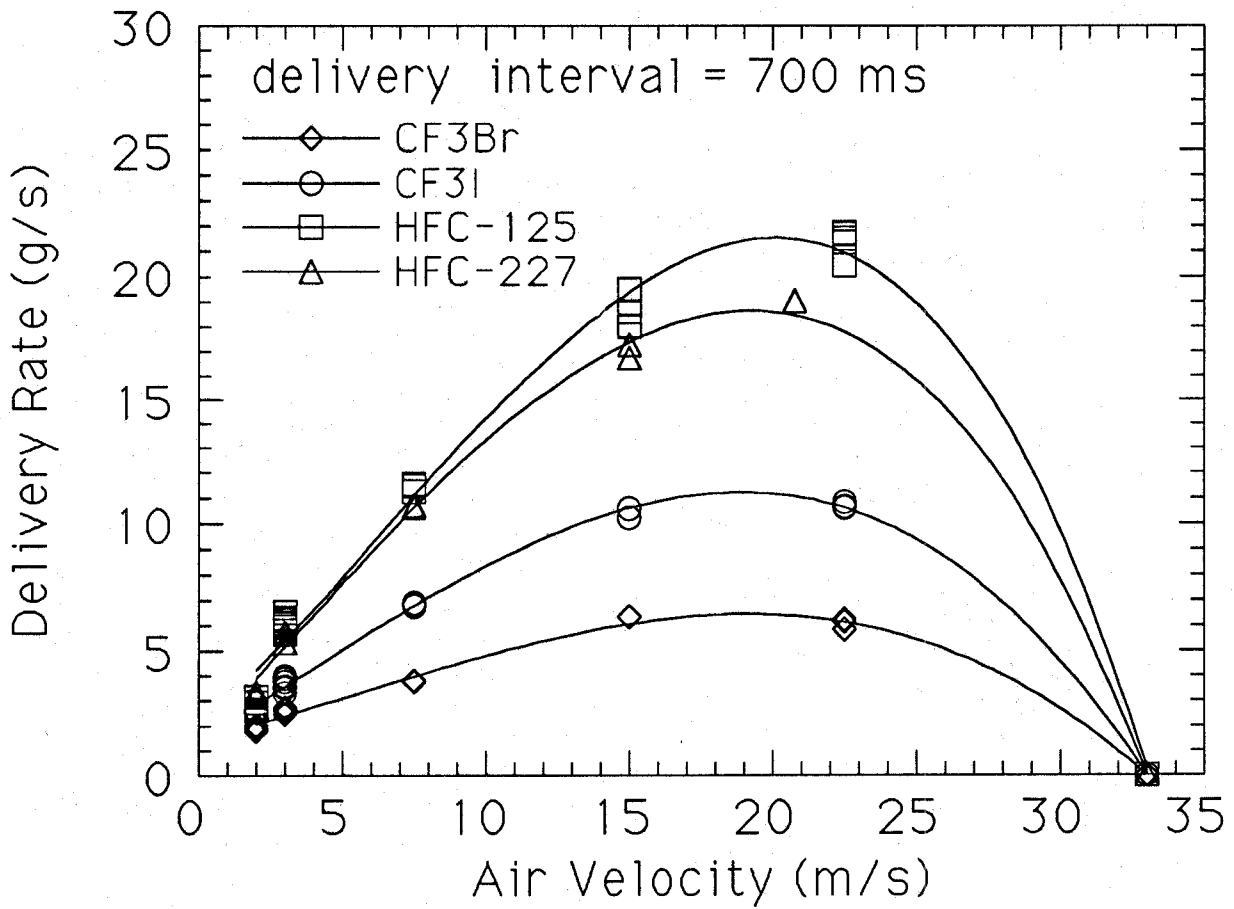


Figure 11. The critical mass delivery rate of agent at extinction as a function of air velocity.

Table 3. Comparison of the critical agent mass fraction at extinction measured in different burners

Agent	Cup Burner	Air Velocity (m/s) in Spray Burner			Strain Rate (s ⁻¹) in OFDF burner		
		3.0	15	22	25	80	175
CF ₃ Br	0.14	0.16	0.085	0.05	0.13	0.080	0.050
CF ₃ I	0.18 ^b	0.21	0.13	0.09	a	a	a
HFC-125	0.28	0.30	0.21	0.17	0.28	0.22	0.16
HFC-227	0.27	0.28	0.20	0.15	0.26	0.20	0.14

a Not measured

b Measured with heptane as fuel. The agent concentration required to extinguish heptane and JP-8 cup burner flames has been measured to be within 4 % of each other for many agents (Grosshandler *et al.*, 1994).

Table 3 shows that a correspondence also exists between the critical agent mass fractions for moderate (80 s⁻¹) strain rates in the OFDF burner (Hamins *et al.*, 1994) and moderate air velocities (15 m/s) in the spray burner. The same correspondence holds for high (22.5 m/s) air velocities in the spray burner and high (175 s⁻¹) strain rates in the OFDF burner.

It should be noted that extinction measurements in the OFDF and cup burner were quasi-steady experiments. Agent concentration was slowly increased until the flame extinguished. The spray experiments involved transient agent injection. Yet, for long injection intervals, the spray experiments were similar to the quasi-steady agent addition methodology and a direct comparison of the results in the three very different configurations is not unreasonable. A plausible explanation of the phenomena follows. As the air flow increased in the spray flame, the characteristic Damköhler number flow time in the recirculation zone decreased and the flow field strain rate increased, facilitating flame extinction with less agent. At high enough air flows, no agent at all was necessary to achieve extinction and flame blow-off was observed. This is analogous to the OFDF results (Hamins *et al.*, 1994). This suggests that the same processes that control flame extinction in simple diffusion flames govern flame extinction in the baffle stabilized spray flame. The correspondence is surprising because a baffle stabilized turbulent spray flame is very different in character from the laminar diffusion flames stabilized in the OFDF and cup burners. Quantitative modeling of the correspondence would require a detailed understanding of the interaction between the chemistry and fluid dynamics/droplet interaction in the recirculation zone of the turbulent jet spray flame. The practical implication of the results shown in Table 3 is that it is not necessary to test the suppression effectiveness of agents in every possible configuration. The results can be scaled from one burner to another.

An interesting model for flame blow-off was reported by Ballal and Lefebvre (1981), who correlated blow-off data for premixed gaseous turbulent flames from many investigators over a large range of velocities and flame holder diameters and shapes. Their model suggests that blow-off is proportional to the product of the square of the laminar flame speed (S_L) and the flame holder diameter (d):

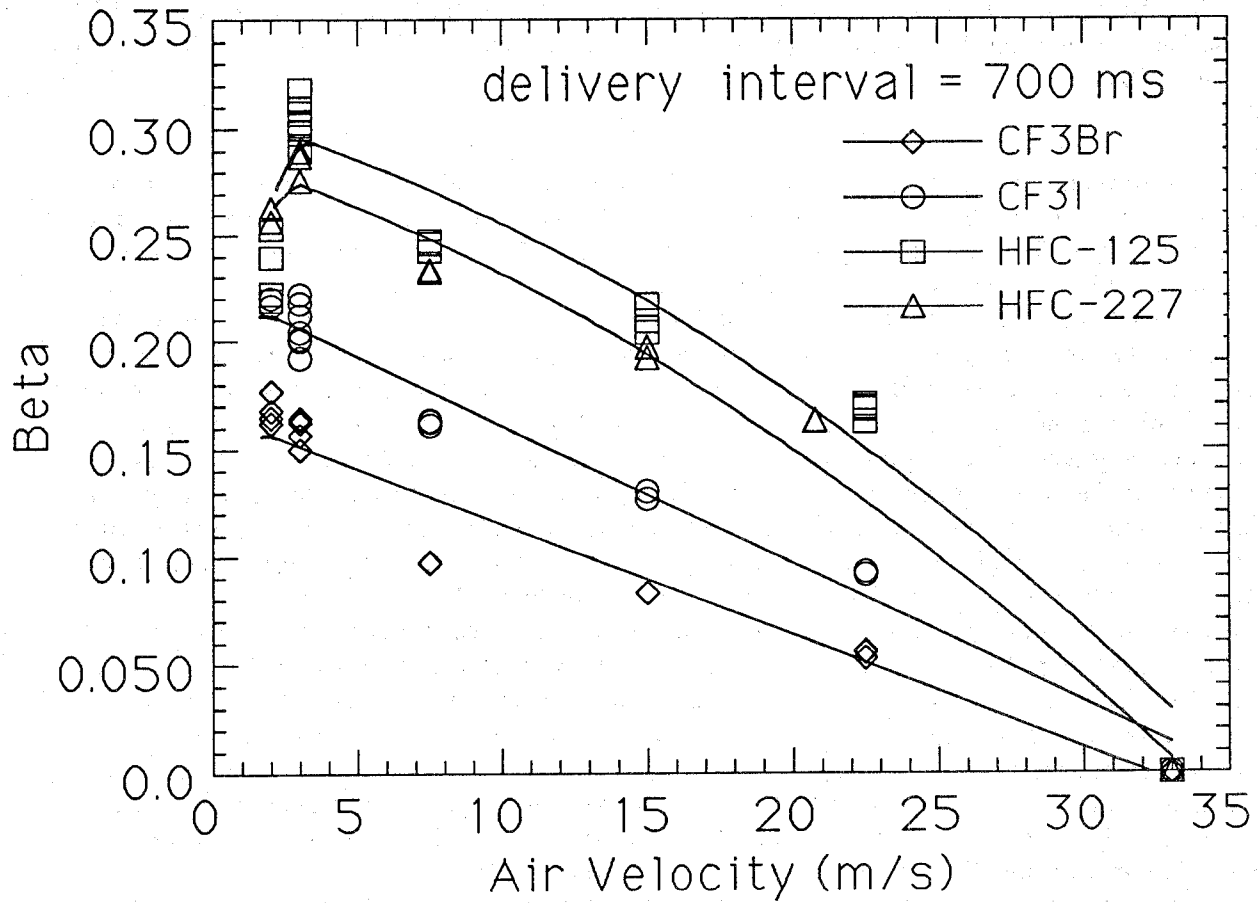


Figure 12. The critical mass fraction of agent at extinction as a function of air velocity.

$$V_{bo} = \frac{d \cdot C_s \cdot S_L^2}{\alpha_o} \quad (12)$$

where C_s is a coefficient which takes into account the drag associated with the geometry of the flame holder and α_o is the thermal diffusivity of the gases. Application of this approach to flames suppressed by agent addition necessitates flame speed information as a function of suppressant concentration. For a particular mixture flow, flame extinction would be predicted to occur for combinations of flame speeds and baffle diameters below a critical threshold. Figure 13 shows the flame speed as a function of CF_3I , C_2HF_5 , and CF_3Br concentration for stoichiometric methane/air flames (Babushok *et al.*, 1995a; Babushok, 1995). Figure 13 shows that flame speeds of 10 cm/s are obtained when agent concentrations obtain values of 1.8 %, 2.1 %, and 3.9 % (by volume), respectively, for CF_3Br , CF_3I , and C_2HF_5 . It is possible to compare these results to the spray flame results in Table 3 for an air velocity of 15 m/s, where concentrations correspond to 1.8 %, 2.2 %, and 6.0 % (by volume) for the same agents, respectively. Thus, the premixed flame results and the results in the spray flame burner follow similar trends when interpreted in terms of Equation (12). Application of Equation (12) to the extinction of baffle stabilized flames merits further investigation. Successful application of this equation would imply that information from premixed flame studies would be an adequate predictor of suppression behavior.

9.3.2.3.4 Effect of Agent Injection Interval. Figure 14 shows the critical mass of CF_3Br and the three alternative agents at extinction as a function of the delivery interval or injection duration for a constant air velocity equal to 7.5 m/s. For conditions below the data points, the flames were stable, whereas for conditions above the data points, the flames were extinguished. As the delivery interval increased, the agent mass required to achieve flame extinction increased in a near linear fashion. CF_3Br required the least amount of mass to extinguish the flames, followed by CF_3I , and the other two agents, C_2HF_5 and C_3HF_7 . These two agents were measured to have nearly identical effectiveness. The relative effectiveness of the various agents is consistent with the results shown in Figure 10-12.

Figure 15 shows the critical rate of mass injection required to achieve flame extinction as a function of delivery interval for the same data as shown in Figure 14. As the delivery interval increased, the critical rate of mass injection decreased and approached an asymptote for long delivery intervals. The relative effectiveness of the various agents is consistent with the results shown in Figure 14.

Figure 16 shows the critical mass fraction (β) as a function of delivery interval for the same data as shown in Figures 14 and 15. The curves are similar to those in Figure 15. As the delivery interval increased, the critical β decreased, and approached an asymptote for long delivery intervals. The curves for all of the agents in Figure 16 were nearly identical in shape, but were displaced along the y-axis.

These data can be explained in terms of a phenomenological model first developed by Longwell *et al.*, (1953) to explain blow-off of premixed flames by treating the recirculation zone as a well-stirred reactor. The key parameter in this model is the characteristic mixing time of reactants to entrain from the free stream into the recirculation zone. Support for this model also comes from Mestre (1955), who found that the blow-off velocity was related to the characteristic time for entrainment into the recirculation zone. Here, the model is extended to treat agent entrainment into the recirculation zone and subsequent extinction of combustion occurring in that zone. The assumptions used to develop the model are as follows. The flame is stabilized in the eddy or recirculation zone

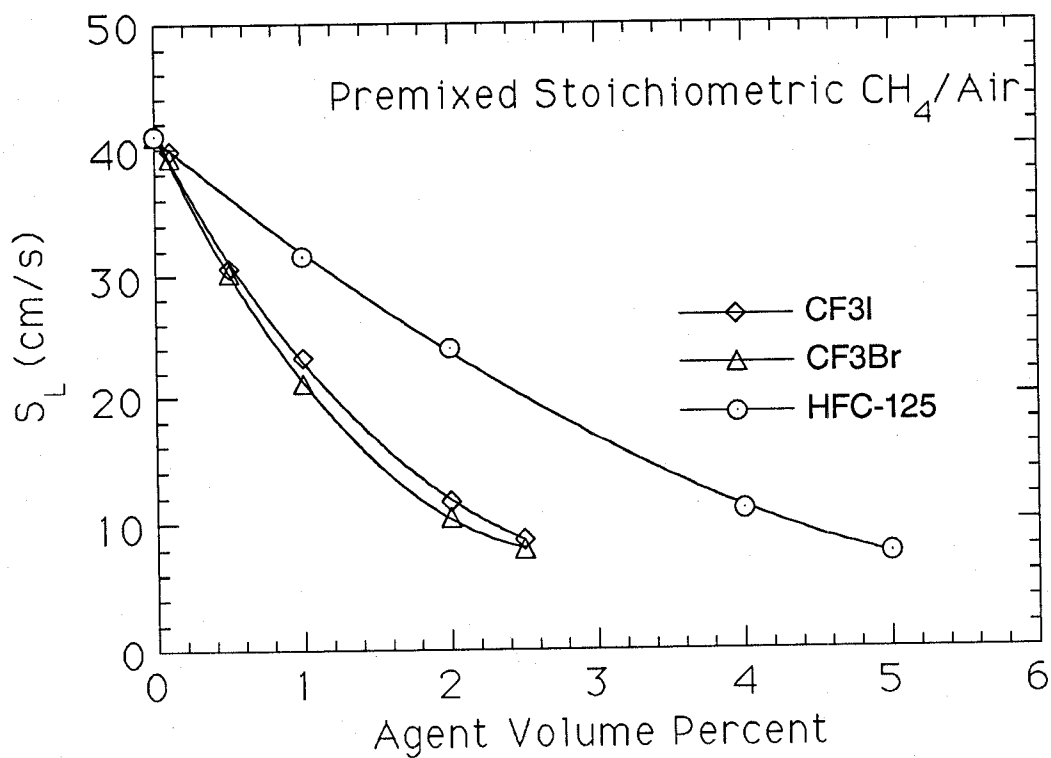


Figure 13. The flame speed as a function of inhibitor concentration in stoichiometric methane/air premixed flames. Results from Babushok (1995) and Babushok et al. (1995a).

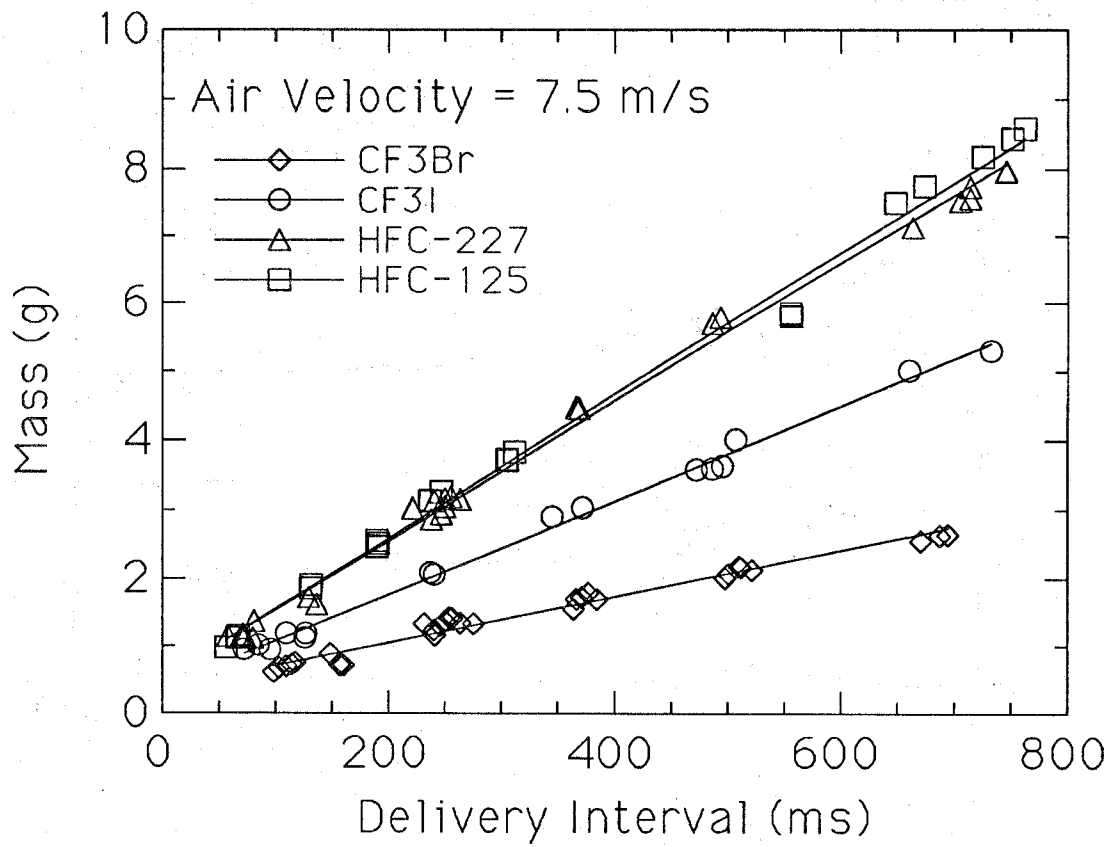


Figure 14. The critical mass of agent at extinction as a function of the agent delivery interval.

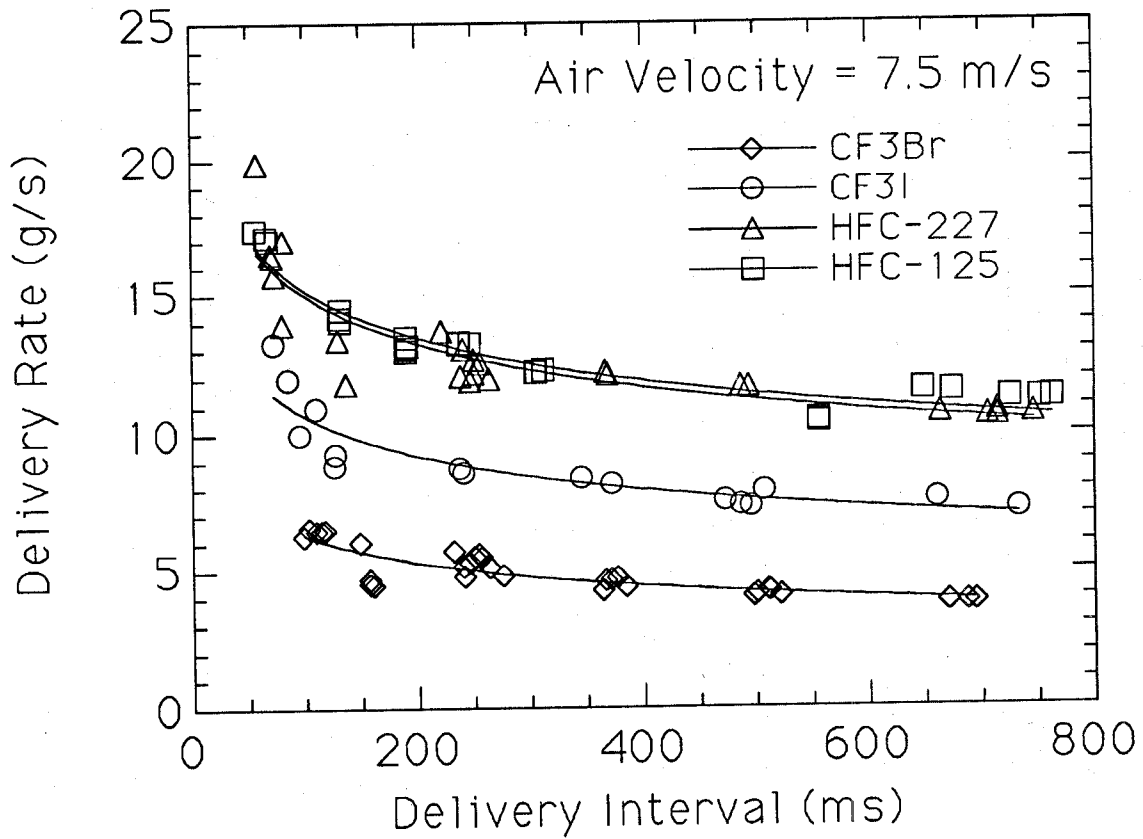


Figure 15. The critical rate of mass injection of agent at extinction as a function of agent delivery interval.

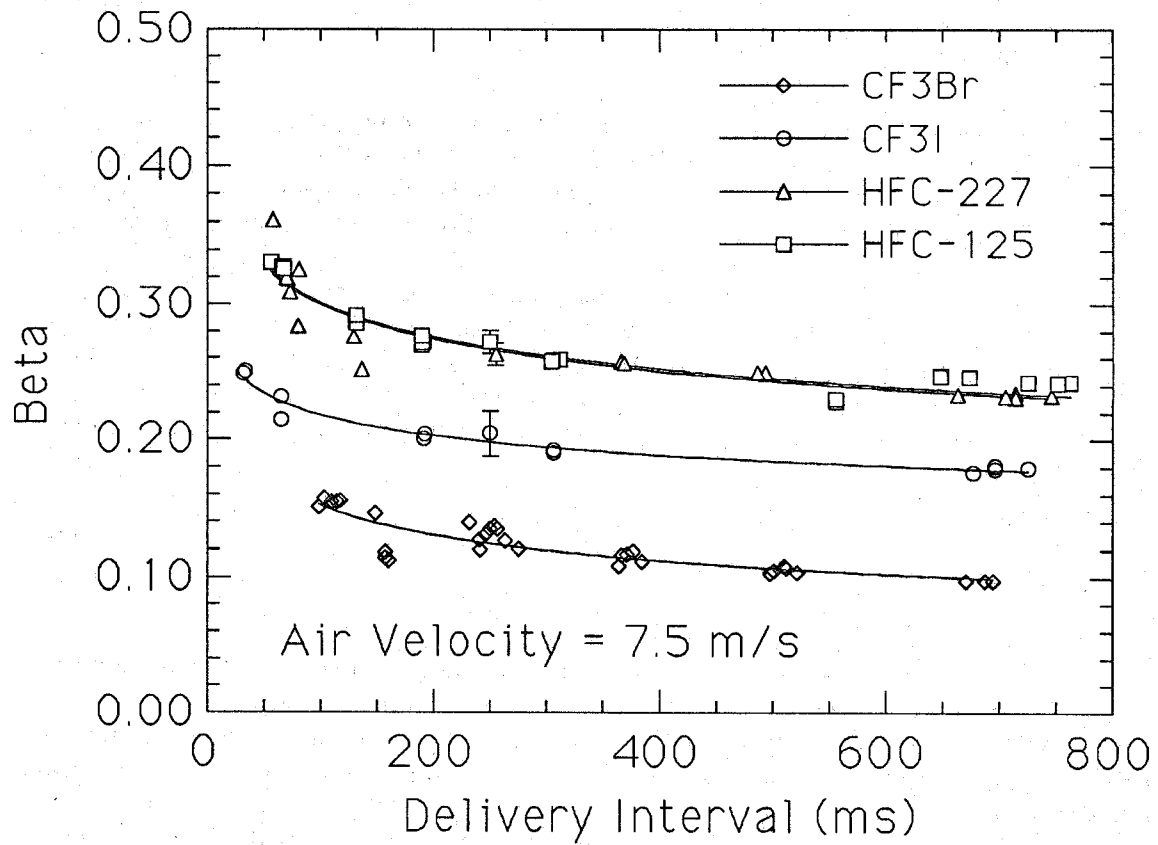


Figure 16. The critical agent mass fraction at extinction as a function of agent delivery interval.

behind the obstacle. To extinguish the flame, the agent (volume based) concentration (X) must obtain a critical value. This concentration depends on the agent type and the free stream air velocity as shown in Figures 10-12. The recirculation zone is homogeneous and mixing of the agent in the zone is instantaneous. Spray characteristics such as the droplet size distribution and momentum are considered unimportant. Applying these assumptions, it is possible to develop a simple model to predict the critical agent concentration at extinction as a function of the injection duration (Δt) and the concentration of agent for long injection times.

Applying this model, the baffle stabilized flame extinction experiments can be interpreted as follows. A pulse of agent is injected into the air stream. The agent/air mixture passes the obstacle and a portion of the agent is entrained into the recirculation zone behind the obstacle. Initially, the agent mole concentration (X) in the recirculation zone is zero. As the agent is entrained into the recirculation zone, the concentration there is given by:

$$X = X_f [1 - e^{(-t/\tau)}] \quad (13)$$

where X_f is the free stream agent mole concentration, t is the time from initial agent entrainment into the recirculation zone, and τ is the characteristic mixing time for entrainment into the recirculation zone. For very long injection times ($\Delta t \gg \tau$), the concentration in the recirculation zone will approach the free stream agent concentration, X_f . Experiments reported by Bovina (1958) confirm the form of Equation (13).

Our well stirred reactor model requires that at flame extinction, the agent concentration in the recirculation zone obtains the same critical value, regardless of agent injection duration. Thus, the model suggests that the critical agent concentration in the free stream required to achieve extinction, $X_c(\Delta t)$, for a finite injection interval (Δt) is related to the critical agent concentration in the free stream, $X_\infty(\Delta t \gg \tau)$, for long injection intervals ($\Delta t \gg \tau$) and an exponential term associated with the extent of mixing:

$$X_c(\Delta t) = \frac{X_\infty(\Delta t \gg \tau)}{1 - e^{(-\Delta t/\tau)}} \quad (14)$$

Interpretation of the spray flame extinction experiments by Equation (14) shows that the critical extinction concentration is determined by the ratio ($\Delta t/\tau$). This relationship is shown in Figure 17 where the term (X_c/X_∞) is plotted as a function of ($\Delta t/\tau$). For long injection durations, the denominator in Equation (14) becomes 1.0 and X_c is equal to X_∞ . For short injection intervals, very high agent concentrations are required to obtain extinction. For example, when ($\Delta t/\tau$) = 1, the critical agent concentration (X_c) is approximately a factor of 1.5 times X_∞ . When ($\Delta t/\tau$) = 0.5, the critical agent concentration (X_c) is approximately a factor of 2.4 times X_∞ . In addition, X_c is constrained such that $X_c \leq 1$. Equation (14), therefore, implies that there exists a critical injection duration (Δt_c) such that no matter how large the agent concentration, the flame cannot be extinguished. The value of the critical injection duration is:

$$\Delta t_c = -\tau \ln\left(1 - \frac{X_\infty}{X_c}\right) \quad (15)$$

For τ equal to 100 ms, representative of conditions in the spray burner for an air velocity of 3 m/s (discussed below), and X_∞ equal to 0.1, Equation (15) yields a value of Δt_c equal to 11 ms. Unfortunately, the minimum solenoid opening time was much larger than this value, so the veracity of Equation (15) was not empirically tested in the spray burner.

Bovina (1958) found that the time constant (τ) in Equations (13)-(15) is related to the baffle diameter (d) and the upstream velocity (V):

$$\tau \approx \frac{d}{V} \quad (16)$$

Bovina (1958) also found that the upstream turbulence level was an important factor in the mixing time. Winterfeld (1965) verified that τ was inversely proportional to the upstream velocity for both combusting and non-combusting cases over a range of Reynolds numbers extending from $\approx 1.5 \cdot 10^4$ to $2.2 \cdot 10^5$. Winterfeld (1965) found that in addition to d and V , the time constant was also a function of the blockage ratio and the geometry of the flame holder. Figure 18 shows Winterfeld's results, where the non-dimensional characteristic mixing time is plotted as a function of the square of the ratio of the baffle diameter (d) to the enclosure diameter (D). Increased blockage (increasing values of d/D) increased the value of τ . Figure 18 shows that τ was approximately a factor of two larger for a combustion situation as compared to an isothermal case, over the entire range of Reynolds numbers tested. Both the isothermal and combusting results were well fit by the form:

$$\tau = \frac{d}{V} \cdot [a + b \cdot \log(\frac{d}{D})^2] \quad (17)$$

Equation (17) is nearly identical to Equation (16), but includes a correction term for the effect of geometric blockage.

The velocity in Equations (16) and (17) refer to the velocity of the air/agent mixture. For cases where the agent composes a small percentage of the mixture, the free stream air velocity is a good approximation of the total velocity (V). Winterfeld's model suggested that mixing actually occurs over the surface which bounds the recirculation zone from the free stream. His measurements showed that the length of the recirculation zone increased significantly with increased free stream velocity. Measurements by others have led to the opposite conclusion (Lefebvre, 1983).

A two parameter fit to the extinction data shown in Figure 16 (after conversion to mole fraction from mass fraction) using Equation (14), allows determination of the parameters X_∞ and τ . By definition, the agent mole fraction (X) is related to the mass fraction (β) by the expression:

$$X = \frac{(\beta/M)}{[(\beta/M) + (1-\beta)/M_a]} \quad (18)$$

where M_a and M are the molecular weight of air (≈ 28.96 g/mole) and the agent, respectively.

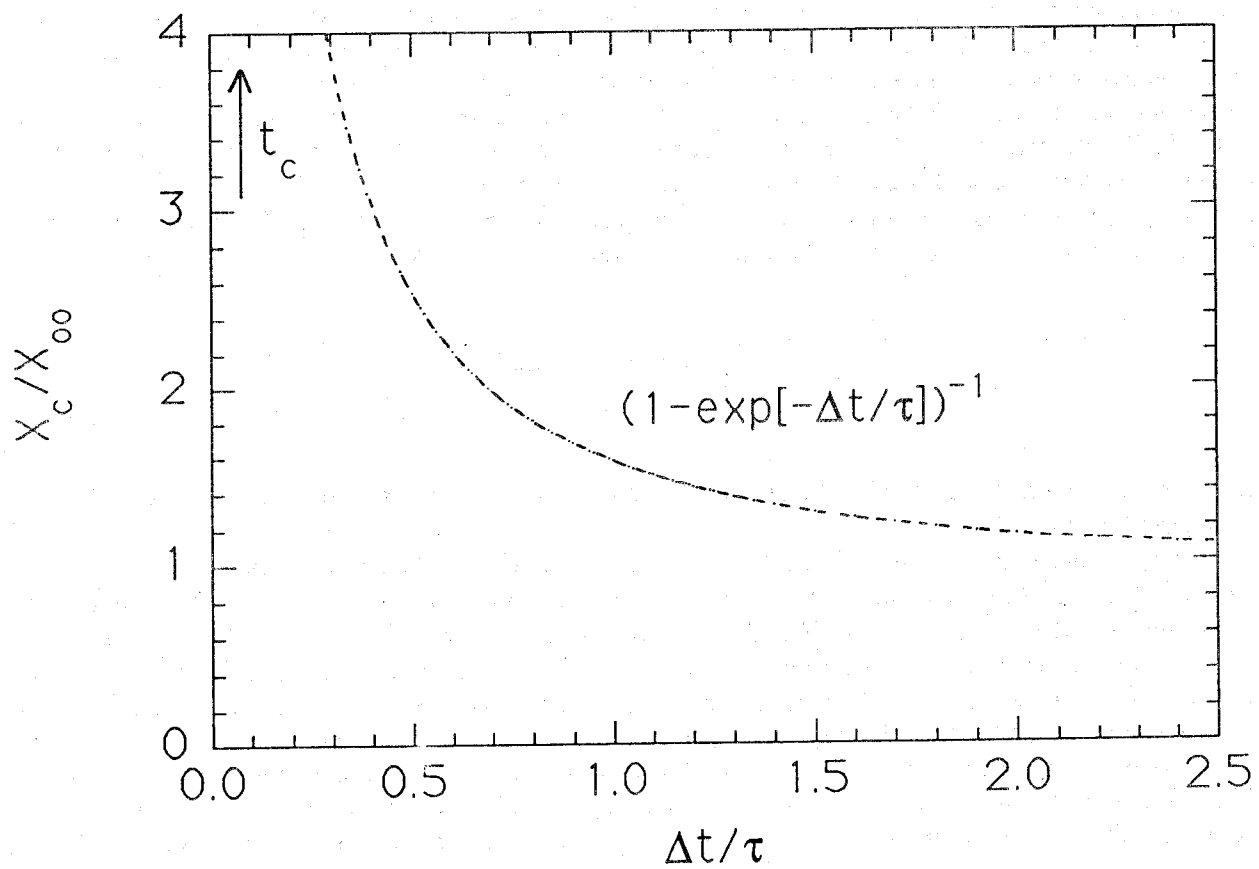


Figure 17. The term (X_c/X_∞) in Equation 14 plotted as a function of $(\Delta t/\tau)$.

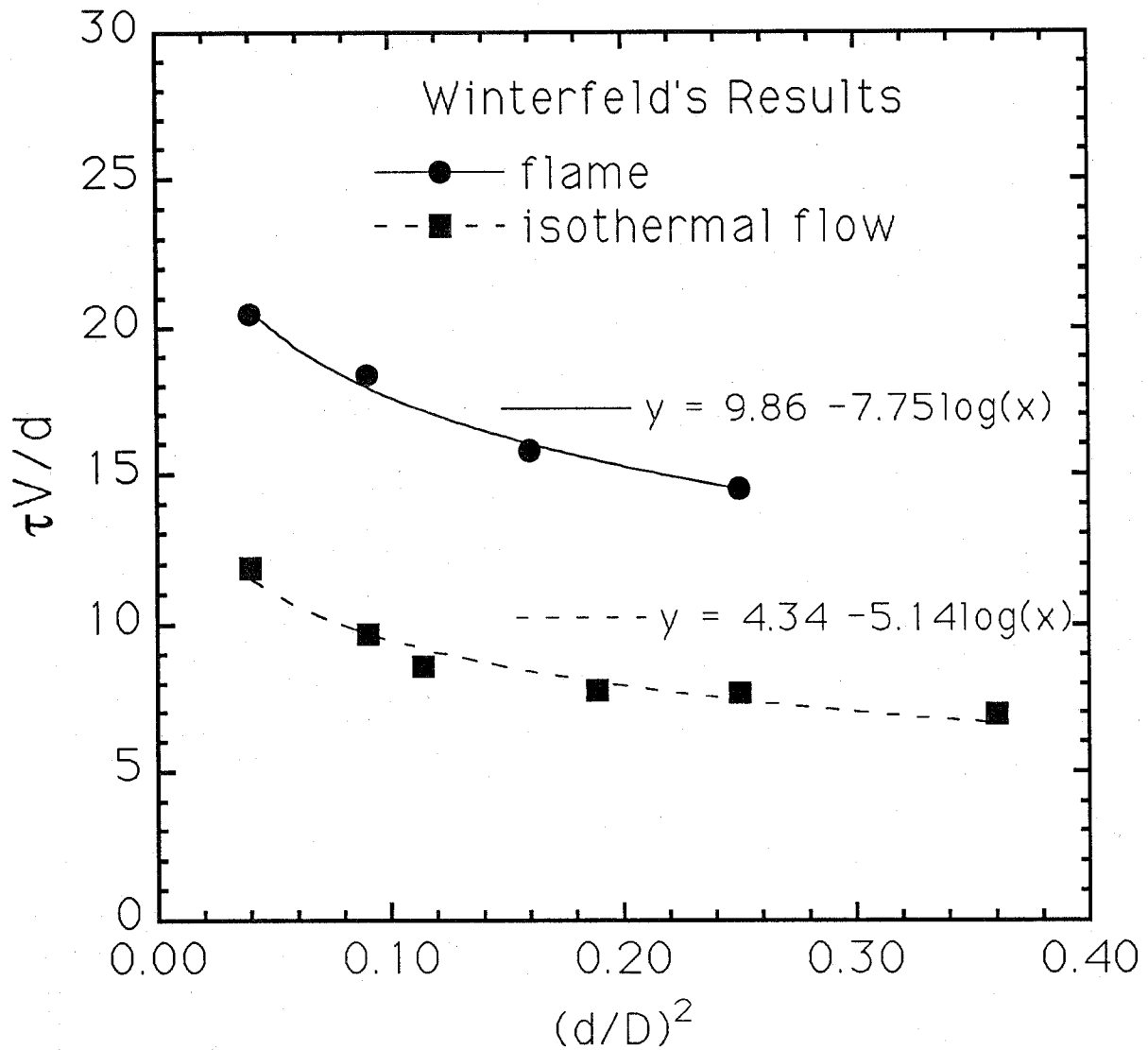


Figure 18. The non-dimensional characteristic mixing time as a function of $(d/D)^2$, as reported by Winterfeld (1965) for baffle stabilized premixed flames in an enclosure.

The critical mole fraction of HFC-125 at extinction for air velocities of 3.0 and 7.5 m/s is shown in Figure 19. The same data presented in Figure 16 for HFC-125 is shown in Figure 19 in terms of the critical mole fraction at extinction. Interpreting the curves in terms of Equation (14) shows that a best two parameter fit for the $V=3.0$ m/s data yields $\tau=99$ ms and $X_{\infty}=0.10$. Because Equation (16) suggests that $\tau \propto (1/V)$, the 7.5 m/s data should be well represented by $\tau=40$ ms ($=99$ ms/2.5). A plot using 40 ms for τ leads to a reasonable fit of the $V=7.5$ m/s data using Equation (14) as shown in Figure 19. The fit yields a value of 0.078 for X_{∞} .

The correspondence between extinction concentrations in the spray burner, cup burner, and OFDF implies that X_{∞} is related to a universal criterion for flame extinction, referred to as the critical Damköhler number. As such, X_{∞} is controlled by the interaction between the chemistry associated with combustion of the fuel/air/agent mixture and the fluid mechanical flow field. Once X_{∞} is known, X_c is controlled by τ , the rate of agent entrainment into the recirculation zone.

Equation (14) and the results in Table 3, suggest that the Damköhler number flow time for flame extinction must be related to the characteristic residence or mixing time, τ , in the recirculation zone of a baffle stabilized flame. For a flame stabilized by an object or a bluff body, this time is related to the free stream air flow, the size of the obstacle, and geometric blockage.

Figure 20 shows measurements of the critical agent mole fraction at extinction as a function of injection interval for two different bluff body disks. The flames behind the 4.13 cm disk were more stable than the flames behind the 2.86 cm disk. The blockage factor, B , (see Equation (11)) for the 2.86 cm and 4.13 cm diameter (4 mm thick) disks were 0.85 and 0.68 respectively. Equation (16) predicts a 30 % increase in the characteristic mixing time based on the increased disk diameter (from 2.86 cm to 4.13 cm). Fitting the 4.13 cm disk extinction concentration data with a two parameter fit for τ and X_{∞} , yields $\tau = 93$ ms.

Winterfeld (1965) studied the combined effect of disk diameter and blockage on the characteristic mixing time for premixed flames over a wide range of blockage ratios. Winterfeld's (1965) results (Equation (17)) predict that the combination of increased disk diameter and increased blockage should lead to a 14 % and not a 30 % increase in τ , yielding a value of 81 ms rather than 65 ms. A plot using $\tau=81$ ms leads to a reasonable prediction of the extinction results for the 2.86 cm disk (4 mm thick) as shown in Figure 20. No direct comparison was made with the results using the reference disk (3.5 cm diameter, 2 mm thick), because disk thickness and material differences influence the measured agent extinction concentrations, presumably through differences in the detailed structure of the recirculation zone. Figure 21 is an example of application of Winterfeld's results for combusting flows (shown in Figure 18), to determine mixing times for various flow velocities in an enclosure of diameter D ($=7.3$ cm). The mixing time is plotted as a function of the square of the ratio of the baffle diameter (d) to the enclosure diameter (D). Relatively large changes in the mixing time occurred for small changes in $(d/D)^2$. The mixing times, determined by fits to the extinction data, for the spray burner were ≈ 99 and 40 ms for air velocities equal to 3.0 and 7.5 m/s respectively (see Figure 19). Winterfeld's results predict mixing times equal to ≈ 170 and 65 ms for $V=3.0$ and 7.5 m/s. The ratio of values determined from Winterfeld's data to our measurements in the spray burner are a factor of 1.7 and 1.6, respectively, for the same air velocities. It was encouraging, however, that the relative difference in the two configurations were nearly the same. These difference are not surprising considering that Winterfeld's results are for premixed flames. In addition, the flows that Winterfeld studied were for relatively high Reynolds numbers and the baffle thickness was not reported nor its material composition.

As expressed through Equation (14), the simple well-stirred reactor/spray flame model has no explicit dependence on pressure, air temperature, or fuel droplet characteristics. These parameters are not thought to impact agent mixing. Molecular diffusion is not expected to play a role either and therefore agent type should not effect the characteristic agent mixing time.

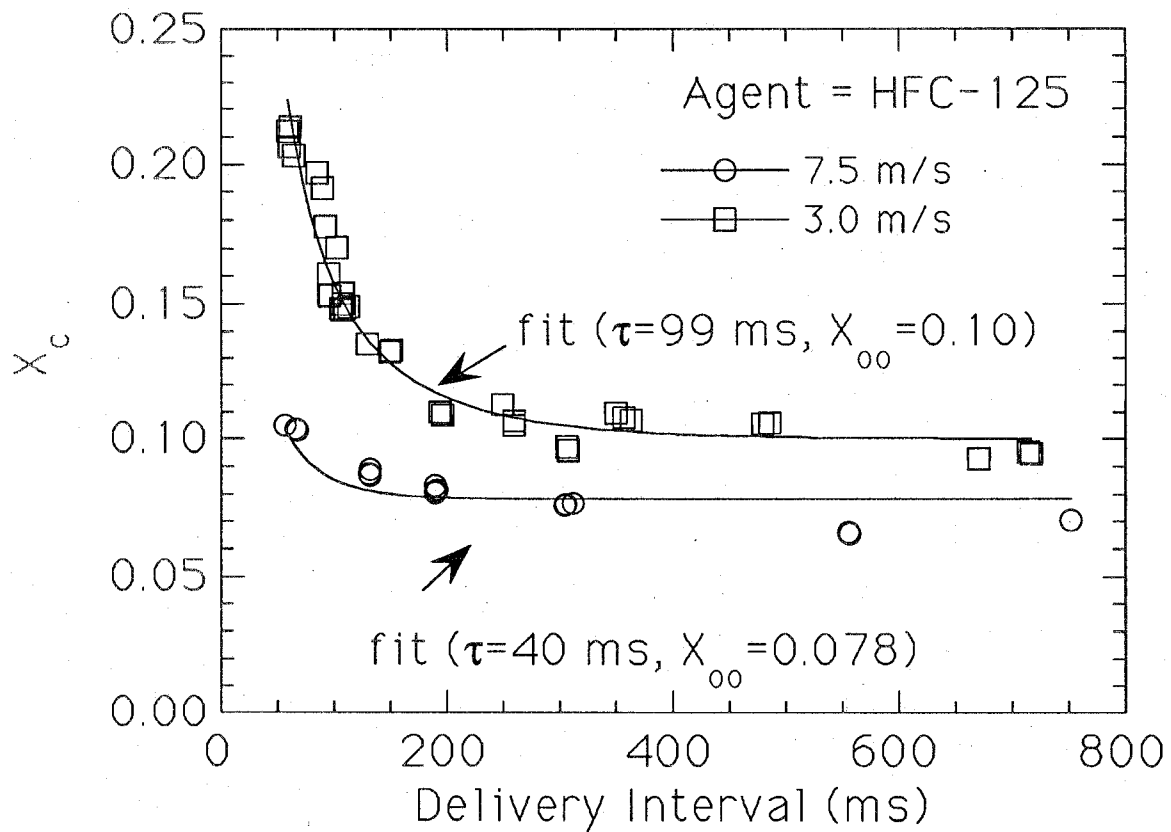


Figure 19. The critical mole fraction of HFC-125 at extinction for air velocities of 3.0 m/s and 7.5 m/s.

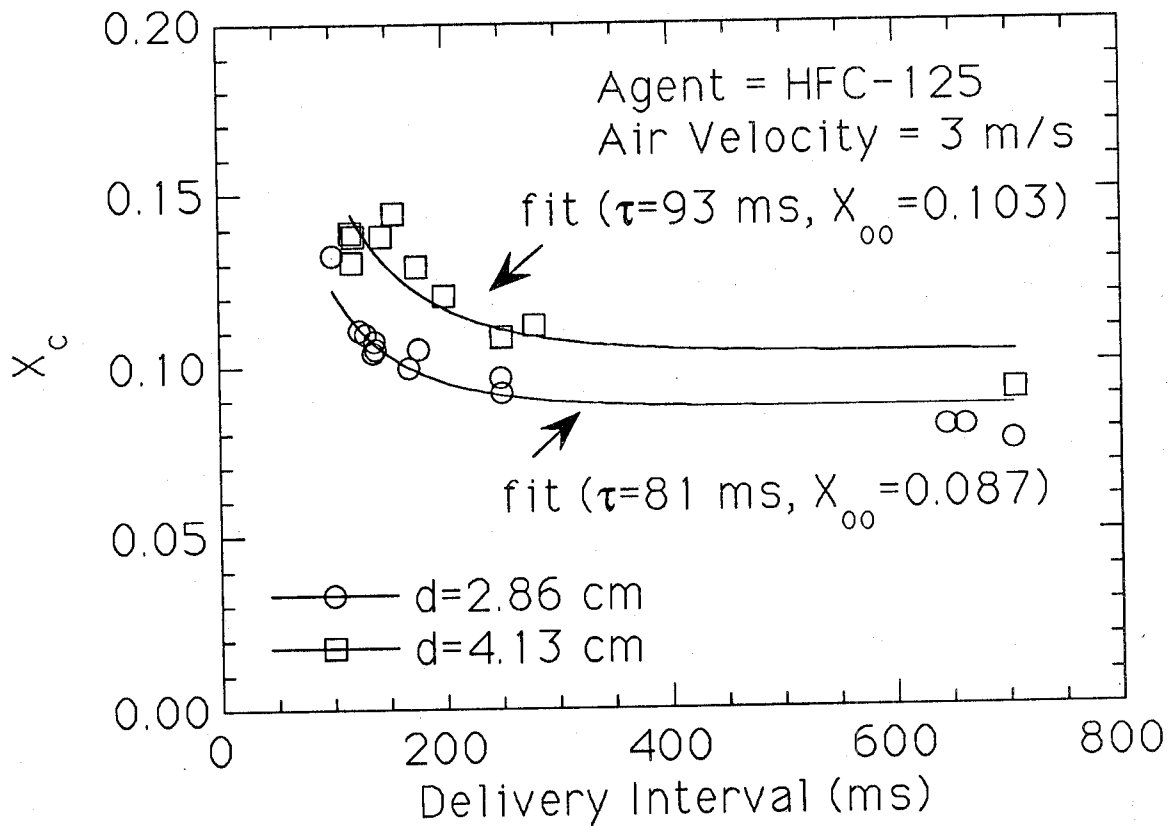


Figure 20. The critical mole fraction of HFC-125 at extinction as a function of injection interval for two different bluff body diameters with the air velocity equal to 3 m/s.

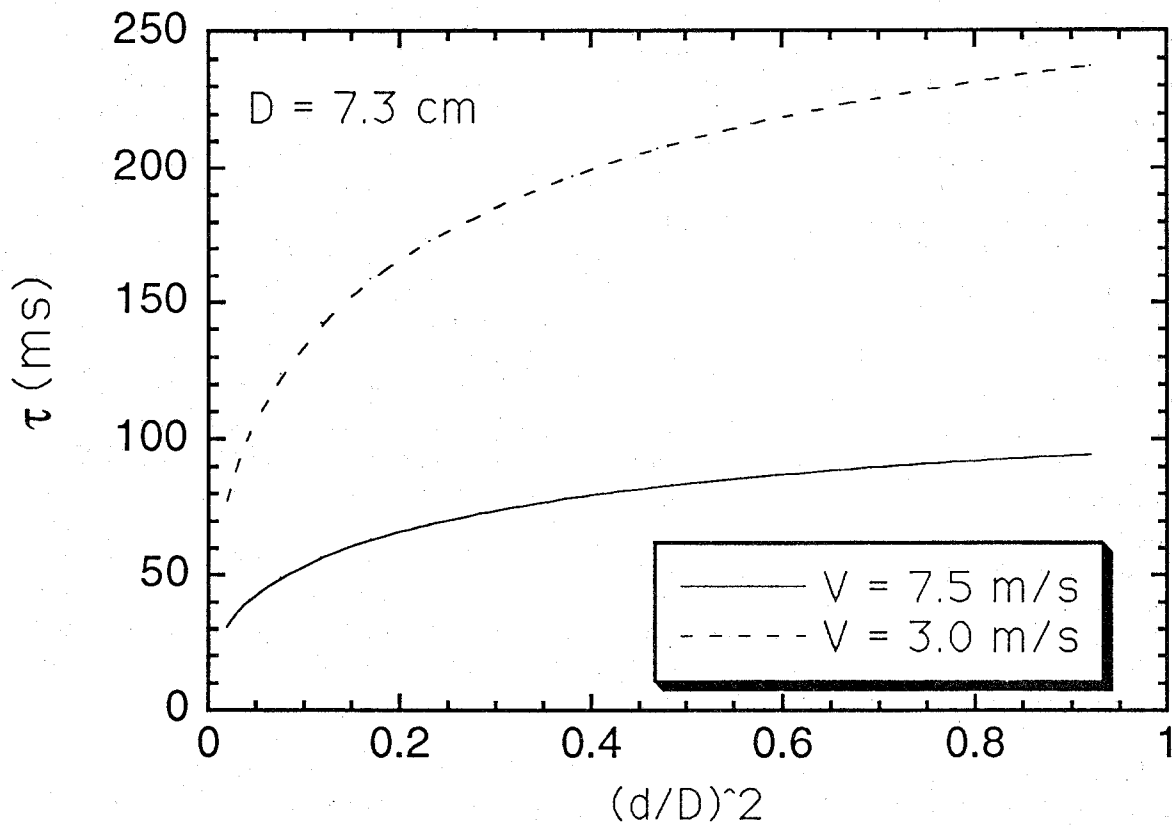


Figure 21. Application of Winterfeld's results to determine the characteristic mixing times as a function of air velocity for a fixed enclosure diameter (D).

The spray flame testing described in this and subsequent sub-sections was conducted with the 3.5 cm diameter disk (2 mm thick) and with air velocities of 7.5 m/s, yielding a mixing time constant equal to approximately 40 ms. In subsequent experiments described below, the agent delivery interval was held constant at 250 ms, yielding a value for the ratio ($\Delta t/\tau$) as approximately equal to 6, indicating that $X_c \approx X_\infty$. Thus, the value of τ is not expected to play a role in the extinction results discussed in this and subsequent sub-sections.

9.3.2.3.5 Effect of Air Temperature. The air was preheated and extinction measurements were conducted with the average air temperature in the burner varying from ambient to 350 °C under conditions of a constant air velocity of 7.5 m/s and for an agent delivery interval of 250 ms. The increase in temperature affected flame stability in several ways. First, since the air velocity at the bluff body was held fixed, the mass flow of air decreased as much as 50 % because of the drop in density. Heating of the JP-8 in the fuel line was minimized because the coaxial water jacket cooled the fuel line. As seen in Figure 22, the agent mass fraction (β) required to suppress the JP-8 spray flame increased as the air temperature increased. This was expected; increased air temperature enhances flame stability through enthalpy addition and the results were also consistent with measurements of the effect of reactant temperature on the stability of baffle stabilized flames as characterized by flame blow-off (Lefebvre, 1983). Surprising, however, was the reduction in the relative effectiveness of CF_3I as compared to the HFCs for moderate temperatures. The relative effectiveness of CF_3I was still better than HFC-125 and HFC-227 for temperatures lower than approximately 100 °C, as noted previously, but was only as effective as those agent for temperature greater than 100 °C. CF_3Br remained the most effective agent over the temperature range studied. In relative terms, CF_3I and CF_3Br required larger relative changes in agent concentration to achieve extinction as the air temperature increased, as compared to HFC-125 or HFC-227. These results were consistent with earlier measurements of the critical agent concentration requirements at extinction for heated air flows in spray flames (Vazquez *et al.*, 1994) and counterflow diffusion flames (Grosshandler *et al.*, 1995), and may be due to diminished chemical effectiveness of these agents (CF_3Br and CF_3I) as the agent concentration increases.

For some aircraft applications, cold temperatures can be expected. For sub-ambient air temperatures, the stability of the spray flame can be expected to decrease and suppression can be expected to require less agent. All measurements reported here, however, utilized gaseous agent. For a two-phase agent delivered under cold temperature conditions, the rate of evaporation and flashing may detrimentally impact the amount of agent required for flame suppression.

9.3.2.3.6 Effect of Agent Temperature. Figure 23 shows the critical β as a function of agent temperature for the three alternative agents under conditions of a constant air velocity of 7.5 m/s and for agent delivery intervals of 250 ms. Extinction measurements were conducted with the three alternative agents heated to temperatures as high as 150 °C (300 °F). The results showed that the gas phase agent temperature had no effect on flame stability. Because the majority of the air/agent mixture was air, the agent was diluted and the final mixture temperature approached the air stream temperature. In addition, the tubing walls were not insulated and the agent pulse was relatively short (less than 1 s), promoting equilibration of the gas mixture to ambient temperatures. These results do not imply that heating or cooling of the agent will not affect the rate of agent dispersion or evaporation. In these tests, the agent was introduced in the gas phase. In the nacelle, the agent will be delivered as a two-phase fluid which raises issues associated with the rate of agent evaporation, etc.

9.3.2.3.7 Effect of Pressure. Figure 24 shows the critical agent mass as a function of system pressure for the three alternative agents under conditions of a constant air velocity equal to 7.5 m/s

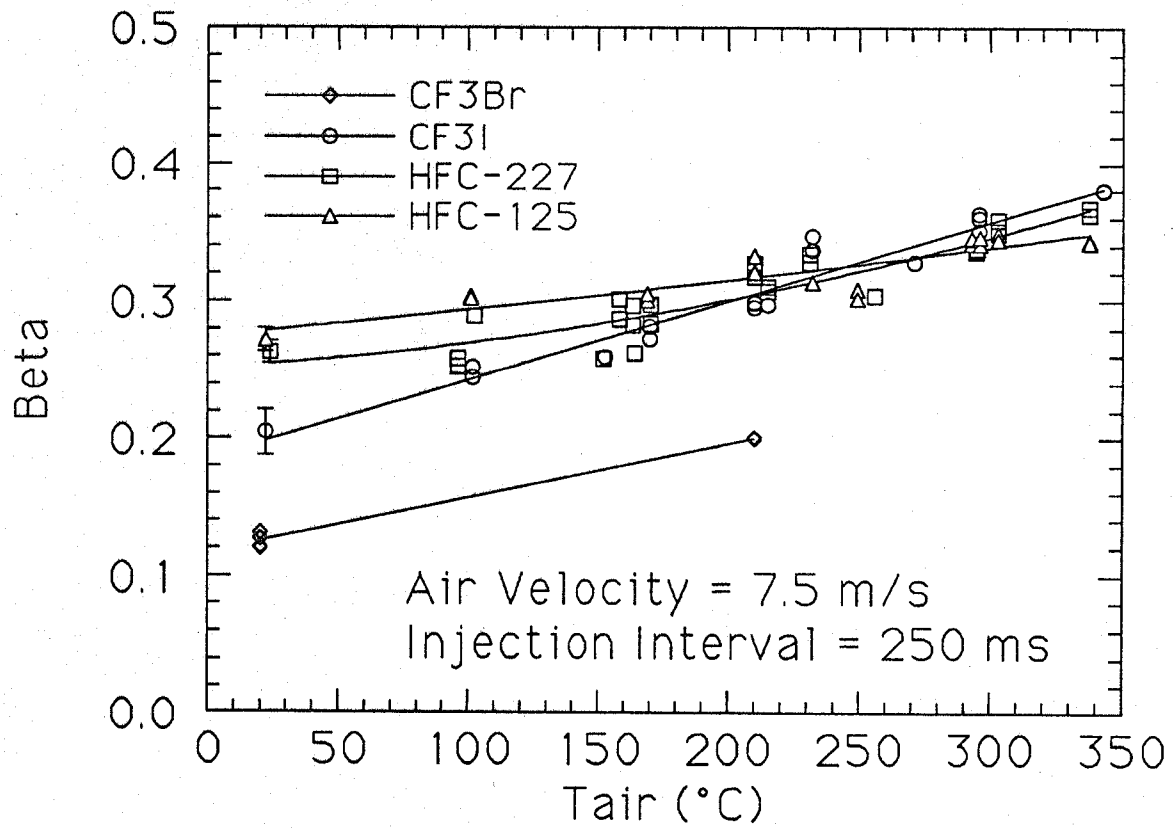


Figure 22. The critical agent mass fraction at extinction as a function of the air temperature.

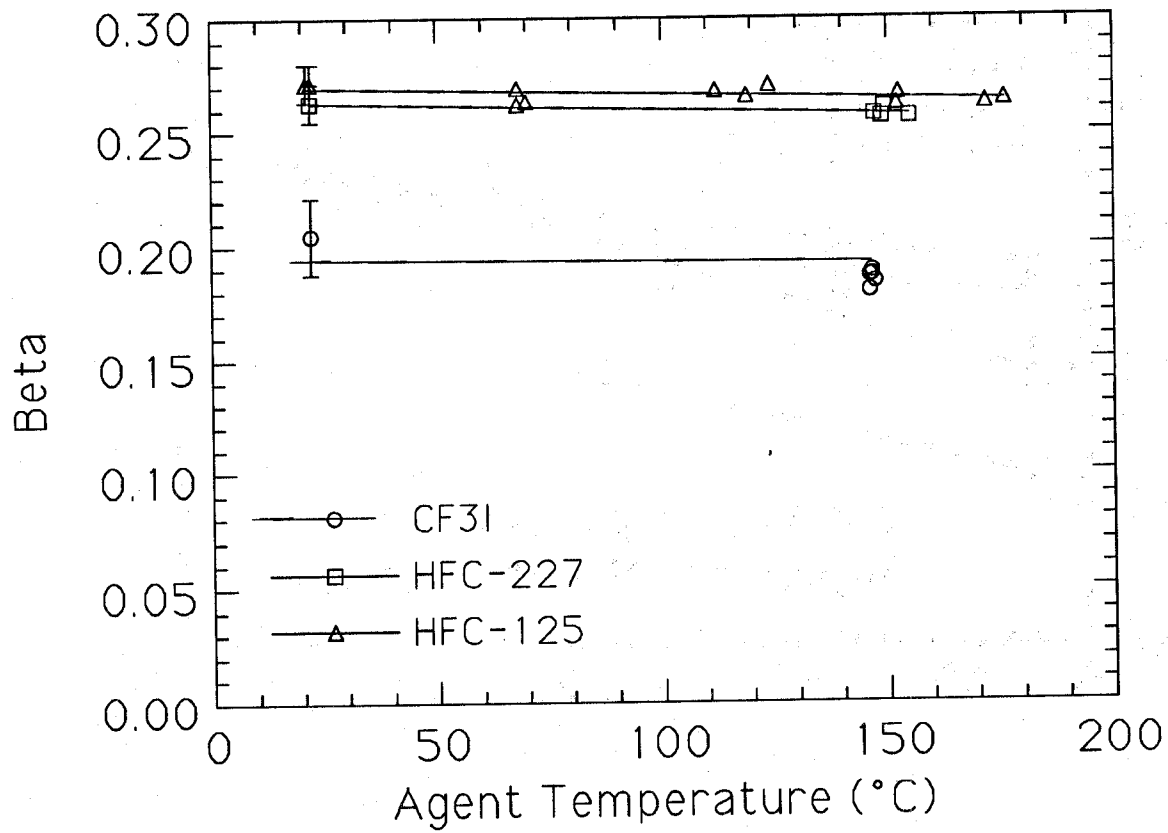


Figure 23. The critical agent mass fraction at extinction as a function of agent temperature.

and for an agent injection interval of 250 ms. As the pressure increased, more agent mass, in a near-linear fashion, was required to extinguish the spray flames. In addition to the super-ambient data in Figure 24, the data representing the ambient case (0 psig or 101 kPa) were also determined utilizing the confined spray apparatus. Those results were similar to the results determined using the standard burner configuration.

Figure 25 shows the critical agent mass fraction at extinction (β) as a function of system pressure for the three alternative agents under conditions of a constant air velocity equal to 7.5 m/s and for an agent injection interval of 250 ms. As the pressure increased, the critical β remained constant for all three agents. Thus, the mass flow of agent required to extinguish the spray flames increased linearly with the mass flow of air. The results imply that the key chemical processes that control flame extinction were not sensitive over the rather narrow pressure variation studied. It should be noted that a small pressure dependence may result for high air velocities. Equation (7) and the results of Hirst and Sutton (1961), who studied the effect of reduced pressure on the air blow-off requirements of baffle stabilized pool fires, predict increased air blow-off velocities (V_{bo}) as the pressure increases. Thus, increases in V_{bo} due to enhanced pressure would alter the profile of the critical agent mass fraction at extinction (β) as a function of the air velocity. For the velocity range of interest (<10 m/s), however, it appears that the pressure dependence is negligible.

In aircraft applications, pressure decreases with altitude. The experimental results suggest that the mass flow of air through the nacelle is the parameter of interest, and that flame suppression will require less mass flow of agent if the mass flow of air decreases with pressure.

9.3.2.3.8 Effect of Fuel Flow. Figure 26 shows the critical agent mass fraction at extinction (β) as a function of fuel flow for the three alternative agents under conditions of a constant air velocity of 7.5 m/s and for an agent injection interval of 250 ms. As the fuel flow increased, β remained approximately constant. As the fuel flow increased, the global equivalence ratio increased, where the global equivalence ratio was defined as the molar fuel/air ratio divided by the stoichiometric fuel/air ratio. It is not clear, however, how changes in the global equivalence ratio impact the combustion processes in the spray burner. A higher fuel flow does not necessarily imply that the fuel concentration in the recirculation zone obtains a higher value. The fuel droplet size distribution may shift to larger sizes as the fuel flow increases. This would actually lead to diminished fuel evaporation rates and decreased flame stability (Lefebvre, 1983). Yet, the results in Figure 26 indicate that the stability of the spray flame is relatively insensitive to the fuel flow over the range of values tested.

Figure 27 shows the critical mass fraction (β) as a function of fuel flow for the three alternative agents under conditions of a constant global equivalence ratio (0.11), for agent injection intervals of 250 ms. As the fuel flow increased, the air flow increased by the same factor. Figure 27 shows that the critical agent mass fraction required to achieve extinction decreased as the fuel and air flows increased. This series of experiments was undertaken to study the effect of fuel flow while eliminating the impact of the global equivalence ratio. Interpretation of the results is difficult, however, because the air flow has a large impact on flame stability as noted in Figures 10-12.

9.3.2.4 Summary of Spray Flame Results. The following equation summarizes the agent mass fraction requirements for flame suppression in the turbulent jet spray burner as a function of operating conditions:

$$\beta = \beta_o f_1(P) f_2(Q_{fuel}) f_3(T_{agent}) f_4(T_{air}) f_5(V_{air}) f_6(\Delta t/\tau) \quad (19)$$

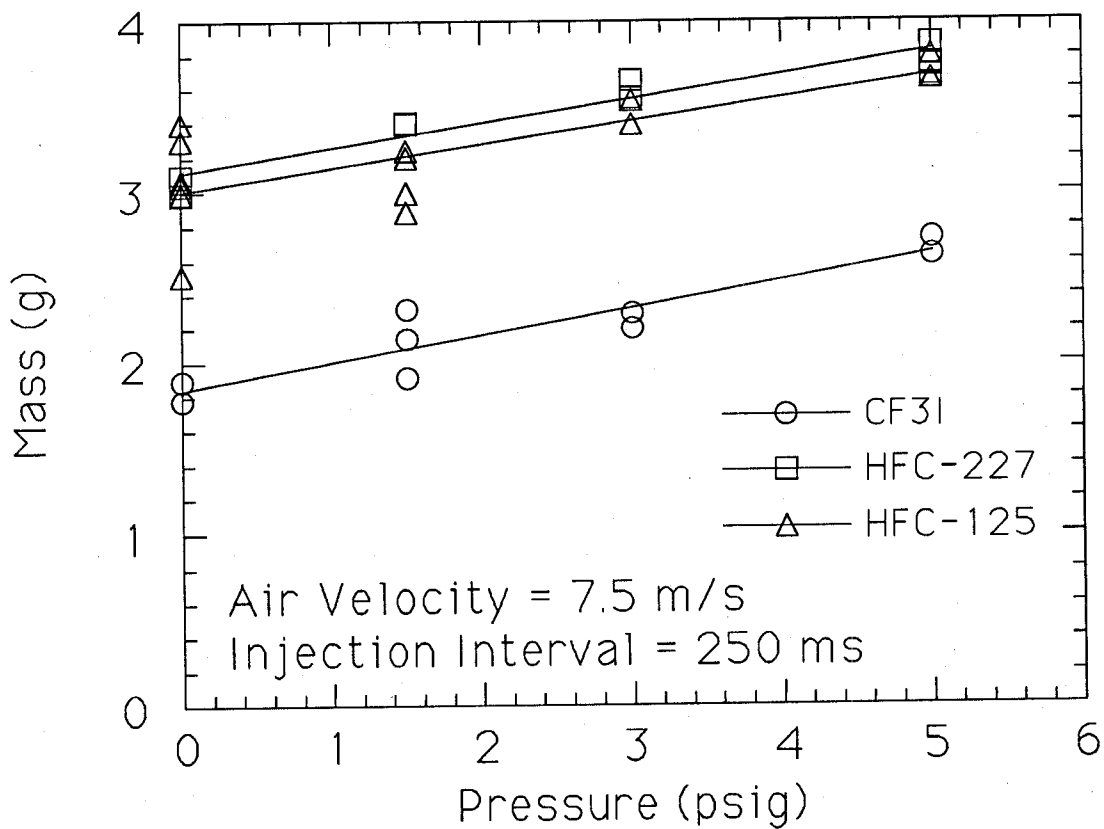


Figure 24. The critical agent mass at extinction as a function of system pressure.

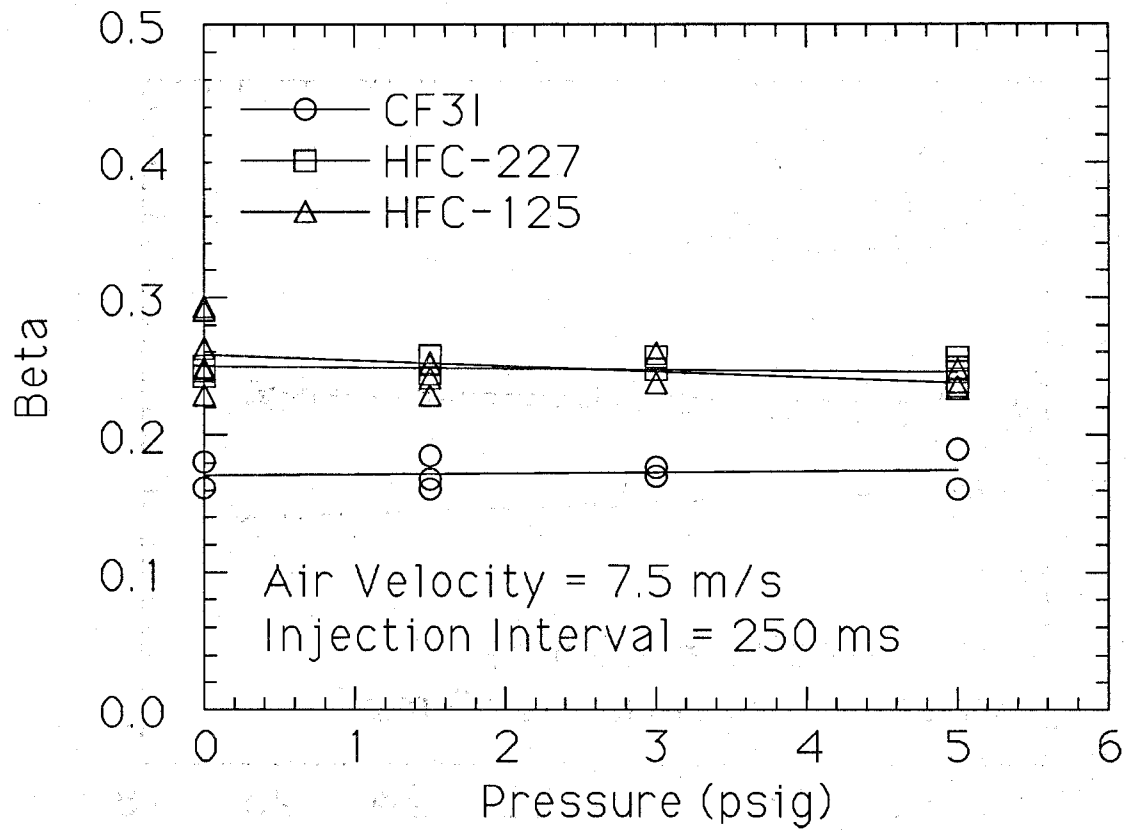


Figure 25. The critical agent mass fraction at extinction as a function of system pressure.

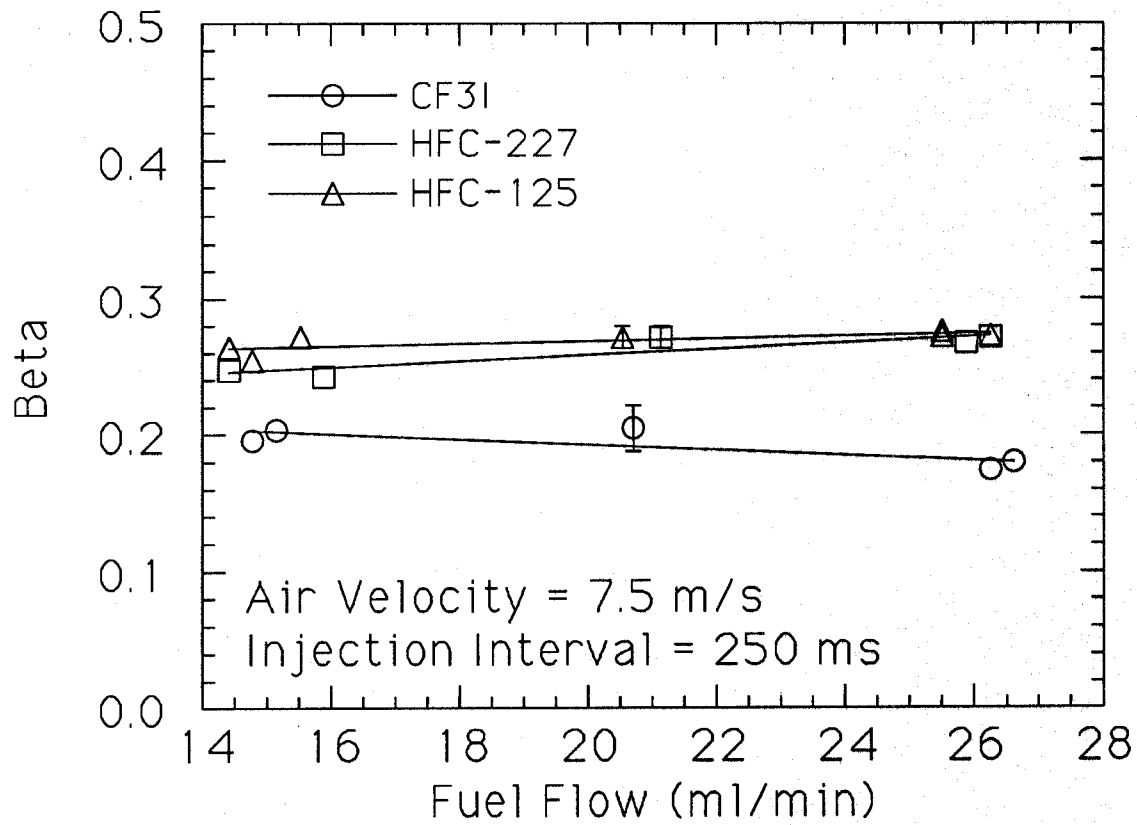


Figure 26. The critical agent mass fraction at extinction as a function of fuel flow under conditions of a constant air velocity ($=7.5$ m/s).

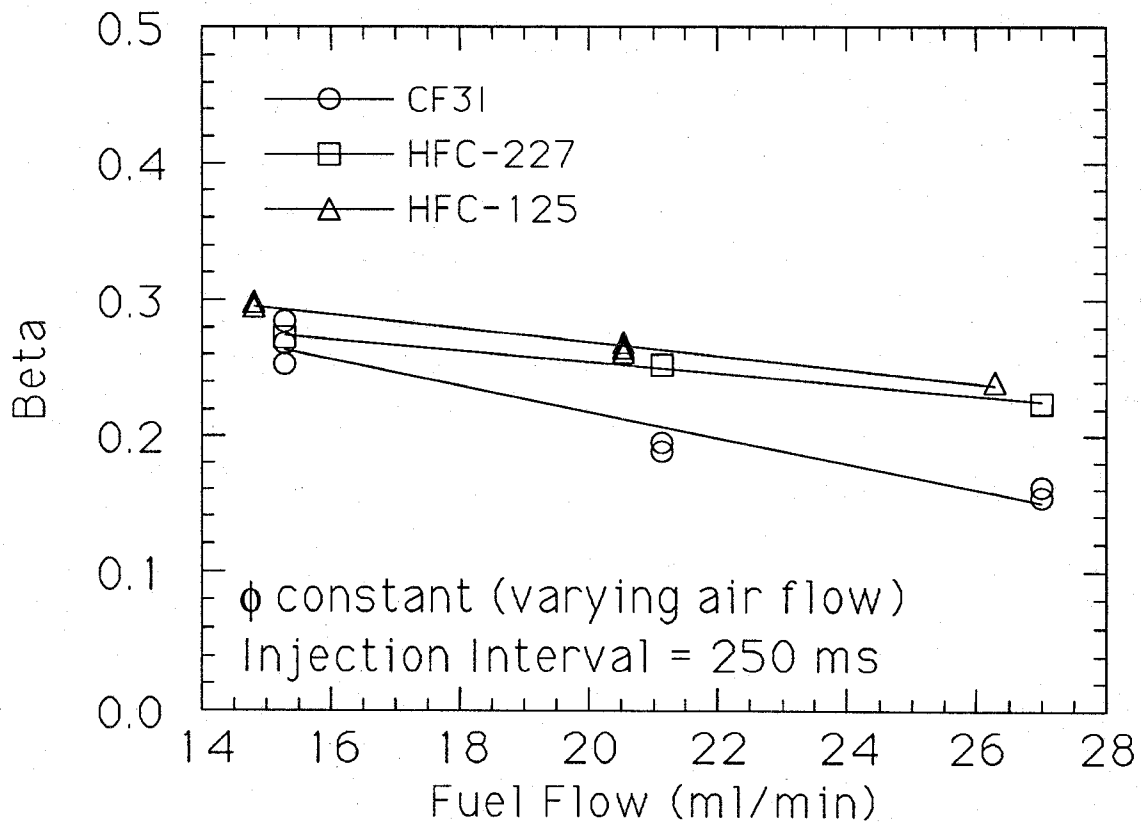


Figure 27. The critical agent mass fraction at extinction as a function of fuel flow under conditions of a constant global equivalence ratio ($=0.11$).

Table 4 defines the symbols, range of conditions, and reference conditions used in Equation (19), where β is defined as the mass fraction of agent at extinction as conditions vary and β_0 is the mass fraction of agent at extinction at reference conditions.

The correction terms to Equation (19) as the operating conditions change are listed in Table 5. Table 6 gives the values of agent molecular weight, β_0 , and the values of the polynomial coefficients for use in the functions $f_4(T_{\text{air}})$ and $f_5(V)$, the correction terms for non-baseline conditions in Equation (19). To determine f_6 , a series of algebraic calculations must be completed as outlined in note "bb" of Table 5. First, X must be determined. This requires input of X_∞ and τ , which can be calculated from the values of d , D , and V , and knowledge of M and β_0 which are listed in Table 6.

9.3.3 Suppression of a Baffle Stabilized Pool Fire. A pool fire resulting from a puddle of jet fuel or hydraulic fluid can pose a serious fire threat under certain conditions in a nacelle. In an air flow, the stability of a pool fire can be greatly enhanced if an obstacle at the leading edge of the pool is present. In some nacelle configurations, obstacles in the form of structural ribs or other bluff bodies are present at locations where combustible liquids could form a puddle. Middlesworth (1952; 1954) reported that the agent extinguishing requirements greatly increased with the presence of transverse structural ribs situated in the lower part of FR-4 and XB-45 nacelles. This was attributed to difficulties in extinguishing pool fires between structural ribs.

The literature on the stability of baffle stabilized pool fires is limited, but many important findings have been reported. Hirst and Sutton (1961) reported the effects of reduced pressure (below 1 atm) and air flow on kerosene pool fires. The pool fire was located on an airfoil in a wind tunnel and the ambient pressure was independently controlled for different air flows. The airfoil provided a smooth transition to the leading edge of the pool (the fuel tray was recessed in the airfoil and was horizontal to the surface). The dimensions of the liquid pool burner were 0.13 x 0.13 and 0.022 m deep. At low air flows, the flame was held near the leading edge of the pool and was blown across the pool surface. At higher air flows (depending on the ambient pressure) the flame was blown off and the fire was extinguished. As the ambient pressure decreased, the air velocity required for blow-off (V_{bo}) decreased. Obstructions in the form of vertical metal plates extending the width of the fuel tray were placed directly in front of the tray. Plate heights varied from 3.2 mm to 51 mm. It was shown that these obstructions had a dramatic impact on V_{bo} . An intermediate obstruction height (16 mm) yielded the highest critical air velocity. Thus, the stabilizing effect of a baffle in front of a pool fire can be very significant.

Hirst *et al.*, (1976) examined kerosene pool fire suppression with methyl bromide (CH_3Br) in a wind tunnel facility similar to the one used by Hirst and Sutton (1961). Minimum agent concentrations required to extinguish pool fires stabilized behind baffles ranging from 10 mm to 64 mm were measured. The baffle height producing the most stable flame (requiring the highest methyl bromide concentration to extinguish) was determined to be 25 mm. The effect of air velocity on the minimum agent concentration required for extinction was examined for the 25 mm baffle. At the lowest air velocity examined, 4.5 m/s, the methyl bromide concentration was the highest (~6 % by volume). The minimum extinction concentration decreased to 4.2 % as the air velocity increased to 15 m/s. Dyer *et al.*, (1977a) examined kerosene pool fire suppression in the same apparatus at lower air velocities, testing methyl bromide, halon 1301, halon 1211 and nitrogen as agents. The minimum extinction concentration for methyl bromide increased to a maximum of 7.5 % (by volume) at an air velocity of 1 m/s. The results for halon 1211 and halon 1301 showed similar trends with the same minimum extinction concentration as methyl bromide, but the air velocity at the peak concentration was from 2.5 m/s to 3.0 m/s. The time to extinguish the baffle stabilized pool fires at low air velocities as a function of concentration was reported for methyl bromide and nitrogen. Figures 28

Table 4. Guidelines for suppression of spray flames

Parameter	Symbol	Parameter Range	Reference Value
system pressure	P	101 - 135 kPa	101 kPa
fuel flow	Q_{fuel}	16 - 28 ml/min	21 ml/min
agent temperature	T_{agent}	20 - 150 °C	20 °C
air temperature	T_{air}	20 - 350 °C	20 °C
free stream air velocity	V	3 - 33 m/s	7.5 m/s
injection interval	Δt	50 - 750 ms	700 ms

Table 5. Correction terms to Equation (19)

Correction term	Value of correction term
$f_1(P)$	1 ^{aa}
$f_2(Q_{\text{fuel}})$	1
$f_3(T_{\text{agent}})$	1
$f_4(T_{\text{air}})$	$a + b \cdot T + c \cdot T_2$
$f_5(V)$	$e + f \cdot V + g \cdot V^2$
$f_6(\Delta t)$	$X \cdot M / [X \cdot M + (1 - X) \cdot M_{\text{air}}] / \beta_0$ ^{bb}

aa some small pressure dependence is anticipated for high air velocities, see text.

bb where $X = X_{\infty} / [1 - e^{(-\Delta t / \tau)}]$

$$\tau = 1.44 \cdot (d/V) \cdot (9.86 - 7.75 \log[d/D])^2$$

$$X_{\infty} = (\beta_0/M) / [(\beta_0/M) + (1 - \beta_0)/M_{\text{air}}]$$

M = the Molecular weight of the agent; see Table 6.

M_{air} = Molecular weight of air (=28.96 g/mole).

Table 6. Values of β_0 and polynomial coefficients for $f_4(T_{\text{air}})$ and $f_5(V)$ of Equation (19)

Agent	M (g/mole)	β_0	a	b (1/°C)	c (1/°C) ²	e	f (m/s) ⁻¹	g (m/s) ⁻²
CF ₃ I	196	0.16	1.1	$3.5 \cdot 10^{-3}$	0	1.4	$-4.0 \cdot 10^{-2}$	0
HFC-125	120	0.24	1.1	$8.2 \cdot 10^{-4}$	0	1.3	$-1.7 \cdot 10^{-2}$	$-5.7 \cdot 10^{-4}$
HFC-227	170	0.23	1.1	$9.0 \cdot 10^{-5}$	$3.8 \cdot 10^{-6}$	1.3	$-2.0 \cdot 10^{-2}$	$-5.3 \cdot 10^{-4}$

and 29 show the reported data, fit to Equation (14). The transport time was subtracted before the data were fit. A best two parameter fit to the data yielded $\tau=6$ s and $X_{\infty}=6$ % for methyl bromide and $\tau=5$ s and $X_{\infty}=38$ % for nitrogen. These values are significantly greater than the spray burner results reported in the previous section.

Since the baffle stabilized pool fire appears to be dramatically more stable than the spray fire, a short series of combustion and non-combustion experiments were conducted in this configuration. For expediency, the apparatus at Walter Kidde Aerospace (WKA) of Wilson, North Carolina was utilized. Tests similar to those reported by Hirst *et al.*, (1976) and Dyer *et al.*, (1977a) were performed at WKA under direction from NIST as part of this project. WKA delivered the test data to NIST for further analysis. These results should be considered preliminary, because the number of experiments and parameters tested were limited due to time restrictions and resource availability.

The main objective of the measurements was to confirm the experimental results of Dyer *et al.*, (1977a), which indicated that the mixing time was very large in baffle stabilized pool fires, that the minimum agent concentration required to achieve flame extinction was significantly larger than the concentration required to suppress cup burner flames under certain conditions, and that the maximum agent concentration approximately corresponds to the peak flammability limit of the agent.

9.3.3.1 Experimental Method and Apparatus. The experimental apparatus was based on the design described by Hirst *et al.*, (1977a). Figure 30 is a side view of the apparatus which consisted of a wind tunnel with a square cross-section (0.30 m x 0.30 m x 3.6 m long) suitable for combustion experiments and a 0.10 m x 0.20 m rectangular liquid pool burner. A cross-sectional view is shown in Figure 31. The burner had a cooling system and fuel level control. The liquid level was maintained 13 mm below the burner rim by replenishing the burned fuel with a gravity feed device (Bajpai, 1974). This prevented fuel spillage at high air flows. An airfoil and an adjustable height baffle were located upstream of the pool fire. Air was supplied by a rotary-vane blower which could produce steady air velocities in the range from 1 m/s to 10 m/s (± 2 %) in the test section. The air velocity was monitored by a vane anemometer. A viewing window provided optical access to the fire location. Each test was videotaped, showing the fire, an event lamp which indicated the agent injection pulse timing, and the vane anemometer readout. Timing sequences were obtained by frame-by-frame analysis of each video record. JP-8 was the fuel tested.

Liquid agent was expelled from a storage container placed on a load cell with a 0.01 kg resolution. The recorded mass loss of agent divided by the injection duration yielded the mean mass flow. To ensure that the mass flow was nearly constant over the injection duration for some of the longer (up to 20 s) injections, the storage bottle was super-pressurized with nitrogen to a final pressure of 2.75 MPa, with make-up nitrogen continuously added from a pressure regulated source during agent injection. The storage bottle was not disturbed during the process, so insignificant amounts of nitrogen would dissolve in the liquid phase. Short and long injection durations yielded the same measured mean mass flows with this configuration for the same needle valve setting.

Agent was introduced through a nozzle in the center of a large plenum connected to a fixed 0.10 m x 0.10 m cross-section of the wind tunnel. After leaving the nozzle, the agent spray hit a deflecting disk which dispersed it radially. A coarse screen was located downstream to improve the agent dispersion by grid induced turbulent mixing. A solenoid valve controlled the agent flow time, while a needle valve just before the nozzle provided a flow rate adjustment.

A series of non-combusting experiments were performed to validate the uniformity of the agent concentration in the tunnel for typical discharges at three separate initial air flows (1 m/s, 2 m/s, and 5 m/s mean velocities in the duct) and four baffle heights (0 mm, 13 mm, 25 mm, and 50 mm). A Statham analyzer was used to measure the HFC-125 concentration as a function of time at various

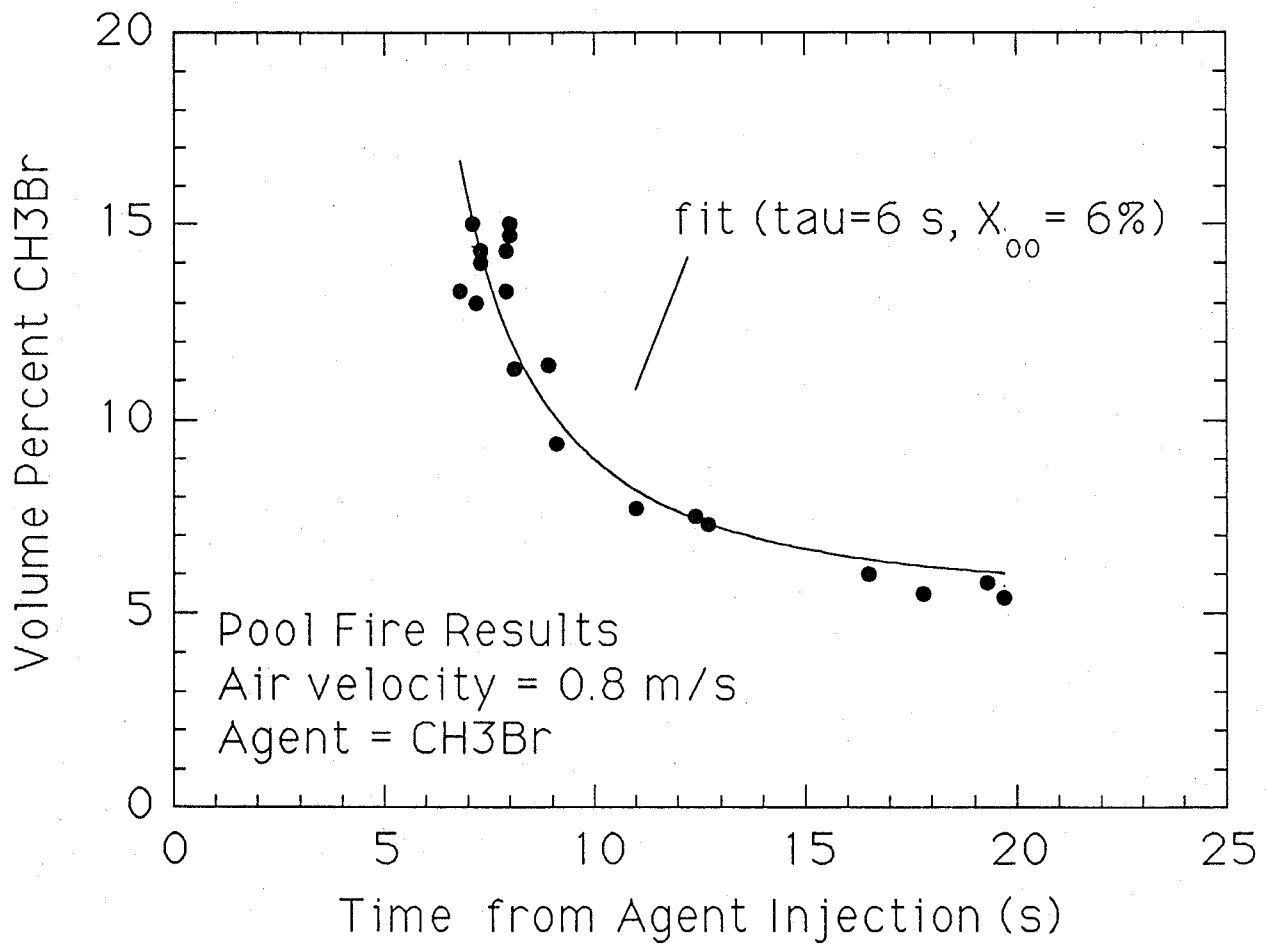


Figure 28. The volume percent of CH₃Br in the oxidizer at extinction as a function of time from agent injection for kerosene pool fires. Data taken from Dyer et al. (1977a).

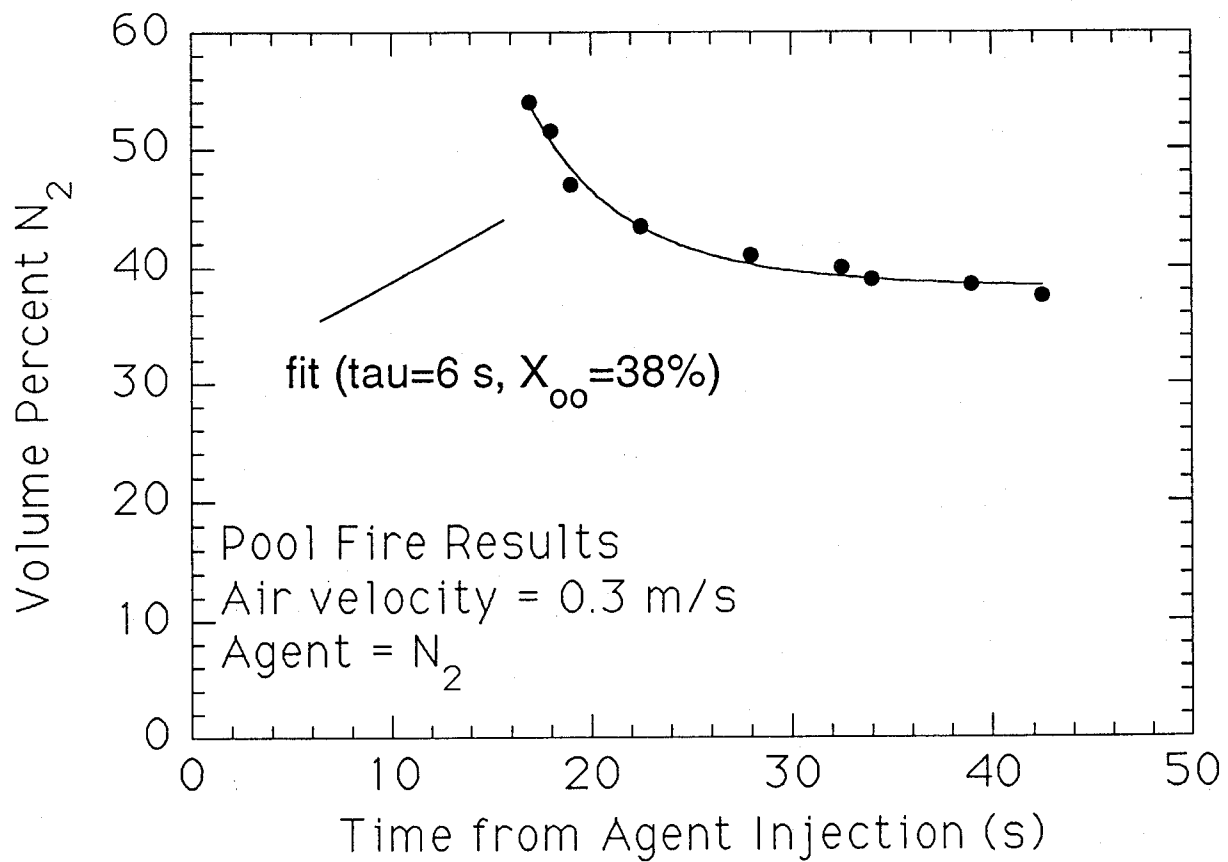


Figure 29. The volume percent of N_2 in the oxidizer at extinction as a function of time from agent injection for kerosene pool fires. Data taken from Dyer et al. (1977a)

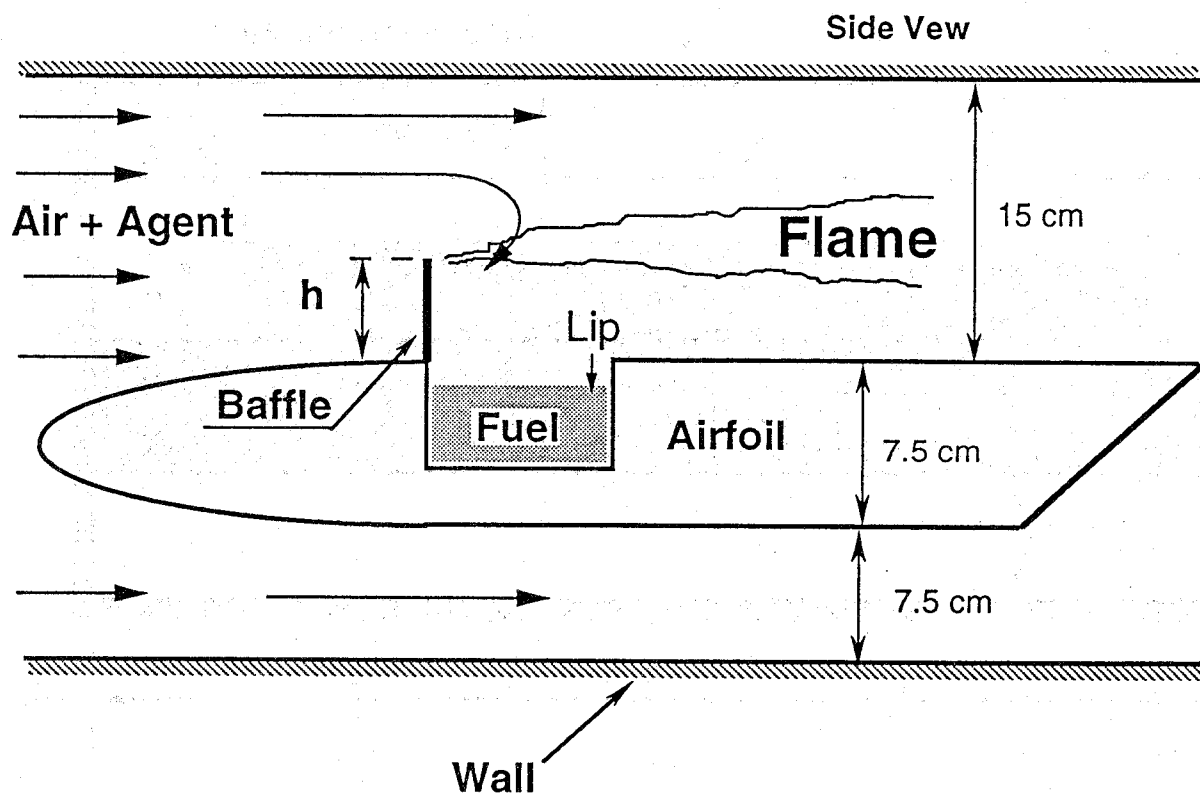


Figure 30. Side view of the wind tunnel/pool fire apparatus:

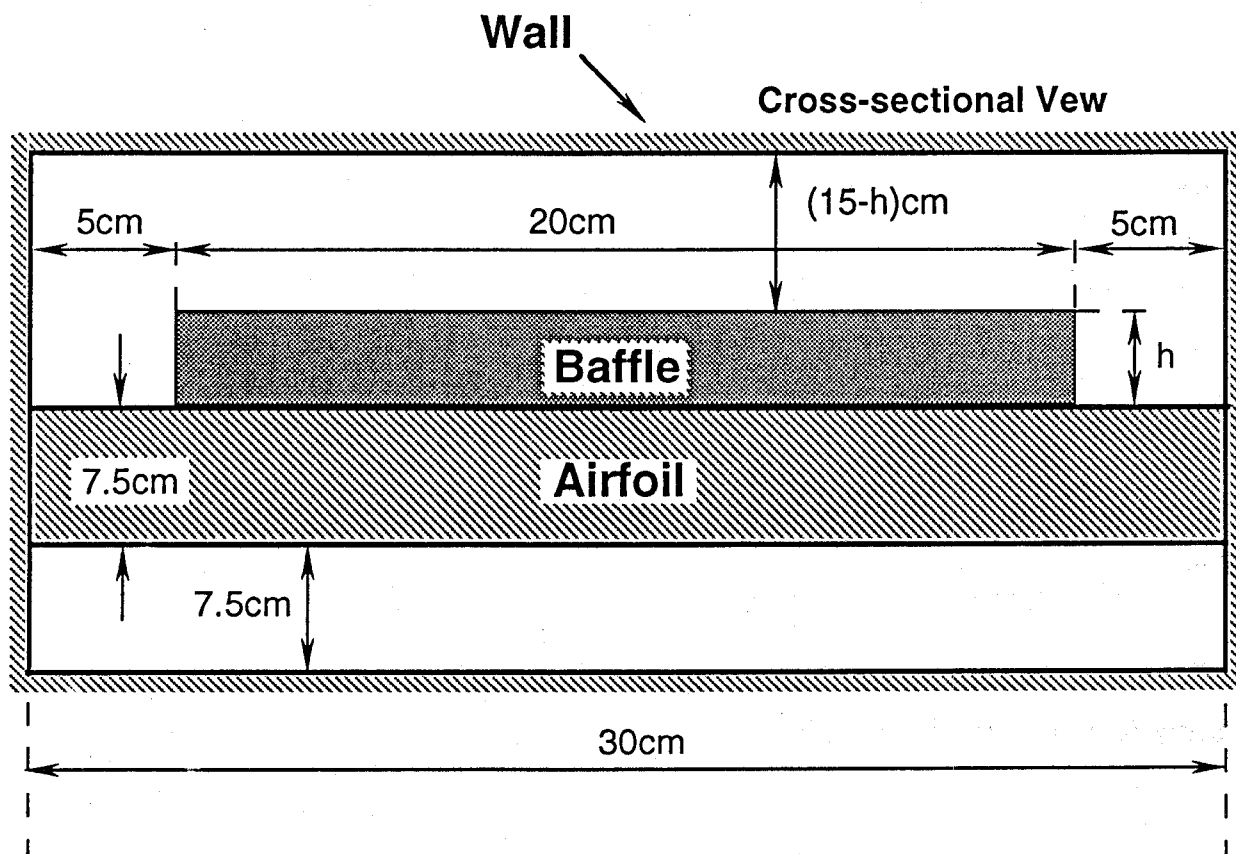


Figure 31. Cross-sectional view of the wind tunnel/pool fire apparatus.

locations upstream from the test section, and at various locations behind the baffle. That instrument was calibrated for HFC-125 and had a relatively fast response time (< 50 ms).

Pool fire extinction tests were conducted in the following manner. The agent mass flow was preset by adjustment of the needle valve, then checked with an automatic valve opening and closing sequence yielding a 1.0 s flow duration pulse. The blower fan was set to give the desired air velocity. Video recording was started, then the pool fire was lit. The agent was injected when the temperature on the top outer wall of the burner pan reached $150\text{ }^{\circ}\text{C}$. The preheat time changed depending on the baffle height, varying from 300 s to 600 s. A manual button controlled the opening and closing of the agent solenoid valve. The valve remained open until the pool fire was extinguished and was then immediately closed to conserve agent. The mass of agent dispensed and the duration of the valve opening sequence were recorded. If the pool fire was not extinguished after 15 s of agent flow, then the test was terminated and the fire extinguished with a back-up CO_2 extinguishing system. The video record provided an accurate means of determining the extinction time.

9.3.3.2 Experimental Results. The non-combusting experiments confirmed the transport delay time of the agent as it traveled from the injection location to the pool fire location. The concentration profile was confirmed to be sufficiently uniform in time and space for the purposes of these tests. The spatial variation was $\pm 10\%$ for the air flows examined in the combusting experiments. It took approximately 0.5 s for the agent to obtain its final concentration from the moment of agent detection by the analyzer.

The pool fire tests were limited in terms of air flows, although five different baffle heights were examined. Tests at an initial air velocity of 2 m/s were conducted with HFC-125, while tests at an initial air velocity of 1 m/s were conducted primarily with HFC-227. An attempt was made to blow-off a pool fire stabilized behind the 6 mm baffle by increasing the air flow. At air velocities of 11 m/s (the limit of the blower) the flame was not blown-off. Tests were conducted well below this value.

Initial calculations of the agent volumetric concentrations (agent volumetric flow/ total volumetric flow) suggested a critical extinction concentration higher than expected for HFC-125. One complicating factor was identified during the analysis of the data. During the agent injections the vane anemometer reading changed from its steady setting. The relative change in the anemometer reading depended on the agent injection rate. It was not surprising that the anemometer reading changed during the agent injection because the anemometer was calibrated for air flows at ambient pressure and temperature. But additionally, the structure of the flame was observed to change almost immediately after agent injection. The flames tended to elongate and appeared more turbulent which is consistent with a higher flow velocity. In light of these observations, along with the higher than expected estimated critical concentrations, an examination of the anemometer discrepancy was performed.

The equation that gives the relationship between the indicated vane anemometer velocity of a fluid at a density different from the calibrated fluid density is $V_1 = V_0(\rho_0/\rho_1)^{0.5}$ (Perry *et al.*, 1984), where V_1 and V_0 are the true and recorded velocities, and ρ_1 and ρ_0 are the fluid density of the flow being measured and the density of air at ambient conditions, respectively. The mixture density of the agent and air flow was estimated by assuming both adiabatic and isothermal mixing at $5\text{ }^{\circ}\text{C}$. The corrected velocity was $\approx 15\%$ less using the adiabatic mixture density as compared to the isothermal mixture density. Gas phase temperature measurements at locations just before the airfoil indicated temperatures on the order of $0\text{--}15\text{ }^{\circ}\text{C}$ (ambient air temperatures reached $30\text{ }^{\circ}\text{C}$ during the testing). For the analysis, a mixture temperature of $5\text{ }^{\circ}\text{C}$ was used.

Figure 32 shows the corrected anemometer velocity for a long discharge test. This corrected velocity is significantly different from the initial velocity of 2 m/s. This implies that the volumetric flow changed dramatically due to agent discharge. An explanation is that the air flow from the blower

is sensitive to the pressure in the duct, since the air flow is not choked. Due to the orientation of the agent nozzle, agent injection induces an ejector-type flow response that pulls more flow from the blower during the injection. The phenomenon was observed during nitrogen injections in the NIST mock nacelle (see Section 9.4).

The digital output from the anemometer was updated at a rate of 0.5 Hz. In addition, it is evident that the instrument electronically averages over the update cycle. Some agent injection events were over before the maximum velocity change was recorded. Therefore, even if the change in air flow due to agent injection was assumed to occur instantaneously, the corrected flow must be estimated for some tests.

The corrected air velocity measurements are listed in Tables 7 and 8, along with the initial air velocity, the mean agent mass flow, the agent concentration and the extinction time or total agent flow time for non-extinguished (N.E.) fires, for the HFC-125 and HFC-227 experiments, respectively. The reported extinction time represents the interval between when agent first reached the baffle, which was evident in the video record as an approaching vapor cloud and the rapid disappearance of flames. Agent transport times were comparable to the transport times inferred from the concentration measurements.

9.3.3.3 Discussion of Experimental Results. Figures 33 and 34 show the agent concentrations as a function of the time required to obtain flame extinction for HFC-125 at an initial air velocity of 2 m/s and for HFC-227 at an initial air velocity of 1 m/s, respectively. The data were consistent with the form of Equation (14), the simple extinction mixing model described for the spray burner. The data were analyzed assuming that the agent concentration pulse was like a step change and that the velocity was constant during the suppression event. Although the results for the different baffle heights showed some variation, the trends did not appear to be significant for the rapid extinction results, and could not be fully characterized from the limited data. Therefore, the solid lines represent a fit to all of the extinction data using the functional form of Equation (14). The values of $X_{\infty}(\Delta t > \tau)$ (see Equation (14)) for extinction by HFC-125 and HFC-227 were measured as approximately 12 % and 11 % (by volume) respectively. These values were greater than the extinction concentrations measured in the cup burner, as expected from the results of Dyer *et al.*, (1977a) for suppression of baffle stabilized pool fires with low air flows. The characteristic mixing times from the data fits were 0.5 s for HFC-125 (with the air velocity approximately equal to 3 m/s) and 0.7 s HFC-227 (with the air velocity approximately equal to 1.5 m/s). Since the characteristic mixing time is independent of agent type, the results display the expected trends. As the velocity increased, the mixing time decreased, but not inversely proportional to the velocity as predicted by Equations (16) and (17). Nor are the values of the mixing times consistent with the results of Dyer *et al.*, (1977a).

The characteristic mixing time inferred from the data of Dyer *et al.*, (1977a) for methyl bromide were much longer than the values reported here. The results for methyl bromide injections were for air velocities of 0.76 m/s. The results of Dyer *et al.*, (1977a) may be partly due to velocity effects (see Equations (16) and (17)), or to a slow increase in the agent concentration, instead of the assumed step function. In any case, the results show that under similar air flow and baffle height conditions, a baffle stabilized pool fire is **much more difficult** to extinguish than a baffle stabilized spray flame (where the baffle is in the middle of the flow field).

9.3.4 Suppression of Re-ignition. After suppression of a nacelle fire, hot fuel vapor may exist at levels which are flammable, leading to the possibility of re-ignition. A puddle of hydraulic fluid or jet fuel from a leaking fuel line will vaporize as heat is transferred from a nearby hot metal surface. Under normal engine operating conditions, hot metal surfaces which could cause ignition exist along the interior wall of the nacelle which separates the jet engine combustor from the nacelle. In addition,

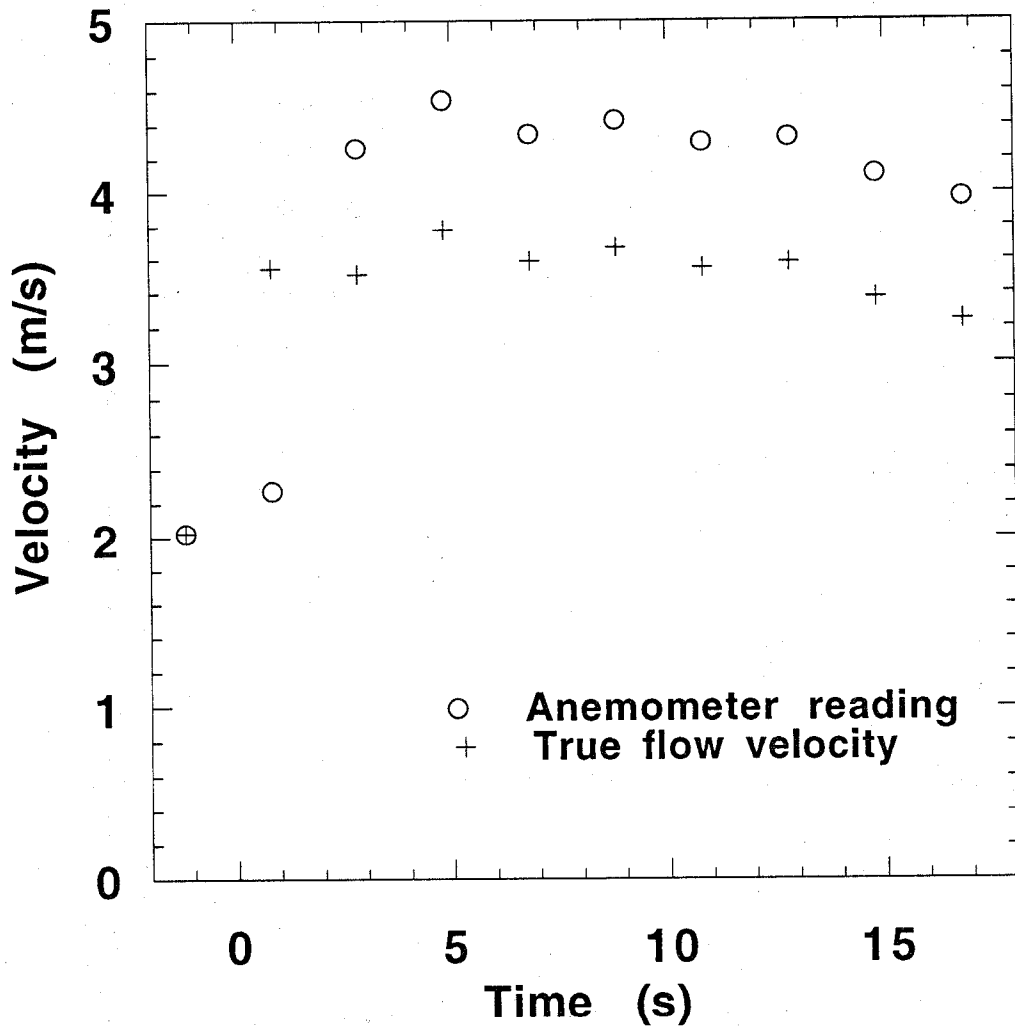


Figure 32. The corrected anemometer velocity as a function of time during agent discharge.

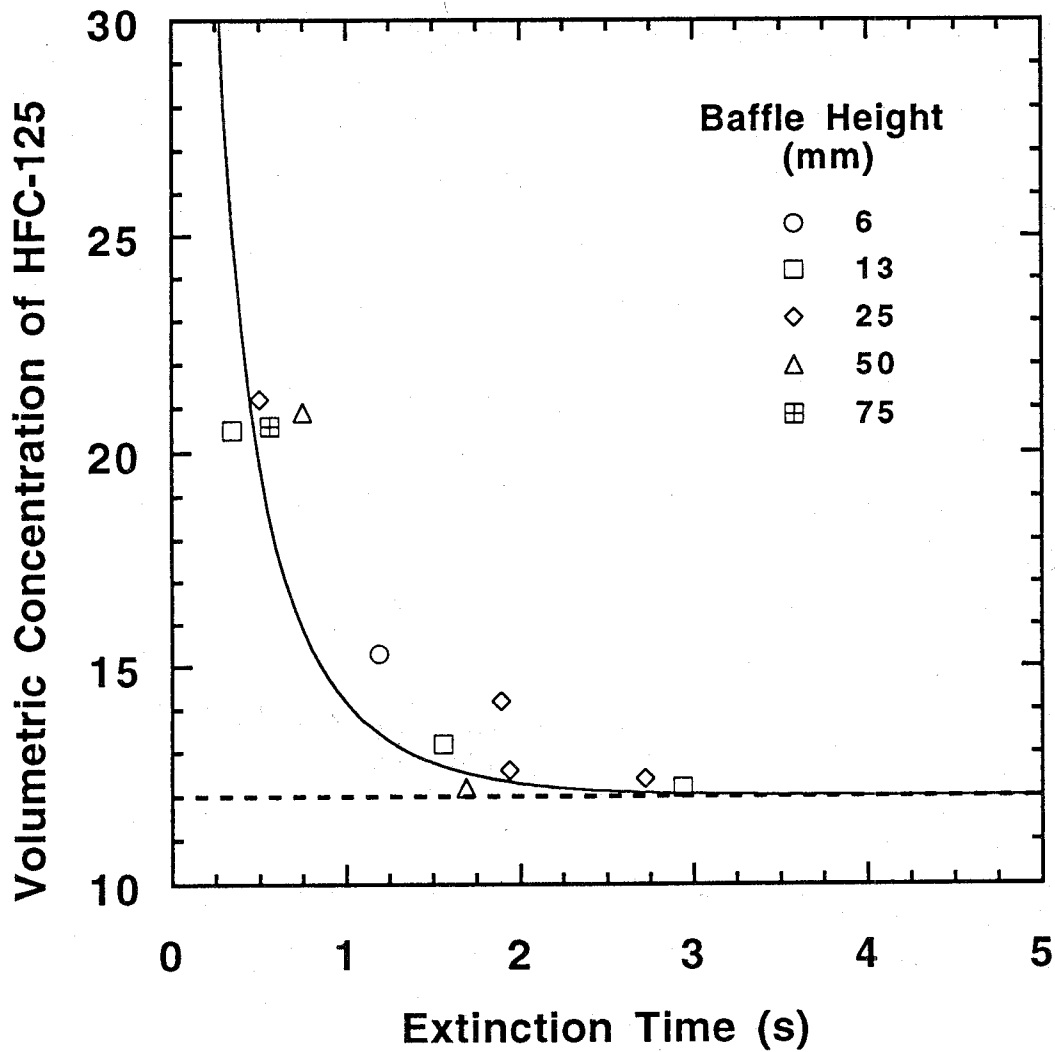


Figure 33. The critical volume percent of HFC-125 in the oxidizer as a function of time to extinguish the flame.

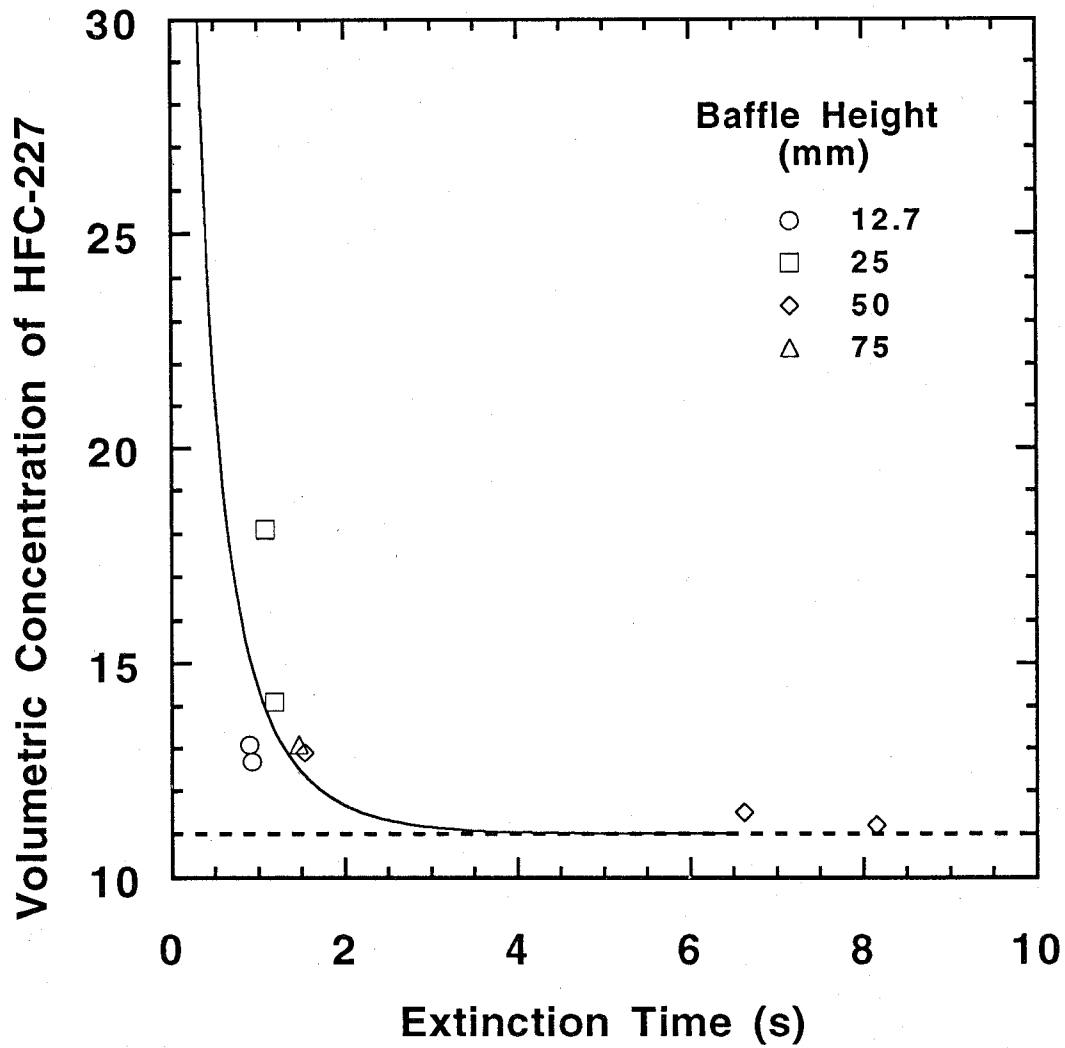


Figure 34. The critical volume percent of HFC-227 in the oxidizer as a function of time to extinguish the flame.

Table 7. Experimental data on the suppression of pool fires using HFC-125

Baffle height (mm)	Initial air velocity (m/s)	velocity during agent flow (m/s)	Mean agent mass flow (kg/s)	Agent Concentration (Vol. %)	Extinction time (s)
6.3	1.90	3.38	0.255	15.3	1.19
13	2.04	3.31	0.175	10.7	24, N.E.
13	1.98	3.45	0.203	11.9	14, N.E.
13	2.03	3.94	0.237	12.2	2.94
13	2.01	3.69	0.241	13.2	1.56
13	1.98	4.23	0.430	20.5	0.34
25	1.96	2.56	0.095	7.5	19, N.E.
25	1.96	2.91	0.143	10.0	19, N.E.
25	2.03	3.59	0.192	10.8	15.5
25	1.92	3.85	0.236	12.4	2.72
25	1.98	3.67	0.228	12.6	1.94
25	1.96	3.44	0.242	14.2	1.89
25	1.95	4.27	0.448	21.2	0.50
50	1.98	3.24	0.142	8.9	17, N.E.
50	1.98	3.64	0.214	11.9	9, N.E.
50	1.85	3.93	0.246	12.2	1.69
50	1.99	4.26	0.441	20.9	0.75
75	2.03	3.67	0.231	12.7	9.97
75	1.96	4.24	0.432	20.6	0.56
25	1.06	2.07	0.105	10.3	15, N.E.
25	1.01	1.90	0.105	11.2	19, N.E.
25	1.06	3.09	0.194	12.7	3.25
25	1.01	2.94	0.202	13.9	1.56

Table 8. Experimental data on the suppression of pool fires using HFC-227

Baffle height (mm)	Initial air velocity (m/s)	velocity during agent flow (m/s)	Mean agent mass flow (kg/s)	Agent Concentration (Vol. %)	Extinction time (s)
13	1.05	1.93	0.145	10.9	11, N.E.
13	1.01	2.47	0.222	13.1	0.90
25	1.05	2.39	0.165	10.1	6.25
25	1.03	2.50	0.243	14.1	1.19
25	0.95	2.09	0.261	18.1	1.09
50	1.00	2.08	0.129	9.0	15, N.E.
50	1.00	2.22	0.172	11.2	8.15
75	0.94	1.69	0.10	8.6	10, N.E.
75	0.94	1.14	0.08	10.4	19, N.E.

hot metal surfaces may occur due to heating by the fire itself. Re-ignition may then arise from contact of the reactive fuel/air mixture with the hot metal surface. Conditions which lead to re-ignition are controlled by the time temperature history of the reactive mixture and to a lesser extent, by the type of metal surface and the chemical composition of the fuel. Recent experiments in the Wright Patterson Aircraft Engine Simulator show that when a hot (700 °C) metal surface was present, flame extinction required almost an order of magnitude more agent than if the hot surface were not present, presumably due to re-ignition (Bennett and Caggianelli, 1995).

Re-ignition is kinetically and phenomenologically distinct from flame extinction and should be independently considered. Historically, the re-ignition problem was a concern long before the search for halon 1301 alternatives. In this sense, the re-ignition problem can be considered as independent from the flame suppression problem, perhaps requiring a separate solution.

A standard test method for determination of auto-ignition temperatures of liquid chemicals is ASTM-E 659-78 (1978), which utilizes a heated 0.5 L borosilicate glass round-bottom, short-necked test flask. The auto-ignition temperature of a fluid is defined as the temperature at which its vapors will ignite in air at atmospheric pressure without an external ignition source. In the auto-ignition test, the ignition delay time varies for each experiment. The fuel/air ratio can also play a role. Because of the long ignition delay times, decomposition of the original fuel molecule into a variety of intermediates may occur. The ASTM-E 659-78 test vessel is not appropriate for use with halogenated compounds, because the decomposition products are known to react with borosilicate glass.

For aircraft applications, the minimum hot surface ignition temperature of a reactive mixture flowing over a hot metal surface may be a more appropriate test. This is because actual nacelle conditions are very different than in the ASTM-E 659-78 test. Surface material, system pressure, air temperature, surface size, air flow, and even the geometry and location of a baffle can all be factors (Johnson *et al.*, 1988; Laurendeau, 1982).

A large number of studies have investigated the ignition of fuel vapor on hot metal surfaces (Smyth and Bryner, 1990; Clodfelter, 1990; Johnson *et al.*, 1988; Kuchta, 1975; Altman *et al.*, 1983; Klueg and Demaree, 1969; Sommers, 1970; Strasser *et al.*, 1971; Cutler, 1974; Detz, 1976; Goodall

and Engle, 1966; Kumagai and Kimura, 1956; Snee and Griffiths, 1989). The purpose of many of these studies was to determine the lowest temperature at which ignition occurs. Residence time was found to be a key factor in the measured ignition temperature. Such measurements also serve as a basis for comparison of the hazard of different fuels. For example, the surface temperature at ignition of alkanes generally decreases with chain length (Smyth and Bryner, 1990). Some testing has focussed on jet fuels and hydraulic fluids used specifically in aircraft applications (Kuchta, 1975; Johnson *et al.*, 1988; Clodfelter, 1990).

Minimum hot metal surface ignition temperatures for JP-8 (or kerosene) for ambient temperatures and pressures and low air flows have been found to vary from 360 °C to 650 °C, depending on test conditions (Parts, 1980; Beardsley, 1967). The minimum hot metal surface ignition temperature was found to increase with increasing ventilation velocity, and decrease with increased ventilation temperatures (Johnson *et al.*, 1988; Strasser *et al.*, 1971). The hot metal surface results can be compared to the measured JP-8 and kerosene auto-ignition temperatures of 224 ° and 229 °C, with associated time delays of 174 and 210 s, respectively (Johnson *et al.*, 1988, Zabetakis *et al.*, 1954).

Few experiments, however, have been conducted to study the effectiveness of halogenated agents in suppressing ignition. Finnerty (1975) studied the effect of halon 1301 on the auto-ignition of propane in a static sub-atmospheric system. Lemon *et al.*, (1980) tested halogenated solid/liquid/binder mixtures which adhere to hot metal surfaces in an attempt to prevent re-ignition. Mulholland *et al.*, (1992) conducted inhibition experiments using chlorinated compounds in well stirred reactors and compared these results to detailed kinetic models. Both ignition and extinction conditions were modeled. Others have modeled ignition using detailed kinetics. Griffiths *et al.*, (1990) compared calculated and measured auto-ignition temperatures for alkanes in a closed vessel. Kumar (1989) and Vlachos *et al.* (1994) modeled stagnation point flow, coupled with detailed kinetics to predict the minimum surface temperature at ignition for H₂/O₂/diluent and CH₄/air mixtures respectively, in the vicinity of a hot surface. Sano and Yamashita (1994) developed a 2-D laminar flow model to investigate the ignition of methane-air mixtures flowing over a hot surface. Their results show that ignition over a hot plate is controlled by the diffusion of heat and mass as well as chemical reactions. They found that the equivalence ratio and the free stream velocity of reactants had little effect on the ignition delay. The ignition delay time decreased exponentially with increases in the area of the hot surface. Sano and Yamashita's investigation was limited to C1 chemistry due to the computationally intensive nature of their model. Others have considered the detailed kinetics associated with inhibition by halogenated compounds on the ignition of fuel/air mixtures in well stirred and plug flow reactors (Barat *et al.*, 1990; Mulholland *et al.*, 1992; Babushok *et al.*, 1995b; 1995c).

The objective of the studies described here was to test the relative effectiveness of halogenated agents in suppressing the ignition of flammable reactants flowing over a hot metal surface under well-controlled conditions.

9.3.4.1 Experimental Method and Apparatus. Two experimental devices were used. Experiments were first conducted to determine the amount of agent needed to suppress the ignition of a JP-8 fuel spray. There were difficulties, however, in obtaining repeatable results. Thus, a gaseous flow of propane replaced the liquid spray. Use of a gaseous fuel represents a most dangerous case, *i.e.*, when a liquid fuel has completely vaporized.

A schematic diagram of the first apparatus is shown in Figure 35. Propane (99 % purity) flowed through a 3 mm (outer diameter) tube in a stagnation point flow towards a heated metal disk located approximately 5 mm away. The disk was 14 mm in diameter, made of a wound ribbon composed primarily of nickel. The metal surface was heated by a regulated power supply which provided up to 200 W. An optical pyrometer was used to measure the surface temperature of the heated disk. With

power applied to the metal disk, a fairly uniform temperature (± 30 °C) was measured in an annular section of the disk, from approximately 2 mm to 6 mm from the disk center. With use, the metal surface oxidized, and the temperature became less uniform requiring replacement of the metal disk. A coflowing mixture of air and gaseous agent flowed through a 86 mm (inner diameter) pyrex tube about the fuel flow. With the fuel and oxidizer flowing, flame ignition occurred in a repeatable fashion by increasing the power through the metal disk. Various amounts of agent were added to the air flow and the temperature of the heated metal disk was measured at flame ignition using an optical pyrometer. The effectiveness of N_2 , HFC-125, HFC-227 and CF_3I were compared in suppressing ignition.

The second test apparatus was based on a device described previously (Smyth and Bryner, 1990). The main difference between this experiment and the first was that the fuel and air were premixed in this apparatus, but were not in the first apparatus. A reactant mixture containing agent, fuel, and air flowed over a heated foil. The temperature of the foil was slowly increased until ignition was observed. Figure 36 is a schematic diagram of this apparatus which included two dc power supplies, a foil holder, rolled thin (13 μm) foil strips, sub-miniature ungrounded type-K thermocouples with a 250 μm stainless steel sheath, fuel gas cylinders (methane, ethene, and propane with purities of 99.97 %, 99.5 %, and 99.0 % respectively), rotameters for fuel, air and agent flow control, the burner assembly and quartz chimney (1.1 cm diameter), and a data acquisition system. The thermocouple was used to measure the temperature of the foil which was held in a unique, spring loaded support (Smyth and Bryner, 1990). Testing with different types of metal foils was attempted and a number of different fuels were tested including methane, ethene, and propane. The distance from the chimney exit to the hot metal surface was maintained at 6 mm for all tests. The flow of reactants was 912 ml/min (16 cm/s), except in one series of experiments using stoichiometric ethene/air mixtures, when the flow was varied to determine its effect on the measured ignition temperature. The angle of the flow impinging on the hot metal surface was maintained at 45°, except in one series of experiments using stoichiometric ethene/air mixtures, when the angle was varied to determine its effect on the measured ignition temperature. In the standard configuration, the reactant mixture flowed near the heated metal surface for approximately 90 ms (Smyth and Bryner, 1990). Reproducibility of the measurements (± 10 °C on average) was similar to that reported by Smyth and Bryner (1990).

9.3.4.2 Experimental Results and Discussion. For small propane fuel flows (<10 ml/min) in the first apparatus, the critical temperature of the hot metal disk at ignition was measured to occur at approximately 1025 °C (± 25), not unlike auto-ignition temperatures reported previously for stoichiometric propane-air mixtures over a heated nickel surface (Smyth and Bryner, 1990). The flame could then be extinguished by decreasing the applied power through the metal disk. Figure 37 shows that the critical ignition temperature increased with increasing fuel flow. This is interpreted as being related to the residence time of the reactive mixture on the hot metal surface. As the residence time decreased, key chemical reactions involving chain initiation and branching have less time to proceed and higher temperatures were necessary to initiate flame ignition. This is consistent with the Damköhler number criteria for flame ignition (Liñan, 1974). Measurements showed that increased or decreased (by 50 %) air flow had a negligible effect on the critical ignition temperature for the reactants flowing over the hot metal surface.

Figure 38 shows the critical ignition temperature of the heated metal disk as a function of agent concentration in the oxidizer stream for a propane flow of 8 ml/min. For small CF_3I concentrations, flame ignition required substantially higher surface temperatures than for the other agents. Thus, CF_3I was significantly more effective than HFC-125 and HFC-227, which were more effective than N_2 , in suppressing ignition.

A second series of experiments were undertaken where agent effectiveness was measured under premixed conditions in the same device used by Smyth and Bryner (1990). A complete description of

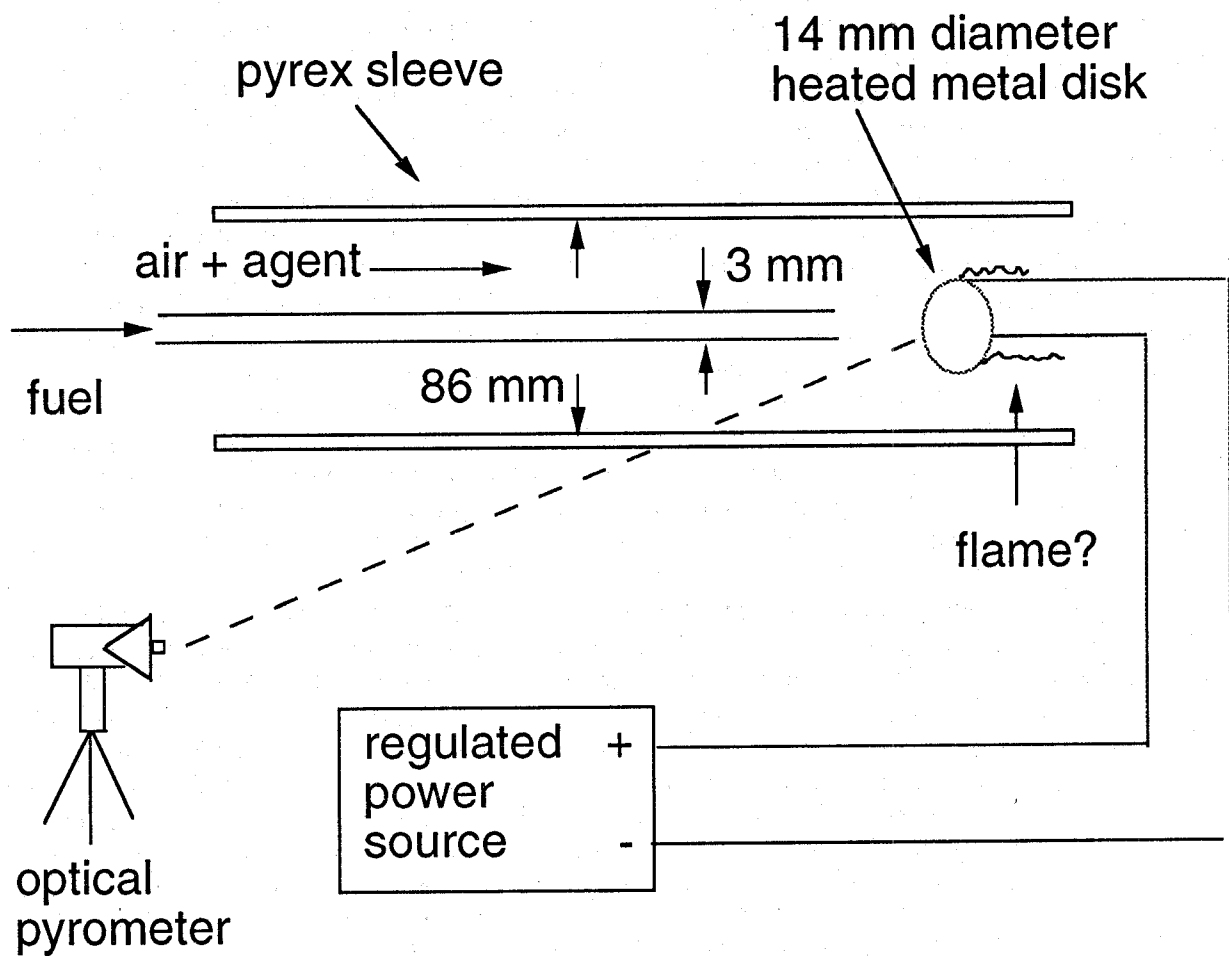


Figure 35. Schematic diagram of the first short residence time hot surface ignition apparatus.

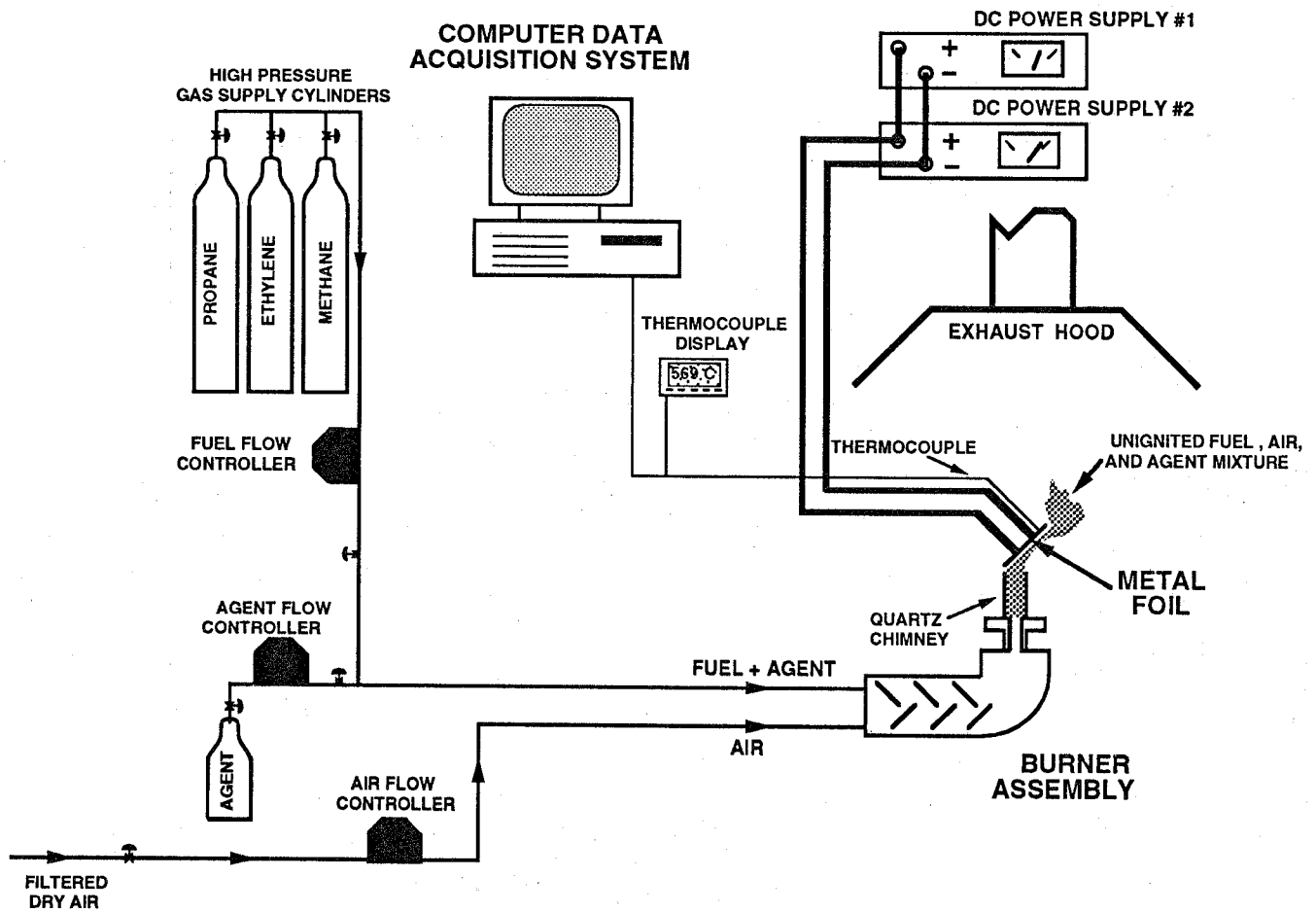


Figure 36. Schematic diagram of the second short residence time hot surface ignition apparatus.

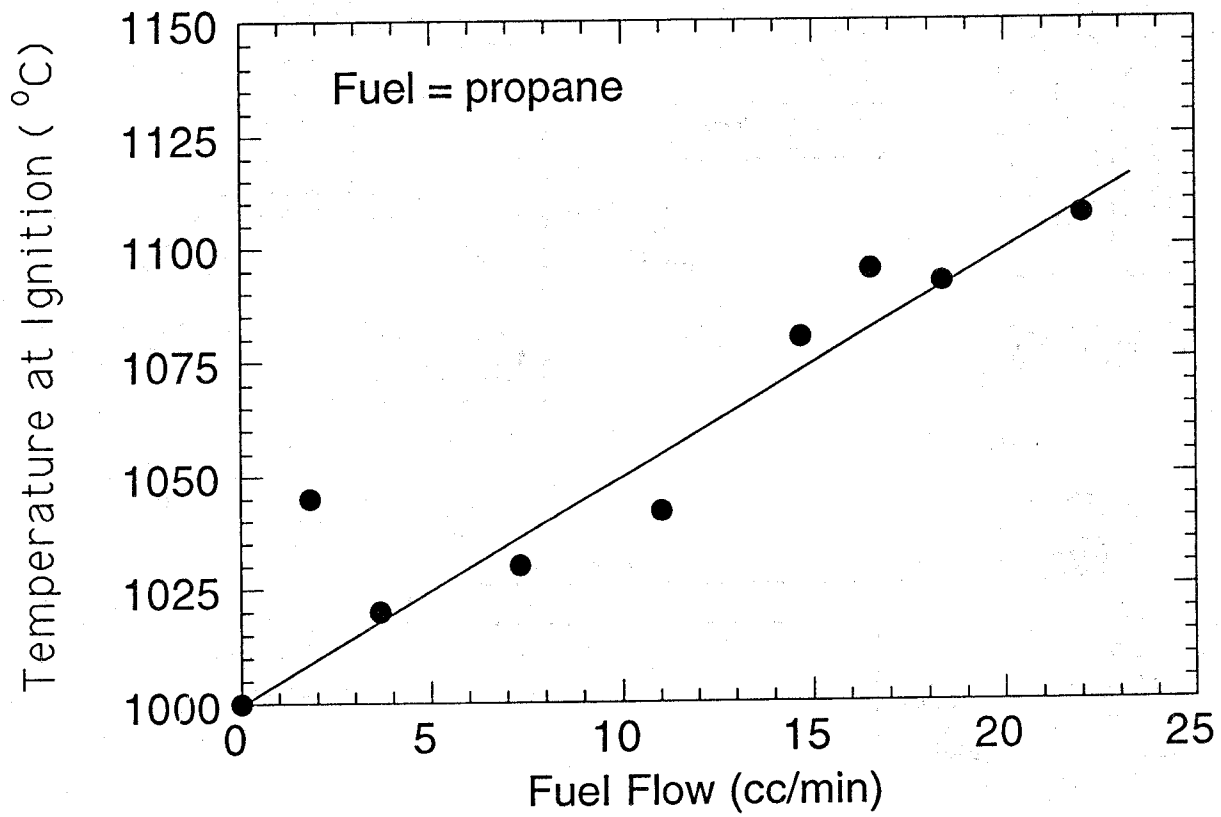


Figure 37. The critical ignition temperature as a function of increasing fuel flow.

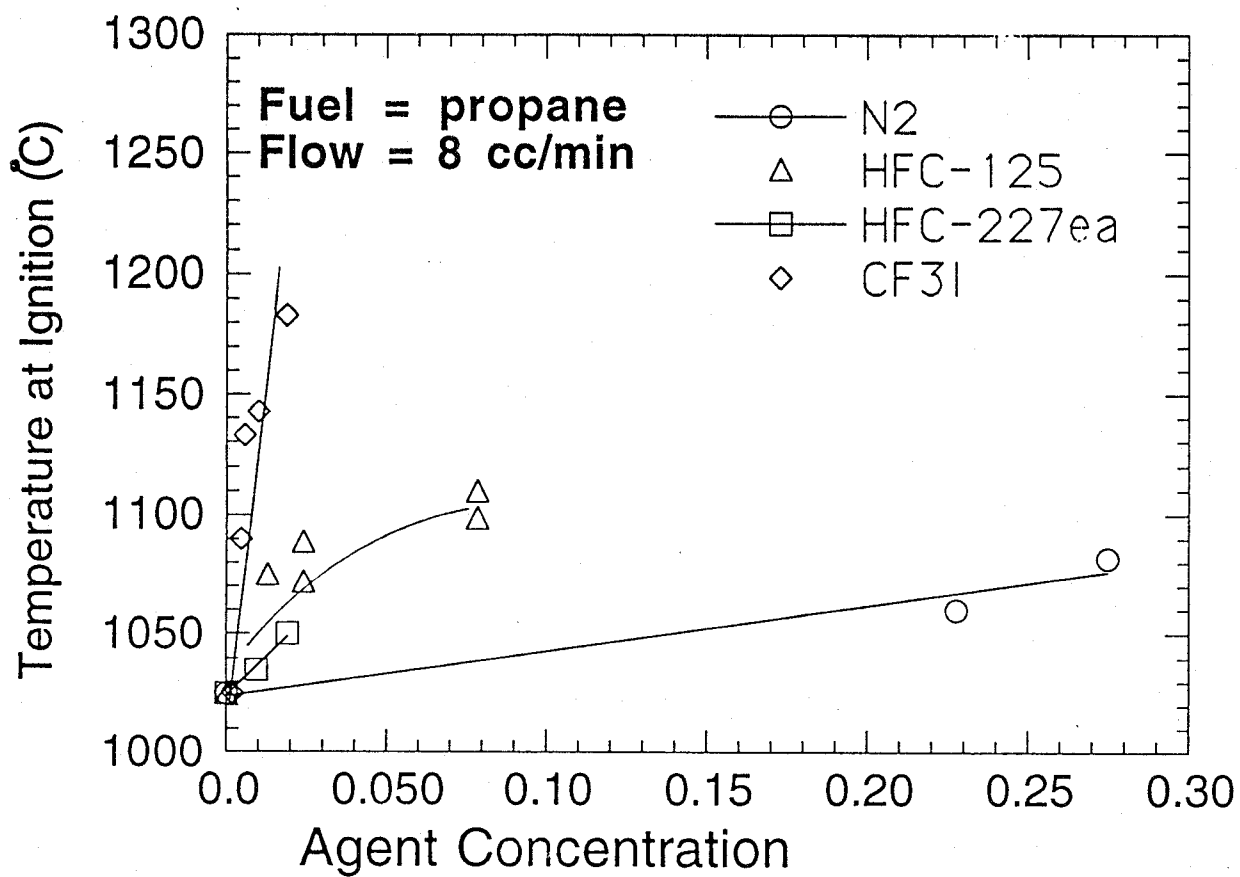


Figure 38. The critical ignition temperature as a function of agent concentration in the oxidizer stream.

the experimental apparatus and procedures is given by Smyth and Bryner (1990). In these experiments, a premixed blend of fuel, air, and agent flowed over a heated nickel surface. Both titanium and stainless steel failed in the presence of even small agent concentrations for temperatures below the ignition temperature, precluding any testing with these metals. The effectiveness of N_2 , HFC-125, HFC-227, CF_3Br , CF_3I were compared in suppressing ignition for stoichiometric mixtures of methane/air, ethene/air, and propane/air.

The angle of the flow impinging on the hot metal surface was varied from 25° to 90° in stoichiometric ethene/air mixtures to determine its effect on the measured ignition temperature. The reactant velocity exiting the chimney was 16 cm/s. The results showed essentially no change in the measured ignition temperature with the reactant approach angle relative to the metal surface until the reactant stream was flowing at an angle equal to 90° , stagnation point flow. Under those conditions, the ignition temperature was measured as nearly $80^\circ C$ less than for the other cases. This result is consistent with the notion that increased residence time leads to a decreased ignition temperature.

Previous results (Smyth and Bryner, 1990) have shown that small changes in the flow rate of reactants over the hot metal surface had little influence on the ignition temperature. Measurements in a stoichiometric ethene/air mixture confirmed the results of Smyth and Bryner (1990), showing that changes in reactant flow had negligible impact on the measured ignition temperature for velocities from 8 cm/s to 24 cm/s. Decreased ignition temperatures were expected from these measurements, because decreased velocities imply increased residence time for the reactants near the heated metal surface. Also contrary to expectations, the measured ignition temperature increased somewhat ($\approx 30^\circ C$) for decreased velocities (at 4 cm/s and 5 cm/s). Although unlikely, a possible explanation of these results was that air was entrained into the mixture as the velocity decreased, altering the mixture from stoichiometric to lean, requiring higher temperatures to achieve ignition. All other tests were conducted for the same reactant velocity, equal to 16 cm/s.

Figures 39 and 40 show the nickel surface temperature required to obtain ignition in stoichiometric methane/air and ethene/air mixtures, respectively, as a function of agent concentration in the mixture. The results demonstrate a close correspondence between the measured temperature increase required to obtain ignition in this apparatus and those measured in the first set of experiments described above. The measured ignition temperatures in the absence of agent were approximately $970^\circ C$ and $760^\circ C$ for the methane/air and ethene/air mixtures respectively, which is consistent with the results of Smyth and Bryner (1990) and Laurendeau (1982). In general, the presence of agent impacted the measured ignition temperature. Figures 39 and 40 show that CF_3Br and CF_3I are consistently effective suppressants of ignition. Of key interest, the results show that HFC-125 slightly promotes ignition in stoichiometric CH_4 /air mixtures. Experiments in C_3H_8 /air mixtures also show a promotion effect. In the C_2H_4 mixture, however, the presence of HFC-125 has very little impact on ignition. HFC-227 was also measured to promote ignition in the CH_4 /air mixtures. The methane results were generally consistent with those for ethene. CF_3I and CF_3Br are highly effective ignition suppressants, whereas HFC-227 and HFC-125 were very poor ignition suppressants and were found to slightly promote methane/air ignition in some instances.

The residence time in these experiments was estimated as 90 ms. This is smaller than residence times that may occur in the nacelle when a fuel puddle sits on top of a hot metal surface and boils. In that case, the residence time may be on the order of seconds. Results in the auto-ignition experiments have shown that as the residence time increases, the ignition temperature will decrease (Zabetakis *et al.*, 1954). Auto-ignition temperatures have been reported with associated ignition delay times that are hundreds of seconds in duration (Zabetakis *et al.*, 1954). Thus, the experiments described here are useful for comparing the relative suppression effectiveness of different agents, but are not useful in a determination of worst case conditions.

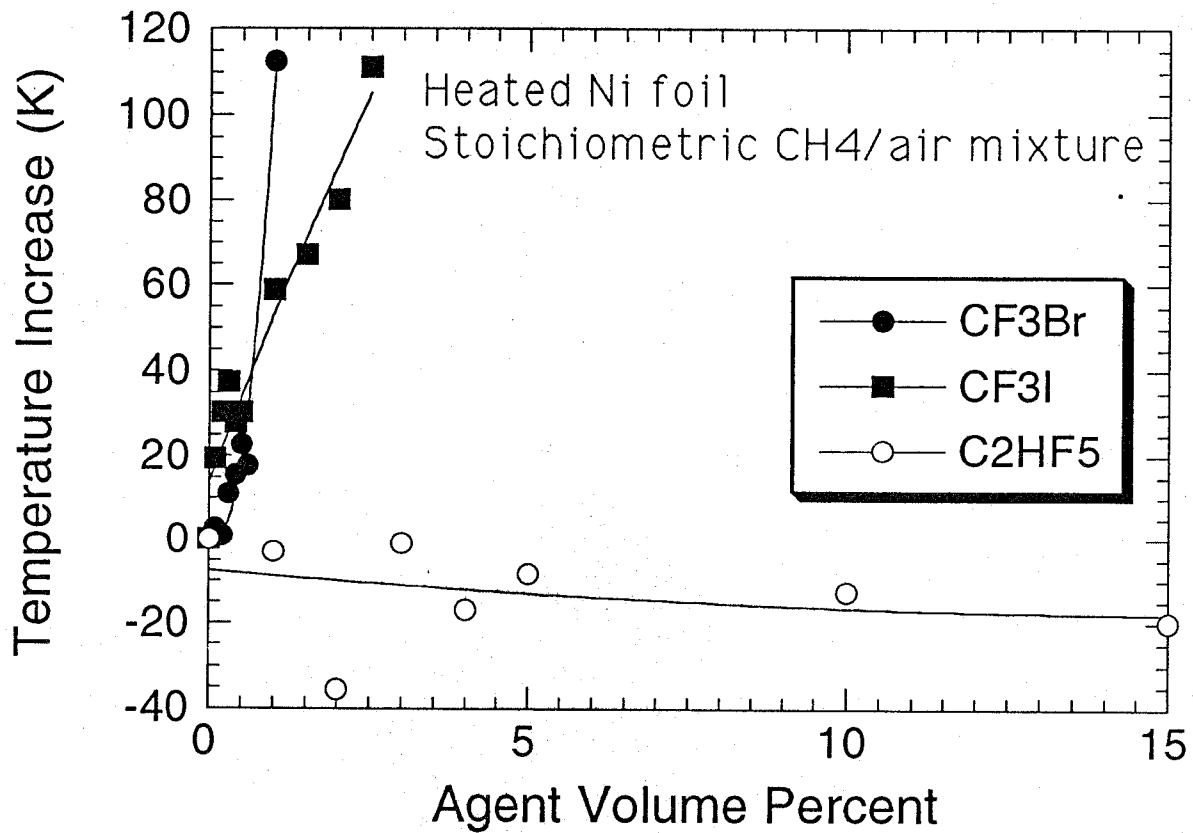


Figure 39. Change in the critical ignition temperature as a function of agent volume percent in mixtures of agent in stoichiometric methane/air.

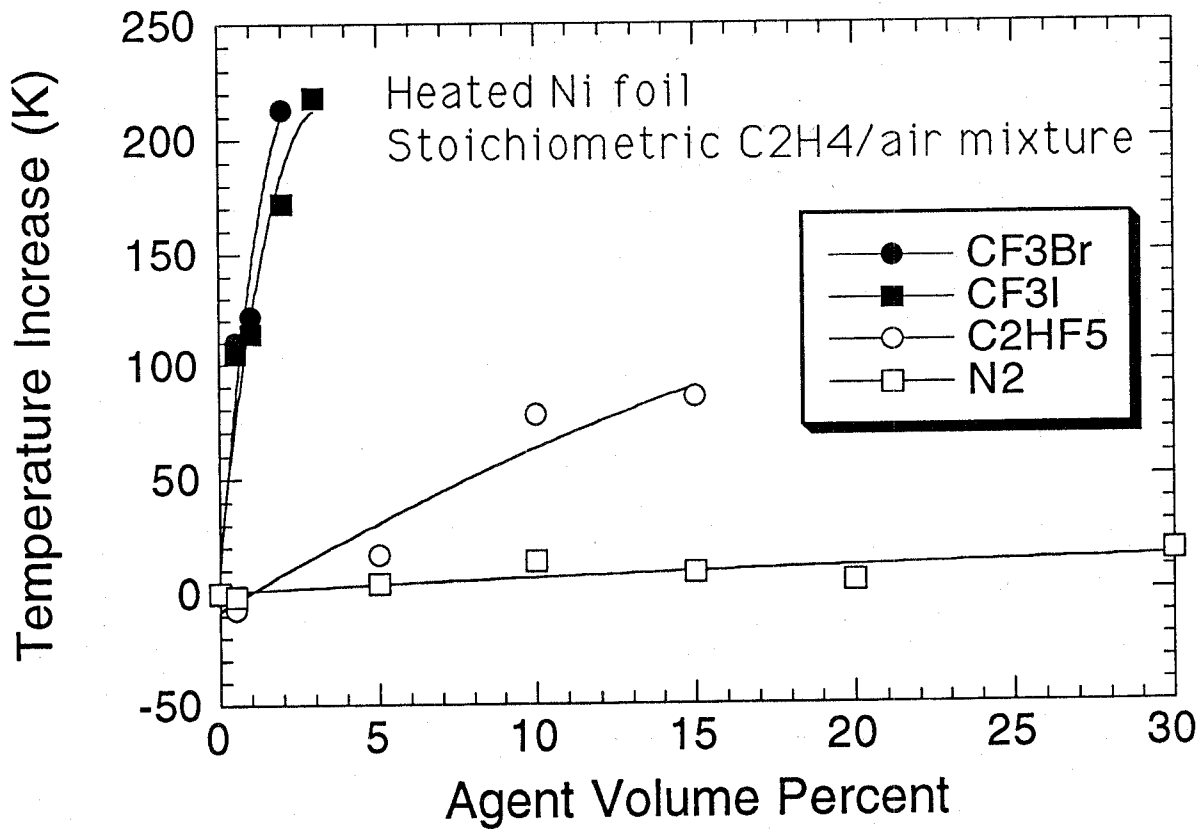


Figure 40. Change in the critical ignition temperature as a function of agent volume percent in mixtures of agent in stoichiometric ethene/air.

Selection of an agent for nacelle applications should carefully consider possible hazards associated with reactant re-ignition. The results determined here indicate that the re-ignition problem in the engine nacelle may be more severe with use of HFC-125 as compared to CF_3Br . At best, HFC-125 has little impact on the suppression of ignition. A possible approach to the re-ignition problem, is to consider using the peak flammability limit as a target concentration for the agent in the fire zone. This insures both flame suppression and the prevention of re-ignition for a period of time on the order of the agent injection duration. After this period, however, it is likely that re-ignition may still be possible and therefore other prevention strategies should be considered.

In future efforts, detailed models of ignition suppression with halogenated compounds would be helpful in predicting ignition phenomena in engine nacelles. Such models will require consideration of detailed inhibition chemistry.

9.3.5 Flammability Limits

9.3.5.1 Background. A large number of experimental arrangements have been used to measure flammability limits. Typical flammability curves take on a "D" like shape when the fuel concentration is plotted as a function of the critical or limiting agent concentration. The fat part of the "D", also called the flammability peak, can be considered the most hazardous condition, because these conditions require the highest agent concentration to inert the mixture. A standard test apparatus is a vessel filled with gaseous reactants equipped with an ignition device as described in ASTM-E 681-94 (1994). Flammability limits have also been determined using one dimensional premixed laminar flames (Lewis and von Elbe, 1961; Strehlow, 1984) and have been related to the extinction of symmetric counterflow twin premixed flames extrapolated to zero stretch rates (Yamaoka and Tsuji, 1978).

Flammability limits for hydrocarbon/air mixtures have been extensively studied (Coward and Jones, 1939). Although flammability limits have been measured for many halogen containing molecules in heptane/air mixtures, no data is available for C_2HF_5 (Malcolm, 1950; Landesman and Basinski, 1964). Fuel type and initial temperature have been shown to impact the halocarbon concentration required to inert a reactant mixture (Malcolm, 1950; Landesman and Basinski, 1964). Thus, care must be taken in interpreting flammability limit data as the peak flammability limits vary with initial temperature, pressure, and reactant type.

The goal of this work was to determine the inerting concentration of HFC-125 for peak flammability conditions in propane/air mixtures.

9.3.5.2 Experimental Method and Apparatus. A detailed description of the experimental apparatus is given by Womeldorf *et al.*, (1995). Two streams of premixed reactants (agent/propane/air) flowed towards each other in a stagnation point flow such that two premixed flames were established between the ducts of an axisymmetric counterflow burner. A nitrogen flow around the reactants was used to reduce ambient disturbances. Flame extinction was determined for several values of reactant flows. The I.D. of the ducts was 25 mm. Stainless steel (40 mesh/cm) screens were used to insure a flat velocity profile of reactants exiting the ducts. The flow of reactants was controlled with rotameters that were calibrated with a bubble flowmeter or a dry test meter. The reactants used were breathing quality air and C.P. grade (99 %) propane. Propane was selected as the fuel because the chemistry associated with its breakdown is not unlike other large alkanes and the experiment required use of gaseous reactants. The agent tested was HFC-125. CF_3Br was also tested to validate the methodology with previous work. The entire apparatus was placed in a negatively pressurized enclosure which was vented to prevent combustion byproducts from entering the laboratory. The distance between the top and bottom ducts was maintained at 16 mm. The composi-

tion and flow of reactants from the top and bottom ducts were kept equal, yielding symmetric twin flames.

The fundamental flammability limit was defined as the critical agent concentration, for a particular fuel/air mixture, at a global flow field strain rate equal to zero analogous to Yamaoka and Tsuji (1978). The global strain rate was defined as the gradient of the mean velocity of reactants exiting the ducts. Because it is not possible to produce a zero strain rate flame, measurements were made at very low strain rates and the results were then extrapolated to zero.

9.3.5.3 Experimental Results and Discussion. Figure 41 shows the measured flammability limits for CF_3Br and C_2HF_5 where the percentage of propane in the reactant mixture is plotted as a function of the limiting percentage of agent in the mixture. Conditions to the left of each curve, represent flammable conditions. Measurements presented in Figure 41 were for low strain rates (15 to 35 s^{-1}). The results appear to be approximately independent of strain rate. Figure 42 shows the limiting C_2HF_5 percentage as a function of strain rate. A linear fit yields a near zero slope line. The low strain rate results shown in Figure 41 can be interpreted as flammability limits with the peak at $12 (\pm 3)$ volume percent for C_2HF_5 .

Previous results for the peak flammability limits for CF_3Br in heptane/air mixtures were reported as 6.1 % (Malcolm, 1950). Although, these measurements were conducted with propane, previous results with N_2 /air/fuel mixtures have shown that the peak inerting concentrations are highly similar (within 5 %) for many alkanes, with only a small shift occurring in the value of the fuel percentage at the peak agent inerting concentration (Macek, 1979). Our results for the peak flammability limits of CF_3Br (shown in Figure 41) in propane/air mixtures are consistent with the results reported previously for heptane/air/ CF_3Br mixtures (Malcolm, 1950).

9.3.6 Discussion and Summary of Combustion Experiments. The key to suppression of a baffle stabilized flame is the characteristic mixing time and the required critical agent concentration. The mixing times are dependent on the interaction of the baffle geometry and the upstream flow conditions, primarily the air velocity. Differences in the flow field associated with the spray flame and the pool fire reported here are likely to have a large impact on the relative ease of fire suppression in these two configurations. Although both flames were baffle stabilized, the flow fields were very different. The baffle in the pool fire was adjacent to a wall, whereas in the spray burner, the baffle was located in the middle of the flow field. In addition, the combustion scenario was distinct in the two configurations.

9.3.6.1 Suppression of Baffle Stabilized Flames. The spray flame represents a two-phase combustion situation where a portion of the fuel droplets were entrained into the recirculation zone, vaporized, and reacted with the oxidizer. In the pool fire, the top of the baffle acts as a flame holder. The appearance of the fire depends on the baffle height and the air flow. For low air flows and small baffle heights, the flame appeared to be laminar. For moderate air flows and baffle heights, the pool fire looked like a ball of flame stabilized behind the baffle. Heat from the flame feeds back to vaporize the liquid fuel. If the baffle was too high the flame was less stable due probably to diminished heat feedback. If the baffle was too low, the flame was less stable, due probably to the relatively large flow field strain rate associated with a small recirculation zone. This idea is consistent with the measurements reported by Hirst and Sutton (1964) who measured peak flame stability for intermediate sized baffle heights. In the spray burner, flame stability also peaked at an intermediate baffle length and it was not possible to stabilize flames for very small or very large baffles as discussed in Section 9.3.2.3.2.

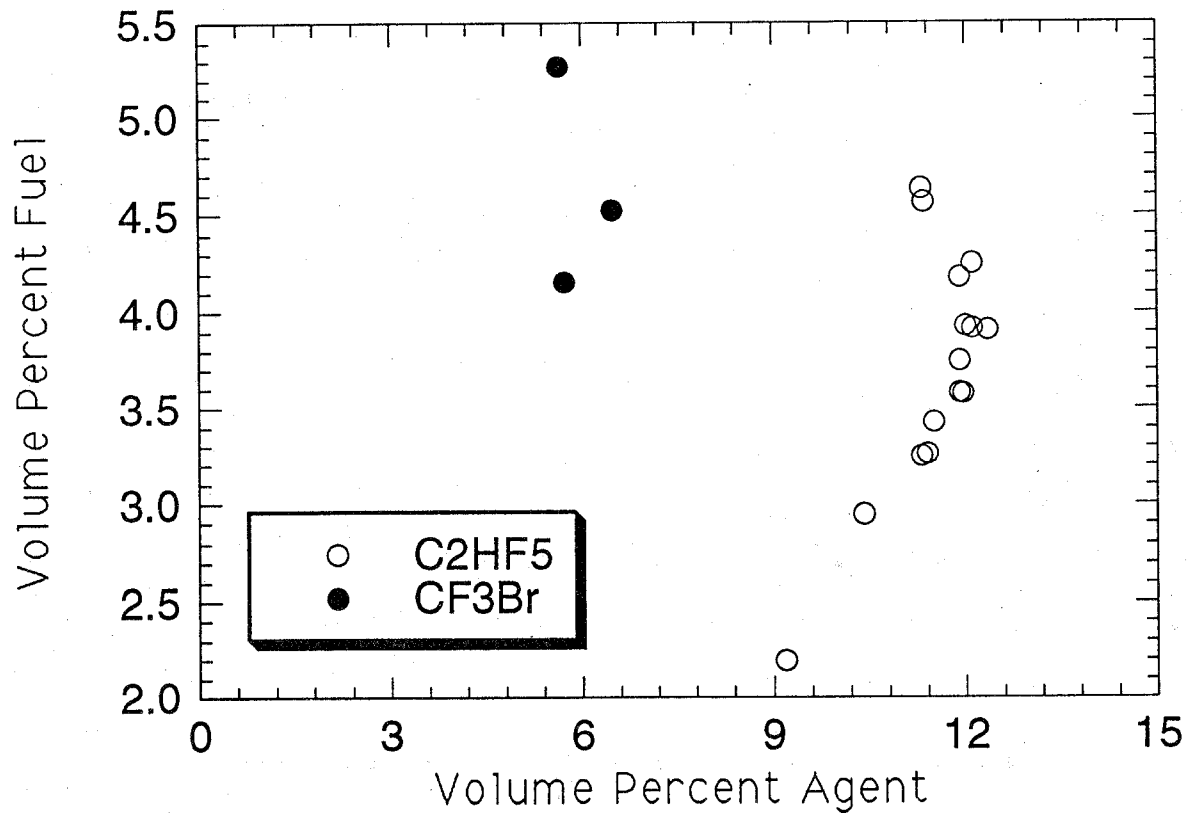


Figure 41. The flammability limits for CF_3Br and C_2HF_5 plotted as the percentage of propane in reactive mixtures of agent/propane/air as a function of the limiting percentage of agent in the mixture.

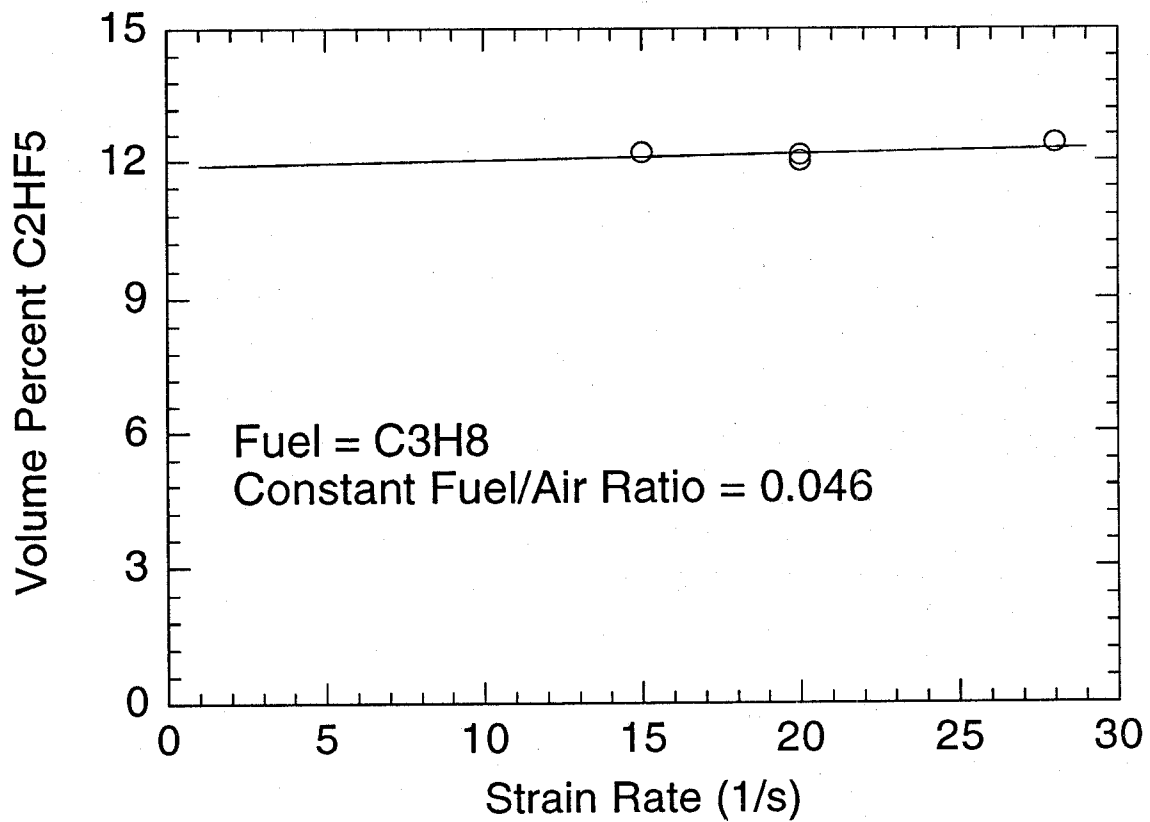


Figure 42. The concentration of C_2HF_5 at extinction as a function of the global flow field strain rate.

Combustion in a recirculation zone is modeled here as a well-stirred reactor (see Section 9.3.2.3.4). For very low air flows, the pool fire extinction measurements (discussed in Section 9.3.3) yield values that are consistent with the inerting of rich premixed combustion, indicating that the flow field could be effectively modeled as a well-stirred reactor. For low air flows in the spray burner, combustion was not observed to occur in the recirculation zone (see description in Section 9.3.2). The flame was a luminous 45° cone of combusting liquid droplets, with a structure not unlike a diffusion flame. The dynamic structures of the recirculation zones were not characterized in either of the configurations. Little is known about even such basic parameters as the size of the recirculation zone or its global equivalence ratio. In the spray flame, for example, only a portion of the fuel droplets may be entrained into the recirculation zone, depending on the relative momentum of the droplets and the toroidal vortex associated with the recirculation zone. Inherent differences in the structure of the combustion zones in each of the configurations could yield differences in agent suppression effectiveness.

The volume fractions of HFC-125 required to suppress the turbulent spray flames and the stabilized pool fires were measured as 9 % and 12 % (by volume) respectively for similar baffle sizes and air flows. This is in comparison to a value of 9 % measured in the cup burner and a 12 % peak flammability limit measured for HFC-125 and discussed in Section 9.3.5. The same type of fuel (JP-8) was used in the spray, pool, and cup burner experiments. The flammability limit study was conducted with propane, yet, it is possible that use of a different fuel can yield a different peak flammability limit. Previous studies, however, using a number of different alkanes showed that the peak flammability limits were highly similar from fuel to fuel for inert agents (Macek, 1983). In general, the spray flame measurements corresponded closely to the cup burner results (as discussed in Section 9.3.2.3.3) and the pool fire measurements corresponded closely to the measured peak flammability limits. The pool fire results of Dyer *et al.*, (1977a) also support the correspondence between agent suppression concentrations in baffle stabilized pool fires and peak flammability limits. Their results for N₂ and CH₃Br were discussed in Section 9.3.3 and are shown in Figures 28 and 29. A fit of their data using Equation (14) yields values of X_∞ equal to 6 % and 38 % for CH₃Br and N₂, respectively. These results correspond closely to the peak flammability limits for these agents in hydrocarbon fuels (Macek, 1979; Malcolm, 1950). It should also be noted, although perhaps only a coincidence, that the current Military Specification of a 6 % nacelle concentration requirement for halon 1301 corresponds to the peak flammability limit for halon 1301 in a heptane/air mixture (Malcolm, 1950). In terms of the re-ignition problem, using the flammability limits as an agent target concentration insures both flame suppression and the prevention of re-ignition.

The limitations of treating the recirculation zone as a continuously stirred tank reactor (CSTR) were tested by using available numerical combustion models (Glarborg *et al.*, 1986) which examine the key parameters that control flame stability such as temperature, pressure, characteristic mixing (or residence time), and equivalence ratio, in addition to detailed inhibition chemistry. Attempts to model the extinction results using detailed kinetics in a CSTR code for stoichiometric methane/air mixtures plus inhibitor (1 % to 6 % agent by volume) yielded calculated residence times at extinction that were approximately two orders of magnitude smaller than the residence times (τ) measured in the spray burner at extinction (Babushok *et al.*, 1995b). This indicated, as expected, that transport effects in the recirculation zone of the spray burner must be considered in detail.

9.3.6.2 Mixing in a Baffle Stabilized Flow Field. Few studies have examined the rate of entrainment into a recirculation zone behind obstacles (Lefebvre, 1983). Winterfeld (1965) found that the mixing time in baffle stabilized premixed flames was approximately a factor of two larger than mixing times for the non-combusting case. Increased blockage ratio was found to increase the characteristic mixing time in an identical manner for both combusting and non-combusting situations

(Winterfeld, 1965). The difference between combusting and non-combusting flows can be partly attributed to increased viscosity in the combusting case, which leads to decreased Reynolds numbers. Unfortunately, Winterfeld's investigation was for Reynolds numbers larger than those utilized in the spray burner or encountered in a typical nacelle. Bovina (1965) also studied entrainment in baffle stabilized flames, but effects due to blockage were not addressed.

Hirst and Sutton (1961) showed that the stability of pool fires was dependent on the size of a baffle upstream of the pool. Pool flames with baffles several centimeters in length were very difficult to extinguish, representing very hazardous conditions. We have shown that the characteristic mixing time for an agent entraining into a baffle stabilized flame is much larger for a baffle against the wall, as in the pool fire configuration, than for a baffle in the middle of the flow field as studied in our spray burner. This confirms the conclusions made by Hirst and Sutton (1961). It should be noted that no experiments were made with the fuel spray stabilized by a baffle against a wall and it is not clear if such a configuration would be more or less hazardous than a baffle stabilized pool fire. In such a case, the recirculation zone may not be very different than the baffle stabilized pool fire. Certainly such a configuration could occur in a nacelle.

To compare mixing in the two flow situations, detailed numerical simulations of the fluid dynamics associated with entrainment of an agent into the recirculation zone behind an obstacle were undertaken. Isothermal flow calculations were performed in an effort to quantify the rate of agent entrainment as a function of Reynolds number and flow field geometry. The Reynolds number (Re) is defined as:

$$Re = \frac{Vd}{\nu} \quad (20)$$

where V is the average upstream velocity, d is a characteristic length scale, and ν is the kinematic viscosity of the agent/air mixture. The characteristic length scale, d , in the Reynolds number was taken as the baffle height in the pool configuration and the diameter in the spray configuration.

The flow field was calculated based on the two dimensional (2D) Navier-Stokes equations describing transient convection in an enclosure. No turbulence model or other empirical parameters were introduced. The details of the methodology are described in McGrattan *et al.*, (1994).

Injection of agent was simulated by slightly altering the density of the fluid in the form of a long square wave pulse. The average density of fluid in the control volume directly behind the obstacle and one baffle diameter downstream was monitored as a function of time. It was also possible to include variation of thermophysical properties of the air/agent mixture.

The concentration of agent (normalized to the free stream) in a region behind the baffle, located adjacent to the wall and in the middle of the duct was calculated as a function of time using the two-dimensional model for flows characterized by Reynolds numbers from 500 to 4000. The blockage factor B was held constant at 0.8. The agent mixes into the recirculation zone and obtains its free stream concentration in 25 to 40 nondimensional time units. A fit to the data using Equation (13) allowed determination of the characteristic nondimensional mixing time constant ($\tau \cdot V/d$) for each corresponding Reynolds number. Thus, a dimensional characteristic mixing time, τ , in units of seconds, could be calculated for combinations of V and d . The dimensional characteristic mixing time determined from this type of calculation is shown in Figure 43 for obstacles 3.5 cm in diameter, located in the center of the flow field and against a wall as a function of time. The mixing times for the obstacle in the center of the flow field is significantly less than the mixing time for the obstacle against the wall. The mixing times decreased as the velocity increased, although the rate of decrease was larger than expected from Equation (16).

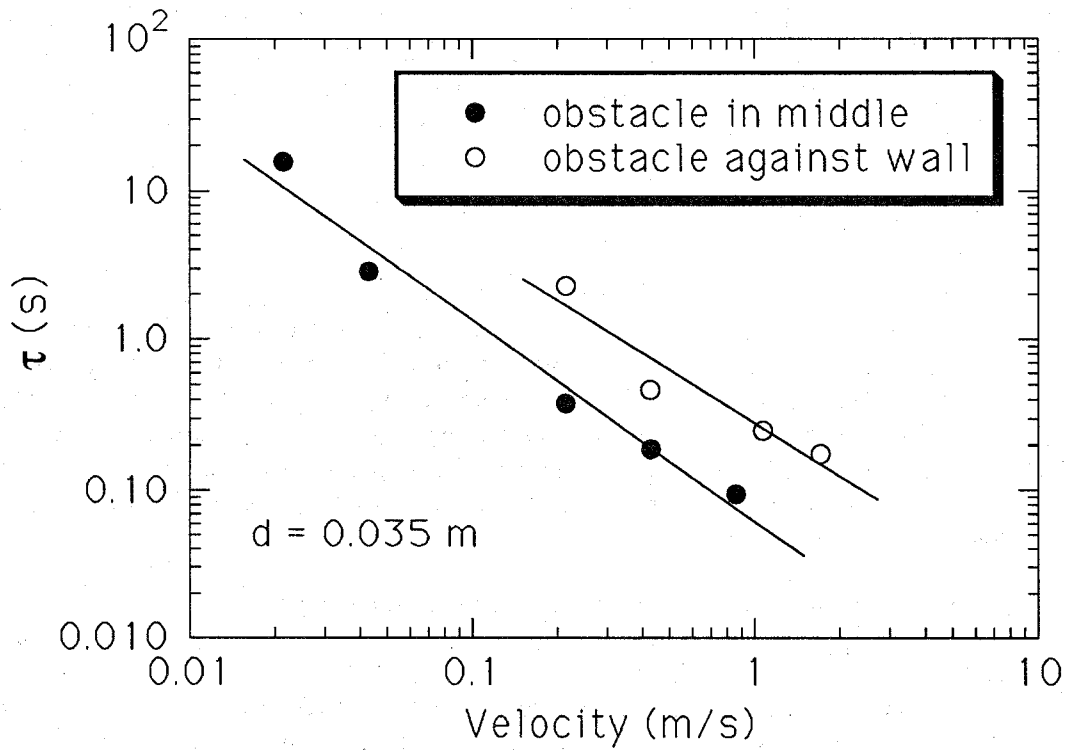


Figure 43. The characteristic mixing time as a function of air velocity for 3.5 cm obstacles against a wall and in the middle of the flow field calculated using the 2D flow model.

These results are consistent with the trends found for the mixing times measured in the spray and pool burners. In those combusting cases, the mixing times in the pool fire (with a baffle against the wall) and in the spray flame burner (obstacle in the middle of the flow field) was measured as approximately 0.7 s and 0.1 s respectively for 3 m/s air velocities and similar baffle diameters. Thus, the difference in mixing times for the two geometries was approximately a factor of 7. It is not surprising that the ratio of mixing times for the simulations and the experiments were not equal. First, the simulations were conducted for an isothermal situation. The detailed structure of the recirculation zones undoubtedly plays a role in the turbulent exchange processes which govern the characteristic mixing time and the structure of the combusting zones are certainly very different from isothermal zones. Second, the detailed geometric configuration used in the pool fire experiments was not as simple as a baffle abutting a wall. The air/agent mixture flowed around the finite sides of the baffle. In addition, a lip was present on the downstream end of the burner to prevent fuel spillage (see Figure 30). Third, the calculations were based on a 2D model. The 3D effects almost certainly play a role. The simulations do, however, confirm the trends in the measurements, which suggest that the baffle stabilized pool configuration is a more dangerous fire scenario in terms of forcing agent into the fire.

Various agents have different thermophysical properties such as viscosity and molecular diffusion coefficients. For example, the molecular diffusion coefficient of HFC-125 is approximately a factor of two less than N_2 under ambient conditions. A calculation was performed to test the effect of molecular diffusion on the characteristic mixing time. This was accomplished by varying the Schmidt number for the agent. The Schmidt number (Sc) is defined as:

$$Sc = \nu/D_m \quad (21)$$

where D_m is the molecular diffusion coefficient. The calculation was conducted for a Reynolds number equal to 500 and with an obstacle in the middle of the flow field. The results showed that changes in the Schmidt number had negligible effect on the characteristic mixing time. These results suggest that agent type will not effect the rate of agent entrainment into a baffle stabilized fire zone for a well dispersed slug of gaseous agent. Other thermophysical properties may play a role however, most notably, the Jakob number which governs the rate of flashing and is indicative of agent dispersion (Grosshandler *et al.*, 1994).

9.3.6.3 System Design Considerations. Safe design of fire protection systems requires an understanding of plausible worst case situations.

- The most dangerous combustion situations, evaluated in terms of Equation (14), are characterized by large values of the parameters τ and X_∞ . For the conditions studied in this report, the most dangerous situations were associated with pool fires rather than spray flames. For the same air velocities and baffle lengths, the values of τ and X_∞ were both larger for the baffle stabilized pool fire than for the spray flame. Furthermore, a comparison between the results shown in Figure 9 and those of Hirst and Sutton (1961), suggest that the blow-off velocity, for baffles with similar diameters, was much higher in the pool fire configuration.
- Besides the fire configuration, other parameters can be considered to add to fire hazard, as discussed above in terms of the spray fire. These include the flow velocity, air temperature, system pressure, fuel flow and other parameters not studied in this report such as fuel volatility, and the droplet diameter distribution of the liquid fuel. In this regard, the results from the

extinction measurements in the spray burner were used to develop simple equations as guidelines for design of suppression systems (see Section 9.3.2.4). However, the spray burner guidelines are applicable to full-scale under certain conditions only. This is because geometric factors, material properties, operating conditions and fire scenario may impact flame stability. For example, the agent concentration at extinction and the blow-off velocity are both affected by the blockage ratio. These are specific not only to each nacelle geometry, but also to each particular fire scenario. The function $f_6(V)$ (see Tables 4-6), related to the free stream air velocity as discussed in Section 9.3.2.4, is another example. As presented in Figure 12, the agent mass fraction at extinction decreased for high air flows. Similar behavior was observed in full-scale testing (Bennett and Caggianelli, 1995; Johnson and Grenich, 1986). Discerning application of $f_6(V)$ would allow a reduced agent weight penalty for high air flows. Yet, for an arbitrary fire in an arbitrary or geometrically uncharacterized nacelle, it is not possible to predict the free stream air velocity at the fire location which is a local parameter. Nor is it possible to predict the total air flow where the required agent mass obtains a maxima, as seen in Figure 10. This is because the nacelle geometry is not a series of simple baffles in a free stream. Fluid flow in a cluttered nacelle environment will cause interaction between the recirculation zones. This may impact the values of the local characteristic mixing times. Furthermore, it is not clear that the blow-out velocity is related only to the baffle length and fuel type. Fire size and fuel puddle dimensions may also be a factor. In addition, only scant data are available for suppression of pool fires at higher air velocities.

- For all of these reasons, agent concentrations in full-scale applications should be at levels such that the maximum agent concentration required for extinction is available for all possible air velocities, unless a full-scale testing program investigating a number of different fire scenarios can prove otherwise.
- Preliminary design guidelines for an alternative agent might consider an agent target concentration in the fire zone equal to the peak agent flammability limit. This would ensure flame extinction and suppression of re-ignition (for a time period on the order of the agent injection duration for typical nacelle conditions). A methodology to achieve such a guideline is suggested in Section 9.5 where agent mixing in the nacelle is viewed as a series of idealized transient processes, amenable to algebraic modeling. The mixing details are not modeled, nor are they known for generic nacelle geometries, but limiting cases are studied which suggest the values of the minimum agent mass delivery rates. The model is based on idealized global mixing models describing agent dispersion and dilution for the bulk temporal concentration, and a local mixing model for flame extinction or concentration build-up at specified locations. The input data for the model were inferred from the results of the small-scale spray and pool experiments described above. It should be noted that the flammability limits are pressure, temperature and probably fuel sensitive as well.

9.4 Flow Field Modeling and Validation in a Mock Nacelle

The agent concentration in the flow field is the key to extinguishing a fire and preventing re-ignition. The character of agent delivery and mixing in the flow field is then a key aspect of a fire suppression system. Because of its low boiling point and other thermophysical properties, use of CF_3Br has ensured rapid evaporation and dispersion of the agent into a target volume. Upon use of one of the candidate replacement agents, it is possible that the evaporation and dispersion characteristics may be diminished. In order to enhance dispersion, the location, number, placement, and orientation, and even

shape of agent injection nozzles may need to be carefully optimized. Computational fluid dynamics (CFD) is a tool that allows three-dimensional modeling of transient problems in non-simple geometries. CFD is a completely accepted methodology in the aircraft industry and is depended upon for aircraft design. The purpose of this subsection is to demonstrate the viability of CFD in treating the problem of agent mixing in an engine nacelle. CFD has apparently been used in the design of the fire protection system for the B2 aircraft (Kinsey, 1994). The B2 has a highly unusual nacelle geometry and standard protection system design was not appropriate. A detailed analysis of agent flow inside of the nacelle under non-combusting conditions was developed. Through use of CFD, a design using multiple agent injection locations was generated to improve agent dispersion (Kinsey, 1994). Unfortunately, no report is available concerning this work.

Since there are many nacelle types, a single representative geometry was considered. The geometric configuration was an idealized reduced-scale version of the Wright Patterson full-scale nacelle test facility. Combusting flow conditions were not considered in the simulations, because the isothermal flow dynamics upstream of the fire source are thought to control agent/air mixing and because agent certification is performed at ambient temperatures. The purpose of this portion of the investigation was to model agent concentration as a function of location, rate, and orientation of agent injection.

Because temperatures as high as 350 °C (650 °F) are not uncommon in engine nacelles and because the candidate agents have relatively low boiling points, evaporation of the liquid-phase agents will be rapid. Under realistic conditions, it is unclear to what extent liquid phase flow phenomena will impact suppression effectiveness through differences in agent dispersion. Because problems associated with modeling an evaporating two-phase flow are much more difficult, only gas-phase phenomena were considered. Information regarding criticality of the number, placement, and orientation of agent injection nozzles as well as the rate of gaseous agent injection were considered.

To insure that the computational results were reliable, a flow tunnel with agent injection was developed and measurements were compared to the computations.

9.4.1 Description of the CFD Model

9.4.1.1 Introduction. Three scenarios were examined. First, agent was injected through a tee so that the initial agent flow was perpendicular to the air flow, and parallel to the plane defined by a cross section of the nacelle. Second, a baffle attached to the inner wall of the nacelle was examined. Third, cases involving agent inlets oriented 15° towards the far end of the nacelle were examined. The geometry of these configurations will be described in detail below. Sensitivity of the agent concentration to various parameters was examined. It was observed that changes to the agent and air inlet velocities caused the most change in downstream agent concentration.

9.4.1.2 Modeling Assumptions. CFDS-FLOW3D (Harwell Laboratories, 1992) was used to perform the numerical simulations described here. This model solves equations for the conservation of mass, momentum and energy. The fully compressible form of these equations was used due to the high velocities at the agent inlet (up to 50 m/s) encountered in these simulations. The conservation of energy equation was neglected since we assume that all flows are isothermal. The standard k-ε model of Launder and Spalding (1974) was used to model turbulence. Various turbulence levels were input at the boundaries without significant changes in the results of the simulations.

The agent, nitrogen, was modeled using the "additional scalar" option of the field model. The field model simulates flow of additional fluids using the species mass conservation equation:

$$\frac{\partial \rho S}{\partial t} + \nabla \cdot (\rho US) - \nabla \cdot \left(\left(\frac{\mu_T}{\sigma_s} + \rho D \right) \nabla S \right) = 0 \quad (22)$$

where ρ is the density of the carrier fluid (air in this case), t is time, U is the fluid velocity, μ_T is the turbulent viscosity, D is a diffusion coefficient, σ_s is the turbulent Prandtl number for the scalar, and S is the mass fraction of the additional scalar. Convection and diffusion control the rate at which the agent moves from one portion of the nacelle to another. It was found that the convection was the dominant mechanism for transporting the agent. Computer simulations were run to steady state and took approximately 7 hours of central processing time on a Silicon Graphics Indigo II workstation.

9.4.1.3 The Computational Grid. The grid used to simulate the cases discussed in this report is illustrated in Figure 44. It consisted of 64,000 grid cells. Simulations with twice the number of grid cells were performed with little change in results. It was therefore felt that 64,000 was a sufficient number of grid cells to resolve the flow. All cases simulated were symmetric about a plane passing through the axis of the nacelle and an agent inlet. Therefore, only one half of the nacelle was simulated with the field model. The control volume sizes ranged from 2 mm on a side near the agent inlet to 4 cm near the far boundary where air/agent mixtures exited the nacelle. Air flowed through the annular region between cylindrical tubes which was modeled as having a 30.4 cm O.D. of the inner tube and a 45.0 cm I.D. of the outer tube. The cross sectional area of the annular region was 0.087 m^2 . Boundary conditions were specified at each inlet, outlet, and walls. The air inlet velocity was taken from the experimental measurements described in Section 9.4.2 below. The velocity was approximately 3 m/s for most cases. The agent inlet velocity was such that the volume flow rate was either 0.012 or $0.025 \text{ m}^3/\text{s}$. The outlet at the far end of the nacelle was modeled as an open or pressure boundary condition. A no-slip boundary condition was used at the walls.

The experimental configuration was used as a basis for the computer simulations. Agent was discharged through a nozzle into the annular test section. Two nozzle types were used. Most experiments used a tee shaped nozzle which injected two round jets perpendicular to the axis of the test section and parallel to a tangent defining the annular region. Some calculations considered a straight round tube (1.5 cm inner diameter) flush to the inner wall of the outer cylinder which defined the test section, with the jet discharging nearly perpendicular to the air flow. A summary of the cases which were studied is presented in Table 9. The agent volume percent varied from 3.4 % to 8.6 % as the agent flow varied from $0.012 \text{ m}^3/\text{s}$ to $0.25 \text{ m}^3/\text{s}$. Geometric details of the air and agent inlets and flow baffles which were attached to the inner nacelle wall are described below.

9.4.2 Experimental Facility. Measurements of the inlet velocity profile dictated the boundary conditions used in the calculations. Figure 45 is a schematic diagram of the flow tunnel which consisted of an air blower, a wood plenum and converging section, and a clear plastic test section. The fan speed was adjustable, providing air velocities in the test section from 1 m/s to 10 m/s. Screens were attached to the end of the converging section to provide a flat velocity profile of air at the test section inlet. The test section consisted of two coaxially arranged plastic tubes, each 2 m long. The inner tube was fitted with an aerodynamic nose section to prevent flow separation.

Two nozzle types were used. Most experiments used a tee shaped nozzle which injected two round jets perpendicular to the axis of the test section and parallel to a tangent defining the annular region. A schematic drawing of the injection tee is shown in Figure 46. The inner diameter of each of the agent flows was 1.56 cm. Some experiments were conducted with a straight round tube (1.5 cm inner diameter) flush to the outer surface of the test section with the jet discharging perpendicular to the crossflow. Mixing was worse in this case, so measurements were focussed on use of the tee.

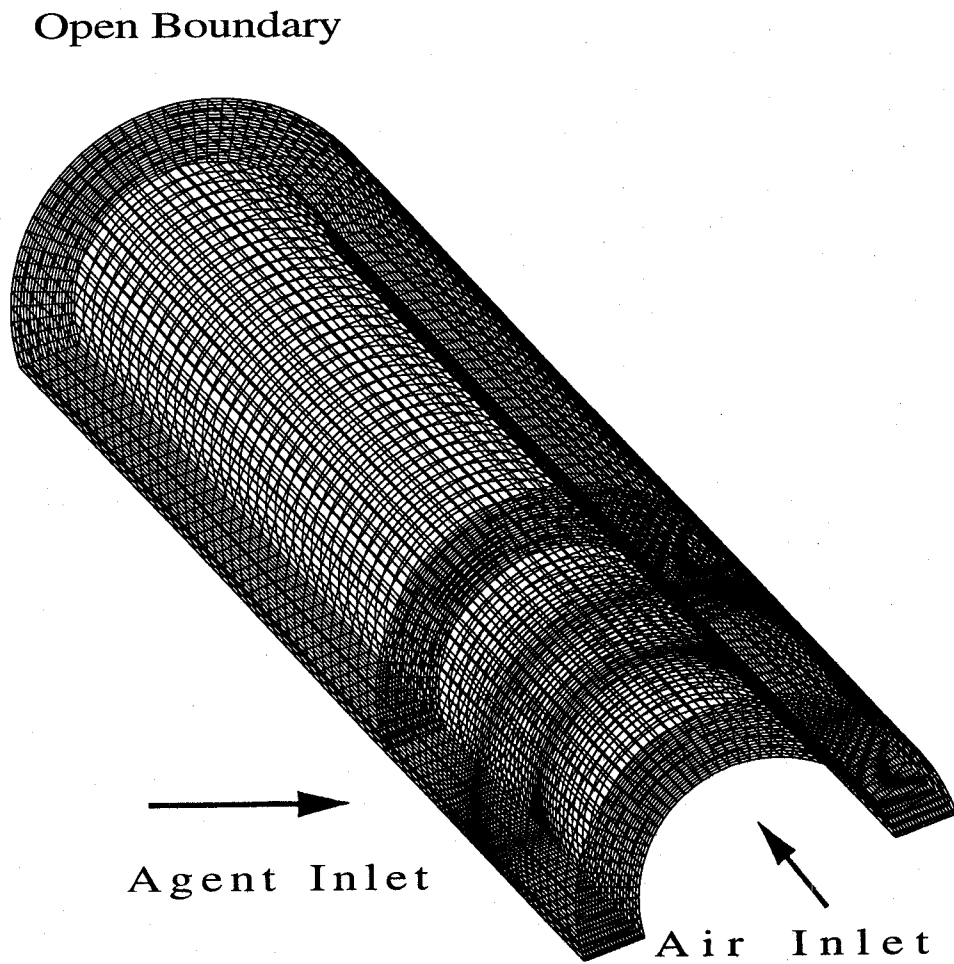


Figure 44. Schematic diagram of the computational grid used in the CFD simulations.

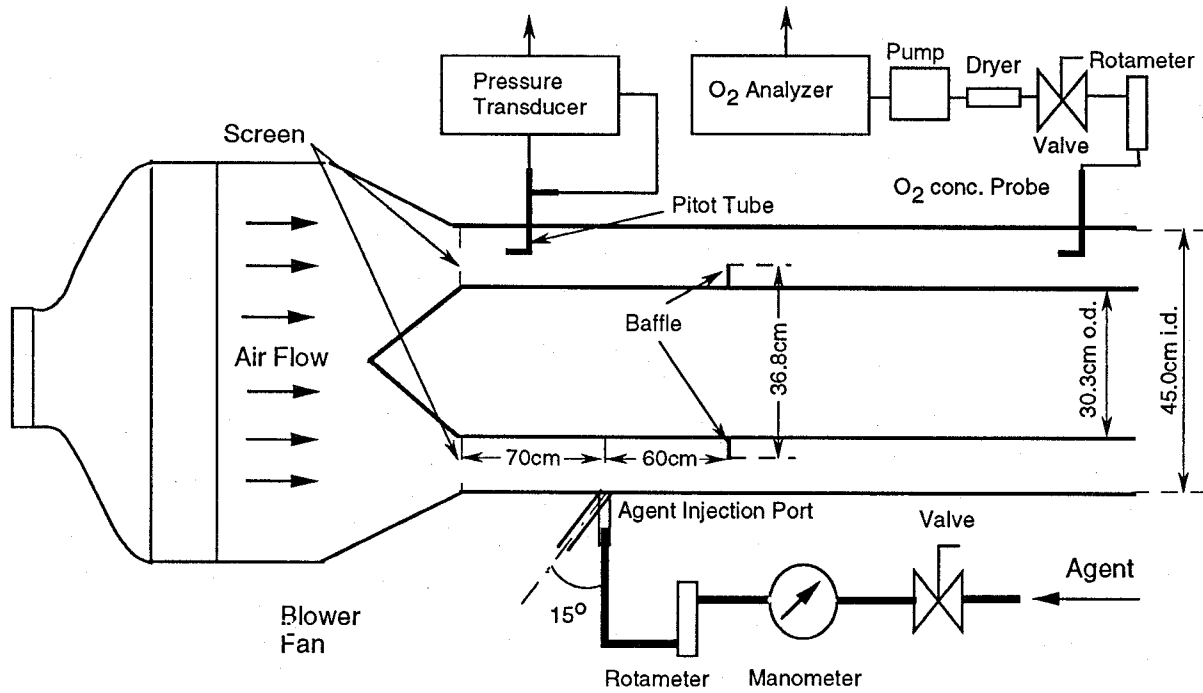


Figure 45. Schematic diagram of the flow tunnel.

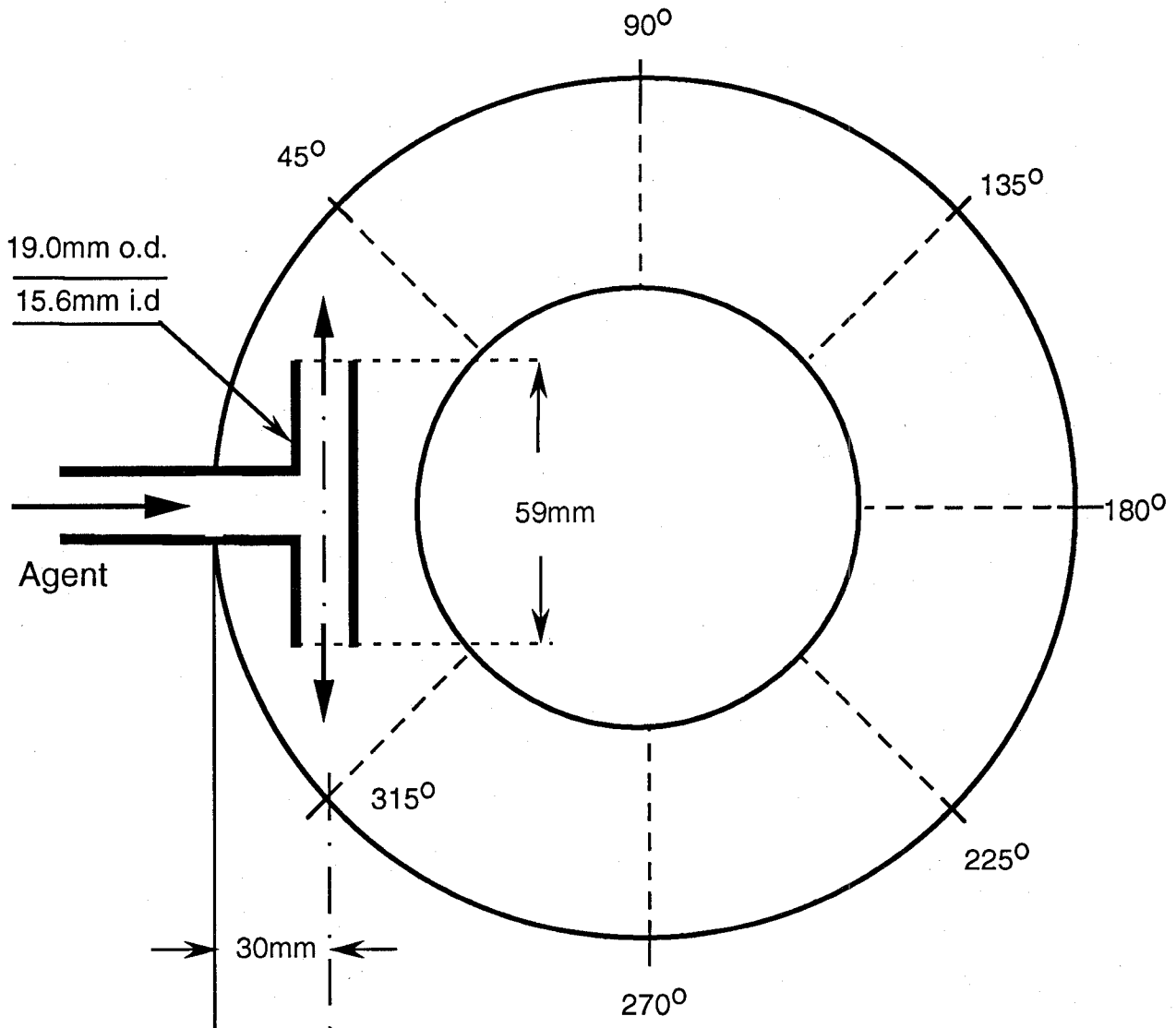


Figure 46. Schematic diagram of the agent injection tee.

Table 9. Description of numerical computations

Case	Injection Locations	Type of Injection	Air Velocity (m/s)	Agent Volume Percent	Agent Flow (m ³ /s)
1	1	tee	3.0	4.5	0.012
2	2	tee	3.0	4.5	0.012
3	4	tee	3.0	4.5	0.012
4	1	tee	3.0	8.6	0.025
5	2	tee	3.0	8.6	0.025
6	4	tee	3.0	8.6	0.025
7	1	tee	3.0	4.5	0.012 baffle on interior wall
8	1	15 degree	3.0	4.5	0.012
9	2	15 degree	3.0	4.5	0.012
10	4	15 degree	3.0	4.5	0.012
11	1	15 degree	3.0	8.6	0.025
12	2	15 degree	3.0	8.6	0.025
13	4	15 degree	3.0	8.6	0.025
14	1	tee	3.3	4.2	0.012
15	1	tee	3.5	3.9	0.012
16	1	tee	4.0	3.4	0.012

Gaseous agent was discharged through a nozzle into the test section at a location 70 cm downstream of the test section inlet. Measurements were made after a steady state flow had been achieved. Gaseous nitrogen was chosen as the agent. N₂ flowed from six cylinders connected in series to the test section through a 2.5 cm pipe. The flow passed through a regulating valve, a manometer, and a rotameter, allowing control and determination of the agent flow. The rotameter readings were corrected for back pressure. Uncertainty in the N₂ flow was estimated as 13 %.

In some experiments, baffles or ribs were placed in the flow field in order to mimic the flow field typically encountered in nacelles. Ribs were installed 60 cm downstream from the point of injection. The ribs were attached to either the inner or outer walls of the annular region with extending from 30.3 cm to 36.7 cm in the radial direction on the inner wall and from 45.0 cm to 39.5 cm on the outer wall.

9.4.2.1 Agent Concentration Determination. The agent concentration was determined by measuring the depletion of oxygen at selected locations within the test section using the following equation:

$$[Agent] = \frac{([O]_o - [O])}{[O]_o} \quad (23)$$

where $[O]_o$ and $[O]$ are the oxygen (volume based) concentrations in the air flow, before and during injection respectively, and $[Agent]$ is the agent volume fraction in the air flow. The local oxygen concentration was measured by a paramagnetic oxygen analyzer in conjunction with gas sampling. The analyzer had a 1 s response time. Gas samples were collected through a stainless-steel cylindrical tube with a 1.4 mm inner and 3.2 mm outer diameter. The probe had a right angle bend 8 cm from the sampling orifice. The probe was inserted into the stream through a hole in the wall of the test section with the orifice facing the flow (see Figure 45). Measurements were made 96 cm and 184 cm downstream from the point of agent injection for many angles and several radial locations. All measurements were time averaged over a period of 10 s. Uncertainty in the agent concentration measurements are estimated as 18 % based on repeat measurements and a propagation of error analysis.

9.4.2.2 Air Flow Measurements. A pitot tube was used to measure the air speed as a function of location in the test section, both upstream and downstream of the agent injection location. Measurements were conducted with a 3 mm diameter stainless steel pitot tube and a differential pressure transducer. All measurements were time averaged for a 10 s period. The pitot tube was mounted facing the incoming flow. Uncertainty in the velocity measurements was estimated as 8 % based on repeat measurements and a propagation of error analysis.

9.4.2.3 Characterization of the Flow Tunnel Without Agent Injection. Figure 47 shows measurements of the inlet air velocity as a function of radial location across the annular region, 65 cm upstream and 90° from the agent injection location. In the absence of agent injection, the air velocity profile is almost flat as a function of radial location. In this case, the average air speed was approximately 3.3 m/s. From measurements taken 35 mm from the inner wall of the test section, Figure 48 shows that the air velocity was uniform as a function of angle around the annulus, except at 0°, where the flow was disturbed by the agent injection tee, causing a 10 % velocity decrement. When the straight tube was used for agent injection, no velocity decrement was observed. The Reynolds number for this flow was equal to $7.5 \cdot 10^4$, where the characteristic spatial dimension (d) was taken as the distance between the inner and outer tubes forming the annular region. Fully developed flow in the tube was expected 2.6 m downstream from the test inlet, which is just beyond the end of the test section (Blevins, 1984).

A hot wire probe was used to characterize the turbulence intensity at the test section inlet. Measurements were obtained at a sampling rate of 2 kHz at several locations across the annular region. The turbulence intensity (TI) was characterized as:

$$TI = \frac{\sqrt{u'^2}}{\langle u \rangle} \quad (24)$$

where u'^2 is the square of the average velocity fluctuations in the axial direction. The average velocity fluctuation is defined as the difference between the time varying (*e.g.*, u) and the time-averaged ($\langle u \rangle$) velocity:

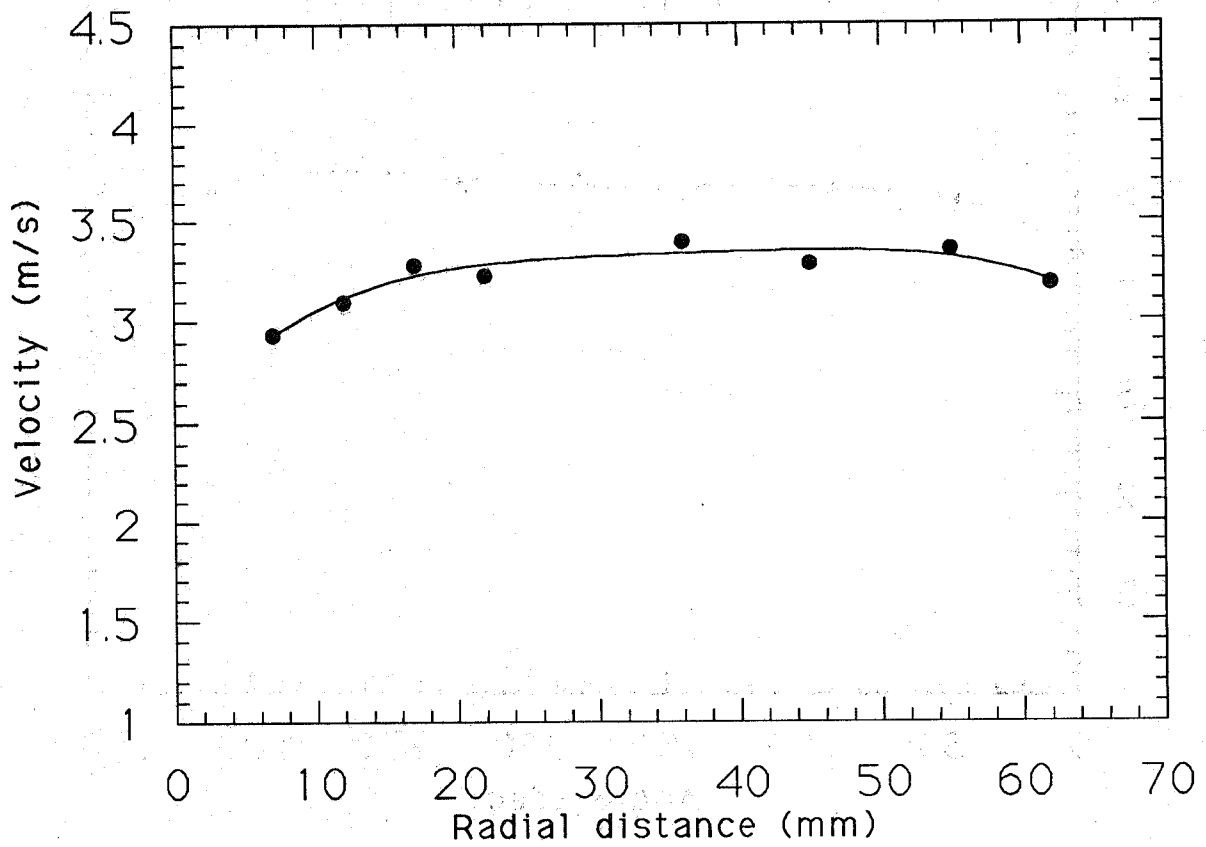


Figure 47. The velocity as a function of radial location, at locations 65 cm upstream and 90° from the agent injection.

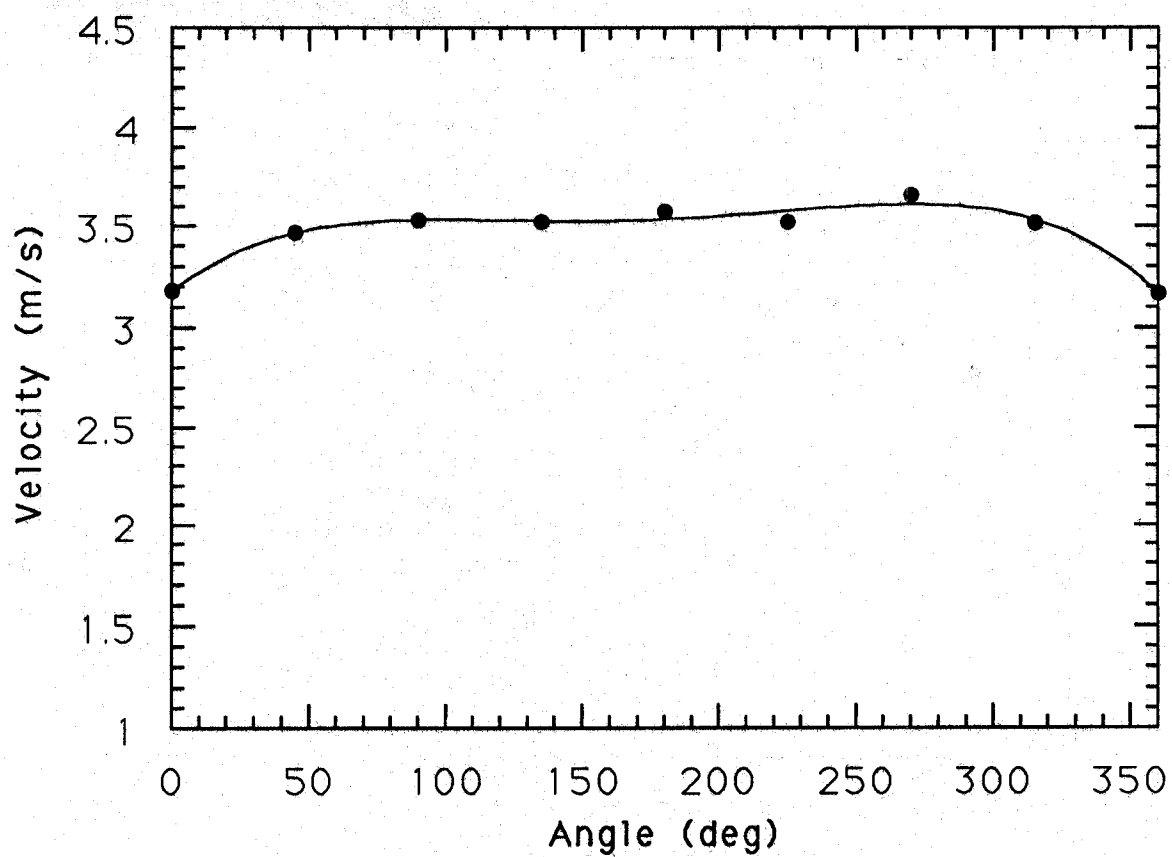


Figure 48. The air velocity as a function of angle around the annular test section at a location 65 cm upstream from the agent injection.

$$u' = \langle u \rangle - u \quad (25)$$

For inlet velocities of ≈ 5 m/s, the turbulence intensity 8 cm downstream of the test section inlet was measured to be ≈ 0.0065 indicating a nearly laminar flow. Because of the Reynolds number, TI increased downstream, obtaining values close to 0.03 on average. Flow visualization using smoke confirmed that the air flow was essentially laminar. The upstream velocity was measured for Cases 1, 4, 7, and 11 (see Table 9), and used as a boundary condition in the corresponding calculations.

9.4.3 Comparison of Calculations with Experimental Measurements. Experimental measurements were performed in an effort to validate the numerical simulations. Measurements were conducted for conditions corresponding to Cases 1, 7, and 14 listed in Table 9. The other cases represent numerical simulations where the effect of varying the location and number of agent injection nozzles on agent dispersion was tested.

Figure 49 compares the experimentally measured agent volume percent to the calculations (for Case 1) as a function of angular location in the nacelle, for positions equidistant from the inner and outer nacelle walls, 96 cm downstream from the agent injection location. Figure 50 shows a similar comparison for locations 184 cm downstream from the point of agent injection. The experimental uncertainty of 18 %, estimated from repeat measurements and a propagation of error analysis, is indicated by the error bars in the figure. In many instances, the calculations fall outside of the error bars. Uncertainty of the input to the model calculation, namely the air and N_2 flows, resulted in an uncertainty in the calculated agent concentration distribution. The magnitude of the uncertainty varies as a function of location in the nacelle and is steepest for locations of large concentration gradients. For example, the uncertainty in the location of the calculated agent concentration maxima in Figure 49 was equal to approximately 40° . A higher air flow or a lower N_2 flow shifted the calculated maxima from 140° to 100° , in better agreement with the measured agent concentration maxima. In general, the computed profiles were characterized by steep gradients and narrow peak half-widths, whereas the measured profiles were relatively broad.

Figure 51 compares the experimentally measured agent volume percent to the calculations for Case 7 with a baffle on the inner wall of the flow field as a function of angular location in the nacelle, for positions equidistant from the inner and outer nacelle walls, 96 cm downstream from the agent injection location. Figure 52 shows a similar comparison for locations 184 cm downstream of the agent injection. The calculations generally follow the trends experimentally measured. Little difference was experimentally measured between the cases with and without the baffle as seen by comparing Figures 49 and 51, or Figures 50 and 52. The agent concentration 96 cm downstream from the agent injection location shown in Figure 51 were asymmetric, whereas 184 cm downstream, they were symmetric. This indicates some asymmetry in the experimental configuration. The measurements were repeated after carefully checking the placement of the tee in the flow field. Measurements yielded nearly the same results. Thus, the reasons for the asymmetry are not clear.

Figure 53 compares the experimentally measured agent volume percent to the calculation for Case 8 as a function of angular location in the nacelle, for positions equidistant from the inner and outer nacelle walls, 96 cm downstream from the agent injection location. Figure 54 shows a similar comparison for locations 184 cm downstream from the point of agent injection. The computations predict agent concentration peaks $\pm 90^\circ$ from the injection location, whereas the measurements show peaks along the angle of injection.

The key difference between the numerical and laboratory experiments which remains unresolved is that agent concentration gradients in the laboratory measurements are smoother and less steep than

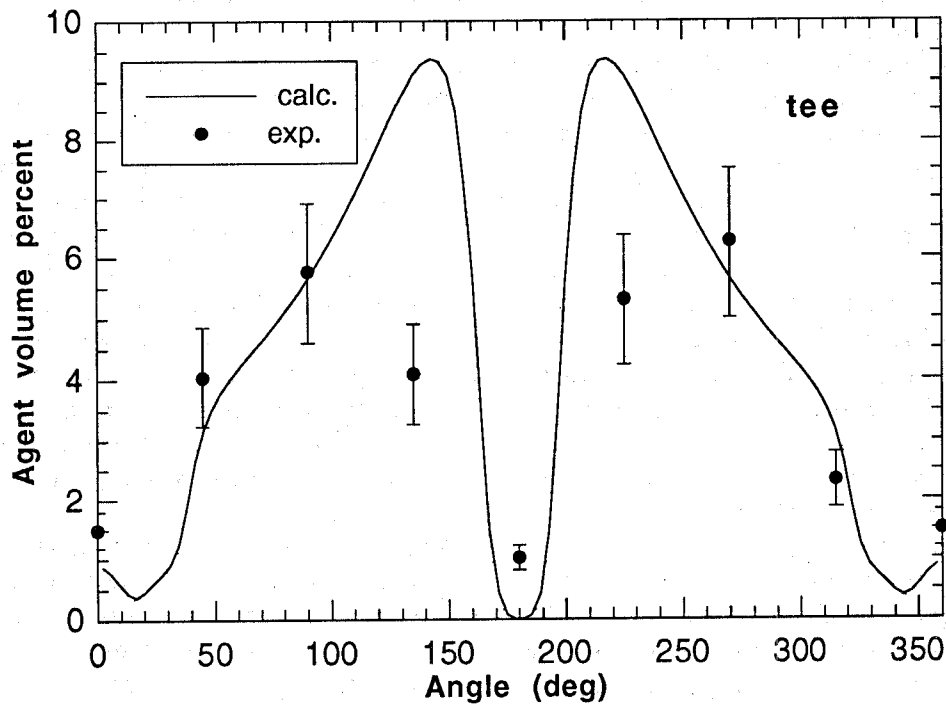


Figure 49. A comparison of the measured and calculated agent volume percent distribution 96 cm downstream from the agent injection tee. The average air velocity was 3.0 m/s and the agent flow was 0.012 m³/s (Case 1).

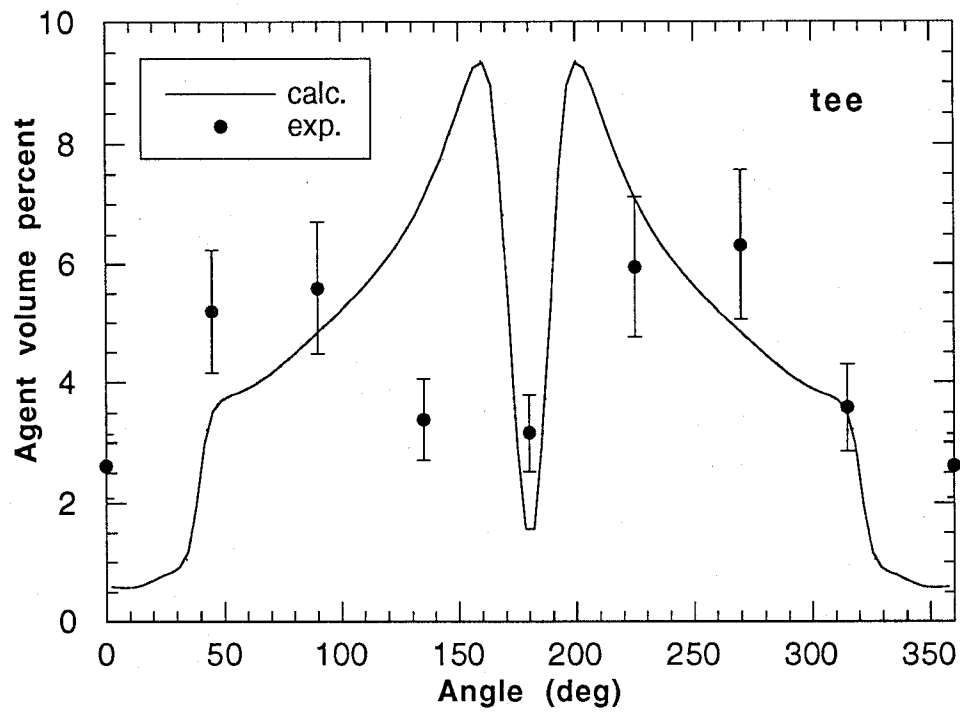


Figure 50. A comparison of the measured and calculated agent volume percent distribution 184 cm downstream from the agent injection tee. The average air velocity was 3.0 m/s and the agent flow was 0.012 m³/s (Case 1).

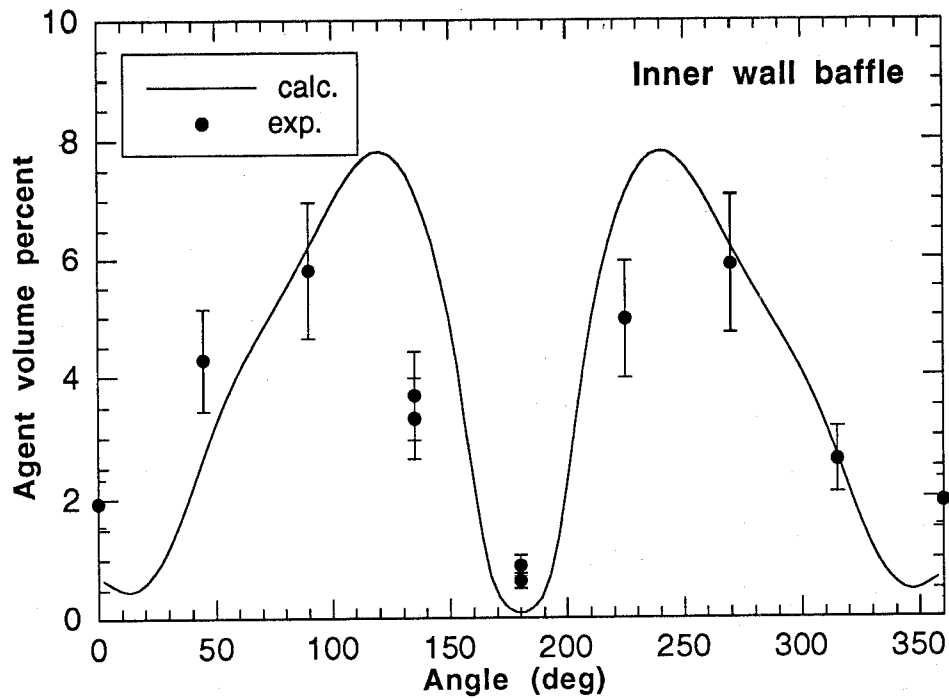


Figure 51. A comparison of the measured and calculated agent volume percent distribution, 96 cm downstream from the agent injection tee for Case 7, a baffle on the inner wall.

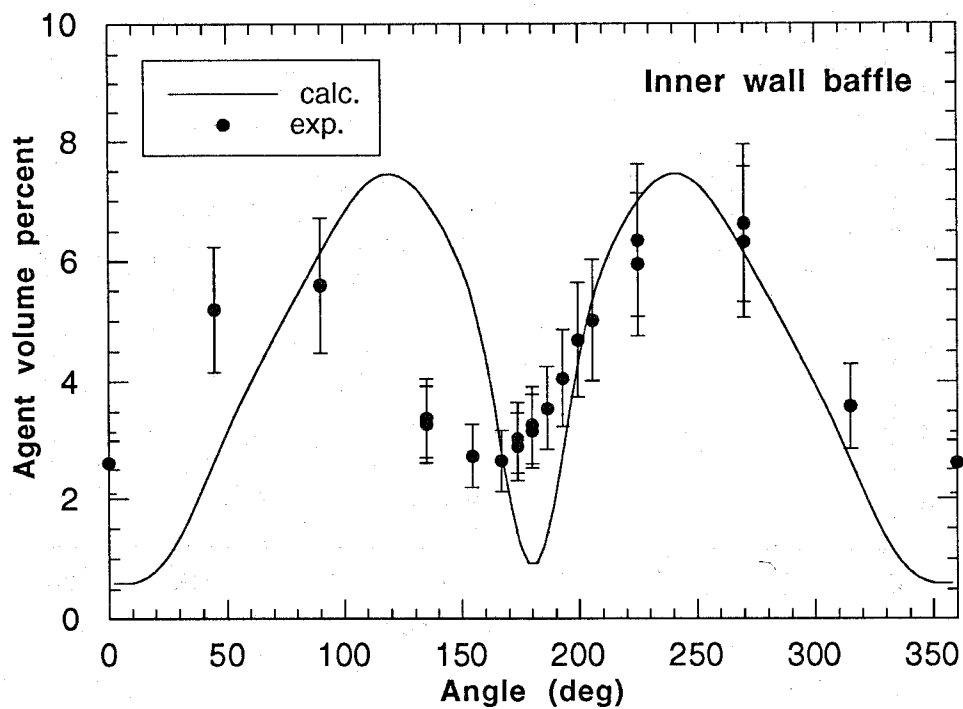


Figure 52. A comparison of the measured and calculated agent volume percent distribution, 184 cm downstream from the agent injection tee for Case 7, a baffle on the inner wall.

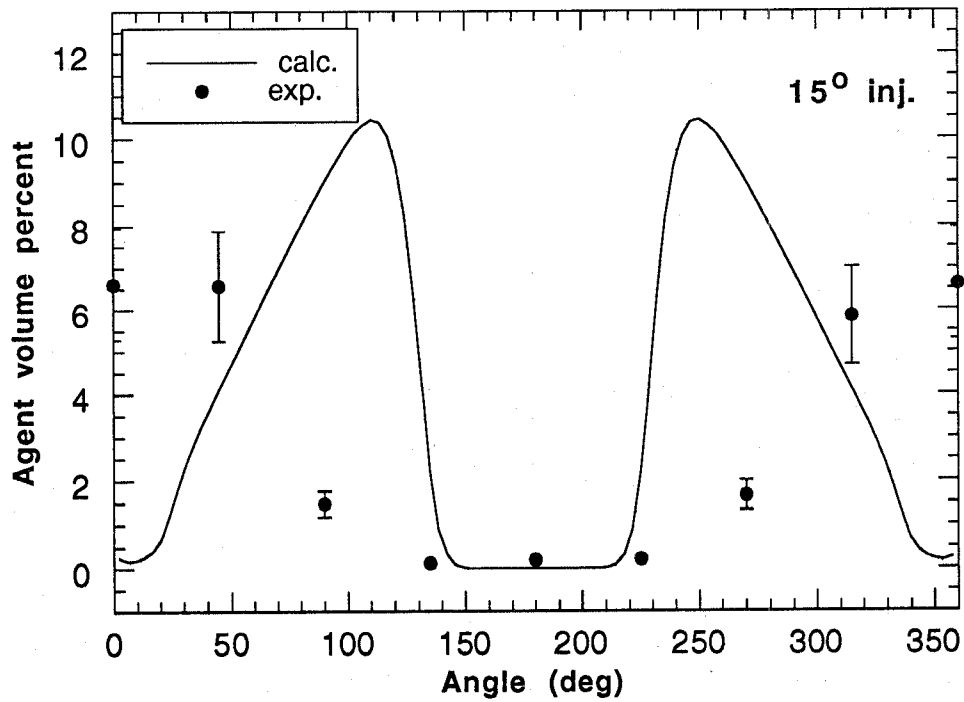


Figure 53. A comparison of measured and calculated agent volume percent distribution 96 cm downstream from the (15°) injection tube. The air velocity was 3.0 m/s and the agent flow was 0.012 m³/s (Case 8).

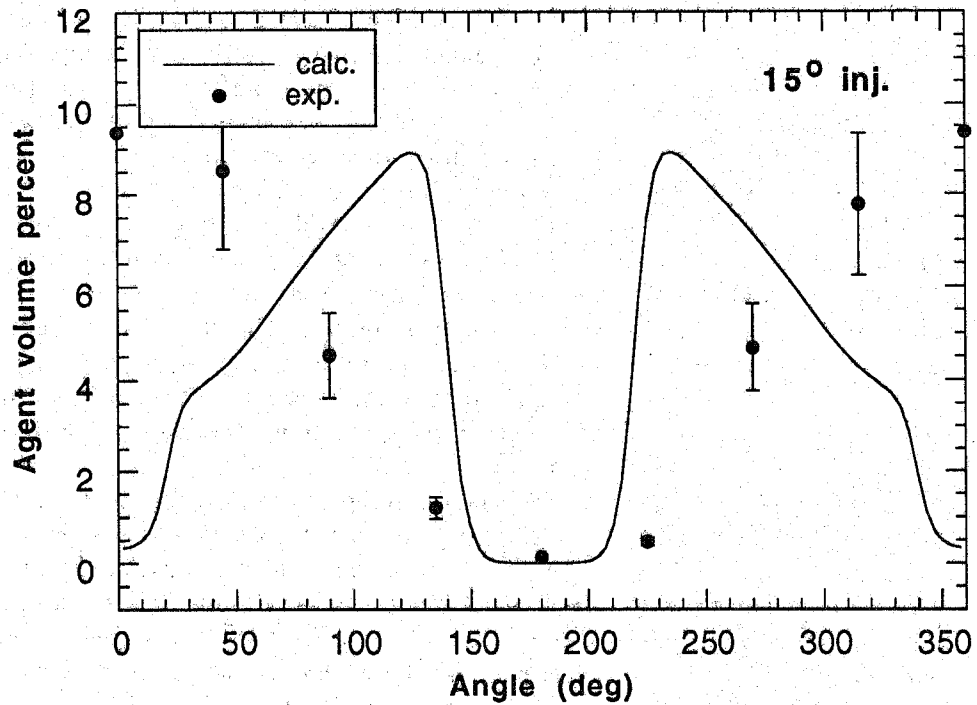


Figure 54. A comparison of measured and calculated agent volume percent distribution 184 cm downstream from the (15°) injection tube. The air velocity was 3.0 m/s and the agent flow was 0.012 m³/s (Case 8).

in the numerical calculations. The numerical computations predict localized regions of high concentrations which are not observed in the experiments.

There are several possibilities that may explain these differences. Most involve the use of correct boundary conditions for the air and agent flows. Another possibility explored was the variation in the spread angle of the agent jet. Several angles from 0° to 5° were examined with little change in agent concentrations. If the actual spread angle was much greater than 5° , then the calculated agent concentration distribution downstream would be more diffuse, more closely matching the experimental measurements.

Another possible explanation for the difference between computations and experiments was that the agent flow exiting the tee was not properly modeled. The assumption that the agent velocity exiting the tee was uniform over the entire opening was tested and the agent flow characteristics inside and near the exit of the tee were examined as illustrated in Figure 55. The grid near the tee exit was resolved into 20×20 grid cells instead of the 2×4 grid cells used in Cases 1 to 13. The fluid velocity is indicated by the length and direction of the vectors. The agent concentration is indicated by the gray scale. Note that the velocities (as indicated by arrow length) are much higher near the top of the tee than the bottom due to the presence of the recirculation zone near the bend in the tee. The agent velocity then was approximately twice the average velocity in the top half and zero in the bottom half. This detailed flow pattern was used as a boundary condition at the tee in a case similar to Case 1 with the result that downstream agent concentrations did not change appreciably.

Another possibility explanation for the modeling/experimental differences is associated with the error introduced through the k- ϵ turbulence model. Empirical parameters were used to calibrate the k- ϵ model. Though the k- ϵ parameters used here were calibrated for applications involving air flow, they may be incorrect for this particular application. Another possibility involves the interaction of the agent jet with the side walls of the nacelle tube. It is important to resolve the boundary layer at the wall properly in order to account for the aerodynamic drag of the bulk flow. It was thought that the grid resolution near the wall was sufficient. This was checked by refining the grid, which resulted in little change in the calculated agent concentration.

Because of the discrepancy between measurements and computations, many model parameters were varied in order to examine the sensitivity of results to changes or uncertainty in input parameters. The model parameters that were investigated were the average agent inlet velocity, the spread angle of the agent leaving the nozzle, the velocity distribution of the agent across the nozzle, the average air velocity, the distribution of the air velocity across the air inlet, and the turbulent intensity boundary conditions for both the air and agent flows. To summarize, the model is most sensitive to the ratio of the agent inlet velocity to the air inlet velocity. The other parameters noted above did not have a significant effect on the simulated distribution of agent in the mock nacelle. Figure 56 shows results from Cases 1 and 14-16. These cases were the same except that the air inlet velocity varied from 3.0 m/s for Case 1, to 4.0 m/s for Case 16. Note that the region of high concentration for Case 1 (3.0 m/s) was located approximately three-quarters (135°) of the way around the tube from the inlet tee (whereas the region of high agent concentration in the 4.0 m/s case was located from one-quarter (45°) to one-half (90°) of the way around the nacelle. Similar results were found when varying the agent inlet velocity (or equivalently the inlet mass flow). Small increases in agent inlet velocity enabled the agent to traverse farther around the nacelle. The model is not sensitive to the velocity profiles of the agent and air (as long as the average velocity across the inlet remained constant), turbulence levels, or the spread angle of agent exiting the injector.

9.4.4 Numerical Simulations. Shaded contours of volume concentration are presented in the plane of injection and at 96 cm and 184 cm downstream from the injection plane in Figures 56-61 for all of the cases listed in Table 9.

Agent Con

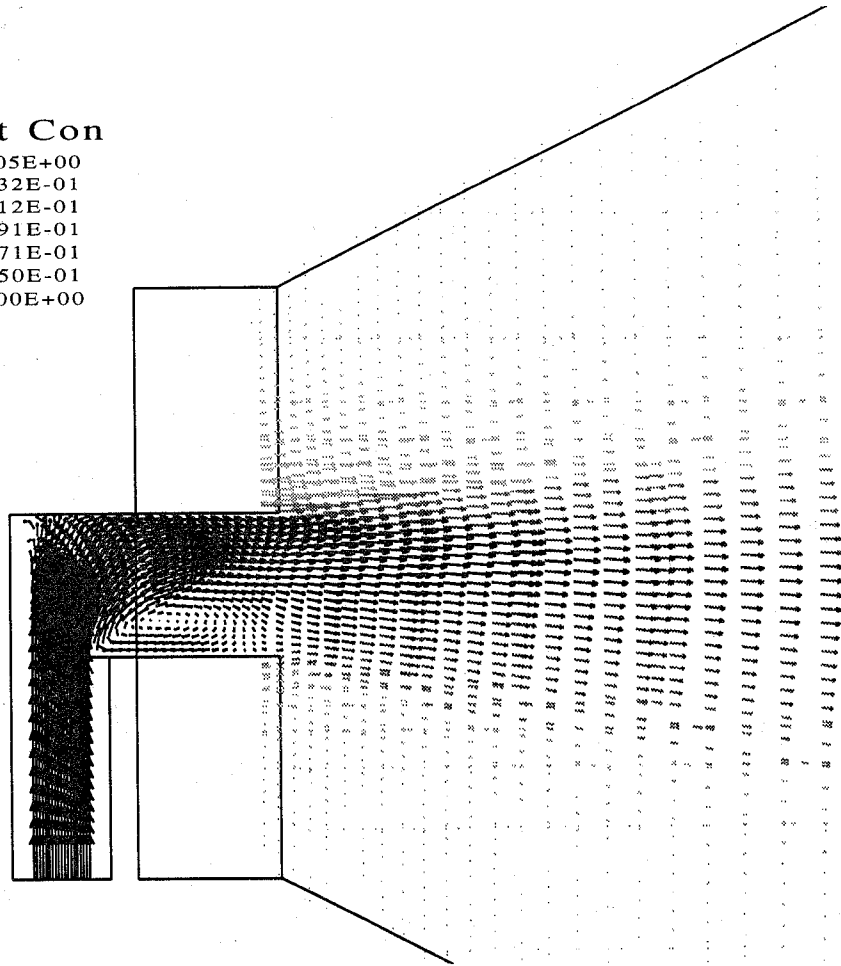
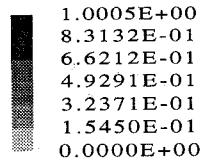


Figure 55. The character of the agent flow inside and near the exit of an injection tee. The fluid velocity is indicated by the length and direction of the arrows.

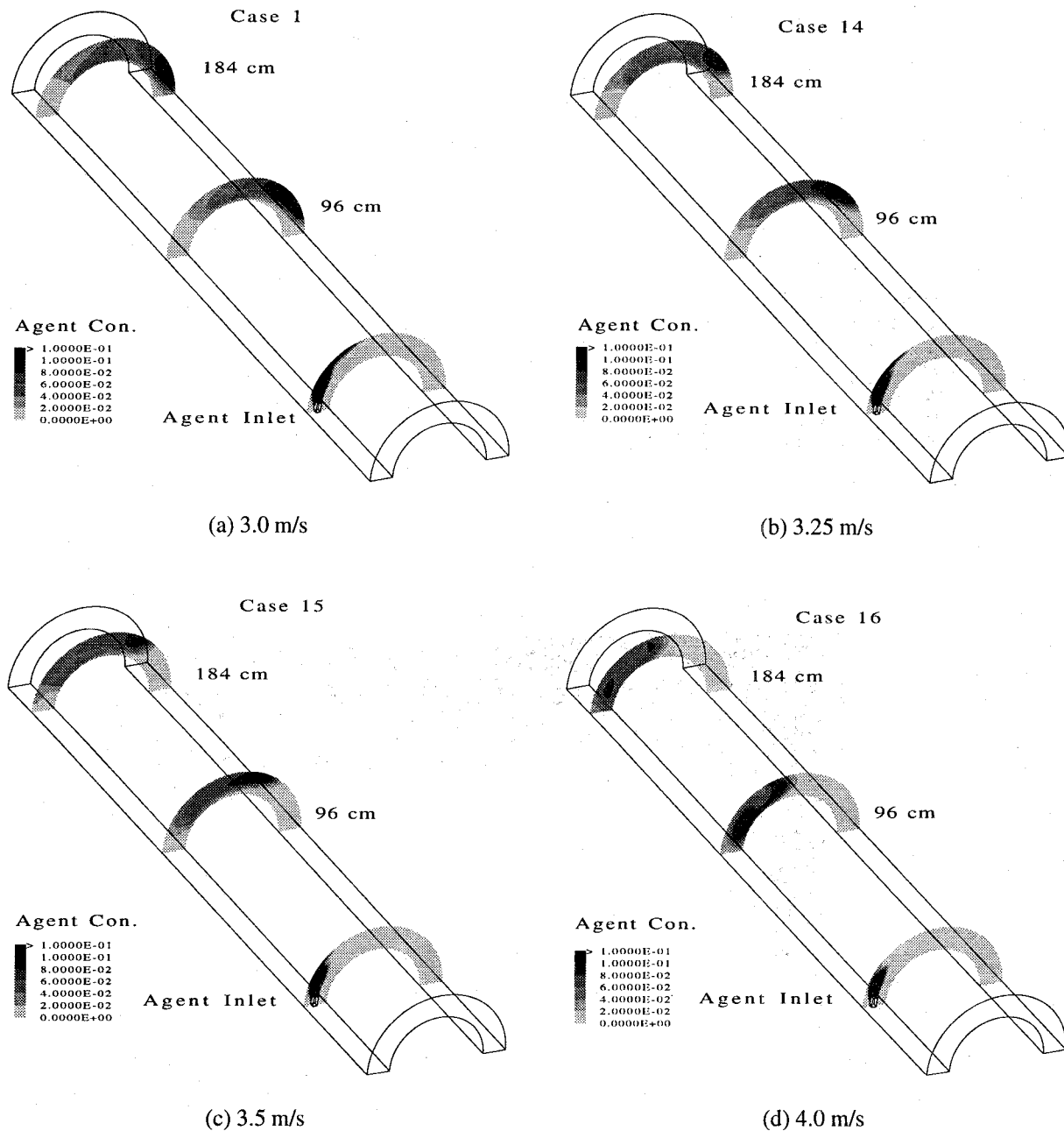


Figure 56. The calculated agent concentration in three vertical planes for Cases 1, and 14-16, for agent injected through a single tee for air velocities vaarying from 3.0 m/s to 4.0 m/s. The agent flow was 0.012 m³/s.

Figure 57 presents results from Cases 1-3 (see Table 9). The total mass flow rate was $0.012 \text{ m}^3/\text{s}$. The agent inlet velocity for the two tee case was 50 % of the one tee case and the inlet velocity for the four tee case was 25 % the velocity of the one tee case, such that the total agent flow into the nacelle was constant. The agent volume fraction in the figure is indicated by the gray scale. Its value varied from near zero to greater than 10 %. The simulations predict that injecting agent at several locations around the nacelle results in a more even distribution of agent down stream.

Figure 58 presents results from Cases 4-6. The conditions were the same as those in Cases 2-4 except that the total agent flow rate was doubled to $0.025 \text{ m}^3/\text{s}$. Again, with more agent inlets, the agent distribution was more even downstream.

Figure 59 shows the computed results for Case 7, where the fluid flows past a baffle on the interior wall of the nacelle. The results for Case 1, with identical conditions except no baffle present, are also shown. The baffle does not significantly influence the agent concentration distribution.

Figure 60 compares Cases 8-10 with the agent introduced through tubes inclined 15° downstream rather than through a tee (see Figure 45). The total agent flow was $0.012 \text{ m}^3/\text{s}$, the same as that used in Cases 1-3. Compared to Figure 58, the agent distribution was marginally better when it was introduced by the tees. Again, the agent distribution was more even downstream when agent was introduced at multiple locations around the nacelle.

Figure 61 compares Cases 11-13 with agent introduced through a tube inclined 15° from the perpendicular to the axis in the downstream direction. The total agent flow was $0.025 \text{ m}^3/\text{s}$, twice that used in Cases 8-10.

9.4.5 Conclusions. The use of flow field modeling can facilitate design optimization of an agent delivery system. The capability of computational fluid dynamics to model gaseous agent concentration in a generic engine nacelle should not, however, be fully accepted until it has been experimentally validated for representative flow conditions. In general, the CFD model has shown that an injector in the shape of a tee (with the tee oriented perpendicular to the flow direction) enhanced agent dispersion as compared to a single agent inlet (oriented 15° downstream). In addition, the simulations showed that increasing the number of agent injection nozzles increased agent dispersion. A baffle had little impact on the downstream agent dispersion for agent injected from a tee. Research remains to properly model two-phase agent flow and rapid evaporation in a nacelle environment (see Section 8 of this report for a discussion of two-phase flow modeling).

9.5 A Simple Model for Agent Delivery Requirements

A simple model describing the agent delivery requirements for engine nacelle fire suppression was developed as a complement to full-scale nacelle fire testing. Preliminary design guidelines for estimating agent mass requirements and the specific system performance criteria, agent concentration and duration, were proposed for each alternative agent using the model results. It must be pointed out that the proposed guidelines must be related to actual fire suppression system performance and appropriate safety factors applied to the mass requirements.

9.5.1 Simple Mixing Models Applied to Engine Nacelle Fire Suppression. The development of Military Specification (Mil E 22285) described in Section 9 suggests a conservative approach in terms of system performance. The sections of that Military Specification of interest here are the guidelines for agent amount, discharge time, and specific performance criteria (agent concentration and duration) of a suppression system. The guidelines for agent amount are meant to aid system designers in

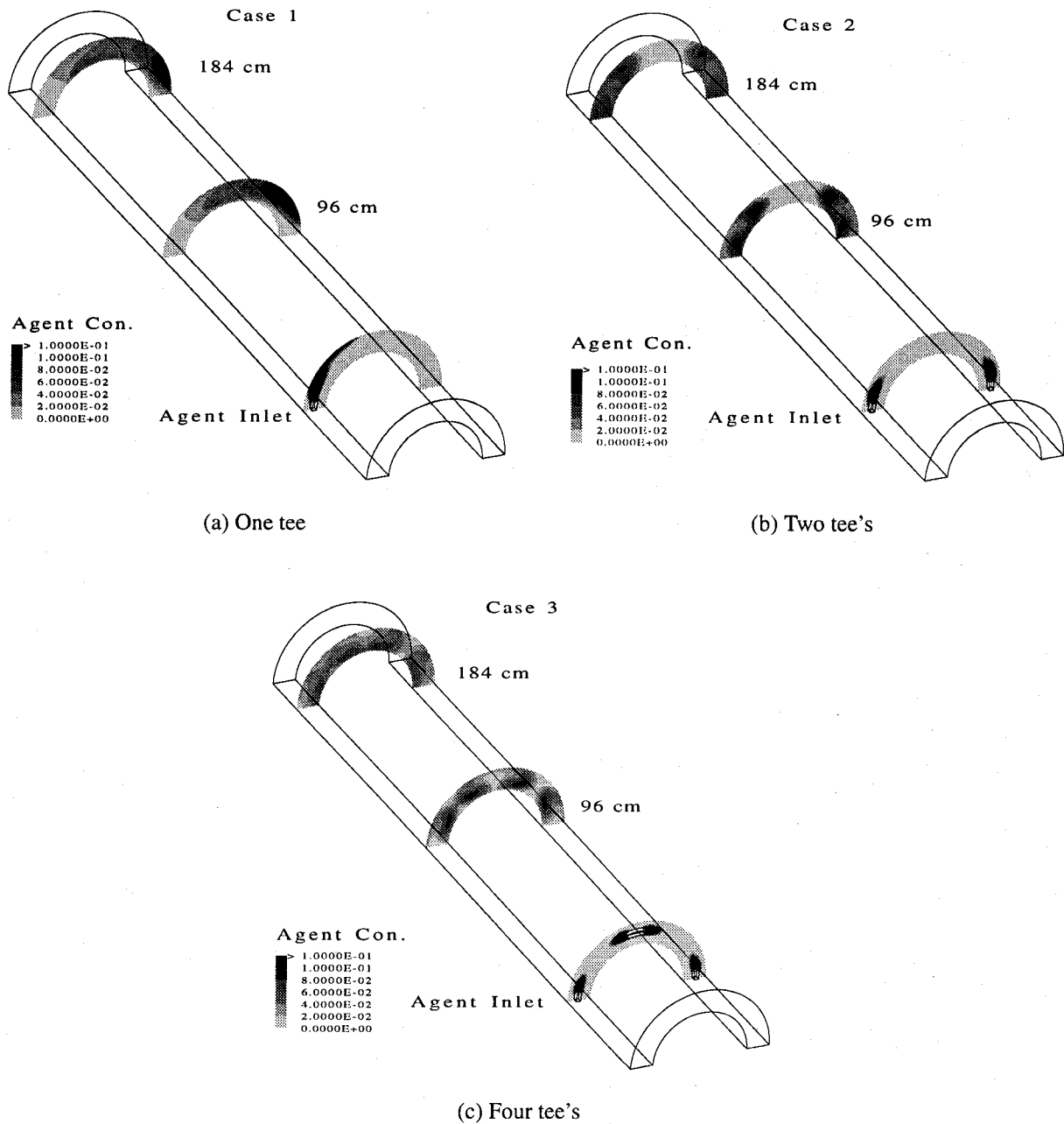


Figure 57. The calculated agent concentration in three vertical planes for Cases 1-3, for agent injected through one, two, and four tees. The bulk air velocity was 3.0 m/s. The agent flow was 0.012 m³/s.

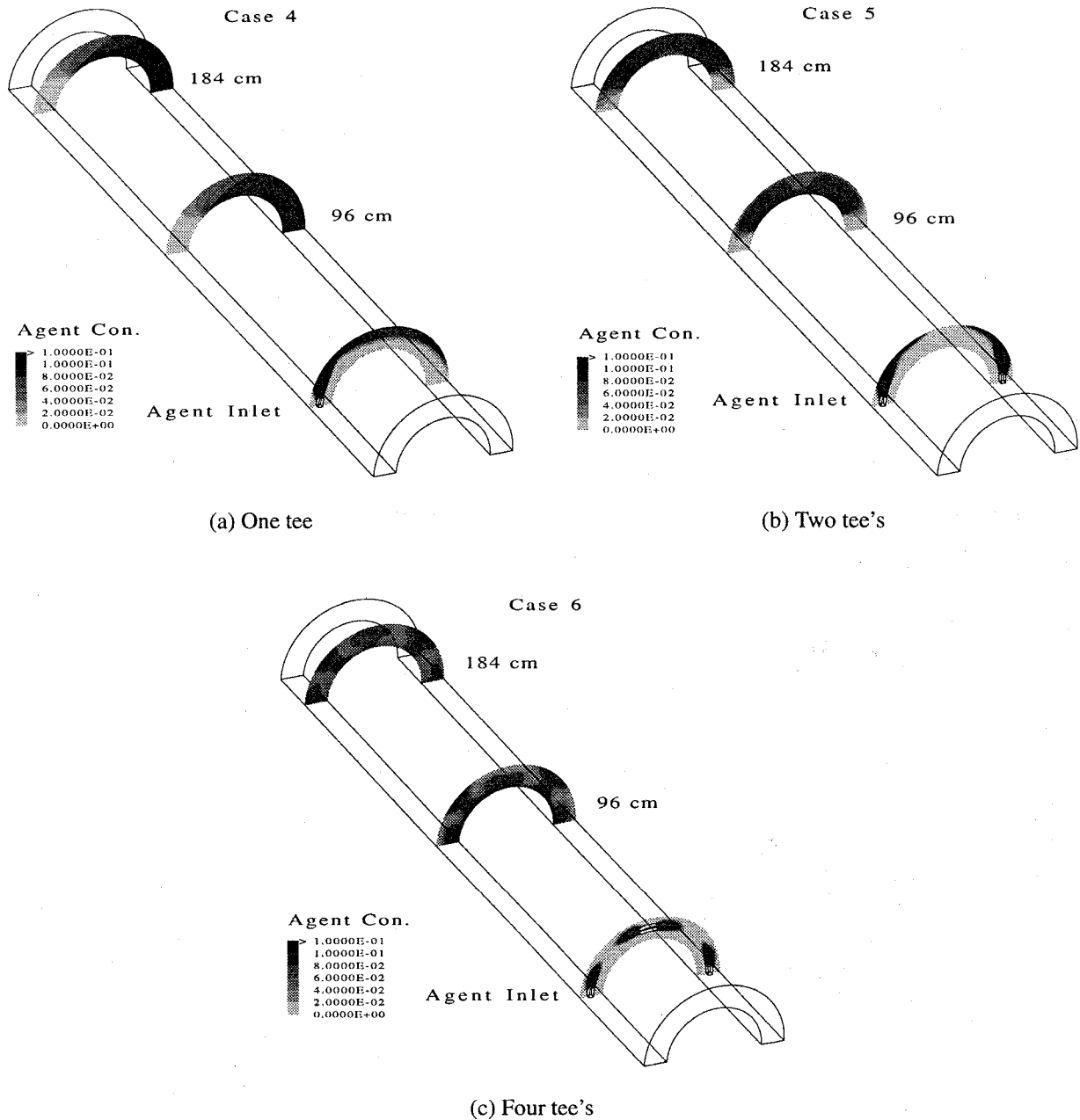


Figure 58. The calculated agent concentration in three vertical planes for Cases 4-6, for agent injected through one, two, and four tees. The bulk air velocity was 3.0 m/s. The agent flow was 0.025 m³/s.

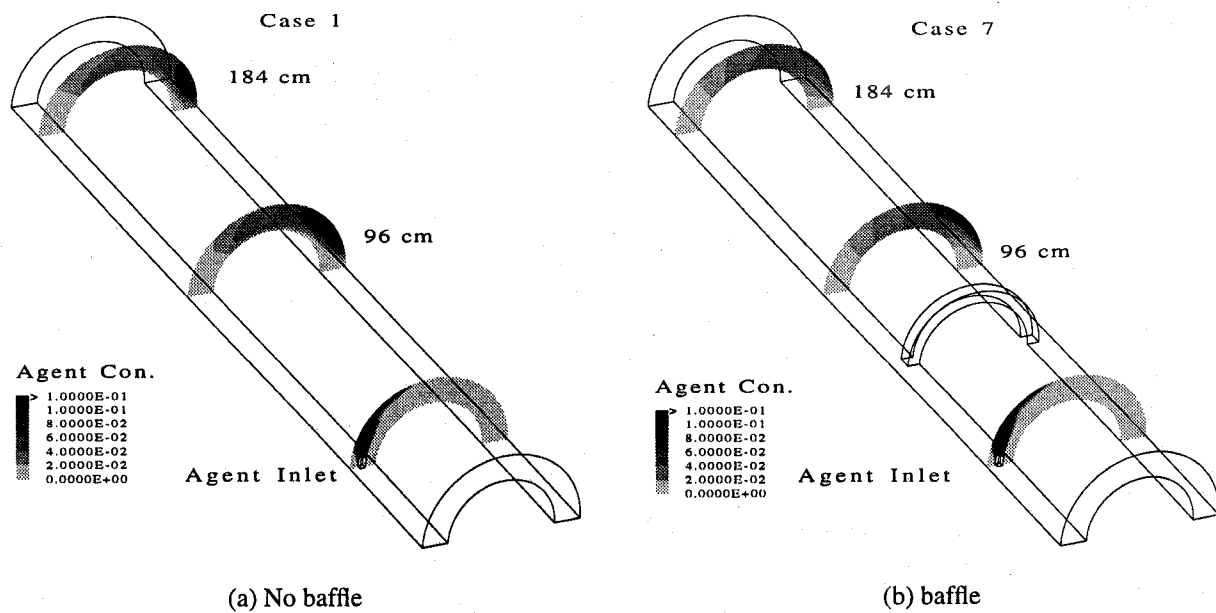


Figure 59. The calculated agent concentration in three vertical planes for Case 7, for flow past a baffle on the inner wall, as compared to no baffle (Case 1). The bulk air velocity was 3.0 m/s. The agent flow was 0.012 m³/s.

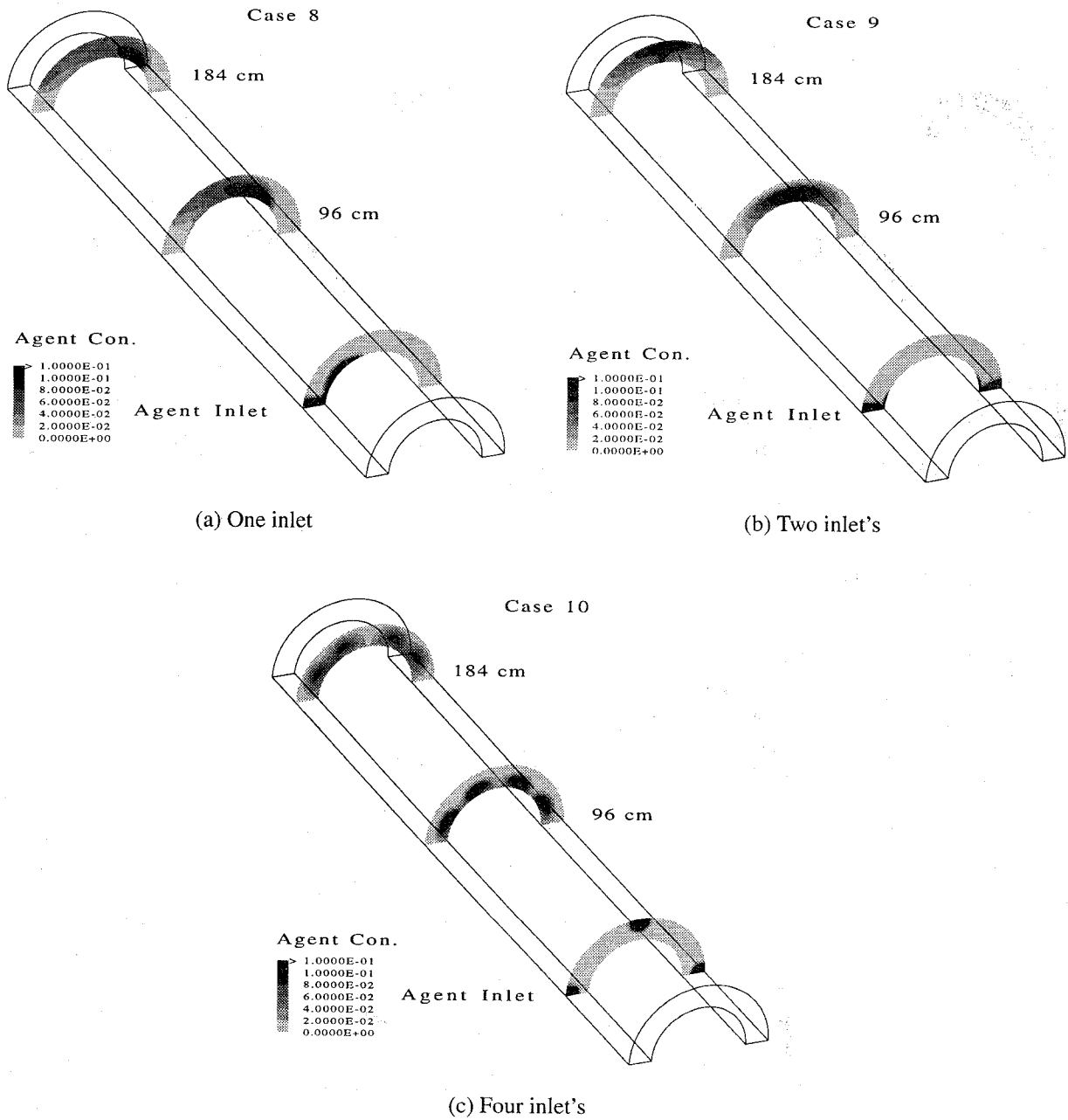


Figure 60. The calculated agent concentration in three vertical planes for Cases 8-10, for agent injected through one, two, and four inclined tubes. The bulk air velocity was 3.0 m/s. The agent flow was 0.012 m³/s.

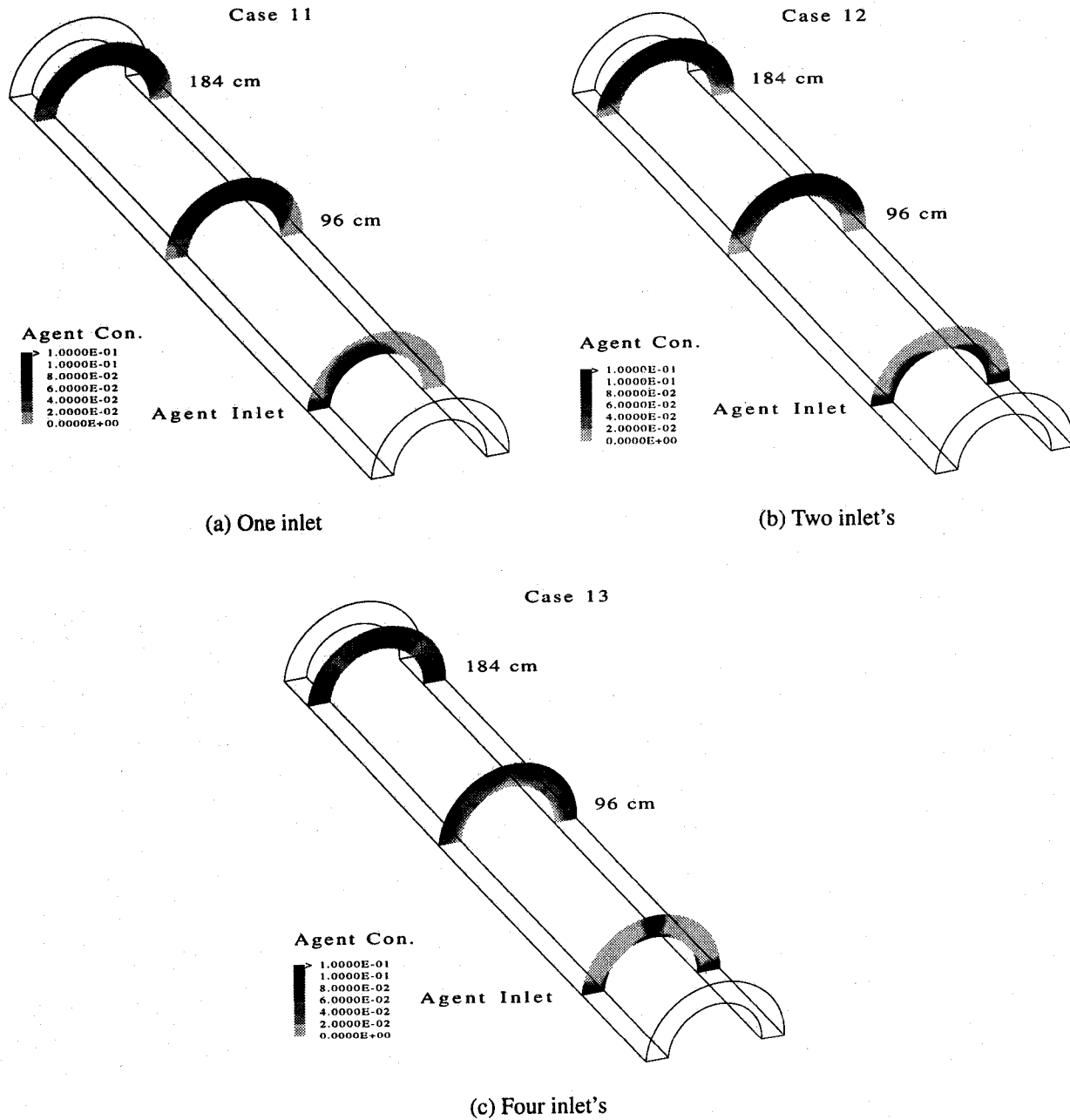


Figure 61. The calculated agent concentration in three vertical planes for Cases 11-13, for agent injected through one, two, and four inclined tubes. The bulk air velocity was 3.0 m/s. The agent flow was 0.025 m³/s.

meeting the performance criteria set forth in the Military Specification. An alternative agent will have different suppression characteristics, which will preclude the use of the Military Specification as it stands. Guidelines for designers and performance criteria for alternatives to halon 1301 are required for safe and efficient system design.

Keeping in mind that the likely halon 1301 replacement may require a much higher volumetric concentration to be effective in extinguishing nacelle fires, a logical question is: "what are the implications of a higher agent target concentration relating to design guidelines and performance criteria?" A direct method to explore the impact of design parameters and system variables is to perform a series of full-scale fire tests, varying design parameters (agent, injection rate) and system variables (air flow, volume, nacelle geometry, fire scenario, etc.) to determine how those variables impact the minimum agent mass required to suppress the fires. Tests with and without fires would also be needed to relate certification test results to the worst case fire scenario suppression requirements. Clearly, the number of full-scale tests would be very large, essentially repeating the early CAA research for each alternative agent. The full-scale testing performed at Wright-Patterson AFB for the Halon Replacement Program for Aviation was limited in terms of air flows, configurations, and fire scenarios, although a number of other variables were examined.

A complementary method to full-scale testing proposed here is a model that describes the agent delivery requirements for generic nacelle geometries. The model was used to explore the impact of air flow, mixing modes, nacelle volume, agent injection duration, and fire scenario on the agent requirements for suppression. All of the details of mixing are not simulated, nor are they known for a generic nacelle geometry, but limiting cases were covered which suggest the values of the minimum agent mass delivery rates to achieve flame suppression. Allowances for un-modeled phenomena such as imperfect mixing, inadequate description of the fire scenario and additional safety factors need to be considered for a conservative design methodology.

The model is based on idealized global mixing models describing agent dispersion and dilution for the bulk temporal concentration, and a local mixing model for flame extinction or concentration build-up at specified locations. The local mixing phenomena were inferred from small-scale experiments previously described in Section 9.3. In principle, computational fluid dynamics (CFD) could provide the answers pertaining to dispersion and the concentration profiles for every single configuration, but at this point, it is impractical to do such calculations because current CFD capability cannot provide a comprehensive description of fire suppression phenomena. Although CFD can provide answers pertaining to agent dispersion and mixing in specific nacelle-like configurations, it is not yet possible to do such calculations with consideration of two-phase flow for both agent and fuel and the detailed inhibition chemistry associated with the replacement agents. Nor is it possible to model all in-flight nacelle conditions, each with its own very different time-varying temperature and flow boundary conditions. Although CFD may prove to be a useful tool in specific applications and future designs, the focus here was to provide simple guidelines on alternative agent delivery rates for engine nacelle fire protection system designers. It is highly likely that discharge testing with concentration measurements for certification will remain relevant to document system performance when an alternative agent is used. Therefore, the relationship between certification criteria and flame suppression requirements needs to be explored for the alternative agents.

The mixing models presented here for the bulk flow are well known, and have been used for decades to describe industrial mixing in blending operations and concentration profiles in chemical reactors. The mixing extremes that are covered are the plug flow "segregated" case and the perfectly stirred "homogenous" case. The plug flow model assumes either no mixing of the components (the extreme) or mixing with the incoming air flow only. The perfectly stirred scenario implies intense, chaotic motion leading to a spatially homogenous system. A definition of a perfectly stirred system is that any given particle after being introduced into the volume has an equal probability of being

anywhere in the mixing volume, and as a consequence, the concentration is uniform throughout the mixing volume. Such a model was successfully employed in Section 9.3 to treat flame extinction in a recirculation zone. In chemical reactors, plug flow is typically assumed for tubular reactors, where the mean velocity profile is unidirectional. An example of a system that approaches perfectly stirred behavior is a liquid-filled tank with an impeller operating at high speed. Deviations from true plug flow occur with turbulent backmixing or molecular diffusion leading to axial dispersion. Deviations from the perfectly stirred case occur from quiescent "dead" spaces in the volume, concentration boundary layers, and by-passing of incoming fluid. In many cases the phenomena giving rise to the deviations from the ideal cases can be modeled or quantified by experiments if sufficient effort is expended.

In the bulk flow models, deviations from the idealized cases were not considered. The description of a particular nacelle is given by any number of perfectly stirred or plug flow regions in series and/or parallel. The transfer of agent from one region to another was taken into account by solving the transient mass balance equations for each region. The agent is assumed to be introduced as a gas, which then mixes isothermally with air.

The agent concentration for any given location as a function of time is required to assess the suppression system performance. One extreme case is to assume that the agent flows as a plug and does not mix with the air stream. Thus, the bulk "free stream" concentration is 100 % for the volume occupied by the plug, and its duration at any location in the nacelle is equal to the nacelle volume (V) divided by the total (air and agent) volumetric flow (\dot{Q}_{total}). The next case is where the agent mixes perfectly with the incoming air stream, and flows downstream as a plug. A good approximation would be agent dispersed from many locations in a cross section with flow in one direction. The bulk "free stream" concentration is equal to the agent volumetric flow (\dot{Q}_{agent}) divided by the total (agent and air) volumetric flow (\dot{Q}_{total}). The duration at any location is equal to the nacelle volume divided by the volumetric flow (V/\dot{Q}_{total}).

For a perfectly stirred region (PSR), the steady-state (long agent injection duration) bulk concentration is equal to the agent volumetric flow divided by the total flow of agent and air ($\dot{Q}_{agent}/\dot{Q}_{total}$). The mixing volume and total volumetric flow determines the dynamics of the concentration build-up. Assuming isothermal, constant volume conditions, the solution to the mass balance equation for a step change in agent flow entering the nacelle is:

$$X(t) = X_f + (X_0 - X_f)(e^{-t/\tau_1}) \quad (26)$$

where $X(t)$ is the volumetric concentration in the nacelle, X_f is the volumetric agent concentration entering the nacelle ($\dot{Q}_{agent}/\dot{Q}_{total}$), X_0 is the initial concentration, and τ_1 is the characteristic mixing time given by the mixing volume divided by the total volumetric flow (V/\dot{Q}_{total}). A step change from a fixed volumetric flow of agent, to zero agent flow gives

$$X(t) = X_p (e^{-t/\tau_2}) \quad (27)$$

where X_p is the concentration in the PSR when the agent flow is stopped (at time $t=0$) and τ_2 is the characteristic time given by the total volume divided by the air flow (V/\dot{Q}_{air}).

The solutions above for step changes in the incoming stream concentration and flow are indicative of cases where the initial agent injection takes place in a perfectly stirred region, or a constant concentration plug flow feeds a perfectly stirred region. Analytical solutions are obtainable for other cases where the concentration of the incoming flow is a known function of time. A relevant case is

when one perfectly stirred region provides the feed to another perfectly stirred region (PSRs in series). This situation is a reasonable model for certain nacelles (see Section 9.5.2). The solution to the concentration in the second PSR is given by one of the following equations below. If the feed concentration is given by Equation (26), the solution to the concentration in the second PSR is:

$$X(t) = X_p e^{-t/\tau_3} + K \left(1 + \frac{\tau_1}{\tau_1 - \tau_3} (e^{-t/\tau_3} - e^{-t/\tau_1}) - e^{-t/\tau_3} \right) \quad (28)$$

if $\tau_1 \neq \tau_3$ and

$$X(t) = X_0 e^{-t/\tau_3} + K (1 - e^{-t/\tau_3}) - \frac{K}{\tau_3} t e^{-t/\tau_3} \quad (29)$$

if $\tau_1 = \tau_3$, where K is the constant feed concentration into the first PSR multiplied by the fraction of the total flow entering the second PSR and τ_3 is the volume of the second PSR divided by the volumetric flow rate into that PSR. If the feed concentration is given by Equation (27), the solution for the concentration in the second PSR becomes

$$X(t) = (X_0 - K_p \frac{\tau_2}{\tau_2 - \tau_3}) e^{-t/\tau_3} + K_p \frac{\tau_2}{\tau_2 - \tau_3} e^{-t/\tau_2} \quad (30)$$

if $\tau_2 \neq \tau_3$ and

$$X(t) = \left(\frac{K_p}{\tau_3} t + X_0 \right) e^{-t/\tau_3} \quad (31)$$

if $\tau_2 = \tau_3$, where K_p is the peak concentration achieved in the first PSR multiplied by the fraction of total flow entering the second PSR and X_0 is the initial concentration in the second PSR. Likewise, solutions for more PSRs in series begin with the solution to the previous PSR.

So far the bulk or "free stream" concentration has been described. A description of agent mixing from the free stream into eddies behind bluff bodies in the case of certification concentration and into fire locations is needed in order to relate certification concentration and duration to agent requirements sufficient to extinguish various types of fires. This local mixing phenomena is described in terms of a characteristic mixing time, analogous to the characteristic mixing time described for the PSR bulk mixing. The location of a certification probe may likely be in an eddy behind a bluff body (rib, etc). In that case the characteristic mixing time depends on the flow velocity, viscosity and characteristic dimension of the bluff body as shown in Section 9.3.6. For the flows considered here, the diffusive term can be ignored since the mixing is convection dominated.

Mixing from the free stream into a fire stabilized behind a bluff body is much slower than mixing into the same location without any fire due to the expanding hot gases increasing the fluid viscosity which affects the flow field and the rate of agent entrainment or mixing. Two different baffle

stabilized fire scenarios were explored; a spray fire, and a pool fire. Extinction times for both scenarios were fit to the same first order equation, Equation (14):

$$X_{\infty} = X_c (1 - e^{-\Delta t / \tau_f})$$

where X_{∞} is the critical free stream agent concentration at extinction for long injection durations ($\Delta t > 3\tau_f$), X_c is the critical free stream agent concentration for short agent injection intervals, and τ_f is the characteristic mixing time associated with the given fire scenario as discussed in Section 9.3.

Considering the characteristic mixing times for combusting and non-combusting cases, it is obvious that local mixing behind baffles is very different. This observation necessitates that relationship between the certification test and real fire scenarios must be explored so that certification criteria specify safe conditions for the worst case fire scenario considered.

9.5.2 Agent Requirements for Generic Nacelles. Two generic nacelle models are described below which represent the extremes in the bulk mixing phenomena.

Model No. 1 It is assumed that the bulk flow of agent is a plug flow and the fire zone or certification locations are located downstream from the injection plane. Perfect mixing of agent and air occurs at the injection plane.

Model No. 2 The entire nacelle volume is treated as a perfectly stirred region. The bulk flow feeds the fire zone or certification locations.

A real engine nacelle may behave closer to one of these generic descriptions than the other. The geometry, air entrance location, air and wall temperatures, agent injection location, and flow exit will impact the mixing and dispersion. For instance, the F-111 has air entering the nacelle uniformly across the radial cross-section, and exits through an ejector at the end of the nacelle. Agent is introduced through a tee fitting located at the most forward position of the nacelle to spread the agent around its co-annular nacelle cross-section (McClure *et al.*, 1974). With this configuration, it is easy to imagine that there is no significant air or agent back flow, and the bulk of the agent would flow as a plug mixed with air. The F/A-18 on the other hand has a much different configuration. The nacelle air is introduced through an air ram located on the bottom of the aircraft and positioned between the forward and aft of the nacelle. The flow exits through two small vents located on the top and the bottom of the aircraft near the aft position (Picard *et al.*, 1993). Agent is introduced through a tube located at the forward-most position of the nacelle. Prior to agent release there must be reversed flows giving rise to recirculation zones and dead zones with no air flow. During and after agent release, the recirculation zones act as perfectly stirred regions. Instead of a plug flow of agent and air, the nacelle will undergo a rapid increase in agent concentration followed by a slower tailing. This behavior was observed qualitatively during some discharge testing with halon 1301 and HFC-125 in an F/A-18 (Leach, 1994). No specification of a smooth or rough nacelle geometry has been made in the generic models. The specific nacelle geometry is handled by the certification and fire characteristic times chosen. It was assumed that in smooth nacelles, no baffle stabilized pool fires could form and for now, the worst case fire for the smooth nacelle geometry was taken as a baffle stabilized spray flame. For rough nacelles (defined as those nacelles with ribs or other obstructions that can stabilize pool fires), the worst case fire was taken as a baffle stabilized pool fire.

9.5.2.1 Minimum Fire Suppressant Requirements. A parametric study was employed to determine the required agent amount for a range of discharge durations for the two nacelle models. The variables were nacelle type (smooth or rough which fixes the characteristic mixing times), free volume, air flow, agent density, discharge duration, and critical extinguishing concentration. The temperature and pressure were fixed at 20 °C and 101 kPa respectively. The nacelle volume range was from 0.25 m³ to 8 m³ in increments that double from the previous value and the air flow range was from 0.25 kg/s to 8 kg/s, also in increments that double from the previous value. These values cover the range of possible air flows and volumes in actual nacelles as listed in Table 1. In the following analysis, the incoming air flow was assumed to be a constant value; agent injection has no effect on the nacelle air flow. This would be the case when the air flow entering the nacelle is choked which can occur for a Mach number greater than one and represents the worst case scenario since dilution air flow is at its highest value. It is also assumed that during agent injection, the pressure rise inside the nacelle volume is negligible. The injection durations examined were 0.25 s, 0.5 s, 1.0 s, 1.5 s, and 2.0 s. This range covers a very rapid injection time (0.25 s) and an injection time twice the value specified in the Military Specification for halon 1301. This range will show when positive effects from rapid injection are to be expected, and when it may be possible to relax the discharge time requirements without having a drastic impact on the agent requirements. The discharge time significantly constrains hardware design (see Section 8.6 of this report). The agent mass flow rate is assumed to be a constant over the injection duration. This is a reasonable assumption given the pipe flow model results reported in Section 8.6.

For the simulations, the mixing times for the fire scenarios were fixed (not a function of air flow) and were specified to characterize worst case fires for these generic nacelles. Two different fire scenarios were considered; a baffle stabilized spray fire, and a baffle stabilized pool fire with characteristic mixing times (τ_f) taken as 0.1 s and 1.0 s, respectively. These values are consistent with the experimental measurements described in Section 9.3. The critical or maximum long injection time concentrations (X_∞) were taken as the cup burner extinction concentrations for the spray fire scenario. For the pool fire scenario, the results described in Section 9.3 served as input or in lieu of this data, the peak flammability limit of n-heptane flames was utilized (Malcolm, 1950). The peak flammability limits are a reasonable target concentration for an agent in the fire zone. This concentration insures that combustion of even the most flammable fuel/air ratio cannot occur and secures both flame suppression and the prevention of re-ignition. Note that the target concentration is for the combustion zone, not the free stream. These values are given in Table 10 along with the gas-phase density of the agent at 20 °C.

For nacelle model No. 1, an analytical expression for the minimum agent mass is given by

$$W_{ag} = \frac{\Delta t \rho_{ag} X_\infty \dot{W}_{air}}{\left(1 - \frac{X_\infty}{1 - e^{-\Delta t/\tau_f}}\right) (1 - e^{-\Delta t/\tau_f}) \rho_{air}} \quad (32)$$

where W_{ag} is the minimum agent mass, Δt is the injection duration, \dot{W}_{air} is the mass flow of air, ρ_{ag} and ρ_{air} are the densities of agent and air at ambient conditions, and τ_f is the characteristic mixing time for the particular fire scenario. Observe that the nacelle free volume is not a variable in the equation, and thus does not impact the amount of agent for this nacelle model. For nacelle model No. 2, the minimum amount of agent is obtained by a numerical iterative procedure using Equations (28) and (31), replacing τ_3 with τ_f and solving for $X(t)=X_\infty$.

The results are presented graphically with agent mass as the dependent variable, air flow as the independent variable, and different symbols for each nacelle free volume. Results for each injection duration are presented in separate figures. Figures 62-66 are for a spray fire scenario with halon 1301 as the agent. In this and all other cases, nacelle model No. 1 (plug flow model) yielded the minimum amount of agent at any given air flow. Note also that as the volume decreased, the results for nacelle model No. 2 approached the plug flow results because the characteristic mixing time for the bulk flow approaches zero as the volume approaches zero. As the air flow approached zero, the agent mass

Table 10. Critical agent volume fraction for spray and pool fires

Agent	X_{∞} , spray fire	X_{∞} , pool fire	Agent density @ 20 °C (kg/m ³)
halon 1301	0.031	0.060	6.2
HFC-125	0.087	0.12	5.0
HFC-227	0.062	0.11	7.2
CF ₃ I	0.032	0.068	8.2

reached a limiting value, independent of injection time. Also, the agent requirements increased as injection time increased. What is not shown is that if the injection time were decreased below 0.25 s, a critical injection time is reached where a fire cannot be extinguished. Recall that agent mass is minimized when the free stream concentration is 100 %. But, in both nacelle models Nos. 1 and 2 the agent always mixes with air flow, therefore 100 % agent concentration cannot be achieved. In practical terms though, this result is unlikely to pose a problem since during any agent injection, there will be some spreading of agent both up and downstream. That spreading effectively increases the injection time and reduces the concentration.

Figures 67-71 are for a pool fire scenario with halon 1301. Again, as air flow decreased, the agent mass tended to a fixed value independent of injection time. The injection time that resulted in the minimum amount of agent was not the shortest injection time, but now depends on nacelle volume and falls between 0.5 s for the smaller volumes and 1.0 s for the larger volumes. In all cases the mass requirements were much higher than for the spray fire scenario.

Figures 72-76 show the results for HFC-125 in the spray fire scenario. Again, agent requirements were minimized for the 0.25 s injection as observed in the halon 1301 simulations. Figures 77-81 show the results for HFC-125 in the pool fire scenario. The minimum agent mass was obtained for injections between 0.5 s and 1.5 s, depending on the volume. In all cases, the agent mass was higher than the predicted values for halon 1301.

Figures 82-86 show the results for HFC-227 in the spray fire scenario. Agent requirements were lowest for the 0.25 s injection time. Figures 87-91 show the results for HFC-227 in the pool fire scenario. Injection durations between 0.5 s and 1.5 s minimized the agent mass requirements. As with the HFC-125 results, the agent mass requirements were higher than the halon 1301 values.

Figures 92-96 show the results for CF₃I in the spray fire scenario. Figures 97-101 show the results for CF₃I in the pool fire scenario. For the spray and pool fire cases, the injection duration that minimized the agent mass was 0.25 s and between 0.5 s and 1.5 s respectively. The agent mass requirements were still higher than halon 1301, but not as high as HFC-125 and HFC-227.

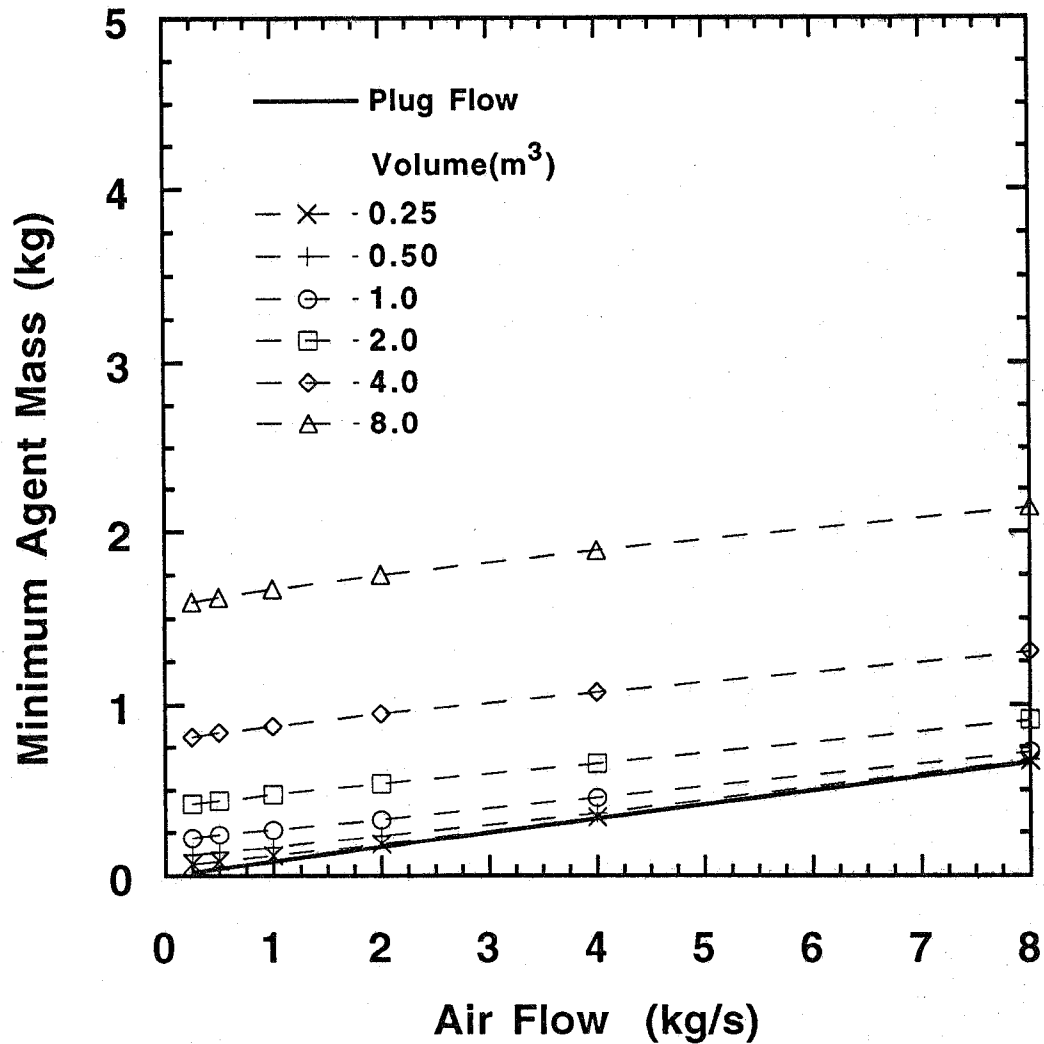


Figure 62. The minimum halon 1301 mass requirements for spray fire suppression as a function of air flow. The agent injection duration was 0.25 s.

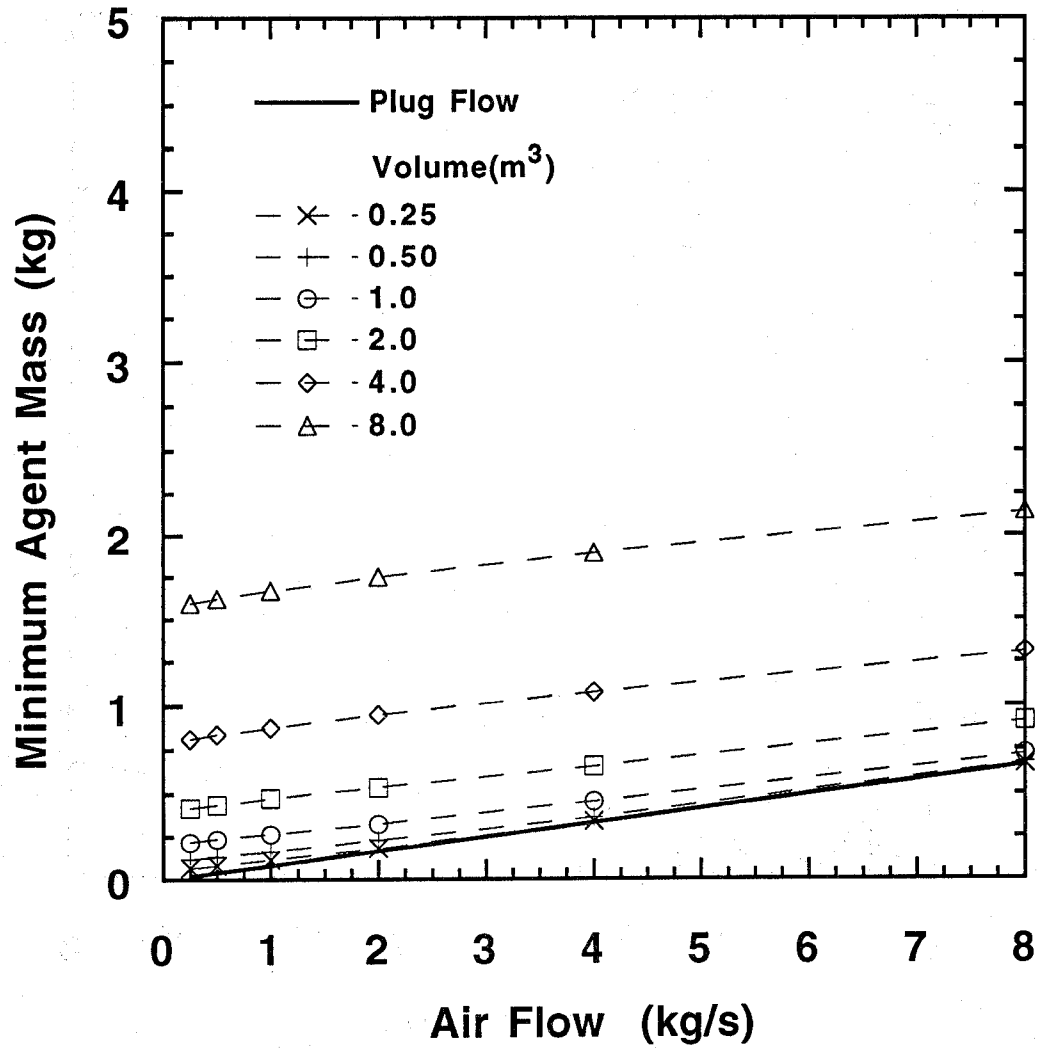


Figure 63. The minimum halon 1301 mass requirements for spray fire suppression as a function of air flow. The agent injection duration was 0.50 s.

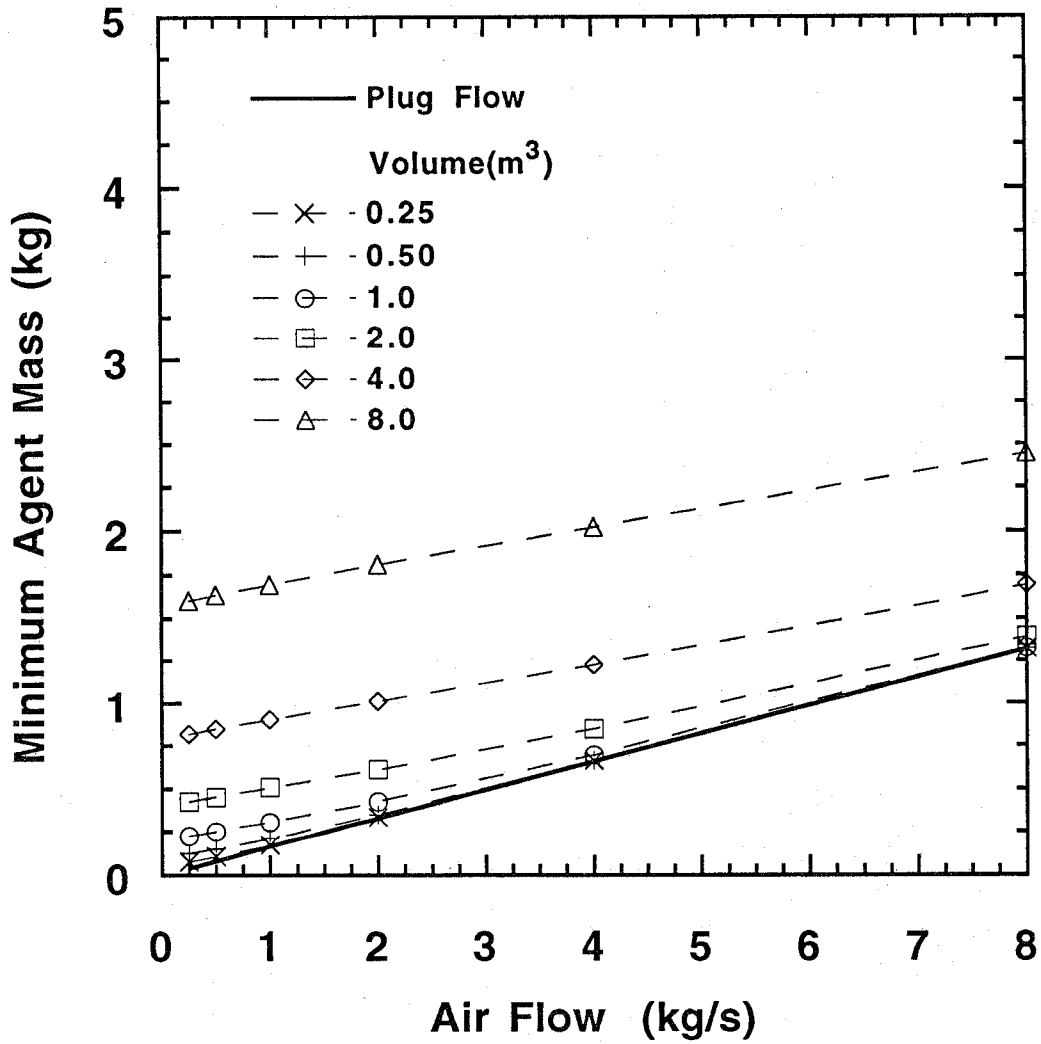


Figure 64. The minimum halon 1301 mass requirements for spray fire suppression as a function of air flow. The agent injection duration was 1.0 s.

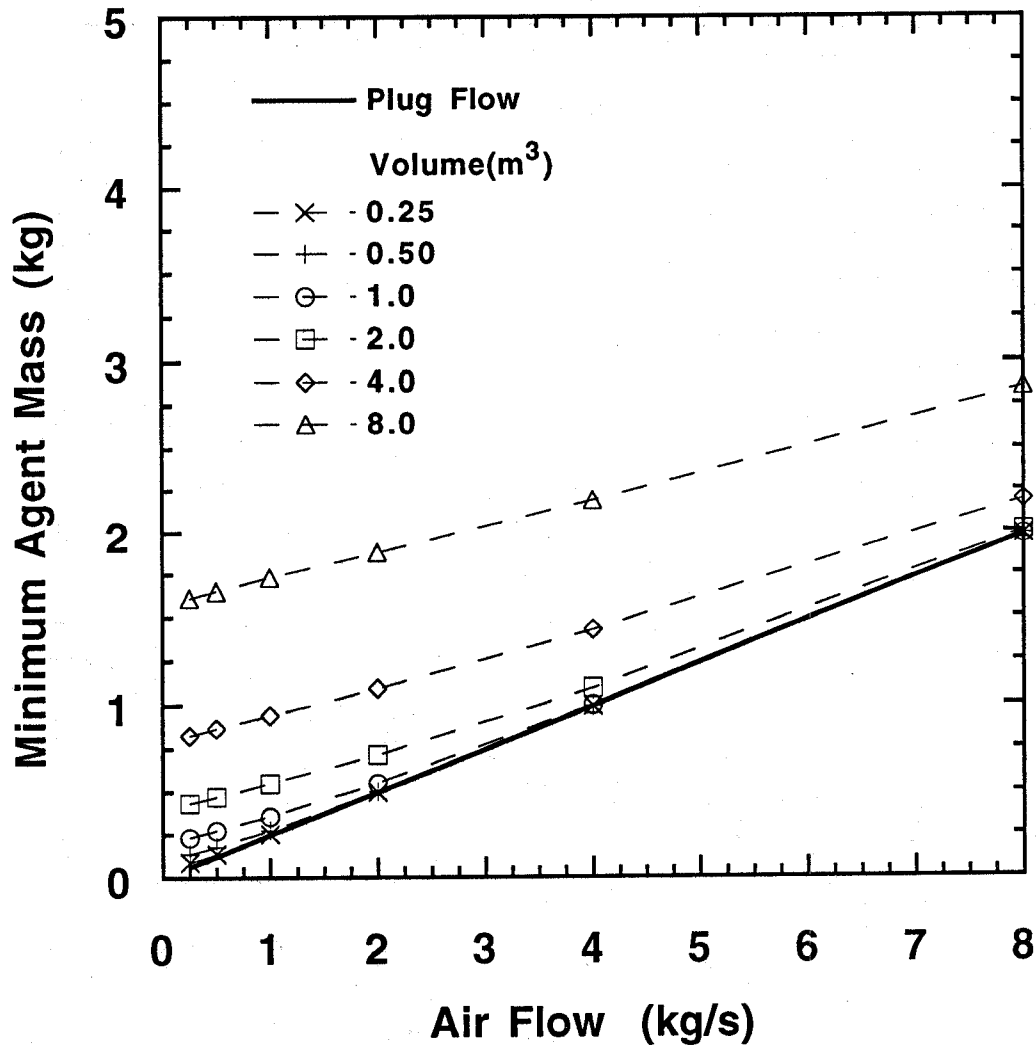


Figure 65. The minimum halon 1301 mass requirements for spray fire suppression as a function of air flow. The agent injection duration was 1.5 s.

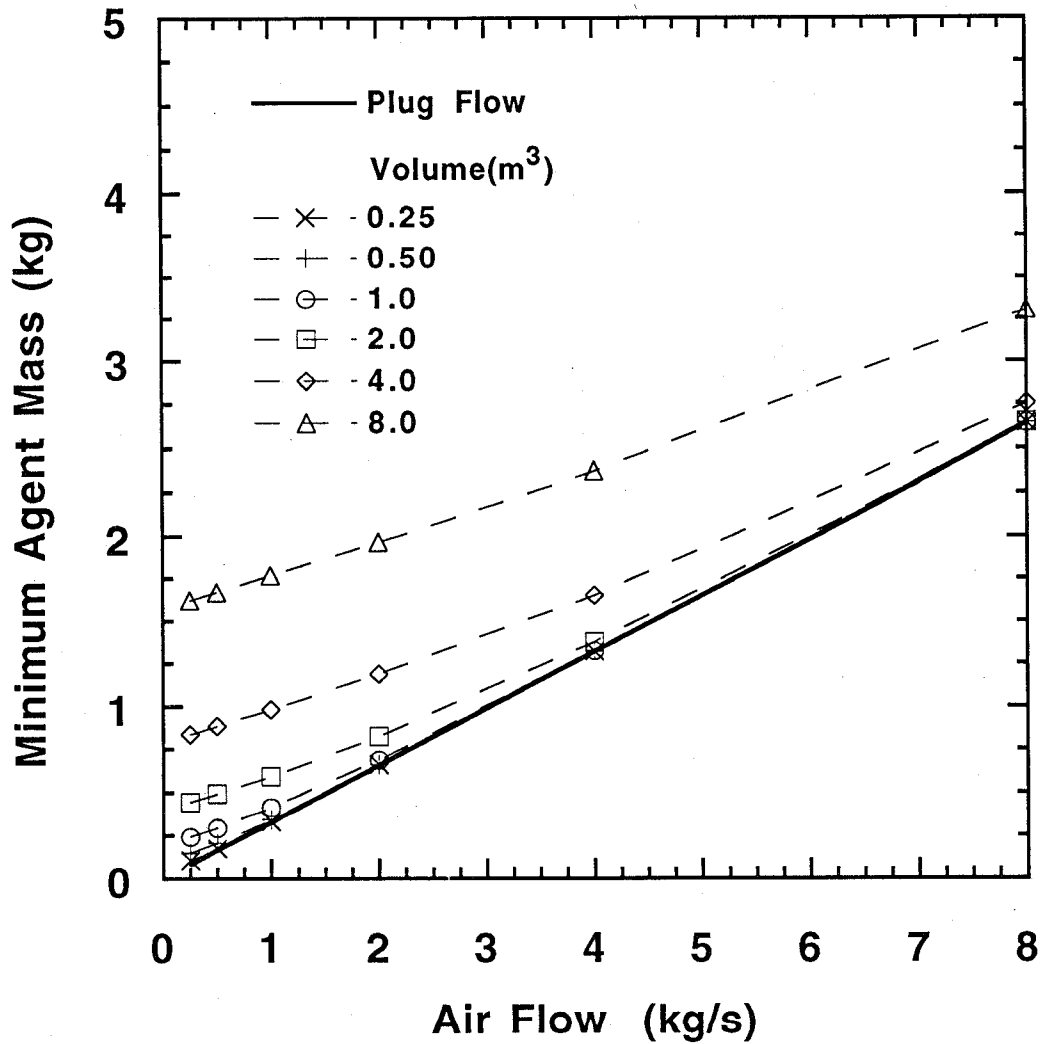


Figure 66. The minimum halon 1301 mass requirements for spray fire suppression as a function of air flow. The agent injection duration was 2.0 s.

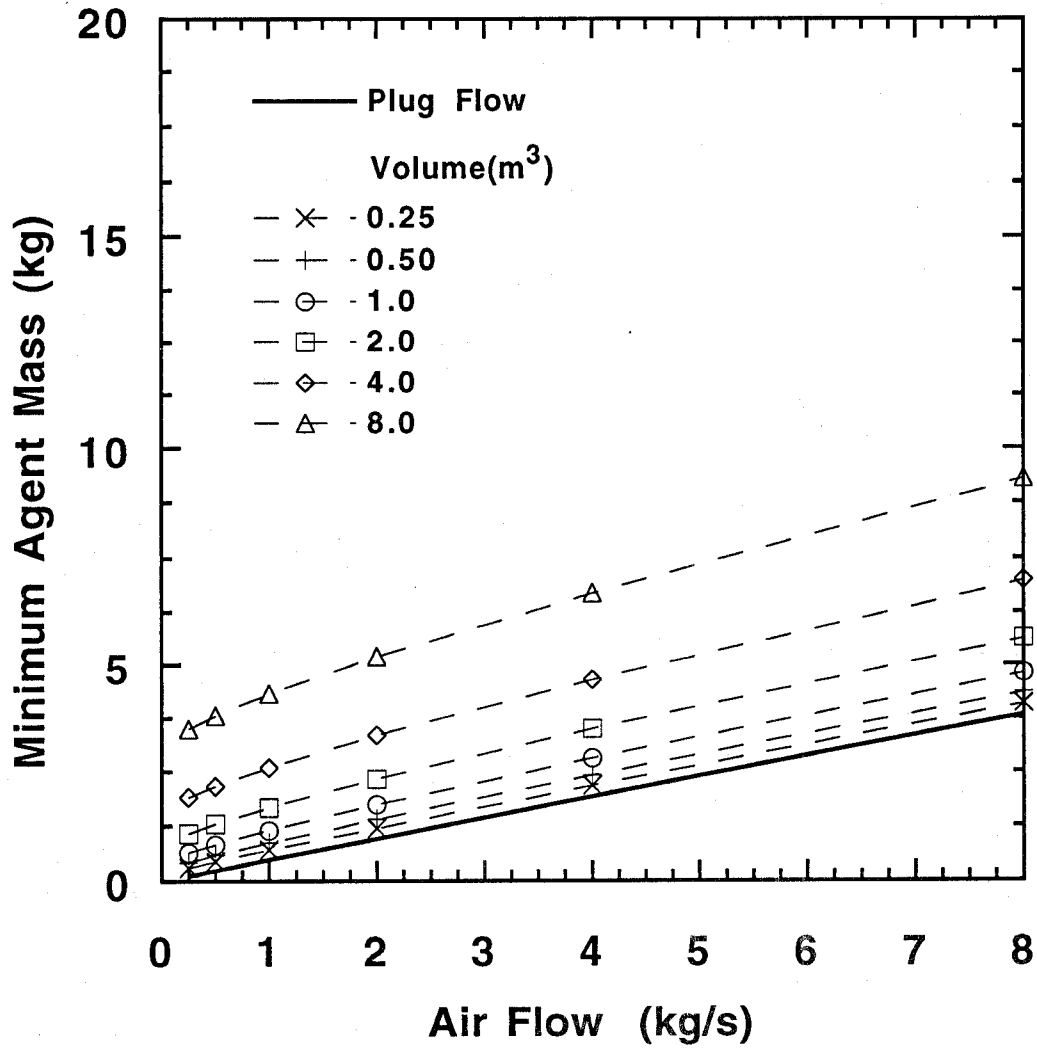


Figure 67. The minimum halon 1301 mass requirements for pool fire suppression as a function of air flow. The agent injection duration was 0.25 s.

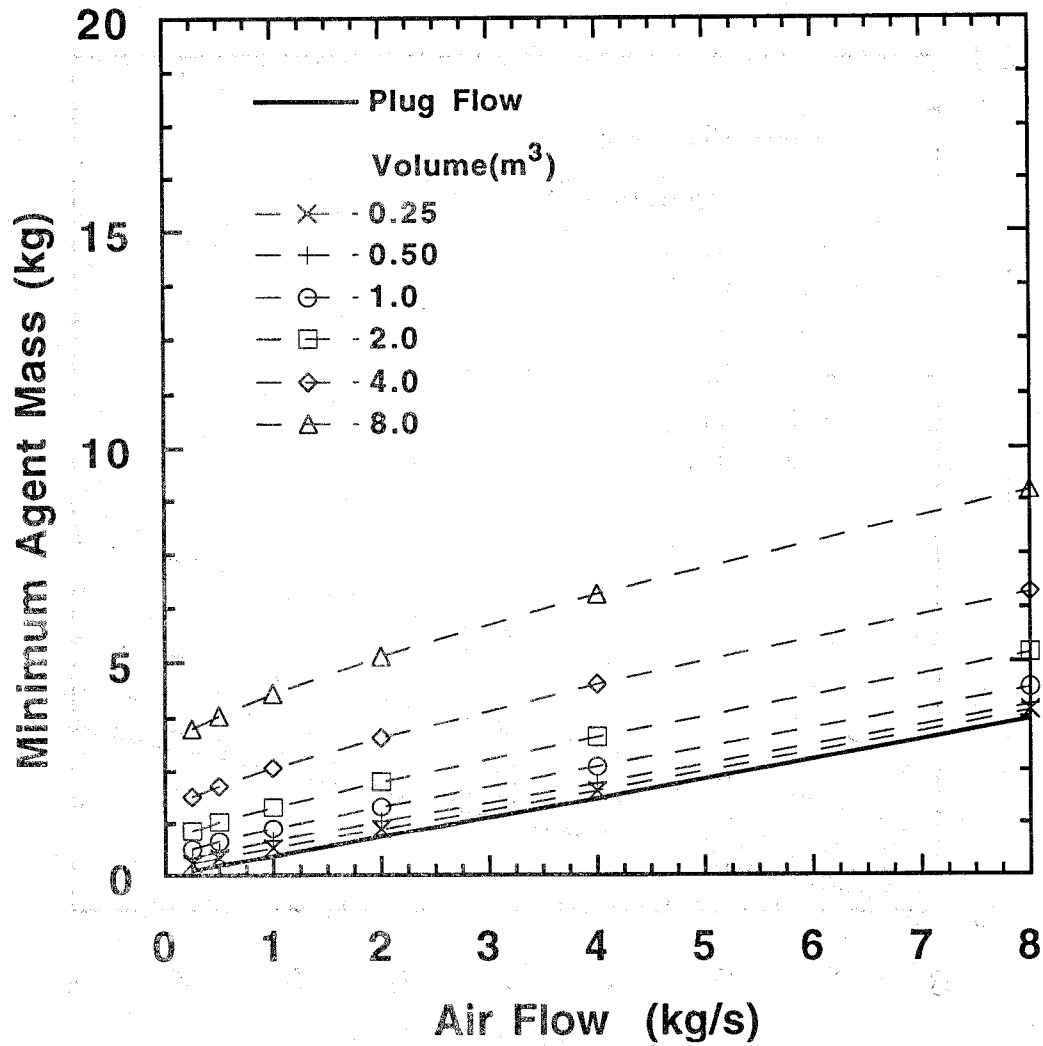


Figure 68. The minimum halon 1301 mass requirements for pool fire suppression as a function of air flow. The agent injection duration was 0.50 s.

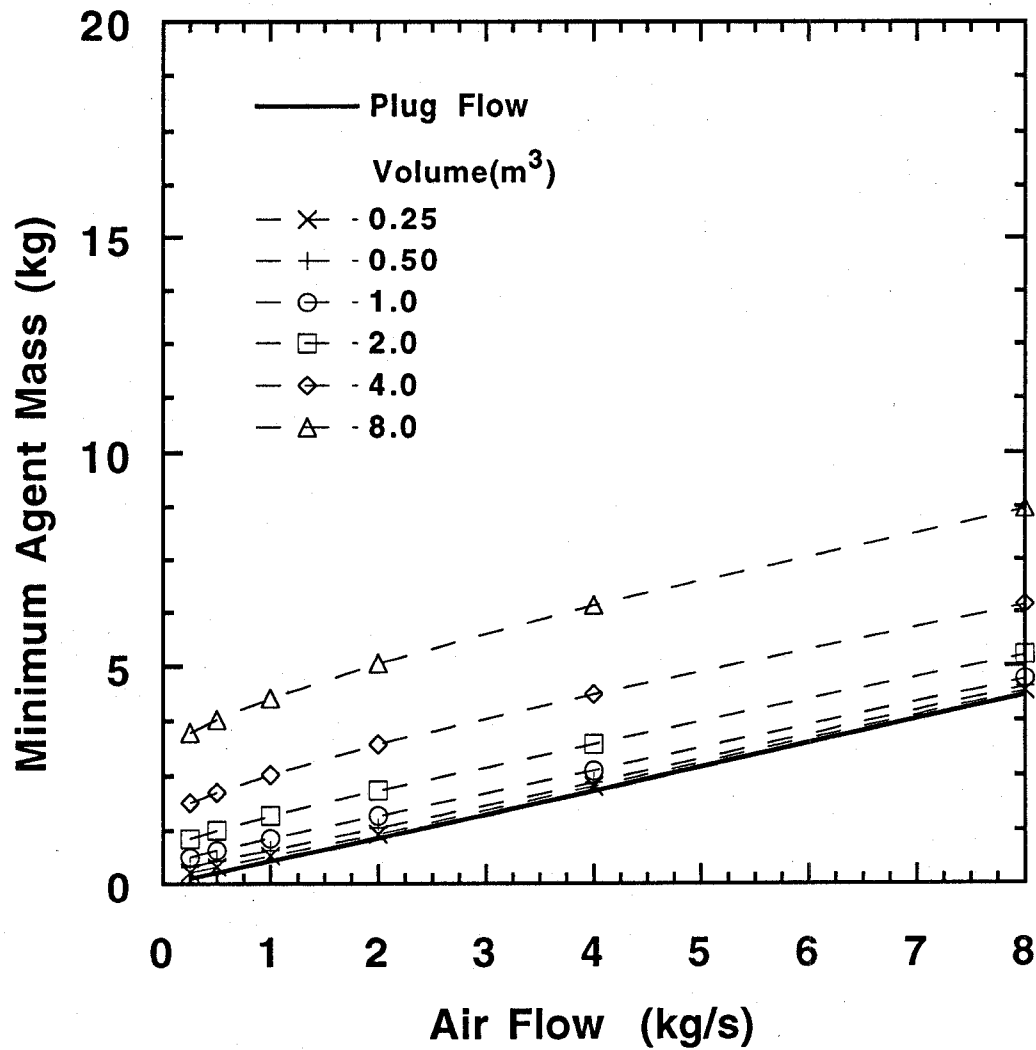


Figure 69. The minimum halon 1301 mass requirements for pool fire suppression as a function of air flow. The agent injection duration was 1.0 s.

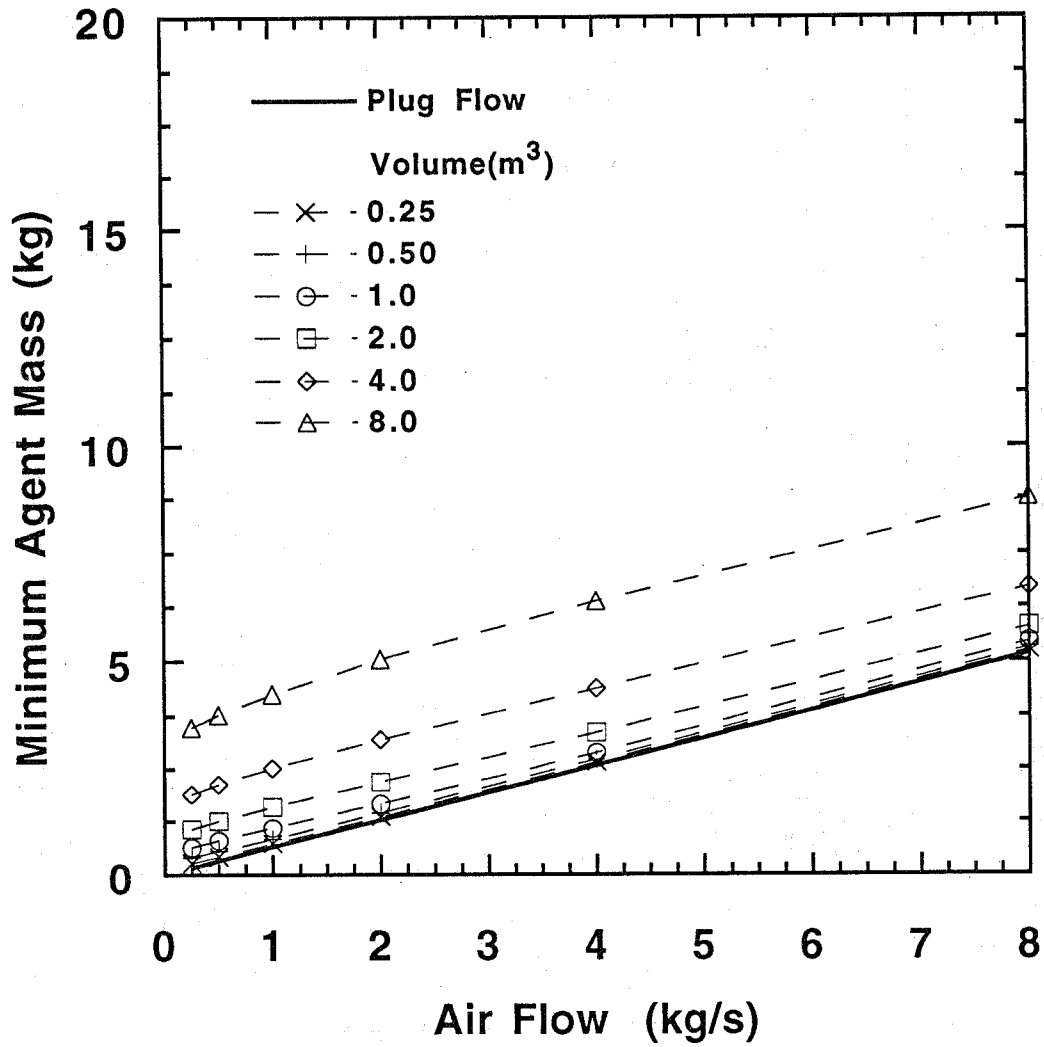


Figure 70. The minimum halon 1301 mass requirements for pool fire suppression as a function of air flow. The agent injection duration was 1.5 s.

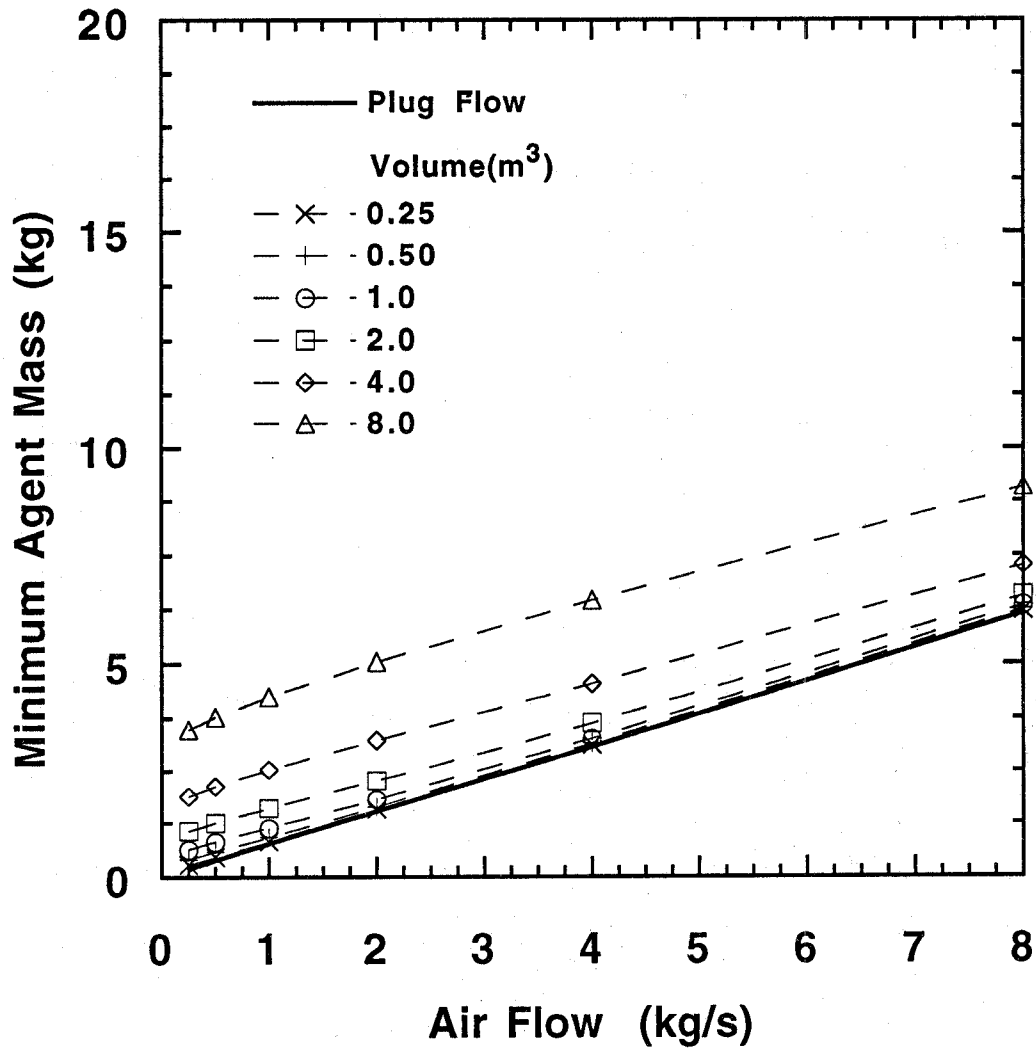


Figure 71. The minimum halon 1301 mass requirements for pool fire suppression as a function of air flow. The agent injection duration was 2.0 s.

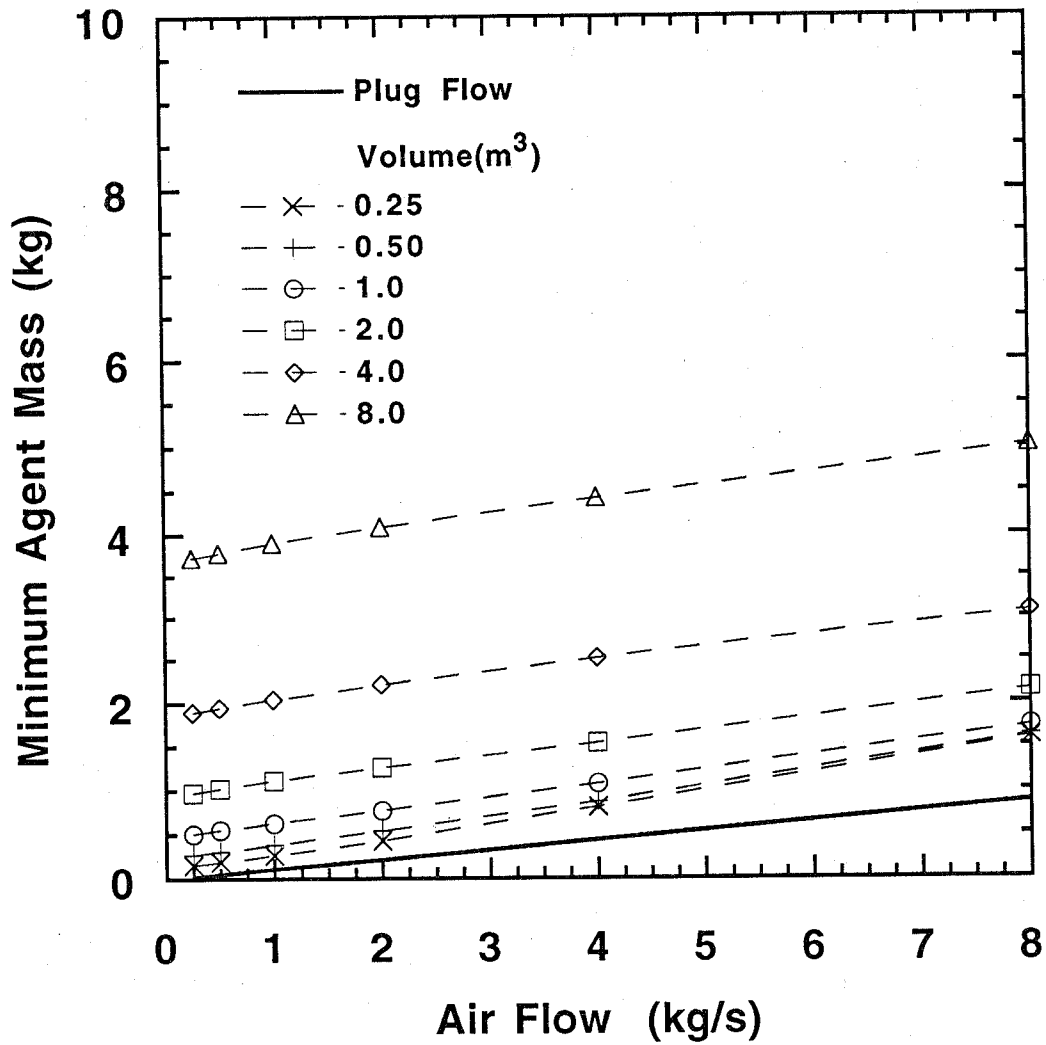


Figure 72. The minimum HFC-125 mass requirements for spray fire suppression as a function of air flow. The agent injection duration was 0.25 s.

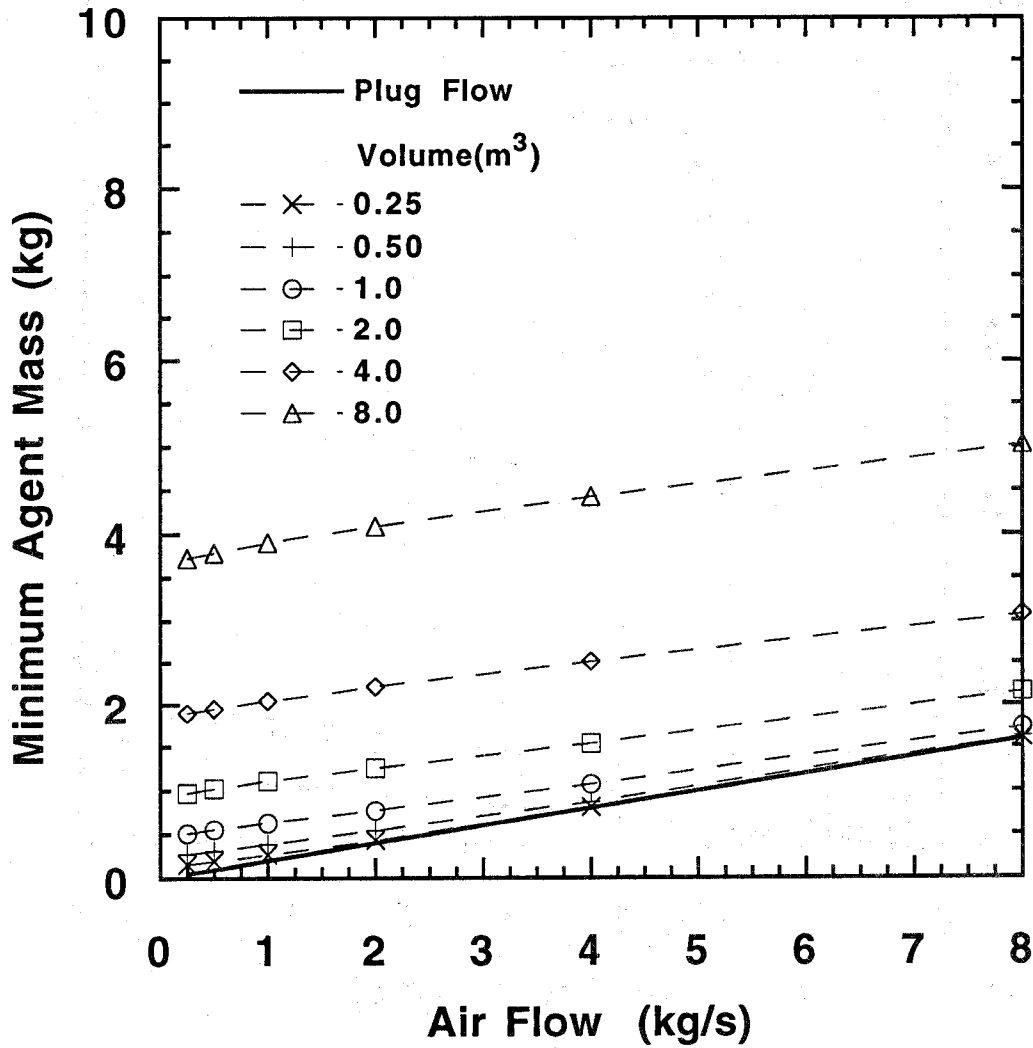


Figure 73. The minimum HFC-125 mass requirements for spray fire suppression as a function of air flow. The agent injection duration was 0.50 s.

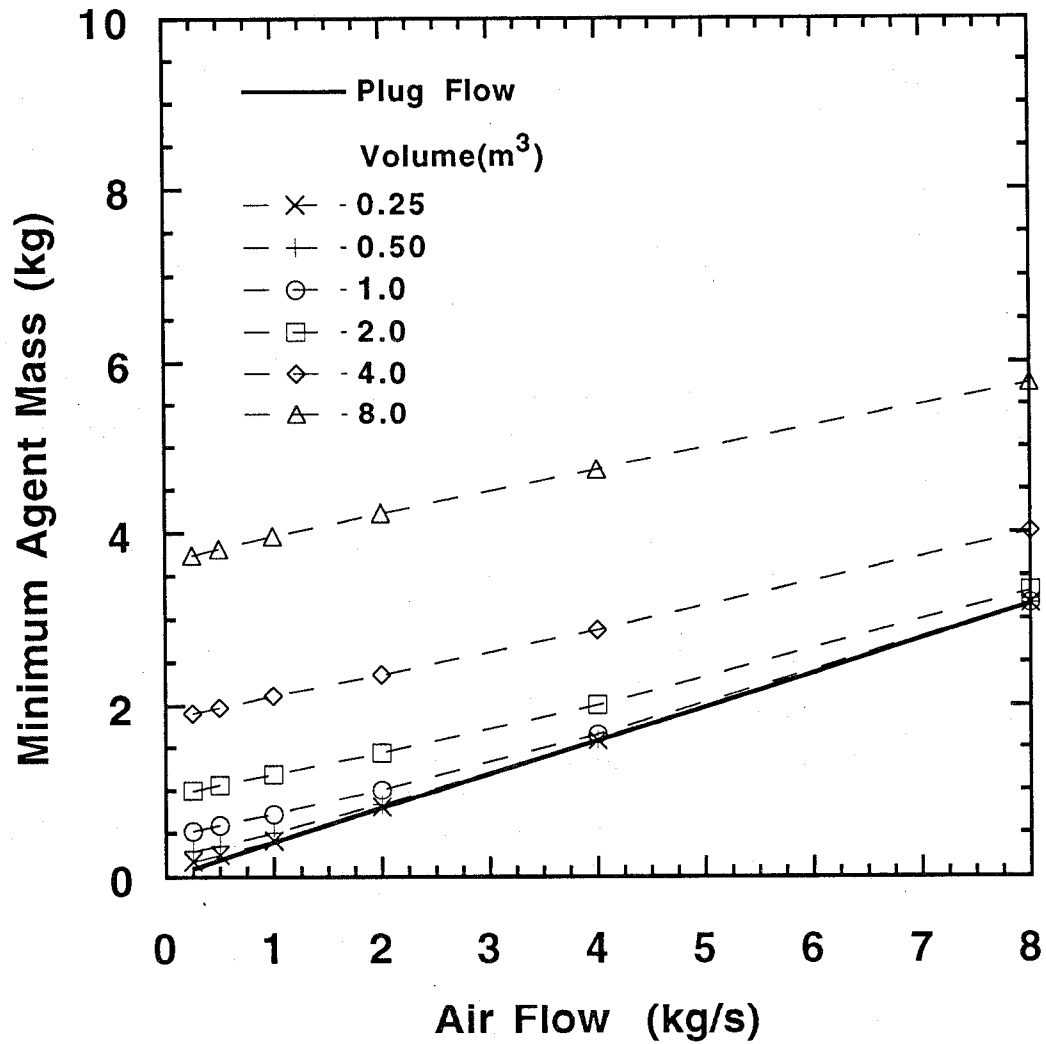


Figure 74. The minimum HFC-125 mass requirements for spray fire suppression as a function of air flow. The agent injection duration was 1.0 s.

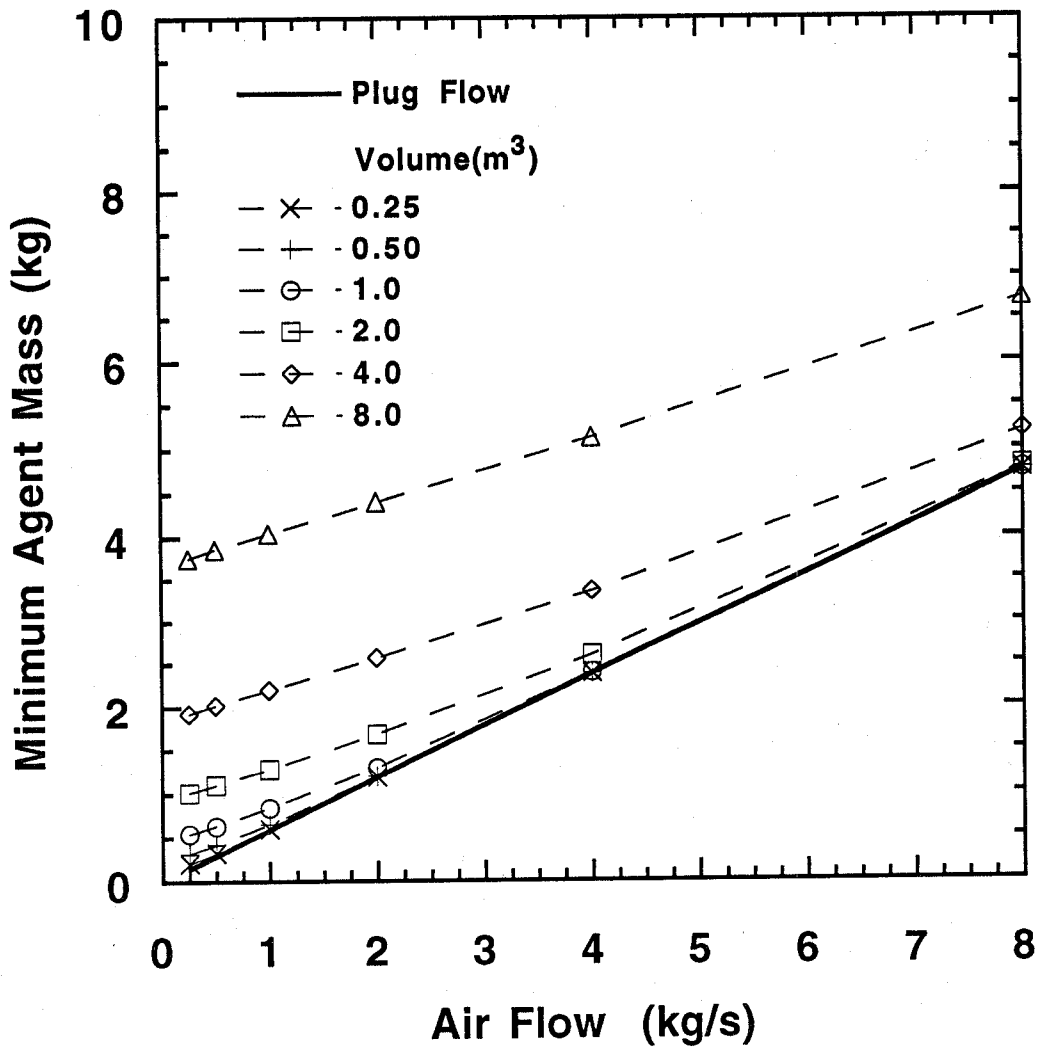


Figure 75. The minimum HFC-125 mass requirements for spray fire suppression as a function of air flow. The agent injection duration was 1.5 s.

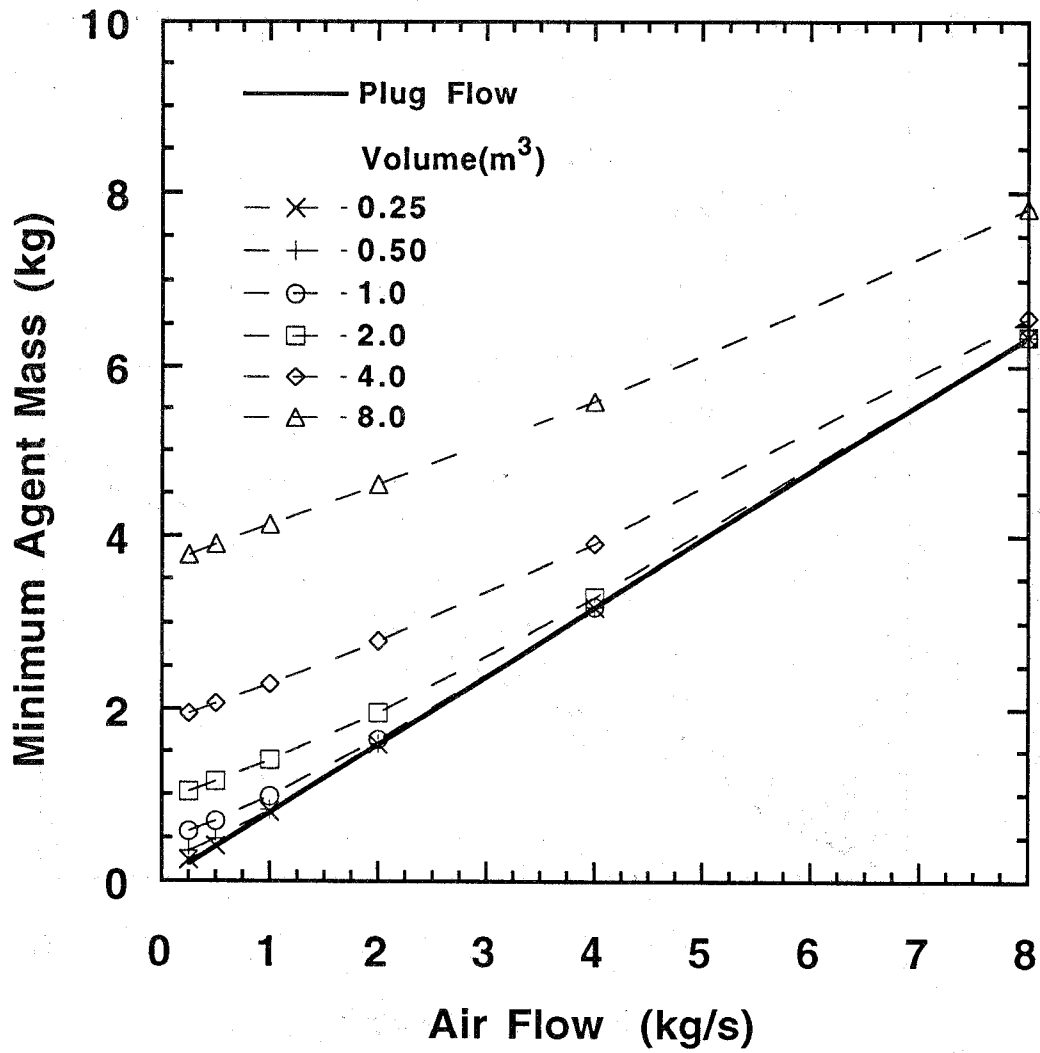


Figure 76. The minimum HFC-125 mass requirements for spray fire suppression as a function of air flow. The agent injection duration was 2.0 s.

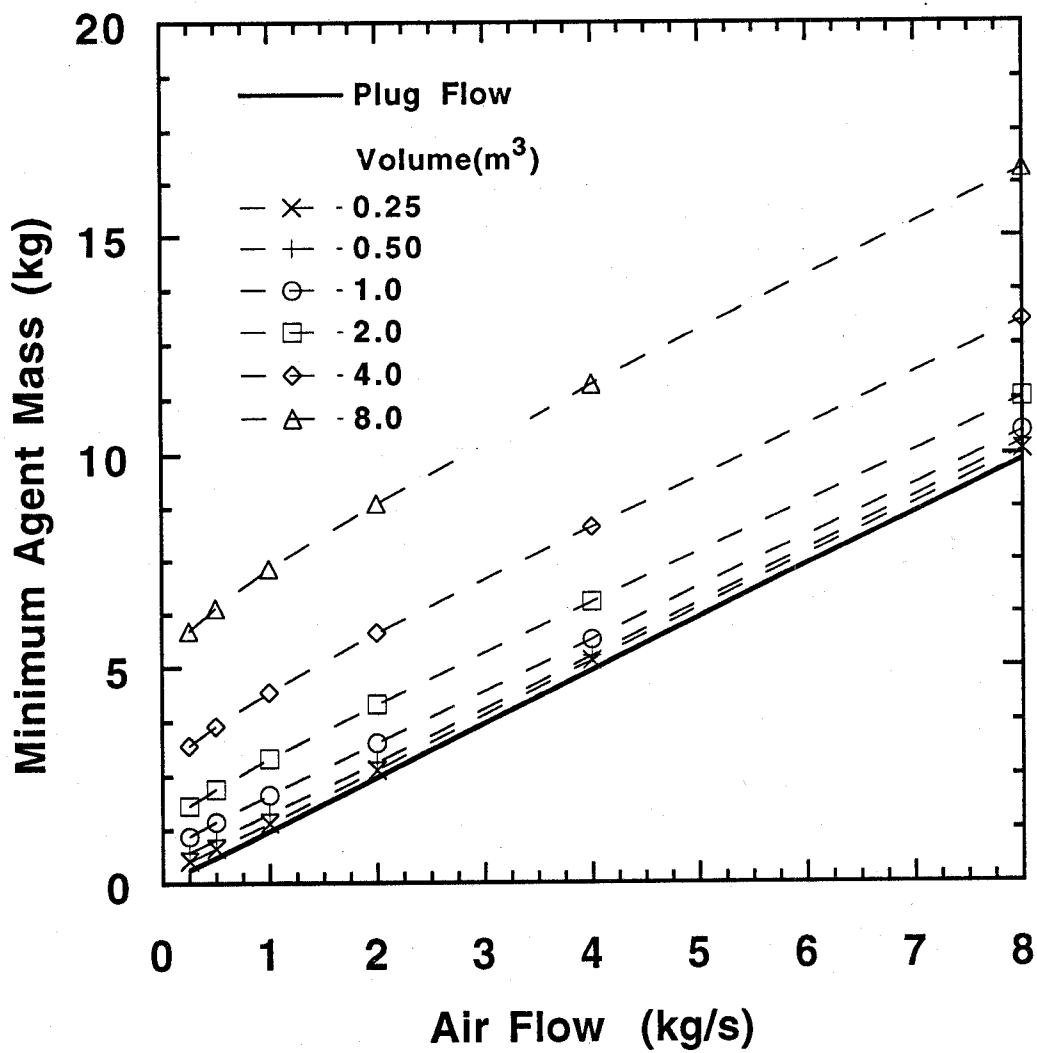


Figure 77. The minimum HFC-125 mass requirements for pool fire suppression as a function of air flow. The agent injection duration was 0.25 s.

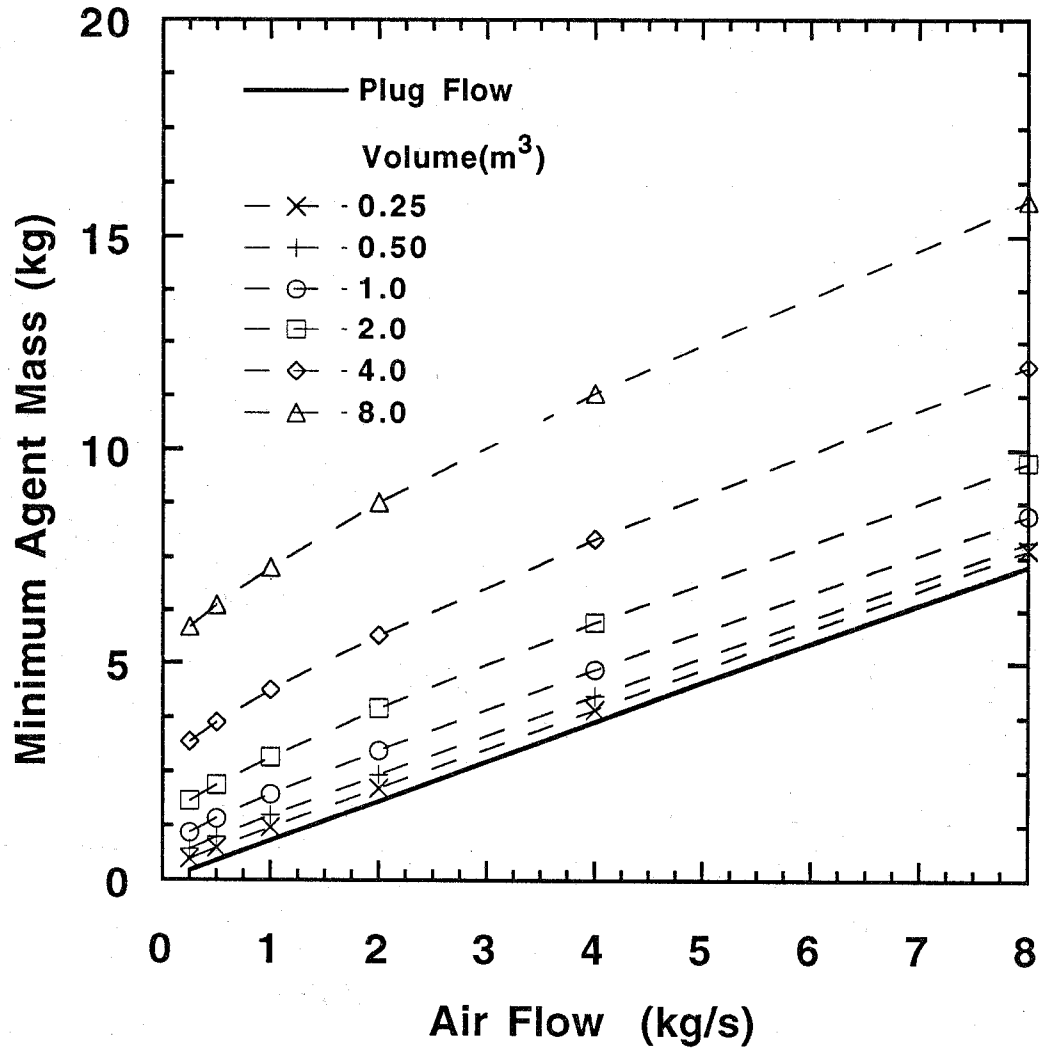


Figure 78. The minimum HFC-125 mass requirements for pool fire suppression as a function of air flow. The agent injection duration was 0.50 s.

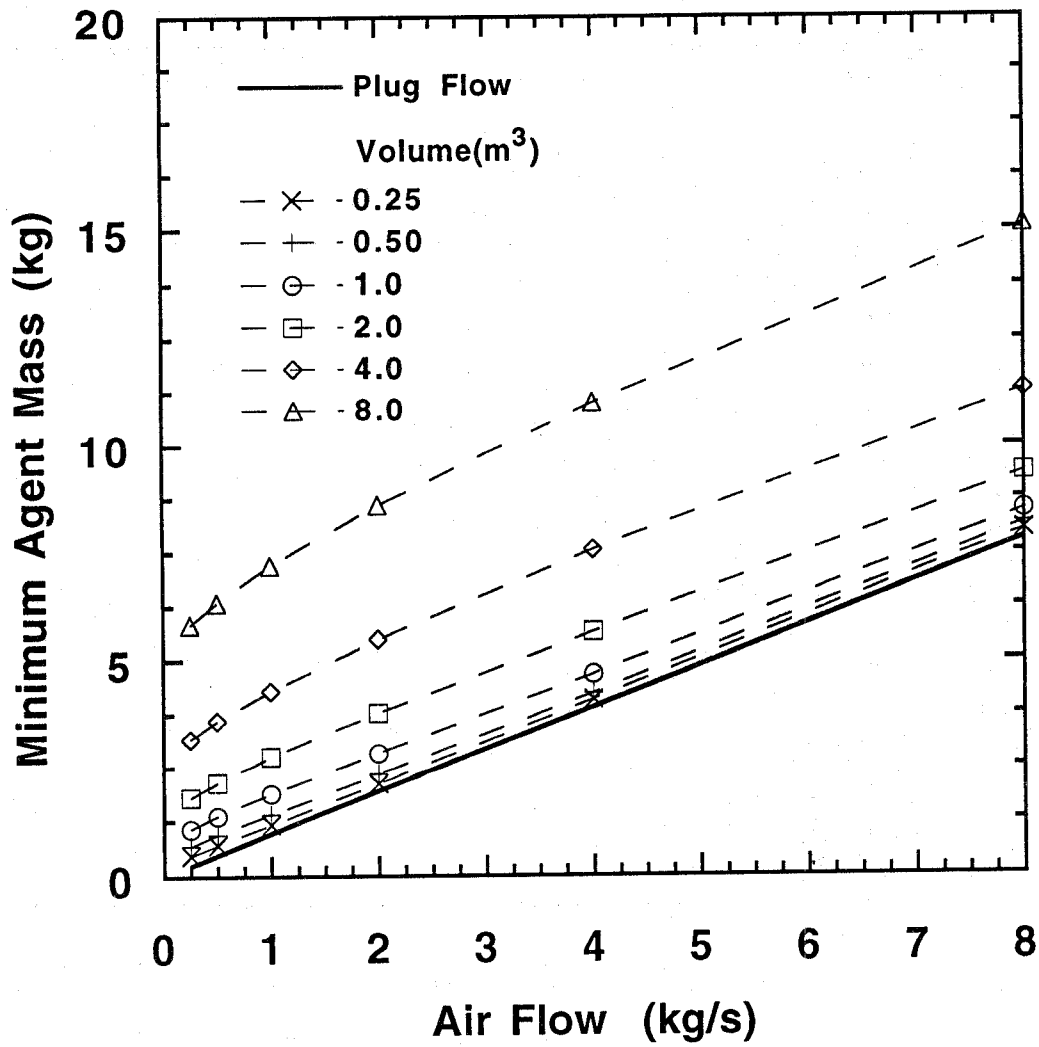


Figure 79. The minimum HFC-125 mass requirements for pool fire suppression as a function of air flow. The agent injection duration was 1.0 s.

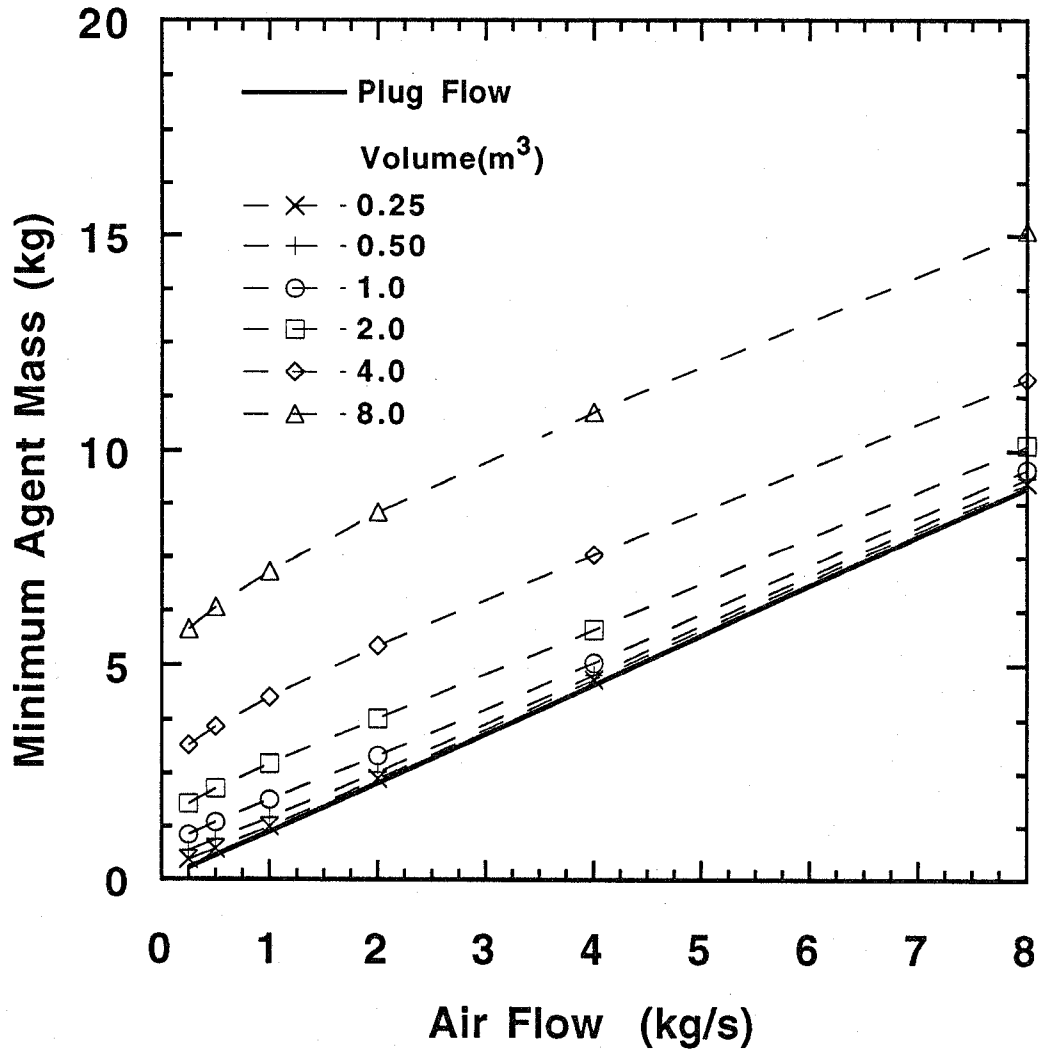


Figure 80. The minimum HFC-125 mass requirements for pool fire suppression as a function of air flow. The agent injection duration was 1.5 s.

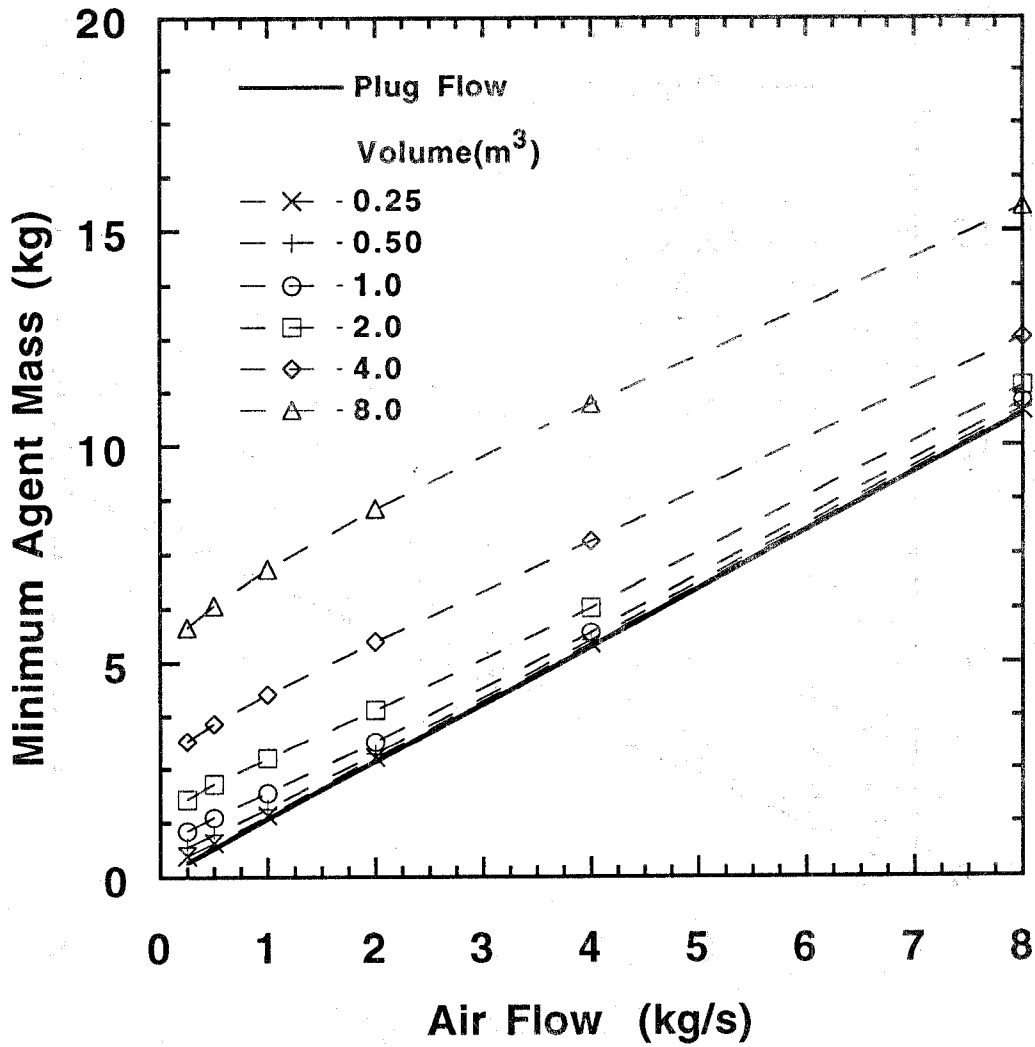


Figure 81. The minimum HFC-125 mass requirements for pool fire suppression as a function of air flow. The agent injection duration was 2.0 s.

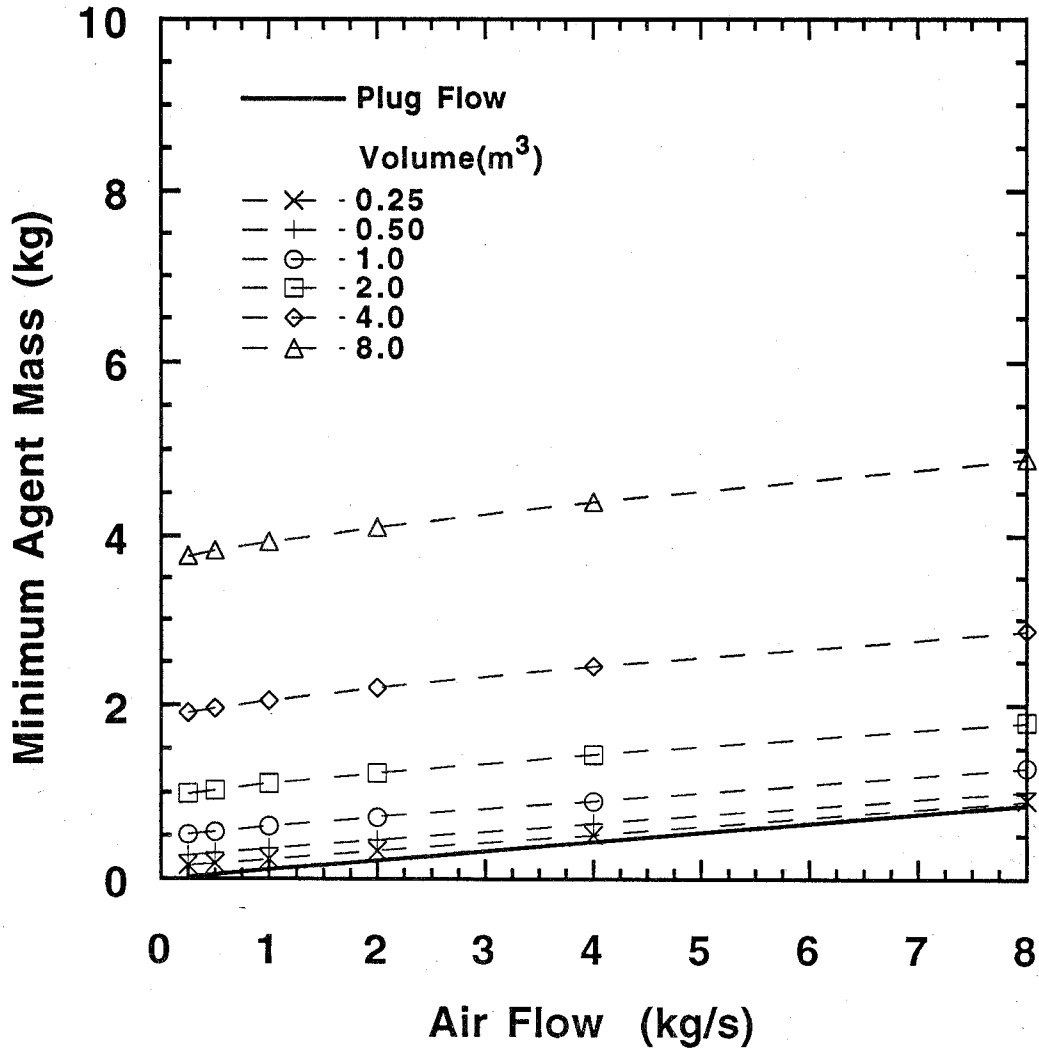


Figure 82. The minimum HFC-227 mass requirements for spray fire suppression as a function of air flow. The agent injection duration was 0.25 s.

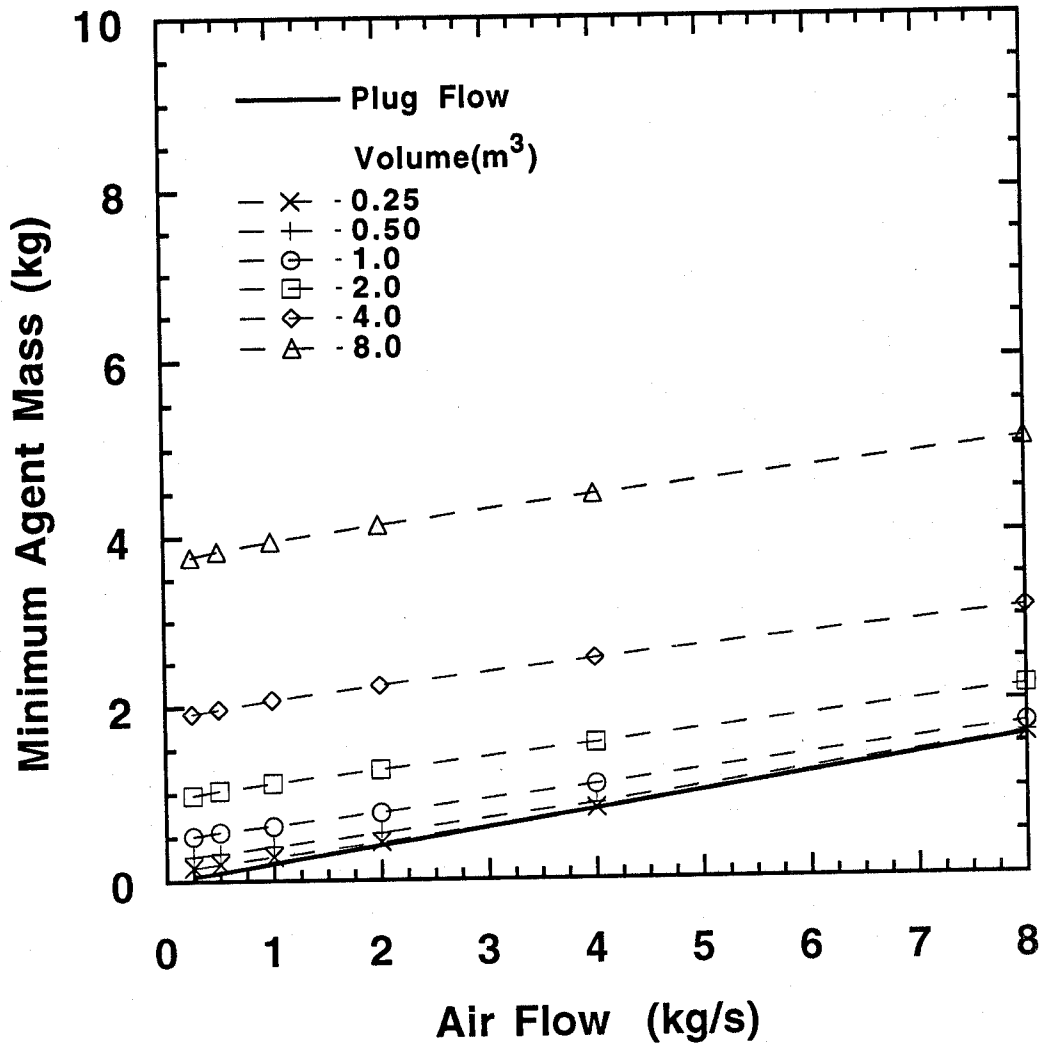


Figure 83. The minimum HFC-227 mass requirements for spray fire suppression as a function of air flow. The agent injection duration was 0.50 s.

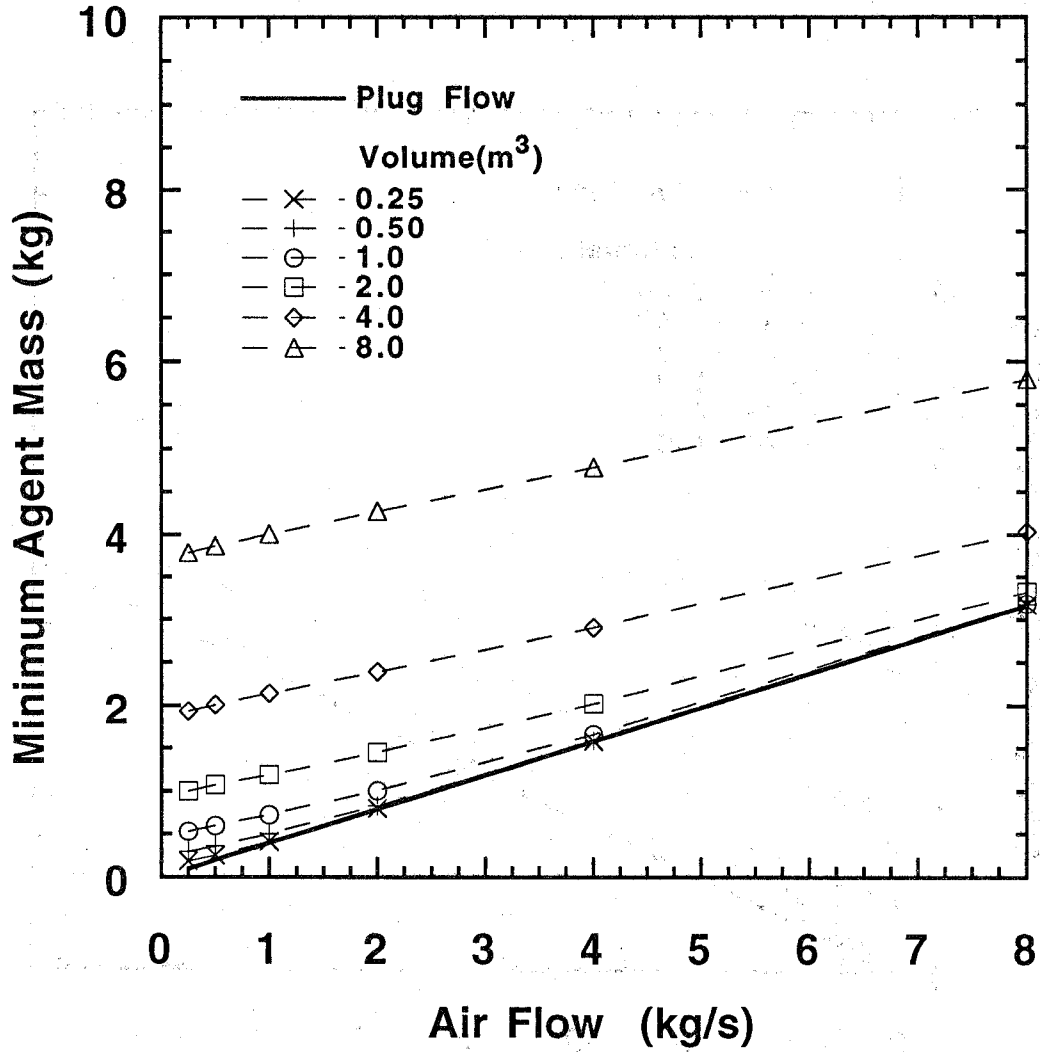


Figure 84. The minimum HFC-227 mass requirements for spray fire suppression as a function of air flow. The agent injection duration was 1.0 s.

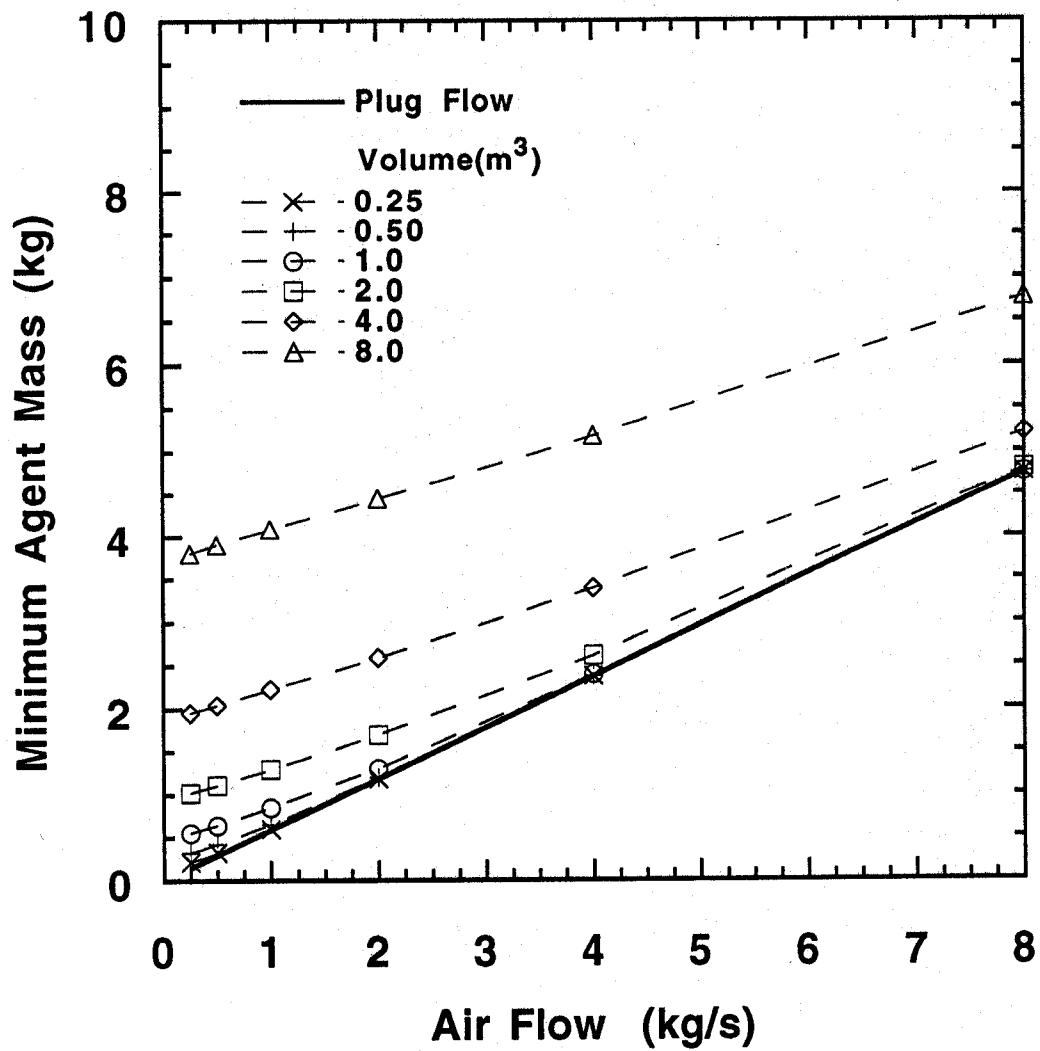


Figure 85. The minimum HFC-227 mass requirements for spray fire suppression as a function of air flow. The agent injection duration was 1.5 s.

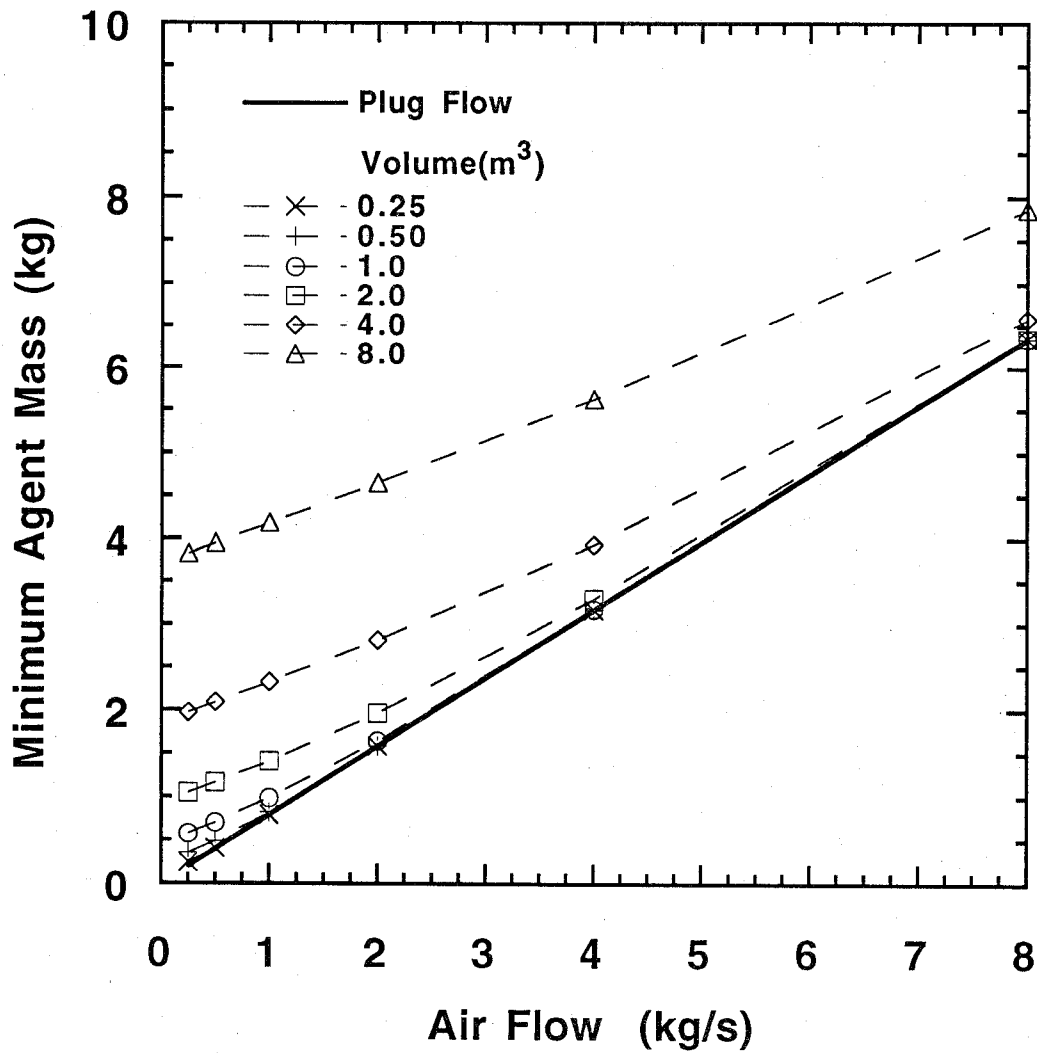


Figure 86. The minimum HFC-227 mass requirements for spray fire suppression as a function of air flow. The agent injection duration was 2.0 s.

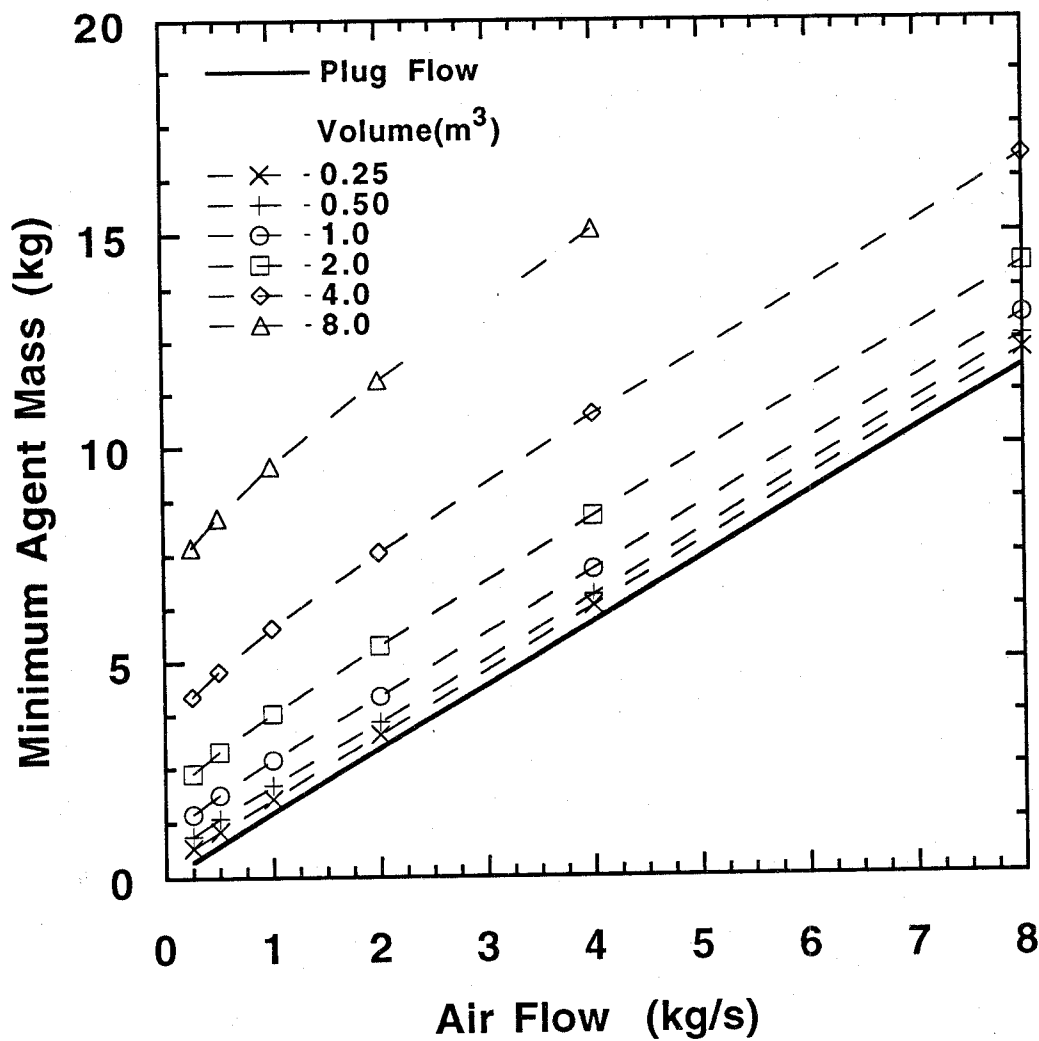


Figure 87. The minimum HFC-227 mass requirements for pool fire suppression as a function of air flow. The agent injection duration was 0.25 s.

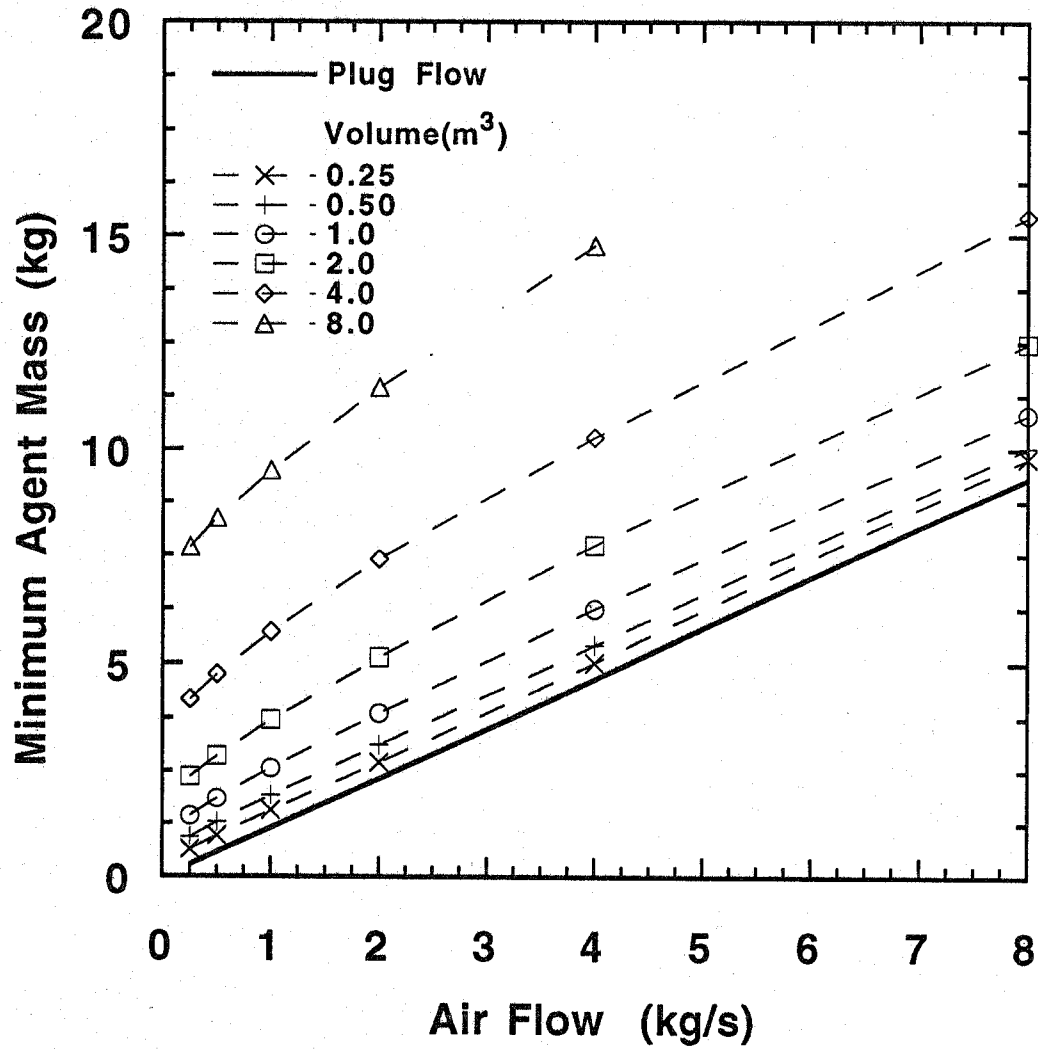


Figure 88. The minimum HFC-227 mass requirements for pool fire suppression as a function of air flow. The agent injection duration was 0.50 s.

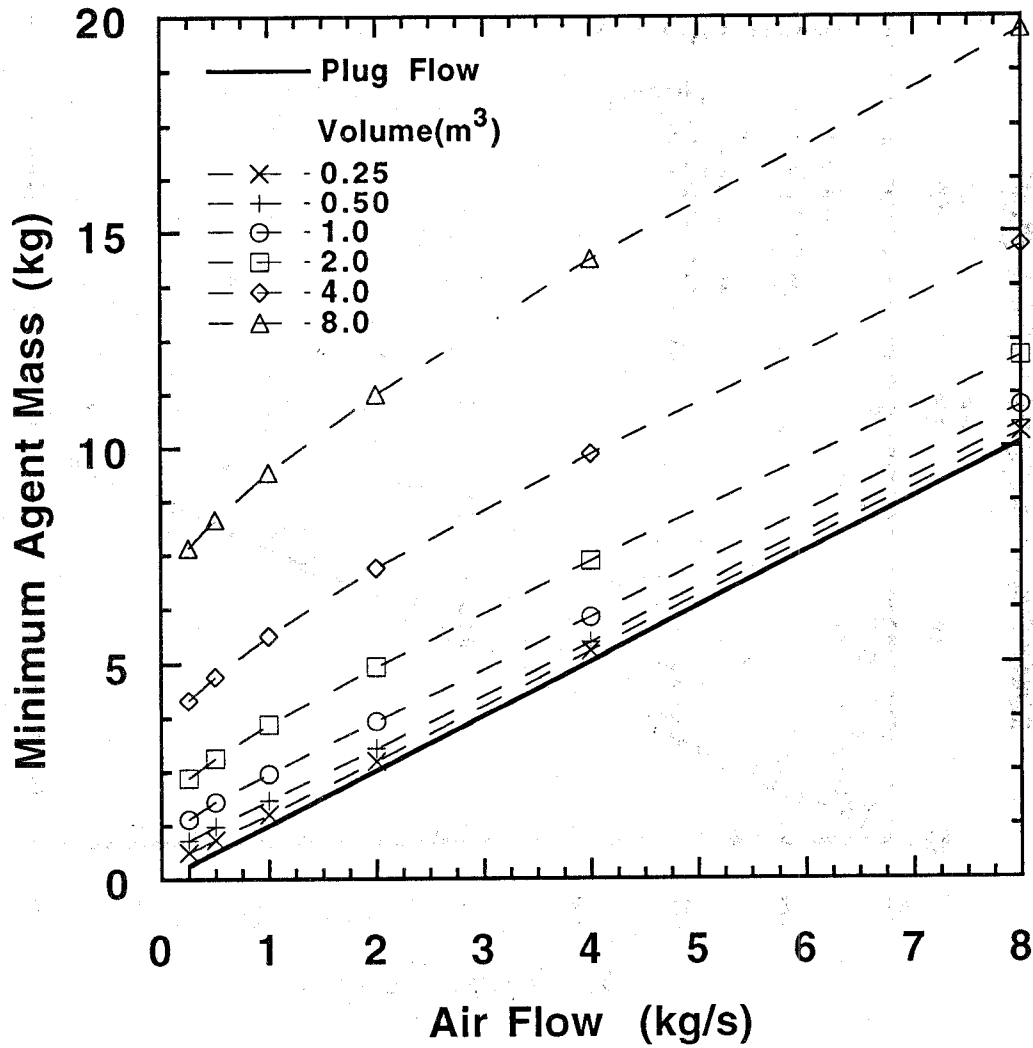


Figure 89: The minimum HFC-227 mass requirements for pool fire suppression as a function of air flow. The agent injection duration was 1.0 s.

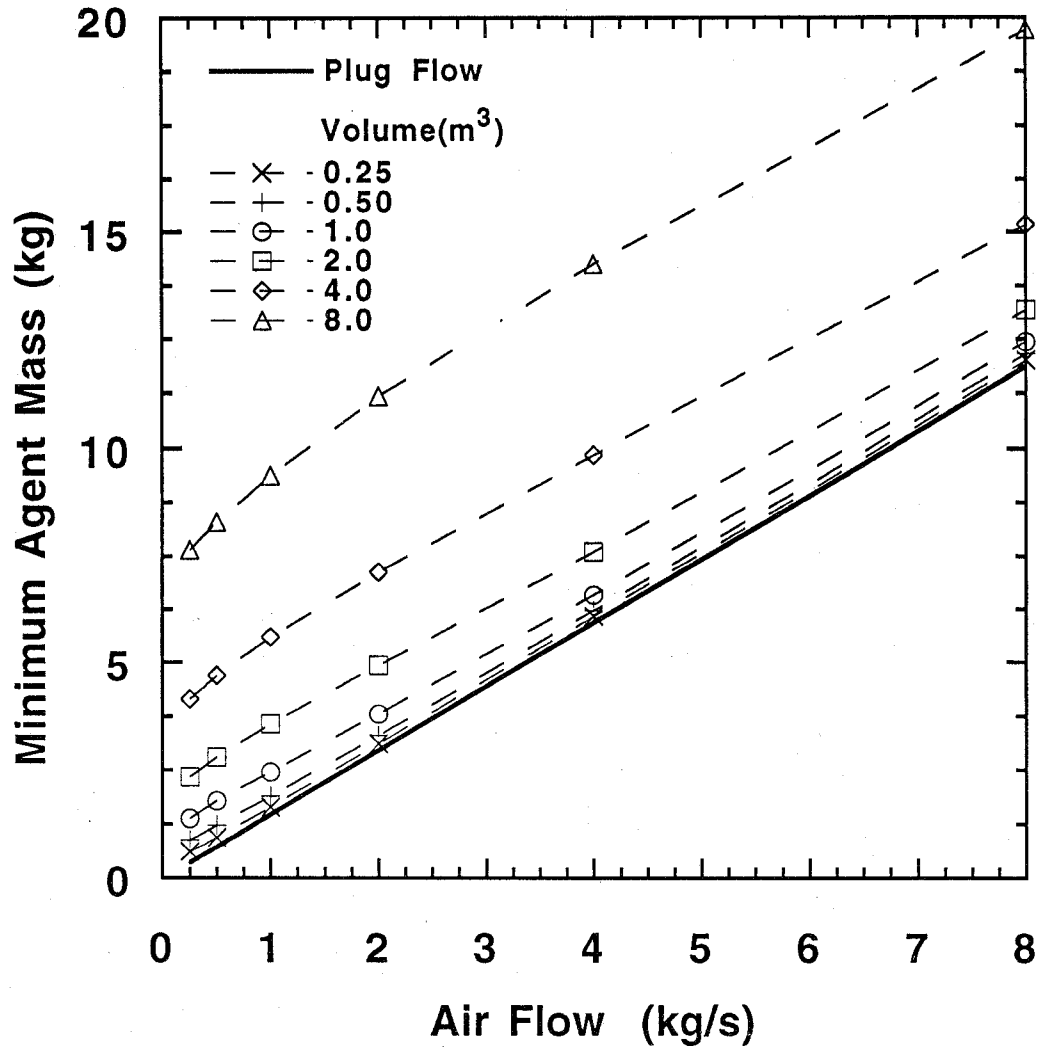


Figure 90. The minimum HFC-227 mass requirements for pool fire suppression as a function of air flow. The agent injection duration was 1.5 s.

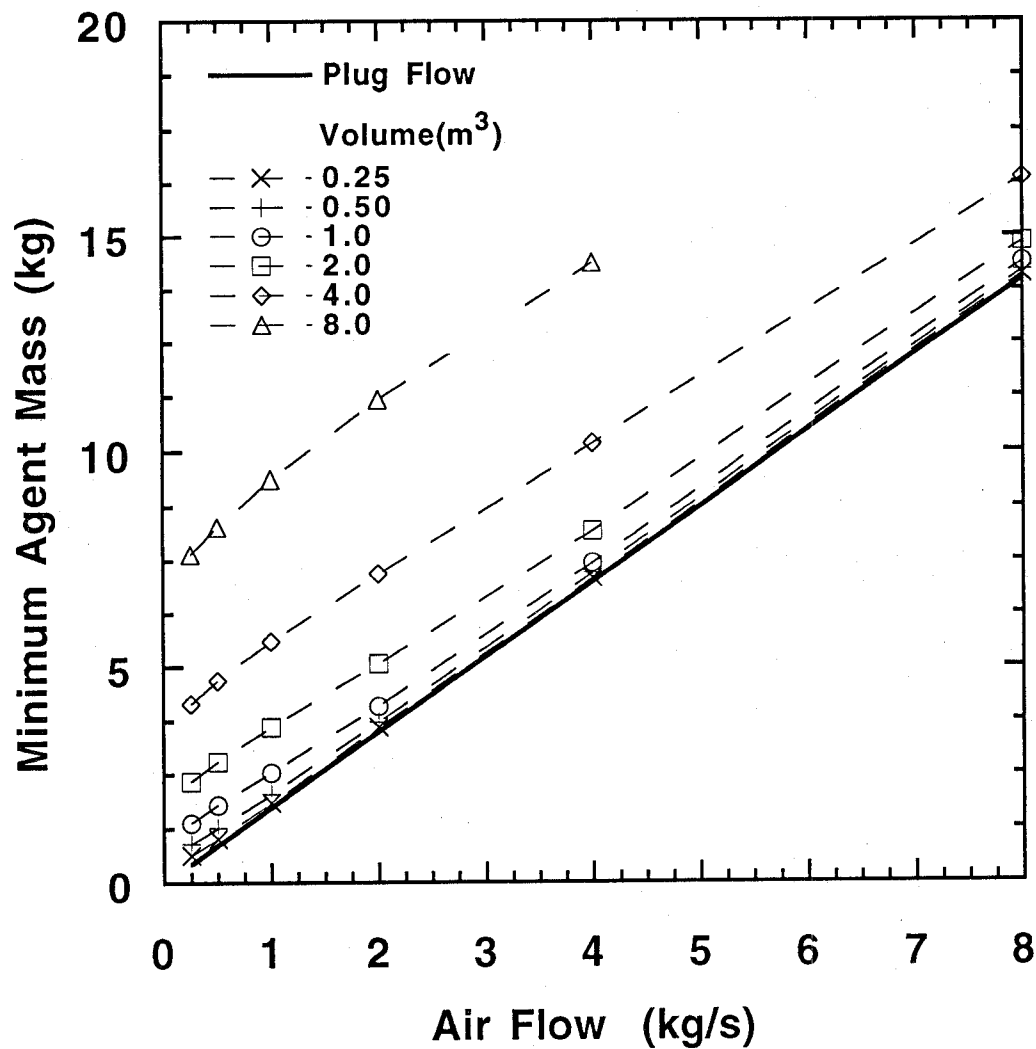


Figure 91. The minimum HFC-227 mass requirements for pool fire suppression as a function of air flow. The agent injection duration was 2.0 s.

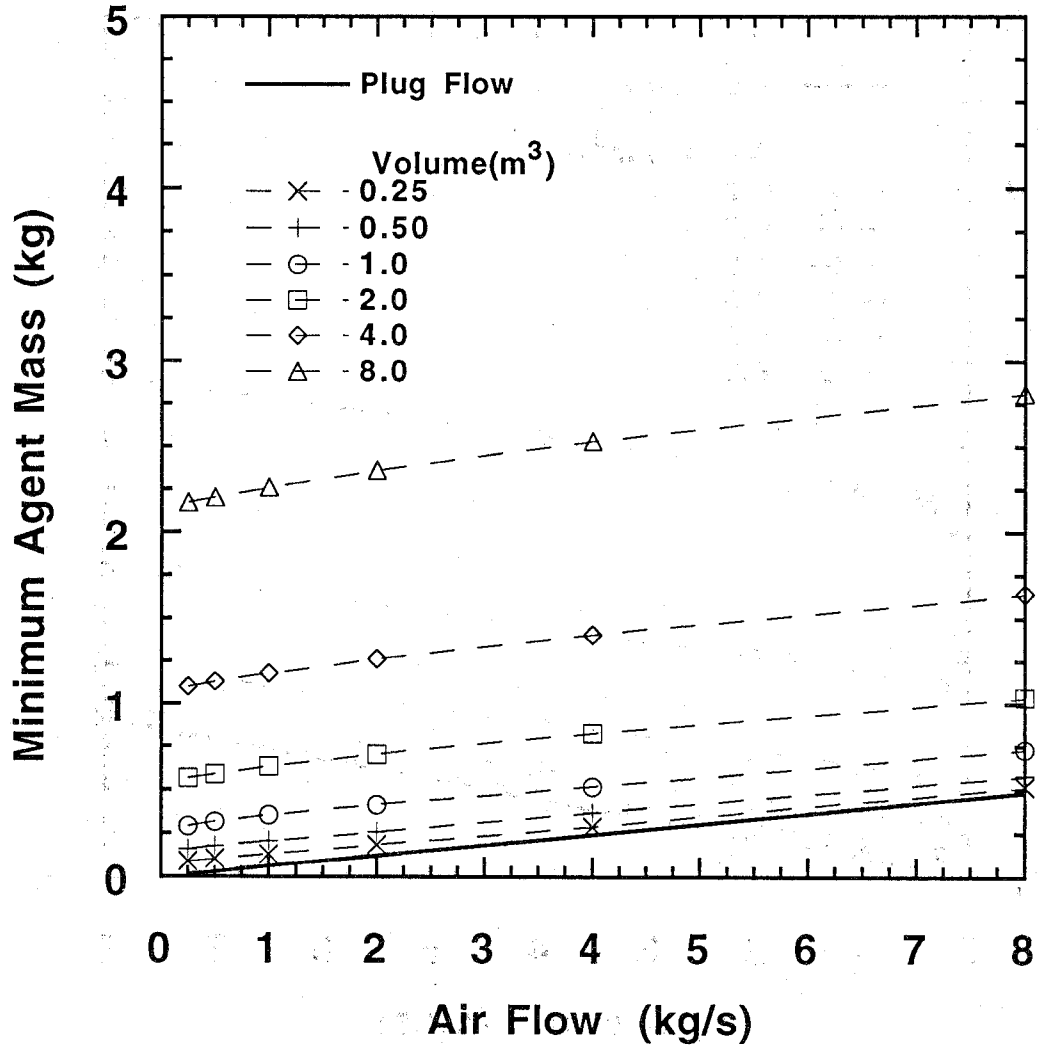


Figure 92. The minimum CF_3I mass requirements for spray fire suppression as a function of air flow. The agent injection duration was 0.25 s.

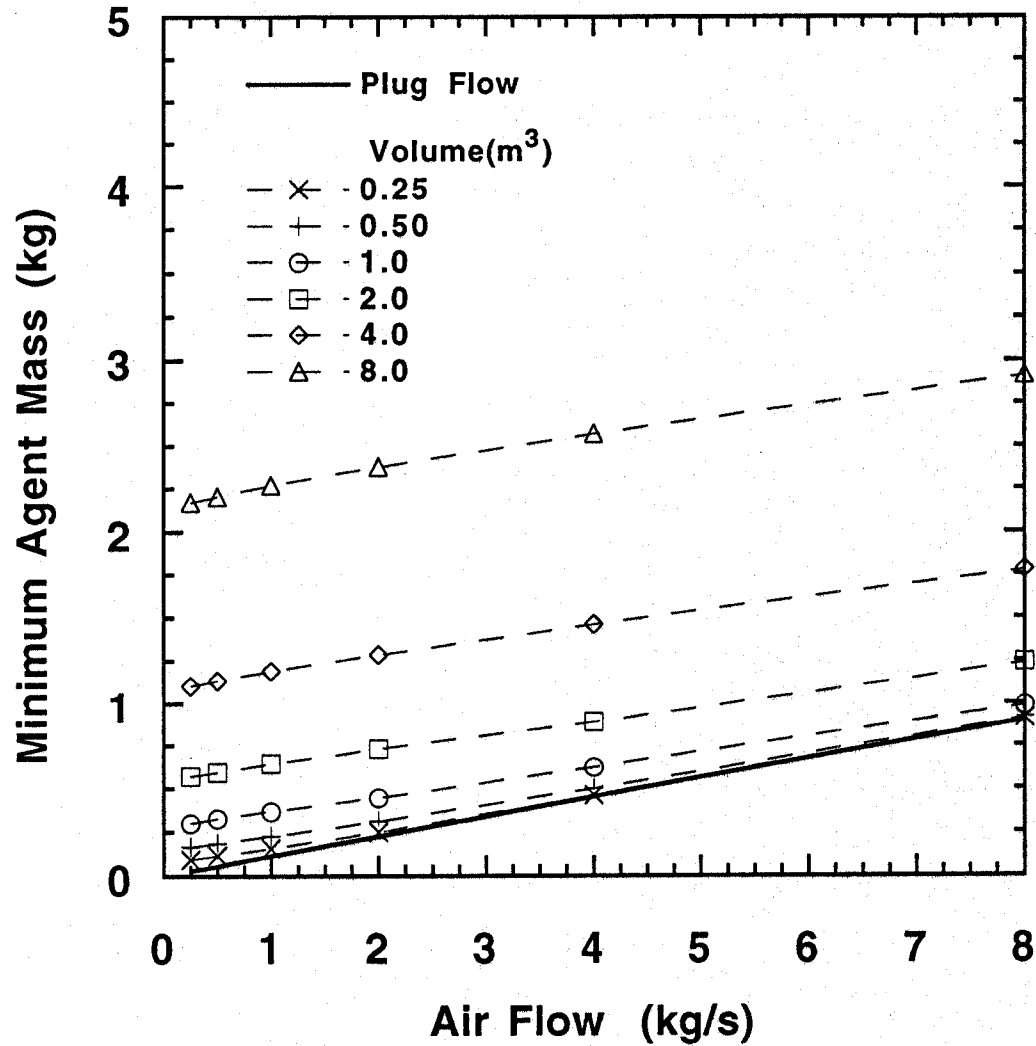


Figure 93. The minimum CF_3I mass requirements for spray fire suppression as a function of air flow. The agent injection duration was 0.50 s.

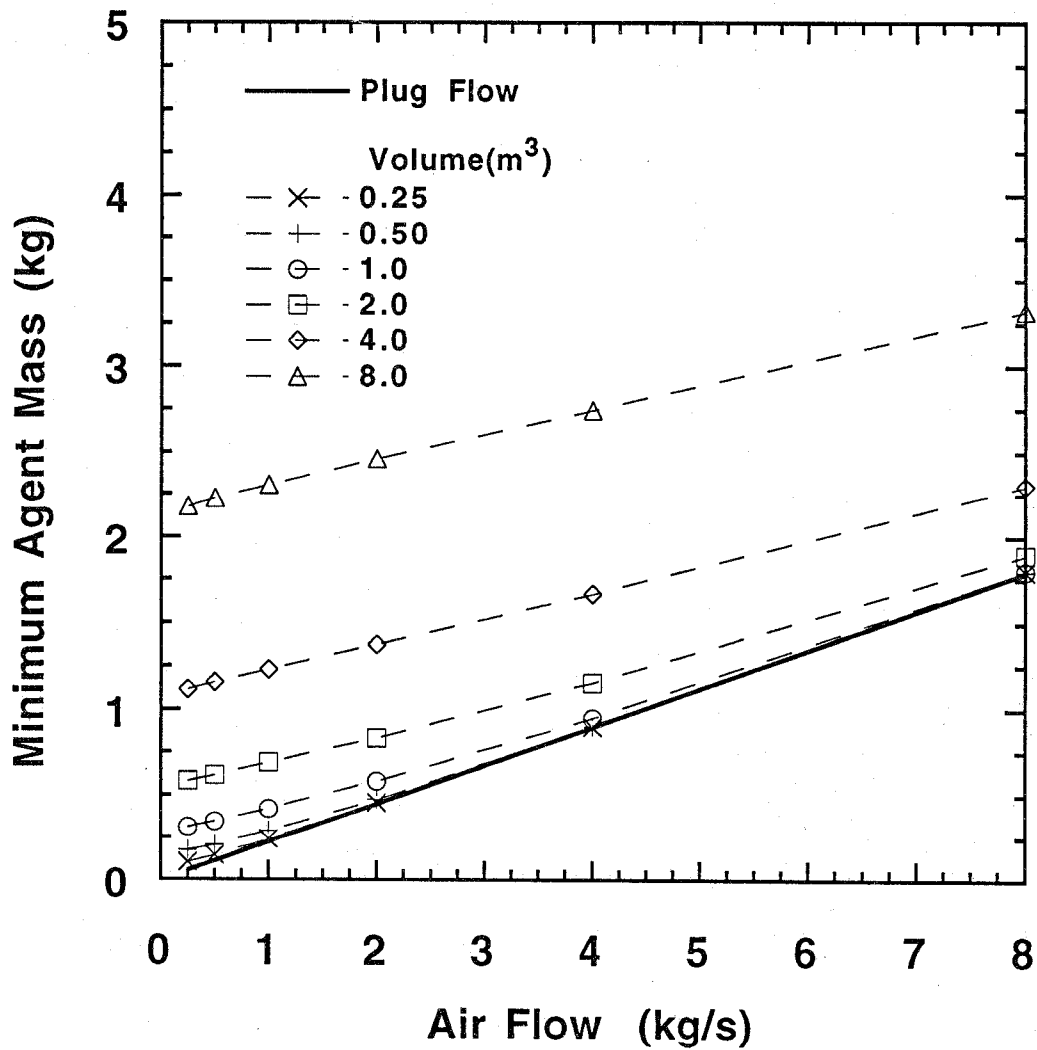


Figure 94. The minimum CF_3I mass requirements for spray fire suppression as a function of air flow. The agent injection duration was 1.0 s.

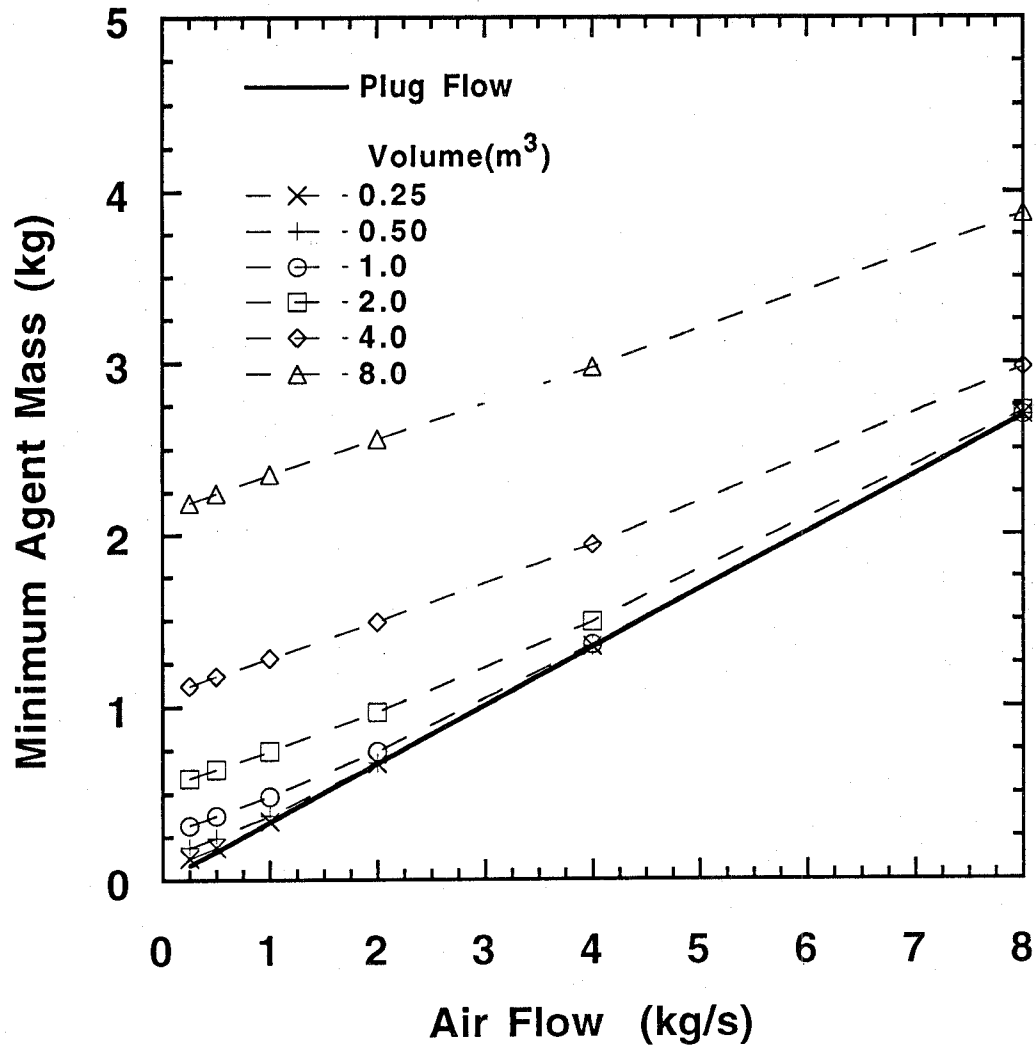


Figure 95. The minimum CF_3I mass requirements for spray fire suppression as a function of air flow. The agent injection duration was 1.5 s.

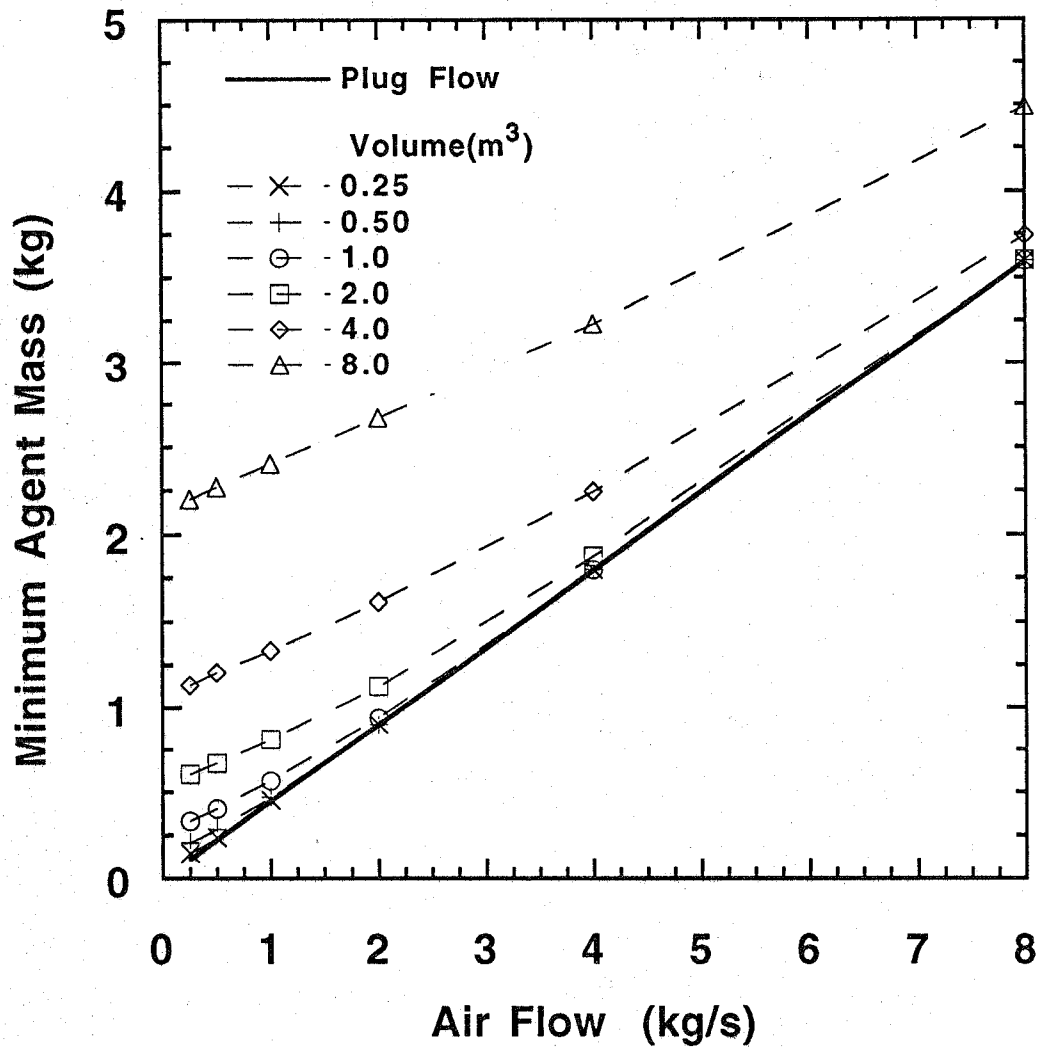


Figure 96. The minimum CF_3I mass requirements for spray fire suppression as a function of air flow. The agent injection duration was 2.0 s.

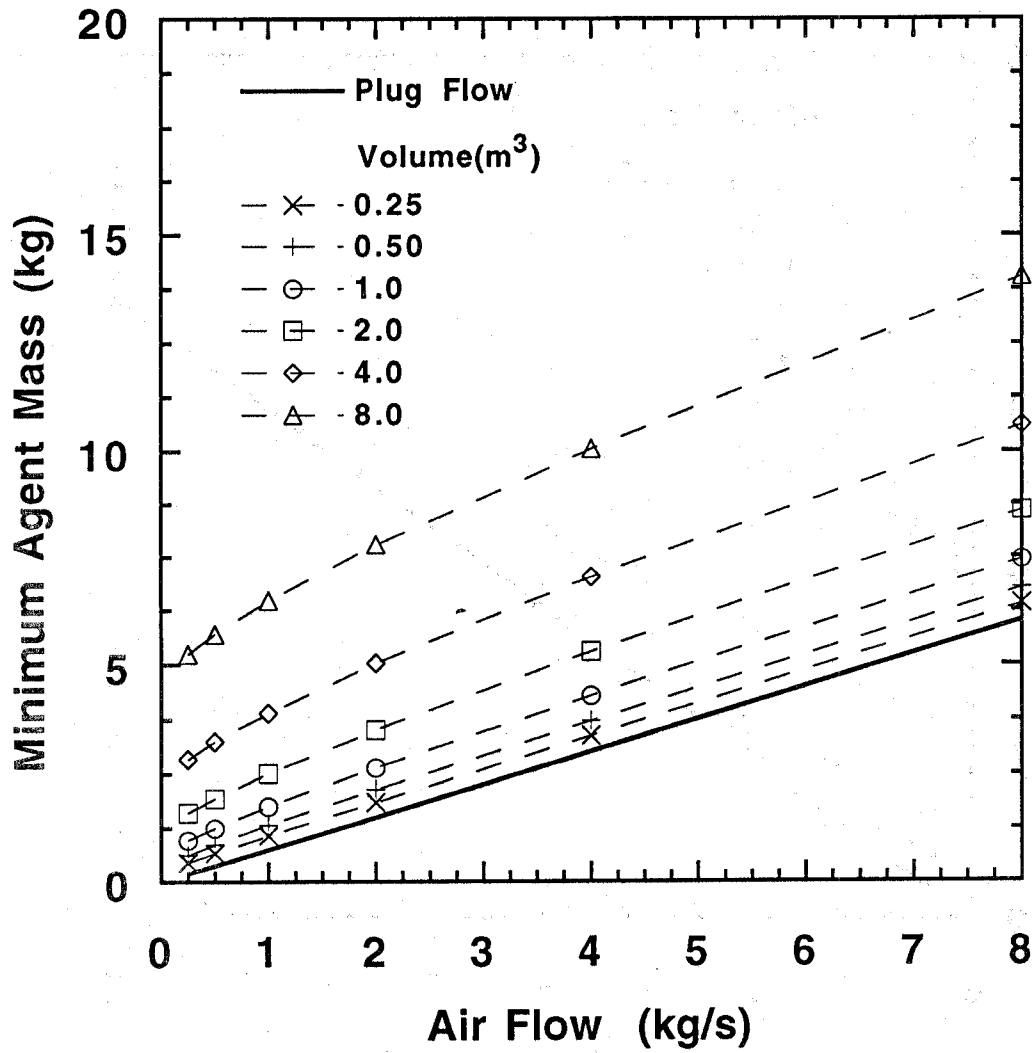


Figure 97. The minimum CF_3I mass requirements for pool fire suppression as a function of air flow. The agent injection duration was 0.25 s.

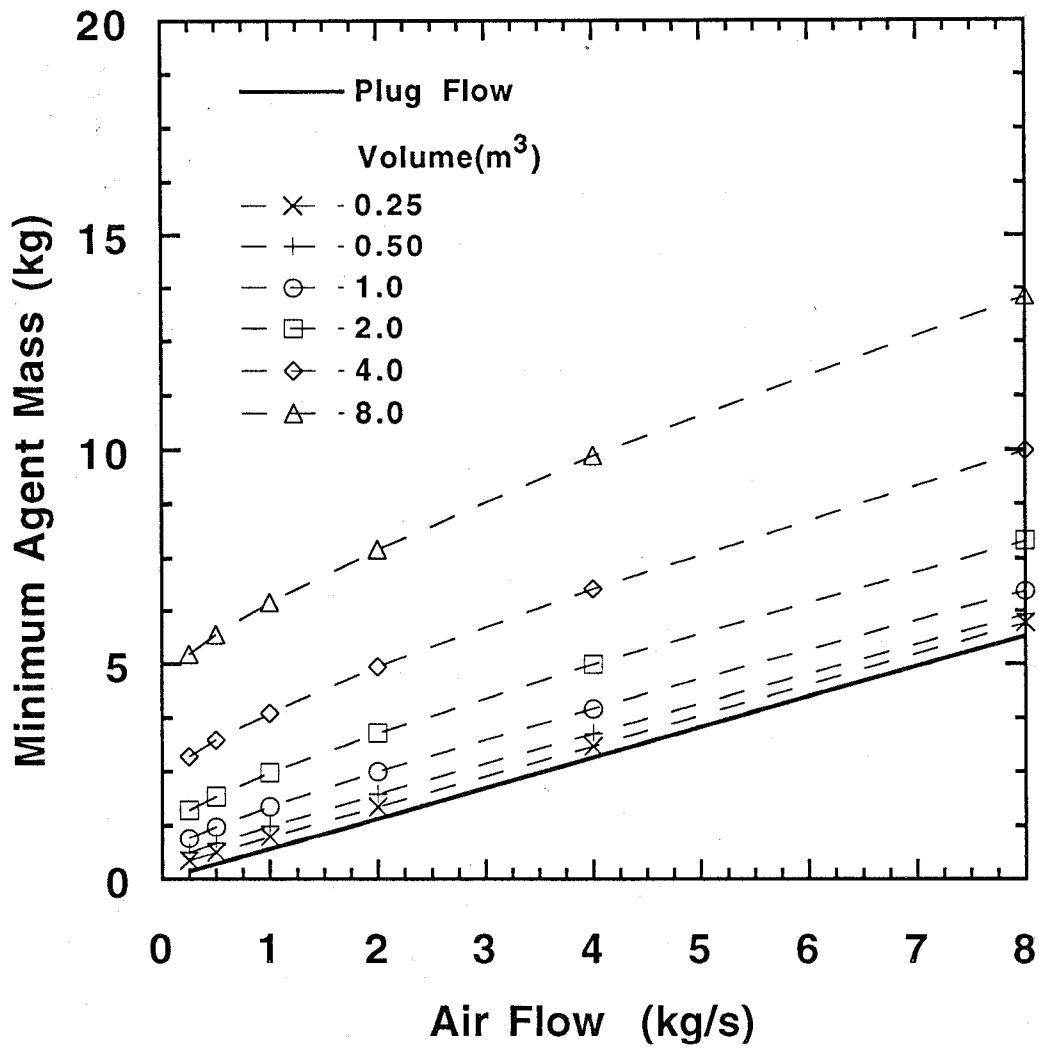


Figure 98. The minimum CF_3I mass requirements for pool fire suppression as a function of air flow. The agent injection duration was 0.50 s.

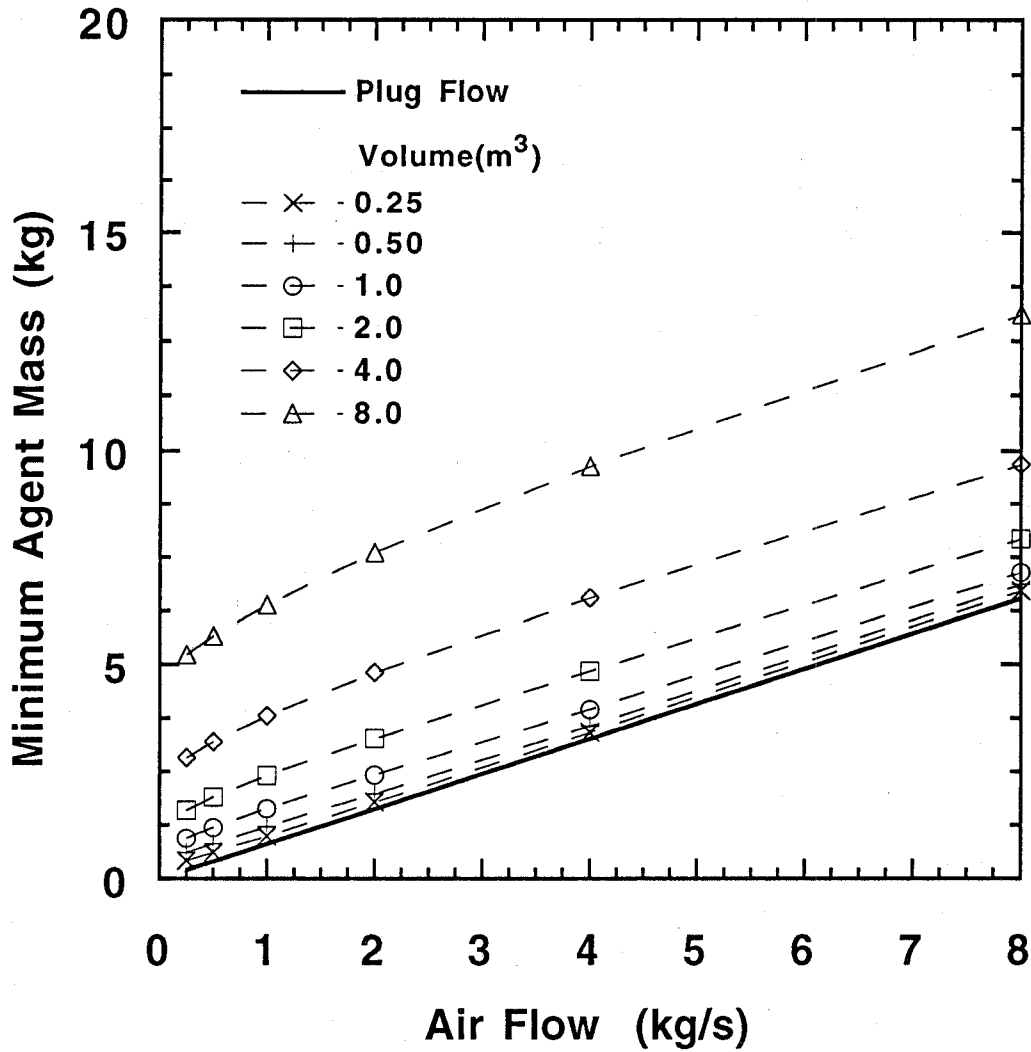


Figure 99. The minimum CF₃I mass requirements for pool fire suppression as a function of air flow. The agent injection duration was 1.0 s.

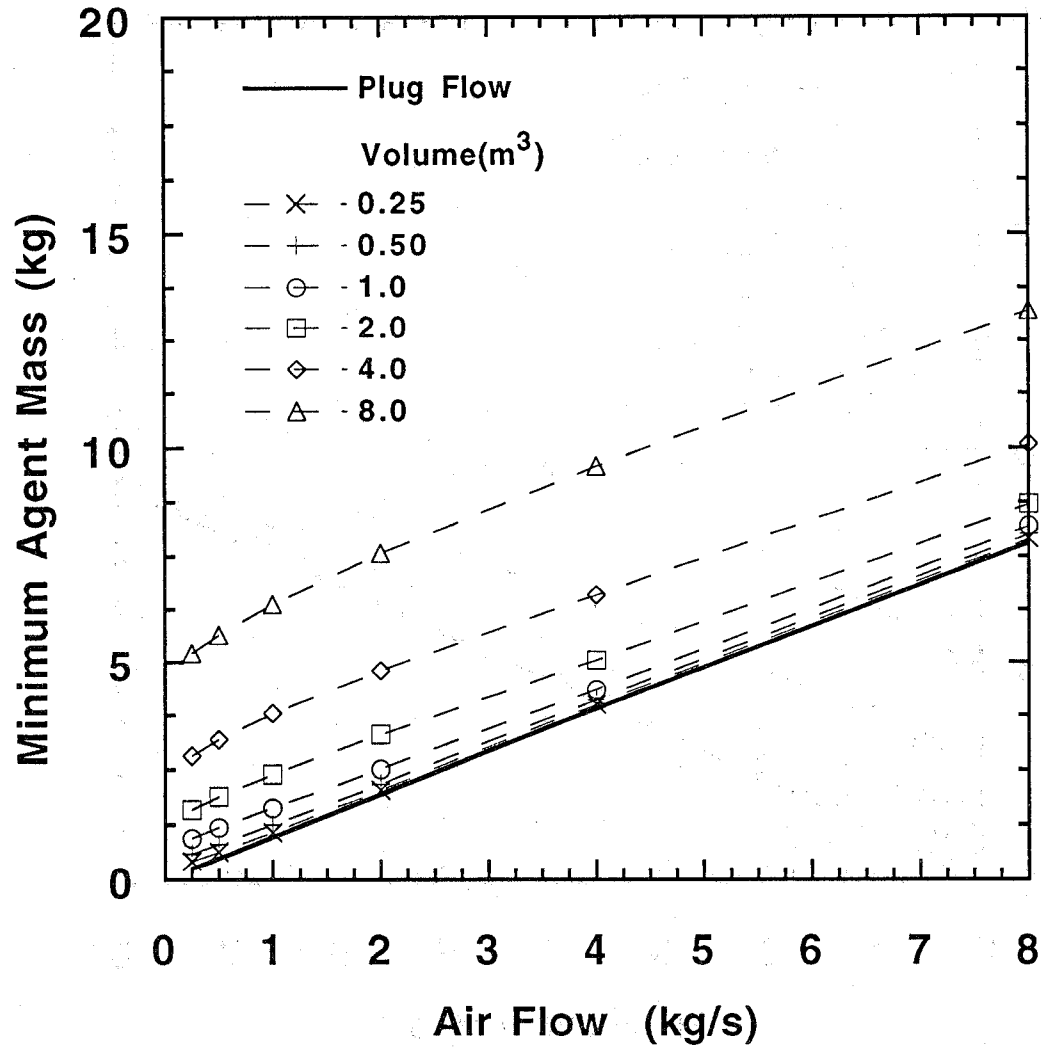


Figure 100. The minimum CF_3I mass requirements for pool fire suppression as a function of air flow. The agent injection duration was 1.5 s.

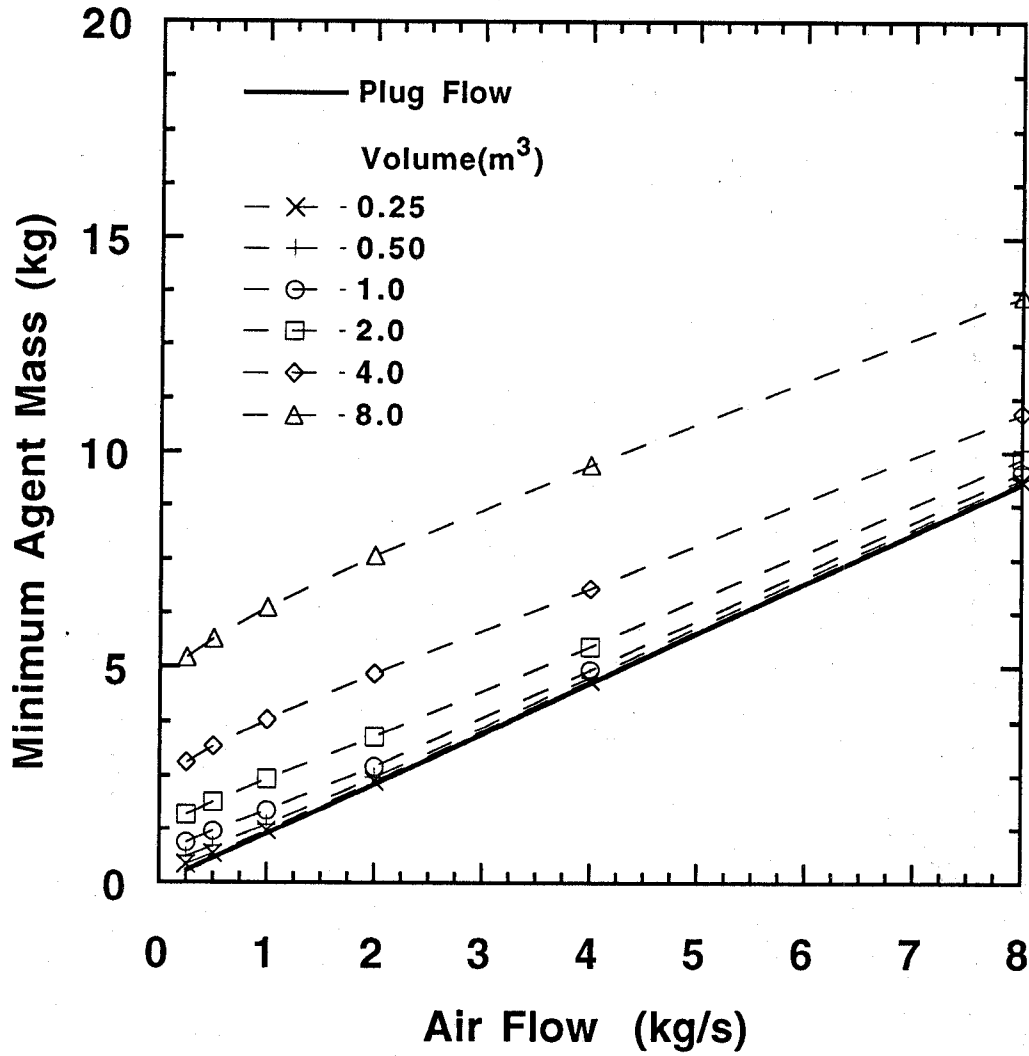


Figure 101. The minimum CF_3I mass requirements for pool fire suppression as a function of air flow. The agent injection duration was 2.0 s.

The minimum agent mass is plotted against injection time for a fixed volume (2.0 m^3) and air flow (1.0 kg/s) in Figures 102-105 to show the effect of injection time on the minimum mass requirements for the different agents, fire scenarios, and mixing modes. Figures 102 and 103 show the spray fire scenario results for plug and PSR-type mixing respectively. The injection time is seen to have a stronger impact on the relative agent mass for plug flow mixing as compared to PSR-type mixing. A comparison of the results in Figure 102 with the spray burner results in Figure 14 show identical trends between the injection time (or delivery interval) and the required mass. The agent rankings are also identical. This observation is not surprising, because the spray fire scenario and plug flow mixing mode is an excellent model for the spray burner. Johnson and Grenich (1986) reported results on the effect of agent injection duration for their "clean" nacelle fire tests in the AEN fire test simulator that are in qualitative agreement with the spray fire and plug flow mixing simulations. Their fire source was a baffle stabilized spray fire, and agent (halon 1301) was injected through a manifold to specifically provide uniform dispersion of the agent in the air flow. In Figure 103, the increase in agent mass from short to long injection times is approximately 30 %. The PSR-type mixing dampens the effect of the rate of injection. Minimum agent mass increases for both nacelle models as the injection time increases. Figure 104 shows the pool fire scenario results for the plug model. In this scenario, the injection time does not have as strong a relative impact, as compared to the spray fire/plug flow mixing model results. The minimum agent mass is a weak function of injection time for the PSR model as seen in Figure 105. Both the plug flow and PSR model results obtain minimum agent mass values at intermediate injection times in the pool fire scenario.

From Figures 102-105, it is inferred that the rate of agent injection can have either significant or negligible impact on the minimum agent mass for suppression depending on the fire scenario and mixing mode. In suppression system design, there may be applications where very short injection times significantly decrease agent mass requirements, which would benefit agent mass and volume storage considerations. Conversely, there may be applications where system constraints (constraints on storage pressure and temperature, bottle location, pipe diameter, etc.) dictate that it is impractical or impossible to achieve rapid discharge. Specific cases, where a relaxation of the discharge criterion (an increase in discharge time) would not have a significant impact on the agent mass, may benefit from flexibility in the system design. For example, in a retro-fit design, if the bottle location does not have to be changed (*i.e.*, its growth potential is sufficient), the original piping may provide an adequate discharge time. This design alternative is probably the second most desirable case, where drop-in replacement is the first.

The impact of a potential cold ambient environment on agent discharge should be considered if the discharge criterion is altered. This is especially critical when the discharge time has a significant impact on the mass of agent.

9.5.2.2 Comparison of the Model to the Military Specification for Halon 1301. The model results for halon 1301 can be compared to the guidelines presented in the Military Specification. The Military Specification used the guidelines developed from data collected by the CAA, where Hansberry (1954) reported that effective suppression occurred for agent injection durations between 0.5 s and 0.9 s. The Military Specification itself requires an injection time of 1 s or less. For comparative purposes, the injection time in the simulations was fixed at 1 s. A distinction between the smooth and rough nacelle configurations can be identified in terms of the worst case potential fire scenario, which is related to air flow and geometry. The smooth nacelle geometry has no ribs and thus pool fires will not be stabilized. In that case, the worst case fire scenario is considered to be a baffle stabilized spray fire ($\tau_f=0.1 \text{ s}$). For the rough nacelle geometry, ribs and other obstructions are available to stabilize pool fires, therefore the worst case fire is considered to be a baffle stabilized pool fire ($\tau_f = 1.0 \text{ s}$).

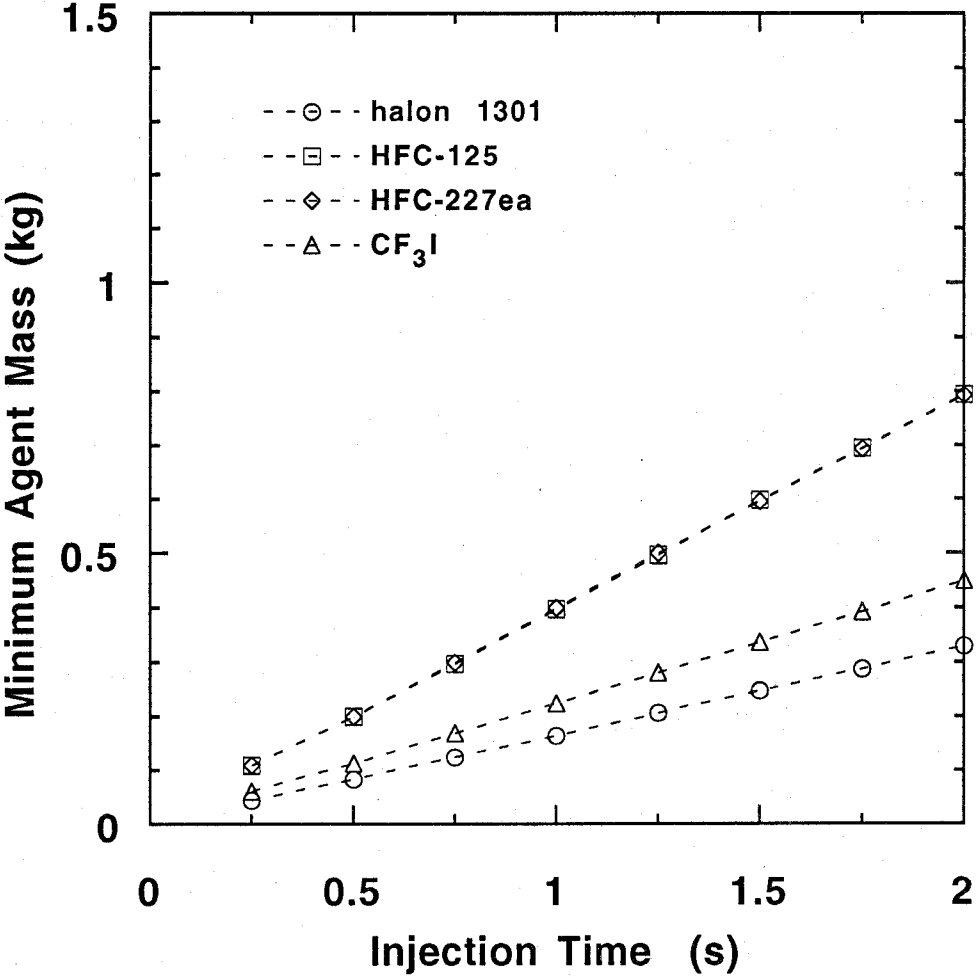


Figure 102. The minimum agent mass as a function of the injection time for the spray fire scenario with plug flow mixing. The air flow is 1 kg/s.

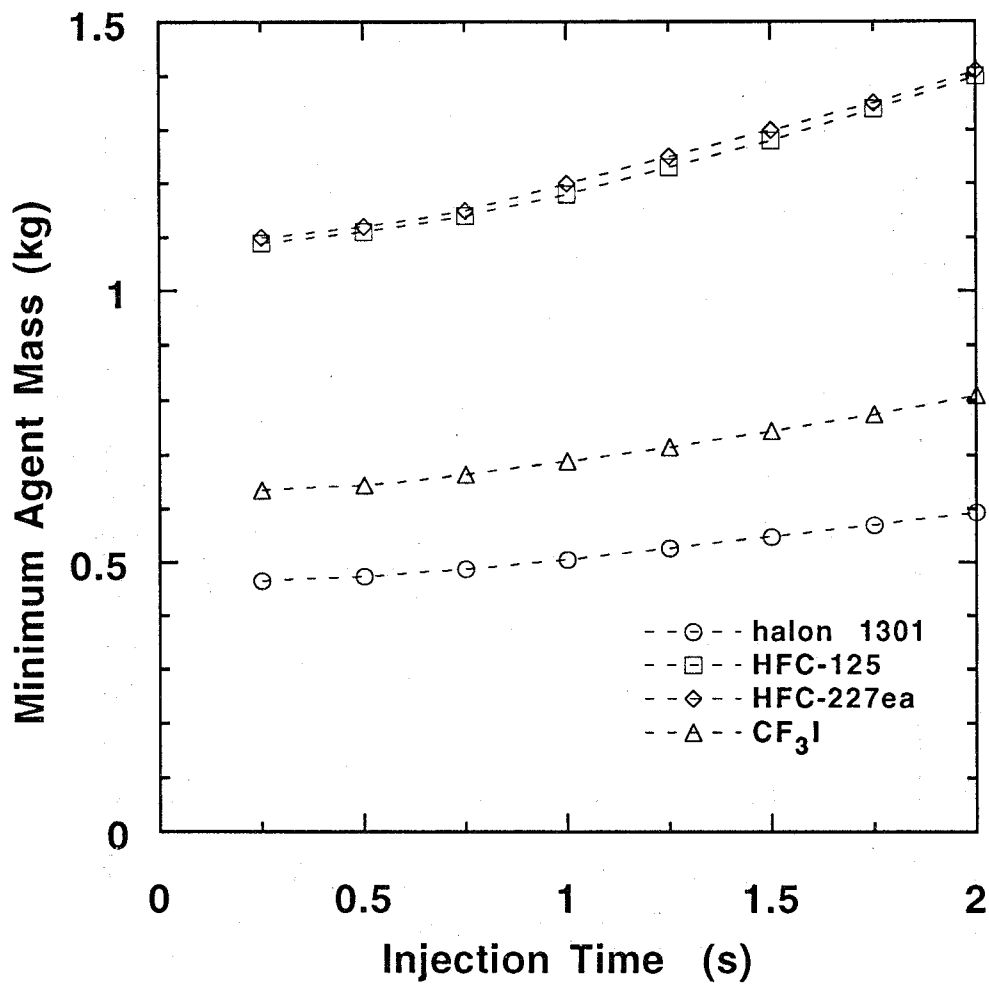


Figure 103. The minimum agent mass as a function of the injection time for the spray fire scenario with PSR mixing. The air flow is 1 kg/s and the volume is 2.0 m³.

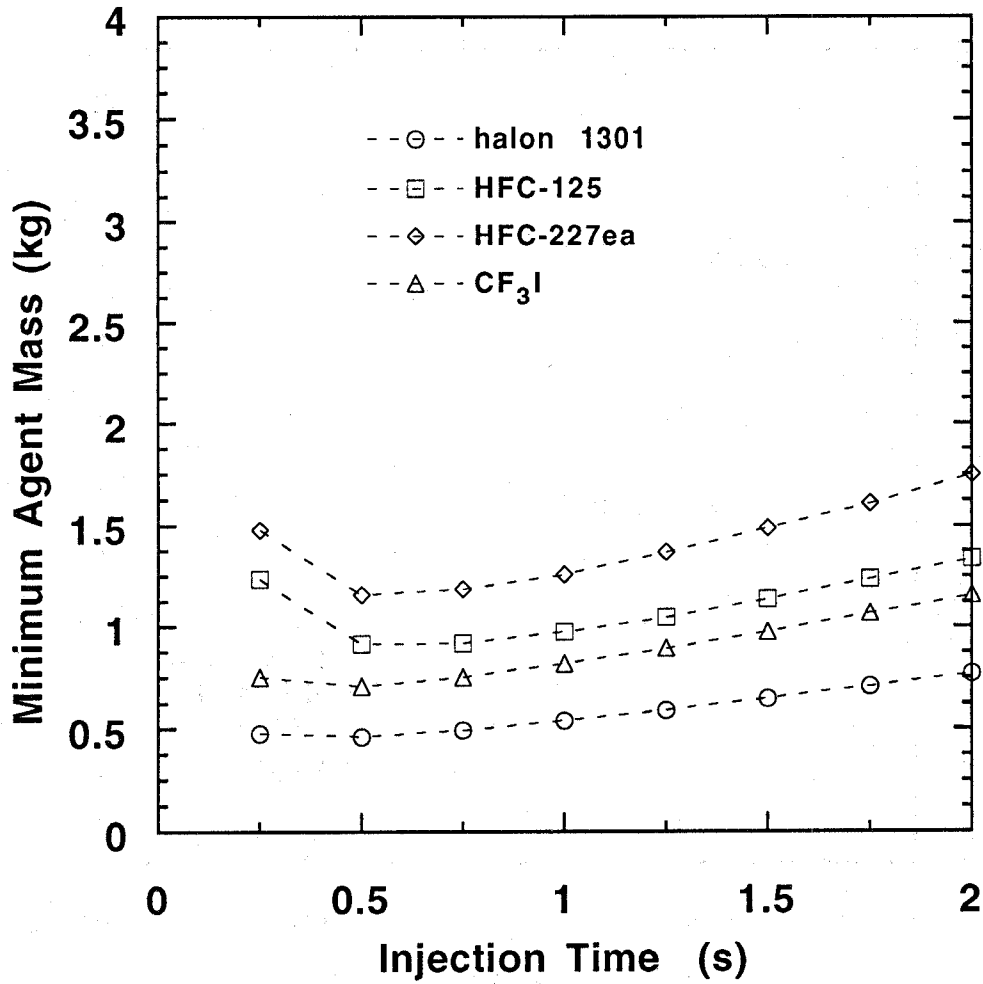


Figure 104. The minimum agent mass as a function of the injection time for the pool fire scenario with plug flow mixing. The air flow is 1 kg/s.

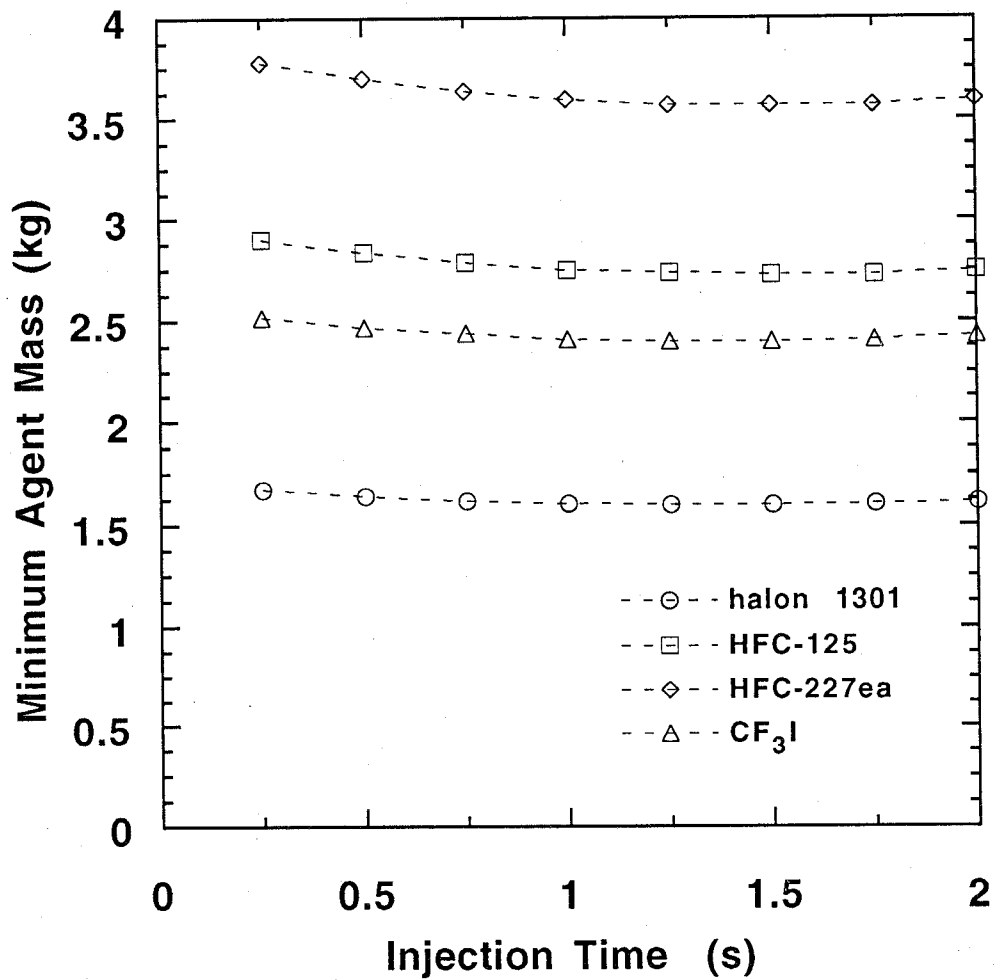


Figure 105. The minimum agent mass as a function of the injection time for the pool fire scenario with PSR mixing. The air flow is 1 kg/s and the volume is 2.0 m³.

Figures 106-109 show the model calculations and the Military Specification agent requirements. Figures 106 and 107 show the spray fire scenario and the guideline requirements for the smooth nacelle. Notice that the Military Specification specifies more mass than predicted from the calculations; in some cases more than three times the predicted amount. If the guidelines were compared to the results for the shortest injection time then even less, and in some cases, much less agent would be predicted. Figures 108 and 109 show the pool fire scenario results compared to the guidelines for the rough nacelle geometry for air flows above 0.45 kg/s. Again the guidelines specify more agent than predicted from the model. The injection time does not have a large impact on the predicted agent requirements; thus, for shorter injection times agent mass will not be substantially less than those for 1.0 s injections and may actually be higher.

The comparison of the Military Specification's halon 1301 requirements and the model predictions indicates that the model predicted the trends as the volume and air flow increased. The fact that no allowances for imperfect mixing or other un-modeled phenomena were included in the predictions suggests that the results are consistent with the Military Specification guidelines. If such allowances were included, a model such as this may have wide applicability.

9.5.3 Comparison of Predicted Alternative Agent Requirements to Halon 1301 Requirements.

The predicted alternative agent mass requirements can be compared to the predicted halon 1301 mass requirements for each given fire scenario, nacelle free volumes, air flow, and agent injection duration. Comparisons of the two fire scenarios, spray and pool fires, at the nominally best agent injection durations of 0.25 s and 1.0 s respectively are shown in Figures 110-112. These figures show the amount of alternative agent required for a given air flow and volume plotted against the amount of halon 1301. Notice that these points fall on a separate line for each fire scenario, and that the lines pass through the origin. The slopes from best fit straight lines indicate a constant multiplier to the amount of halon required to that of the alternative agent required for each fire scenario. This comparison is analogous to the Flame Suppression Number (FSN) introduced in Section 4 of NIST SP 861 (Grosshandler *et al.*, 1994) where the experimental results for the minimum halon 1301 mass required to extinguish various flames were compared to the minimum mass requirements of a number of other agents. Table 11 shows the slopes for the best-fit straight lines for each alternative agent and fire scenario.

As expected, CF_3I is the closest in terms of mass requirements to halon 1301 for both the spray and pool fire scenarios. For the spray-type flame, there is little difference between HFC-125 and HFC-227, but there is a significant difference between HFC-125 and HFC-227 for the pool fire scenario. This comparison has important practical implications. For two very different fire scenarios, there is a linear relationship between the amount of halon 1301 and alternative agent over a wide range of air flows and volumes. Even though idealized mixing and isothermal conditions were assumed, this relationship may still hold for non-idealized real fire scenarios. Therefore, knowledge gained from halon 1301 systems in terms of agent mass requirements may be directly applied to alternative agents. In addition, Table 11 suggests that HFC-125 is almost as efficient as CF_3I for the pool fire scenario. This is not surprising, after all, the input for X_∞ in the pool fire scenario was related to the peak flammability limits, which when written in terms of mass rather than mole fractions (as in Table 10) were 0.247, 0.361, 0.420 and 0.331, for halon 1301, HFC-125, HFC-227, and CF_3I respectively. This follows the same trends as the results for the pool fire scenario as seen in Table 11.

9.5.4 Comparison of the Model to Full-Scale Test Data. It is of interest to compare the model to full-scale data. Data is available from the Phase II full-scale Wright-Patterson study on halon alternatives (Bennett and Caggianelli, 1995). The tests were performed in the AEN fire test simulator, and the data included the minimum agent required to suppress a fuel spray fire. This is the only

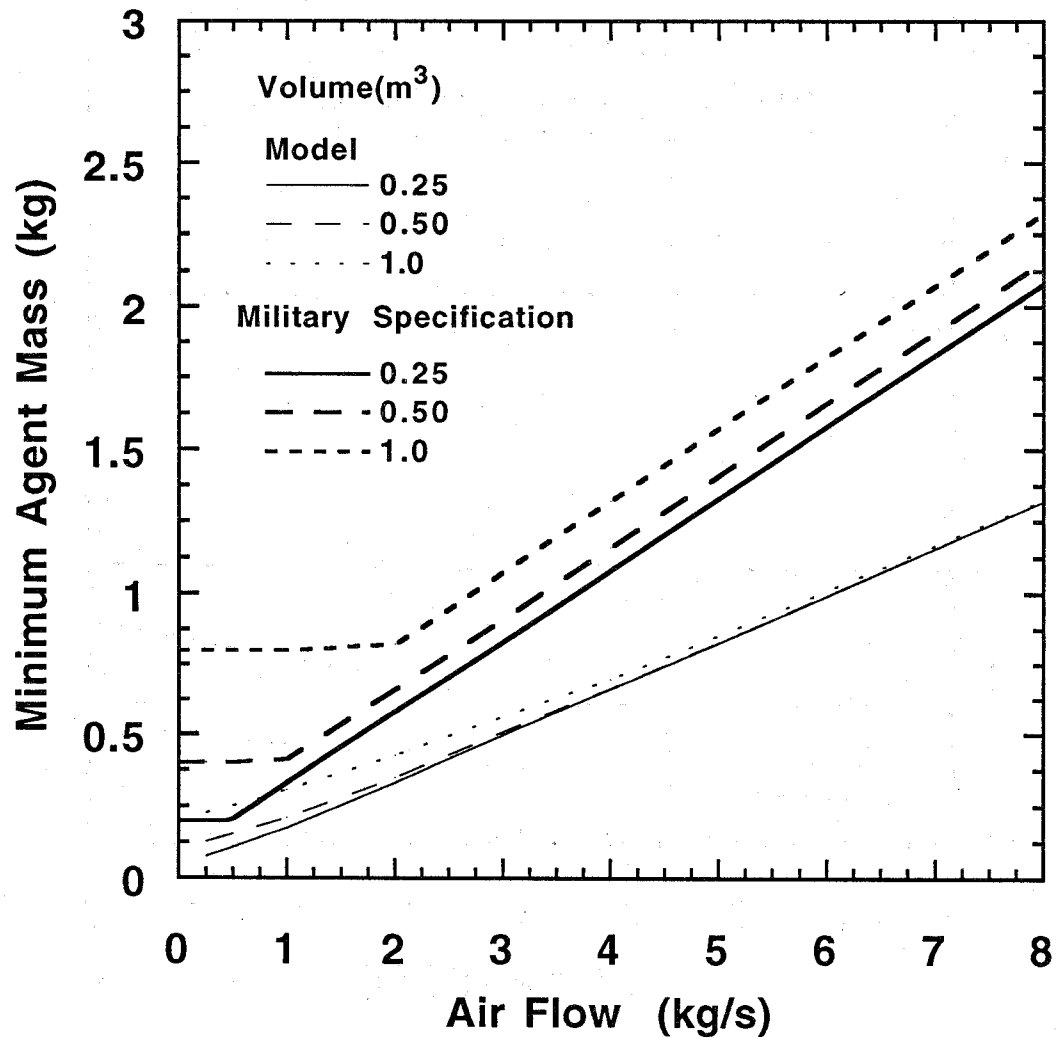


Figure 106. Comparison of calculated minimum halon 1301 mass requirements for spray fire suppression to Military Specification guidelines for low nacelle volumes.

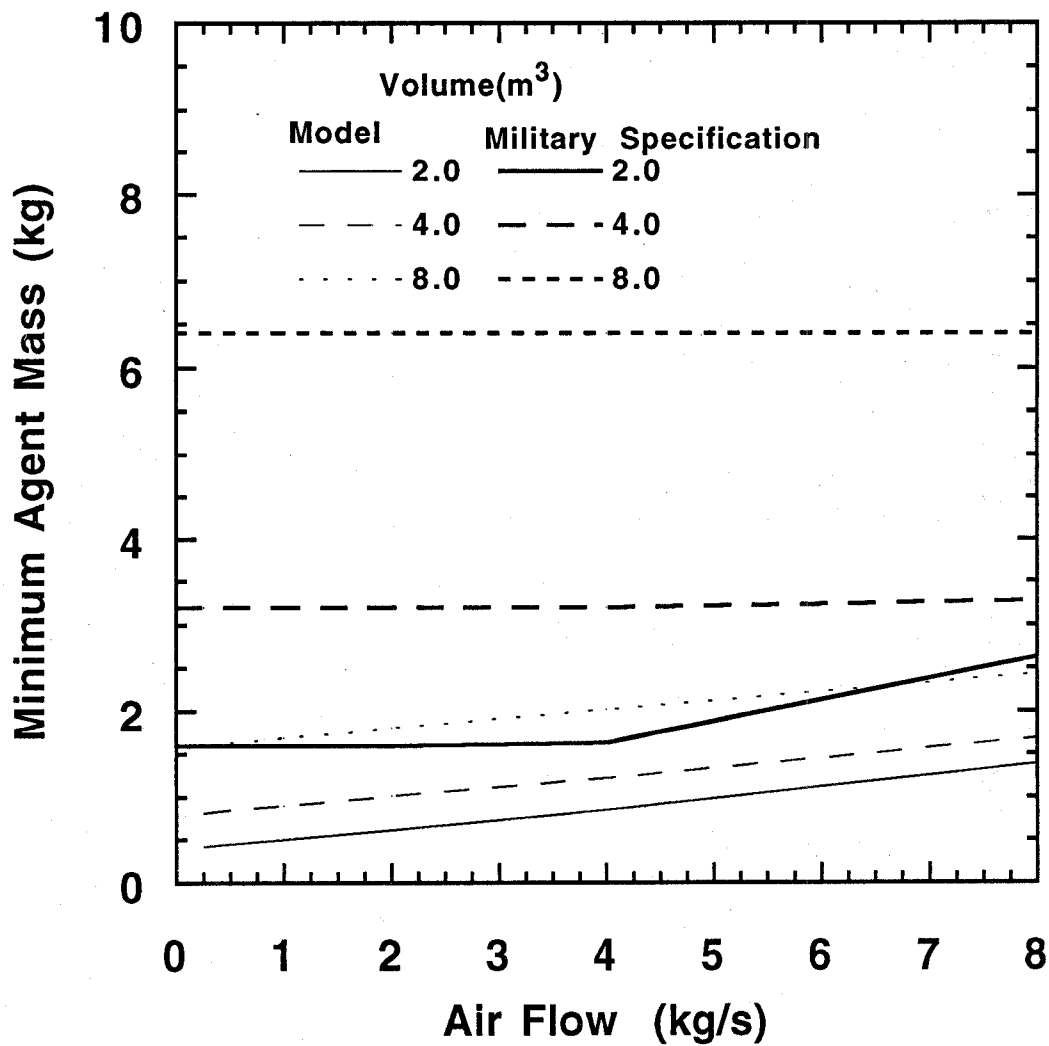


Figure 107. Comparison of calculated minimum halon 1301 mass requirements for spray fire suppression to Military Specification guidelines for high nacelle volumes.

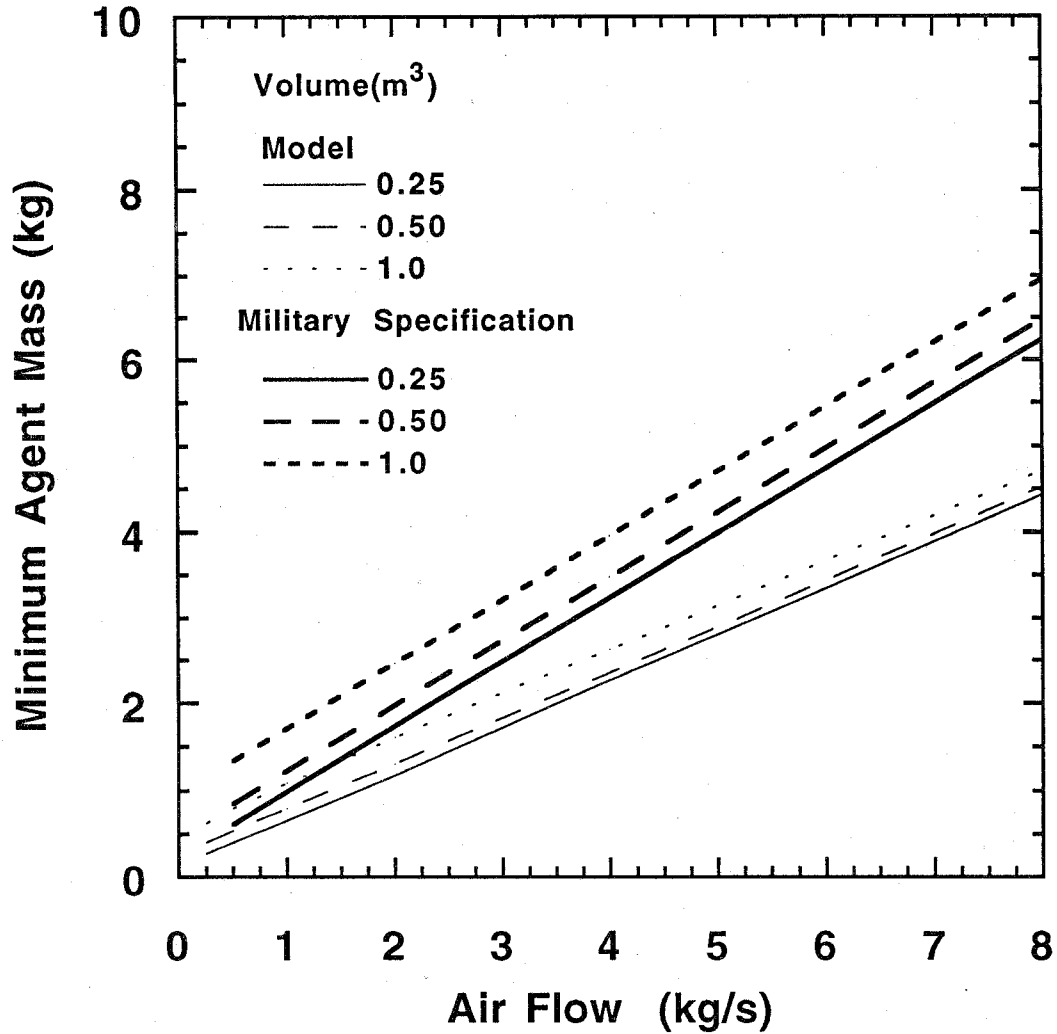


Figure 108. Comparison of calculated minimum halon 1301 mass requirements for pool fire suppression to Military Specification guidelines for low nacelle volumes.

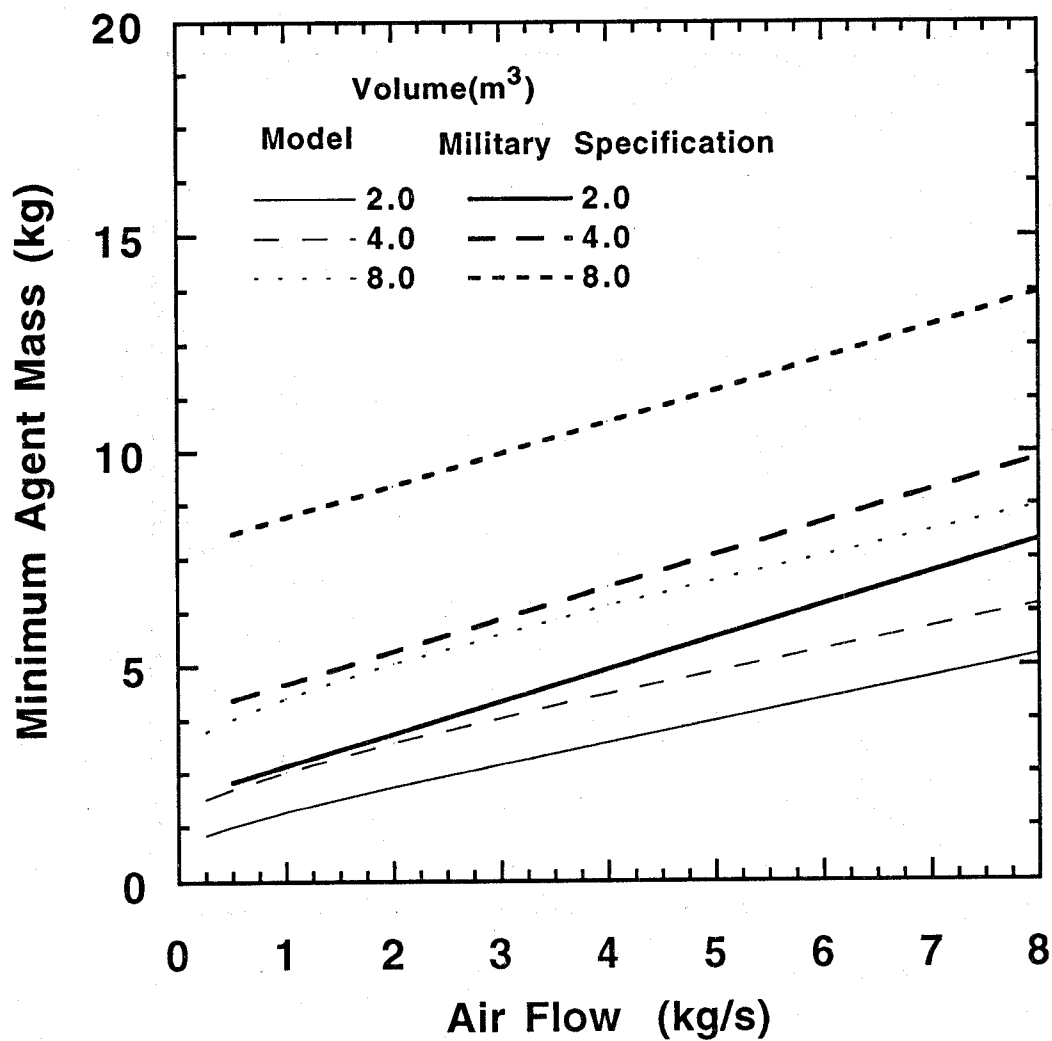


Figure 109. Comparison of calculated minimum halon 1301 mass requirements for pool fire suppression to Military Specification guidelines for high nacelle volumes.

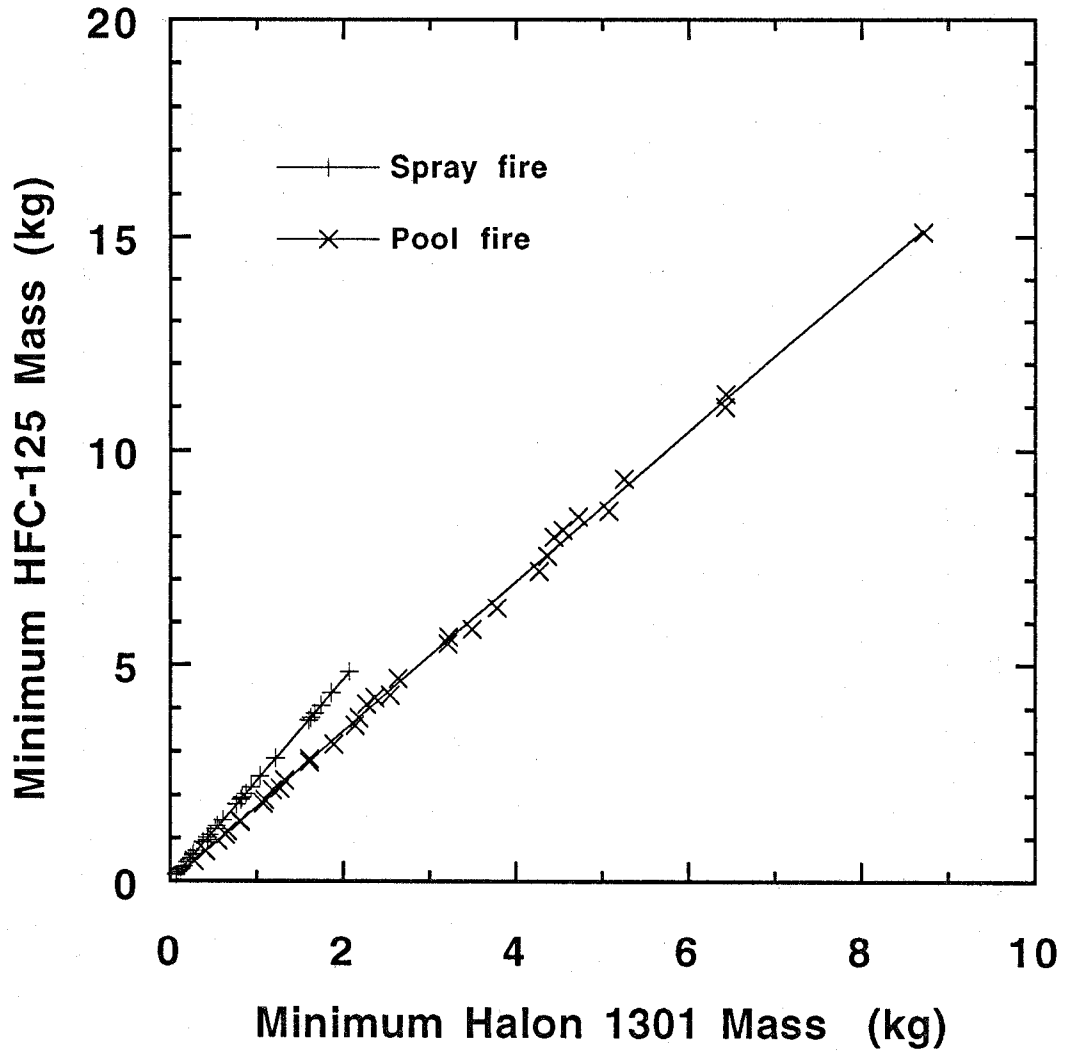


Figure 110. Comparison of minimum mass requirements of HFC-125 to halon 1301 for 0.25 s and 1.0 s injection durations in the spray and pool fire scenarios respectively. Solid lines indicate best-fits through the data.

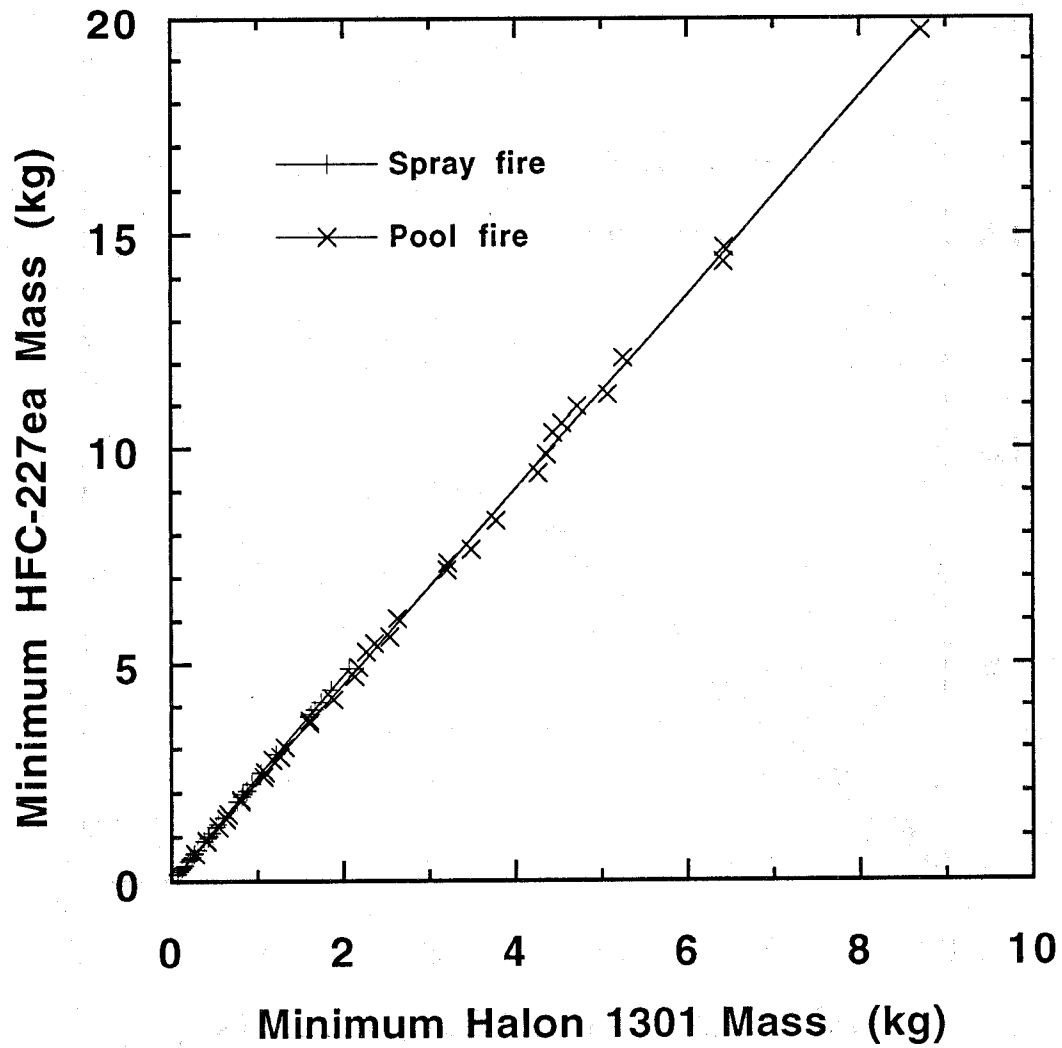


Figure 111. Comparison of minimum mass requirements of HFC-227 to halon 1301 for 0.25 s and 1.0 s injection durations in the spray and pool fire scenarios respectively. Solid lines indicate best-fits through the data.

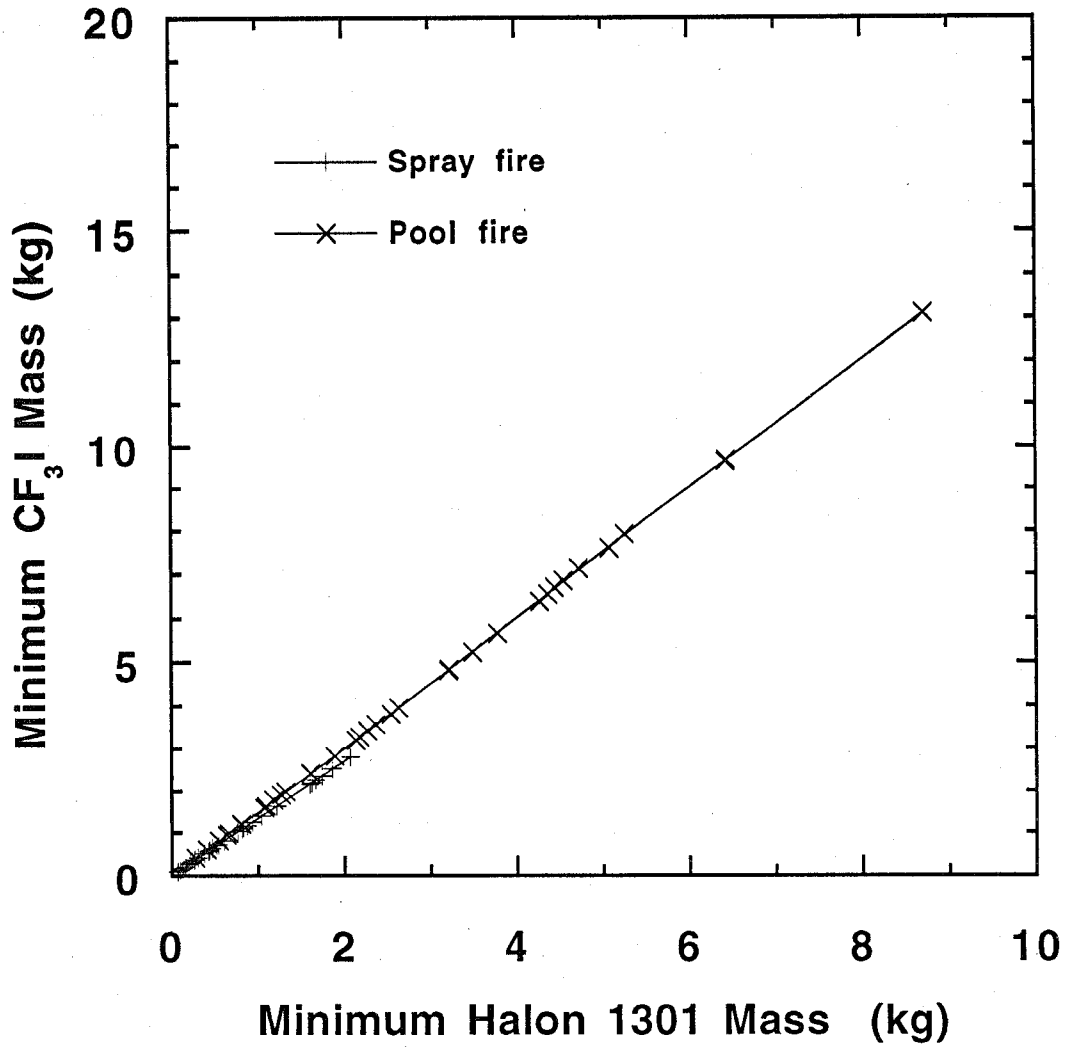


Figure 112. Comparison of minimum mass requirements of CF₃I to halon 1301 for 0.25 s and 1.0 s injection durations in the spray and pool fire scenarios respectively. Solid lines indicate best-fits through the data.

known full-scale data for the alternative agents. Model calculations were compared to this data set. Only tests where the surface temperature was not above 79 °C (175 °F) were considered since hot surface re-ignition was not included in the model at this time. Two nacelle volumes, 2.5 m³ and 4.2 m³, and two air flows, 0.4 kg/s and 1.2 kg/s were examined in the full-scale tests. Agent injection duration varied depending on the bottle conditions and the amount of agent required to suppress a given fire. Estimated times were in the range from 0.05 s to 0.4 s. For the purposes of comparison an effective injection time of 0.25 s was assumed, since at very rapid injection rates some spreading of the agent as it penetrates up and downstream from the injection location must occur. The data for each agent were compared to the model calculations for baffle stabilized spray and pool fire scenarios over a range of air flows and volumes. Figures 113-118 show the comparisons. The test data fall between the plug

Table 11. Best-fit Flame Suppression Number for each alternative agent and fire scenario

Agent	(Mass of agent) / (Mass of halon 1301)	
	Spray Flame ($\tau_f=0.1$ s)	Pool Fire ($\tau_f=1.0$ s)
HFC-125	2.34	1.74
HFC-227	2.36	2.27
CF ₃ I	1.36	1.51

flow results and the PSR results for the spray fire scenario. The test results lie above and then below the plug flow results for the pool fire scenario as the air flow is increased. One possible explanation of these observations is that the experimental results are consistent with a spray fire and plug flow with poor radial mixing. The details of the AEN mixing are not known, but it is unlikely that recirculation of agent and air occurs, which suggests a plug flow mixing scenario.

9.5.5 Re-ignition Suppression Requirements. Re-ignition suppression requirements are very dependent on the specific scenario. At this point, there is no reliable method to predict the optimal agent requirements to prevent it. Re-ignition is always a threat as long as fuel vapor and air can come in contact with sufficiently hot surfaces. Strategies to prevent re-ignition include removing fuel vapor, reducing surface temperatures (either through design changes or active cooling), and inerting the fuel/air mixture with a suppressant.

Fuel vapors are removed by the air flow in the nacelle, liquids are removed by drain holes or sump ejectors. Typically, before activation of the engine nacelle fire suppression system, the jet fuel and hydraulic fluid flow to the particular engine is shut down. This limits the amount of fuel in the nacelle, but it could take a relatively long time to remove the combustibles from the nacelle, especially the low vapor pressure liquids.

Surface temperatures can be reduced either by design changes such as insulating hot surfaces, or through active cooling. Air flow over hot surfaces will lower the surface temperature, but may not be available in sufficient quantity. A mechanism that should be considered is the effect of surface cooling from the agent after it is discharged into the nacelle. For instance, mass requirements for HFC-125 will probably be at least twice that of halon 1301 and, given the heat of vaporization and heat capacities for those two agents, the HFC-125 discharge would provide more cooling relative to halon 1301. It is possible, although unlikely, that cooling may be sufficient to decrease surface temperatures below ignition temperatures.

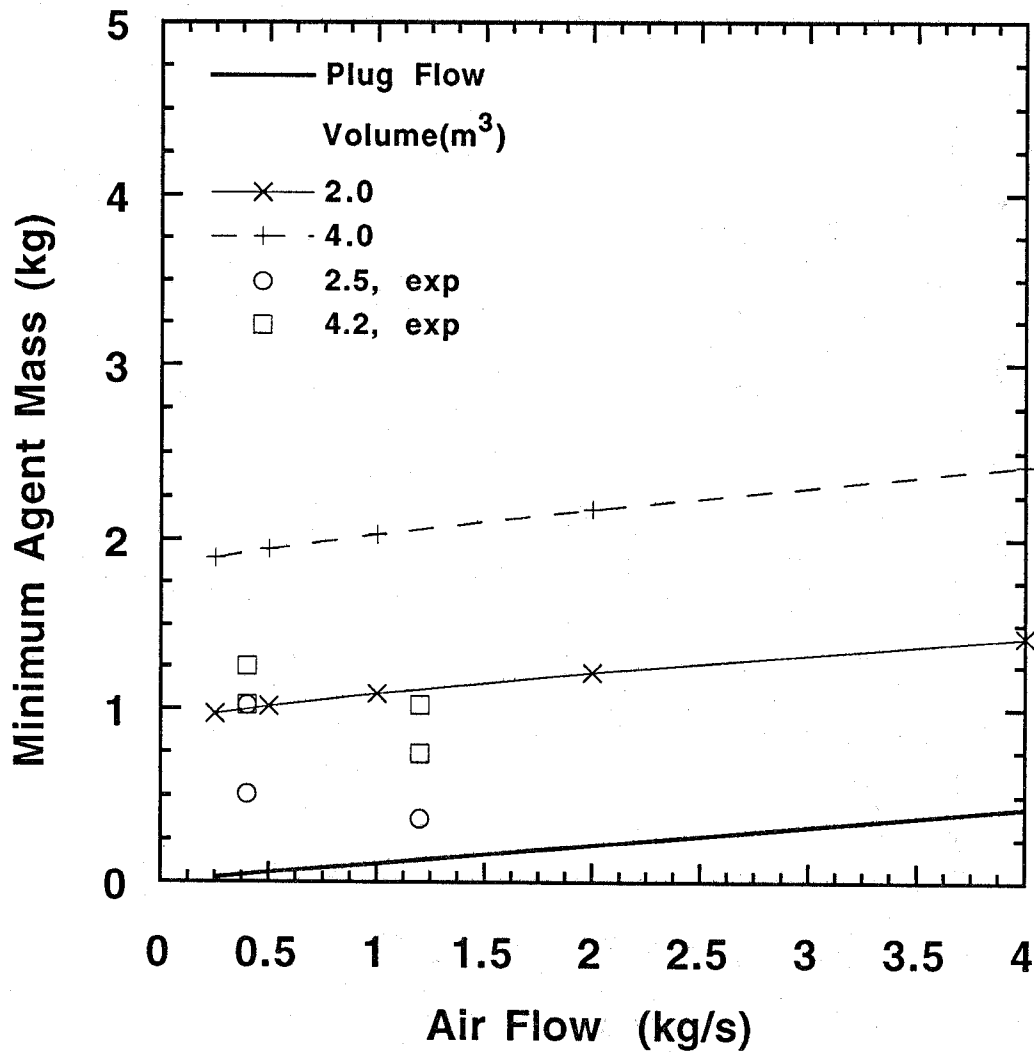


Figure 113. Minimum HFC-125 mass requirements for full-scale AEN simulator tests and the simulated spray fire scenario for an agent injection duration of 0.25 s.

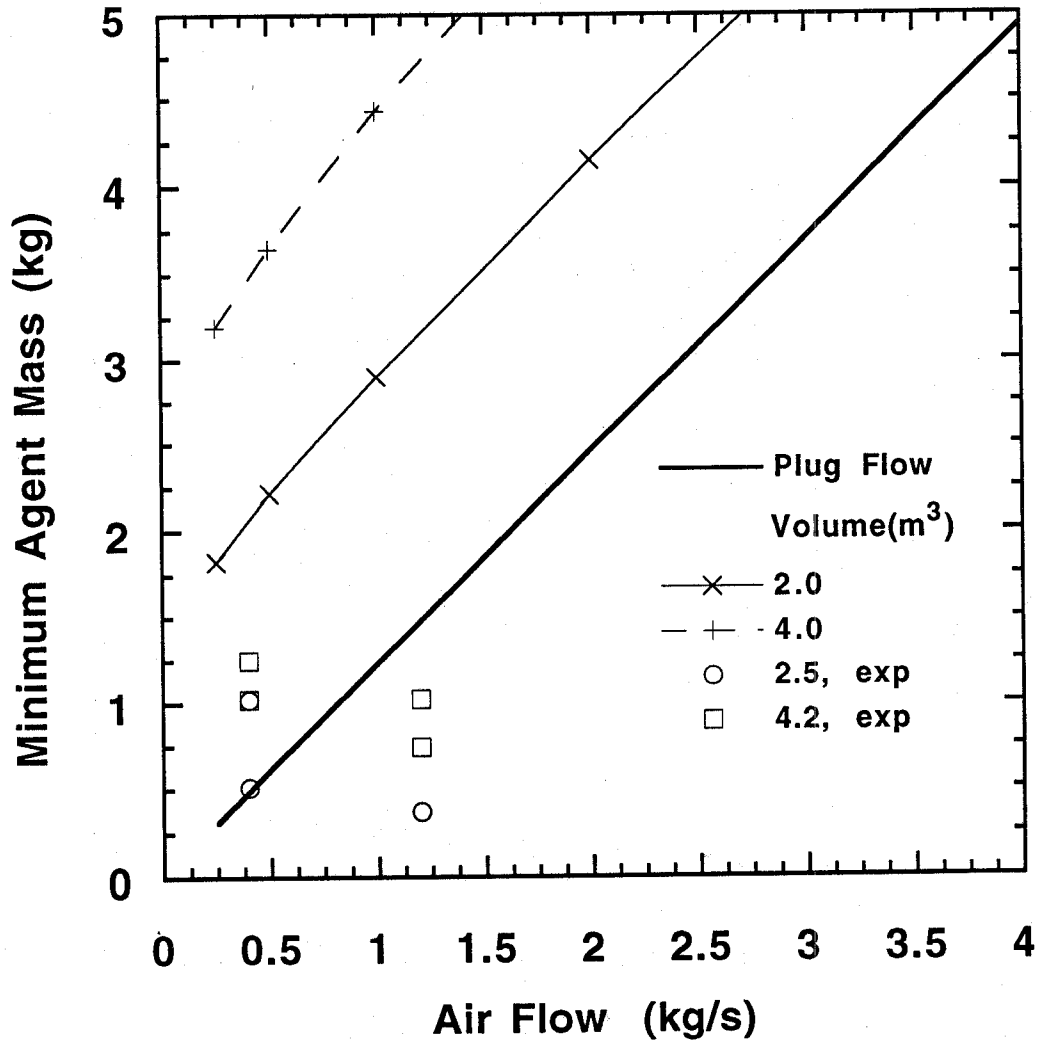


Figure 114. Minimum HFC-125 mass requirements for full-scale AEN simulator tests and the simulated pool fire scenario for an agent injection duration of 0.25 s.

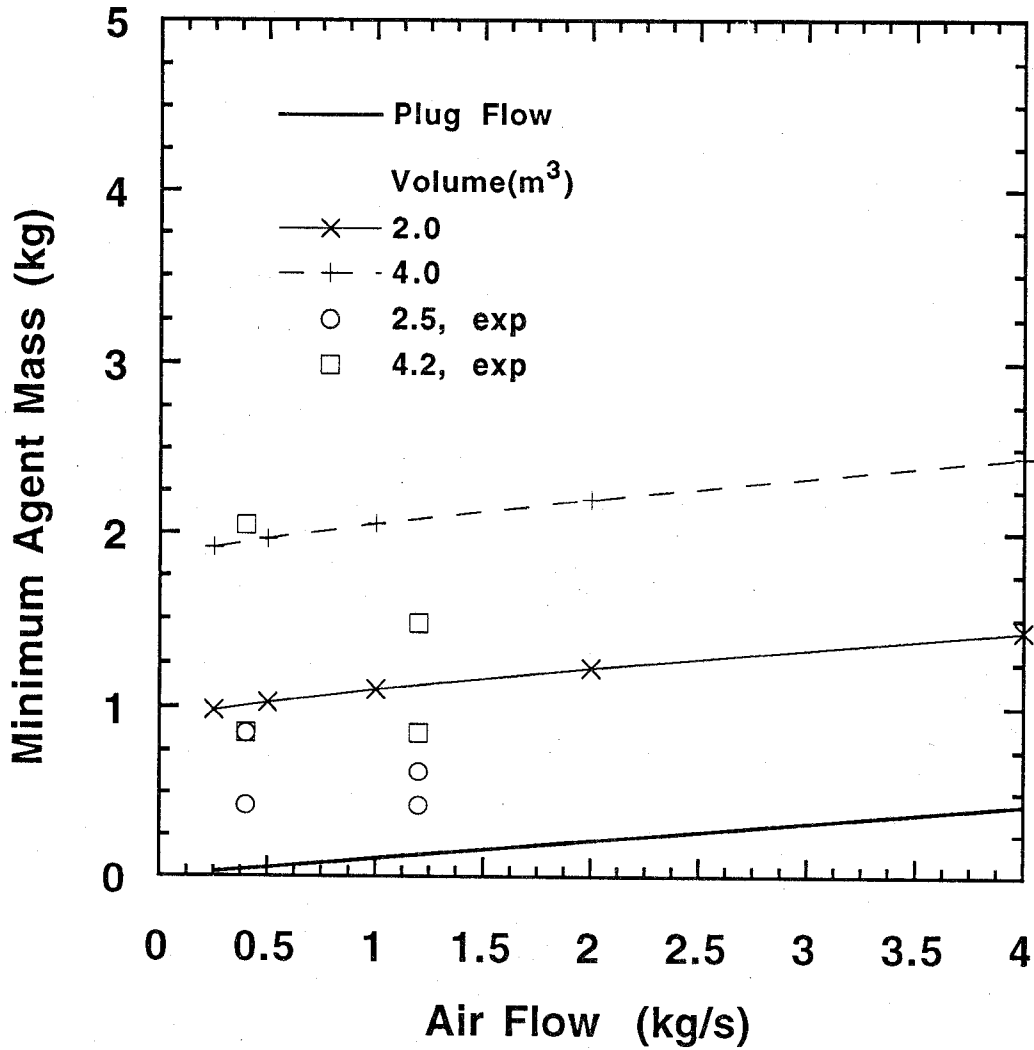


Figure 115. Minimum HFC-227 mass requirements for full-scale AEN simulator tests and the simulated spray fire scenario for an agent injection duration of 0.25 s.

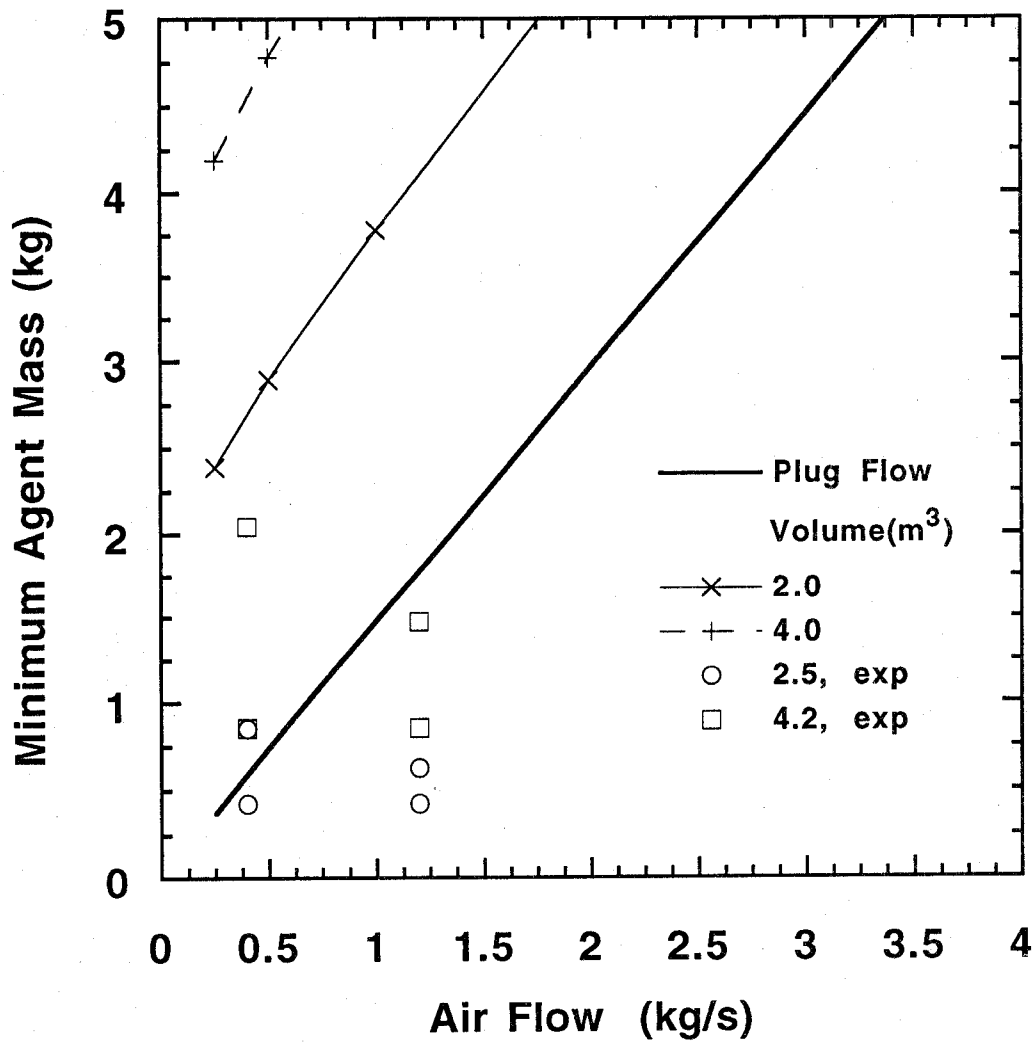


Figure 116. Minimum HFC-227 mass requirements for full-scale AEN simulator tests and the simulated pool fire scenario for an agent injection duration of 0.25 s.

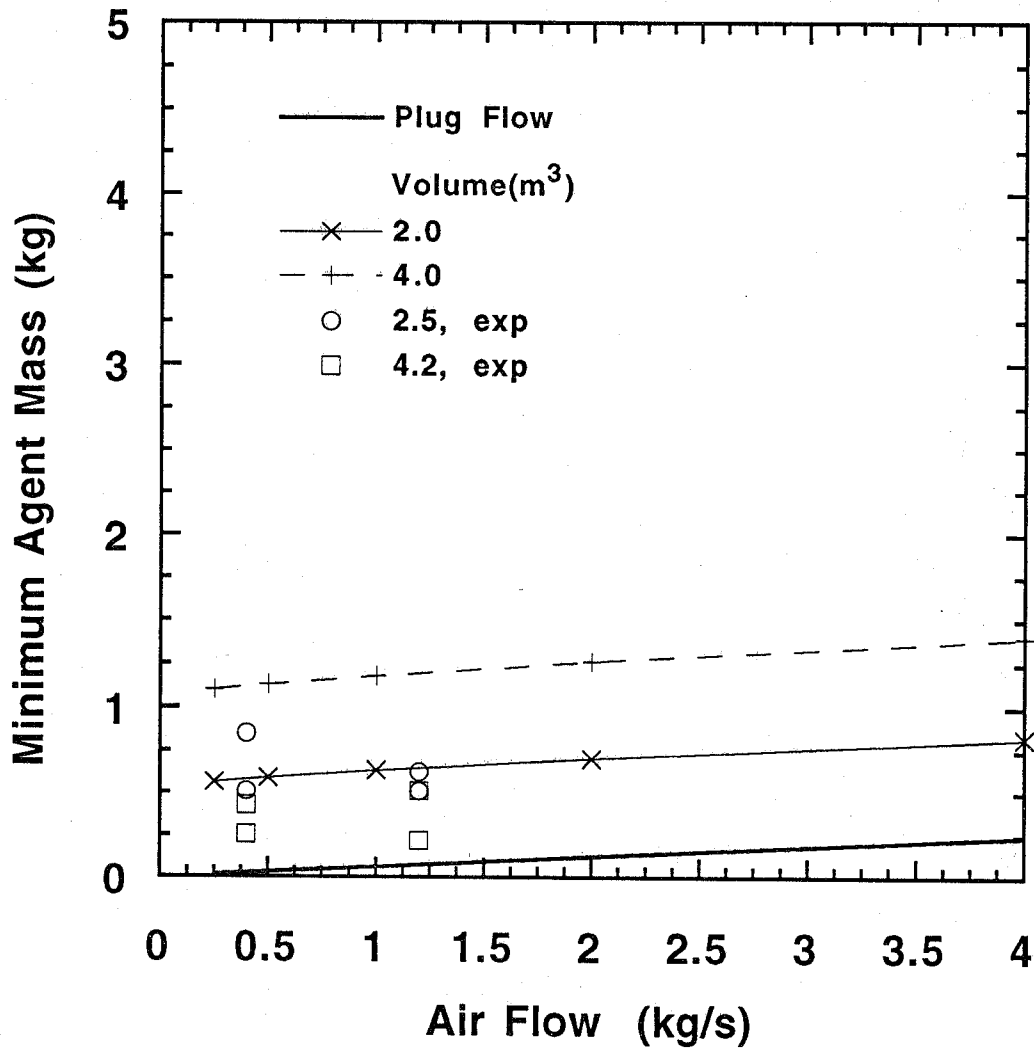


Figure 117. Minimum CF_3I mass requirements for full-scale AEN simulator tests and the simulated spray fire scenario for an agent injection duration of 0.25 s.

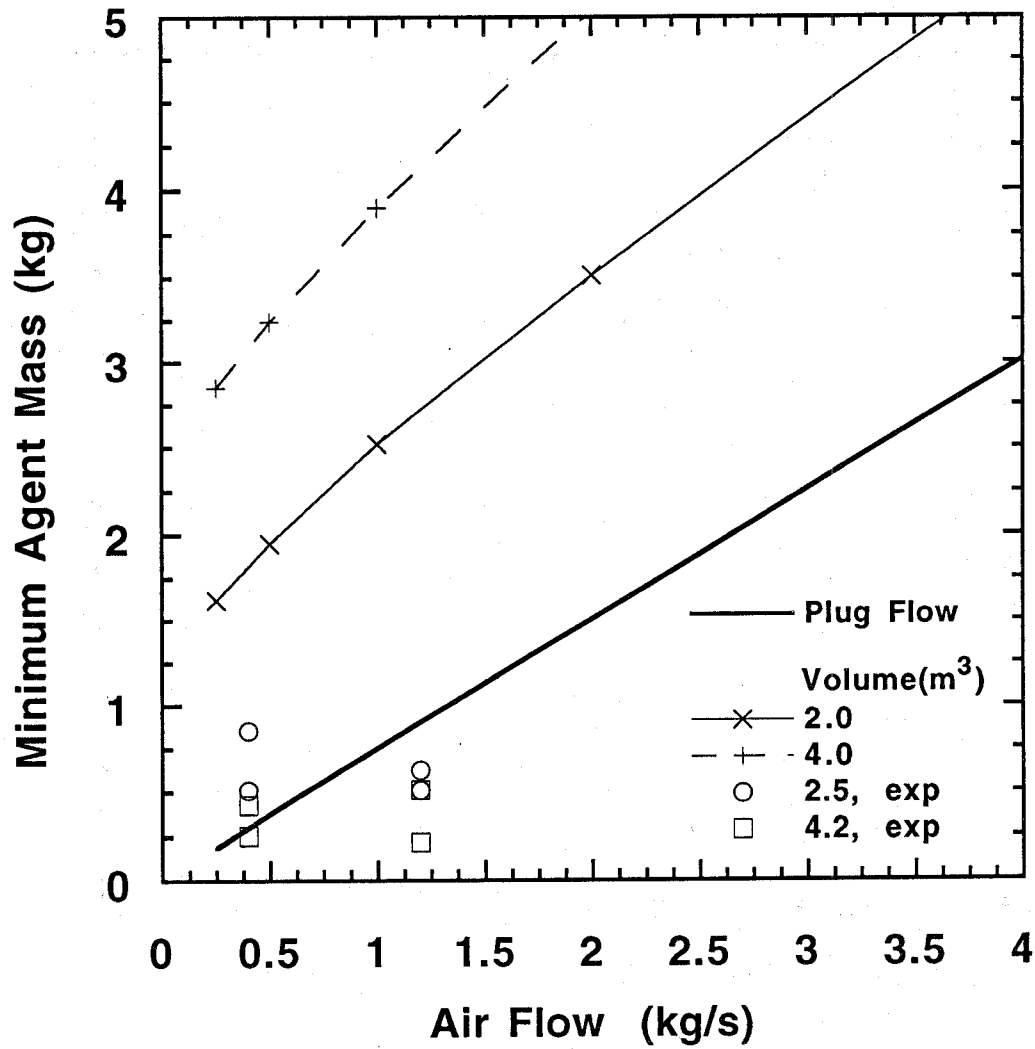


Figure 118. Minimum CF₃I mass requirements for full-scale AEN simulator tests and the simulated pool fire scenario for an agent injection duration of 0.25 s.

Unfortunately, it has been shown that the replacement agents are not very efficient in suppressing hot surface ignition at low agent concentrations as measured by relative increases in the ignition temperature (Section 9.3.4). The model developed here uses the agent concentration which inerts the peak flammability limit as a target for the combustion zone (see Section 9.5.2.1), insuring suppression of possible re-ignition. Yet, the duration of that target concentration was not specified. To insure prevention of re-ignition, a high concentration must be held until surface temperatures decrease sufficiently, or fuel vapors are removed from the nacelle.

9.5.6 Impact of Unmodeled Phenomena. In all of the model calculations above, the fire scenarios were defined by fixed characteristic mixing times and fixed critical concentrations. No allowances were made to account for the effects the local velocity has on the ease of suppression, because for the generic nacelle models, no relationship between the flow and velocity was introduced. The only constraint was that the characteristic mixing time for each fire scenario represented the worst case possible for those models. In real nacelles, geometric factors such as objects, upstream from a baffle, can significantly impact the flow field near the baffle. Therefore, it is impossible to utilize the known effects of velocity on the characteristic mixing time and flame stability unless detailed flow calculations or measurements are performed for specific nacelle configurations. See Section 9.3.6.3 for a more detailed discussion of this issue.

In the model, agent injection occurs isothermally and the agent is assumed to be in the gas phase to simplify the equations. An assumption is made that there is sufficient heat available to vaporize the agent soon after mixing with the nacelle air. Typically the agent enters the nacelle as a two-phase gas/liquid mixture and at a cold temperature due to adiabatic expansion and flash evaporation. The air flow may be approximately 20 °C during a certification discharge, or at cold or elevated temperature during flight depending on flight conditions, with the possibility of hot surfaces present. Upon mixing with air, agent will continue to vaporize while cooling the air; also heat transfer from the nacelle walls can add heat to the agent/air mixture. It is possible to numerically solve the mass and energy balance equations simultaneously to determine the impact of non-isothermal conditions for the plug flow and perfectly stirred nacelle volumes, but given the simplified mixing assumptions, such details do not significantly affect the results in terms of the predicted trends of this analysis.

9.5.7 Conservative Design Allowance. Allowances should be made to account for imperfect mixing, uncertainty in input parameters, and other un-modeled phenomena. The model calculations assume that the agent is mixed perfectly with the air flow. In reality, some areas will have relatively lower agent concentrations due to real dispersion effects; therefore, more agent must be added to protect such areas. The relative increase needed to protect such areas is configuration dependent and is not known *a priori*.

In terms of a safety factor, one question is: "Is it better to increase concentration or duration when adding additional agent mass?" Assuming that the minimum agent mass and injection time are known, to affect an increase in the agent concentration in a fire zone, the additional agent mass is injected over the original injection time. This increase in the mass injection rate will increase the turbulent mixing and local velocities in the nacelle, impacting flame stability in a favorable manner. Likewise, to increase the duration, the minimum and additional mass are injected over a longer injection time such that the mass injection rate is equal to the original mass injection rate. This increase in injection duration will increase the duration of agent at all locations. An increase in duration may be required if the nacelle volume is to be "inerted" (held at concentrations above the peak flammability limit) for a period of time. Thus, there are trade-offs associated with each choice.

9.5.8 Preliminary Agent Mass Guidelines. The model calculations show that the agent mass needed for extinguishment is not a function of the nacelle volume in the plug flow model if the cross section of the nacelle is held constant. That is to be expected since the nacelle volume does not play a role in free stream concentration or duration for the plug flow configuration. The perfectly stirred nacelle results do show variation with air flow and nacelle volume. In addition, it appears that air flow and total volume are essentially independent parameters for the ranges of air flow, free volume, and injection times examined. It follows therefore that a "design equation" of the form:

$$W = a V + b \dot{W}_{air} \quad (33)$$

could fit the model results for fixed characteristic mixing times. Here, W is the agent mass (kg), V is the nacelle free volume (m^3), and \dot{W}_{air} is the mass flow of air (kg/s). Indeed, suitable equations were obtained for each agent and worst case fire scenario. This equation is of the same form as the design equations in the Military Specification (see Equations (1)-(4)). Figures 119-126 show the "new" design equation (Equation (33)) for the spray and pool fire scenarios for agent injection times of 0.25 s and 1.0 s respectively as a function of the model calculations for all of the agents. Thus, Equation (33) represents a simple algebraic equation which may be used as a design guideline. Table 12 gives the coefficients for each agent and fire scenario. The (a) coefficient is not simply the critical concentration divided by the agent density. These results approach those limiting values at very low air flows only, much lower than the flows considered here. Again, no allowances for un-modeled phenomena are included in the above design equations, and appropriate safety factors must be applied.

It should be noted that Equation (33) was developed for ambient conditions and the coefficients (a) and (b) are functions of temperature. It is anticipated that the pressure dependence is small. The temperature dependence can be obtained from calculations using the model and based on the results discussed in Section 9.3.2.3.5.

9.5.9 System Performance Criteria. For halon 1301 systems, system performance is validated through a non-combusting certification discharge test. The test involves discharging the agent into the nacelle with air flow provided to simulate cruise conditions and making temporal concentration measurements at various locations. The performance criteria specifies that the halon 1301 concentration be 6 % by volume or greater at all locations in the nacelle for a minimum of 0.5 s. Replacement agent(s) for halon 1301 will likely have to be tested in a similar manner. Here, a method to back-out agent concentration and duration requirements from flame extinction experiments is presented to provide a rational approach for the development of alternative agent system performance criteria. As presented previously, (Section 9.3) there is a relationship between the free stream agent concentration (X_f) and duration (Δt) required to suppress a given fire. Assuming a step function free stream agent concentration (plug flow), that relationship is given by Equation (14) which is re-written here as:

$$1 - \frac{X_\infty}{X_f} = e^{-\Delta t/\tau}$$

Section 9.3.2.3.4 describes this relation in detail. Figure 127 illustrates the equation as it is presented above. For conditions above the curve, a flame would be extinguished. The critical injection duration (Δt_c) shown in Figure 127 is obtained when the free stream agent concentration is equal to 100 % (see Equation (15)). Below this value, the duration is too short to extinguish the flame. For known values of X_∞ and τ , assuming that the agent and fire scenario are known, the required duration (Δt) can be

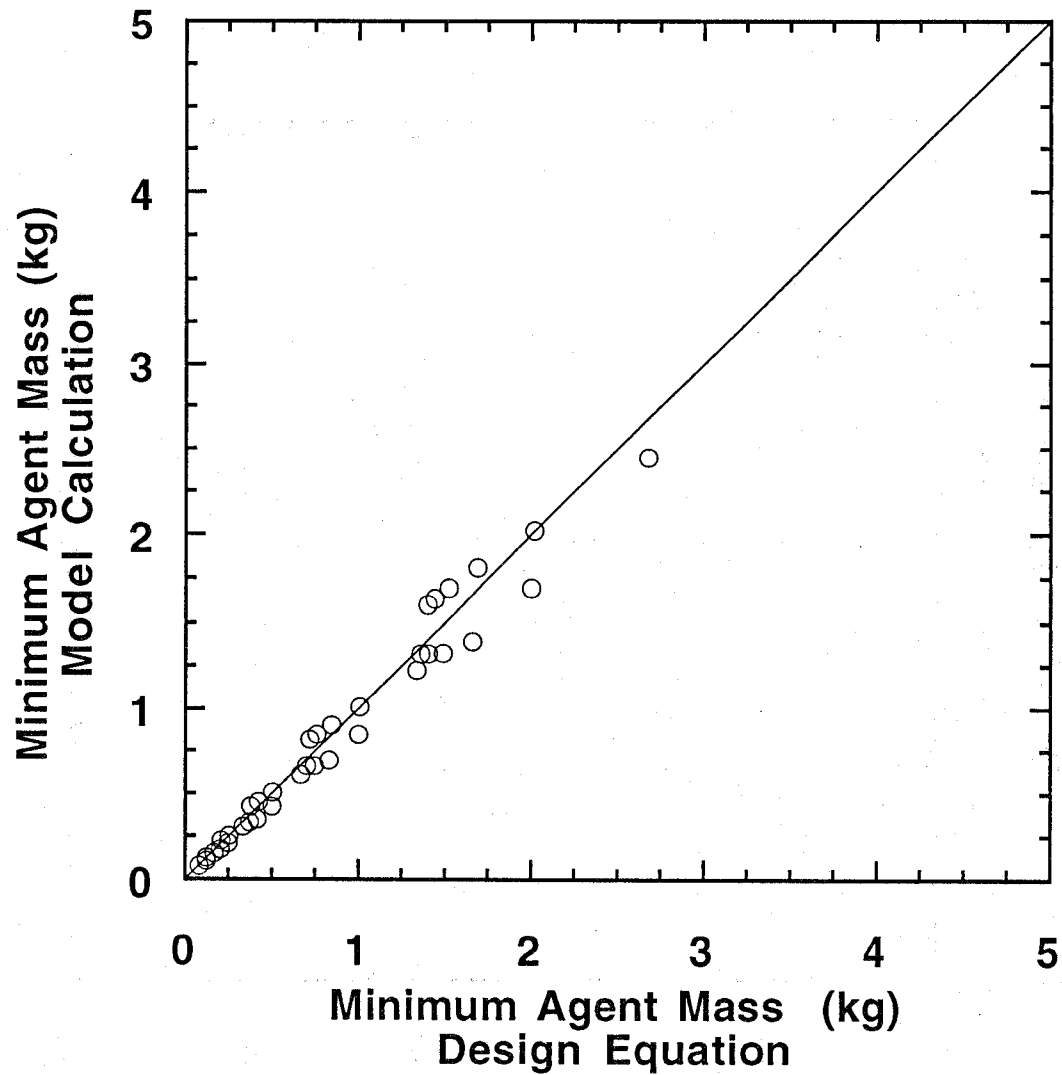


Figure 119. Comparison of the minimum halon 1301 mass from the model calculations and the "design equation" for the spray fire scenario with an agent injection duration of 0.25 s.

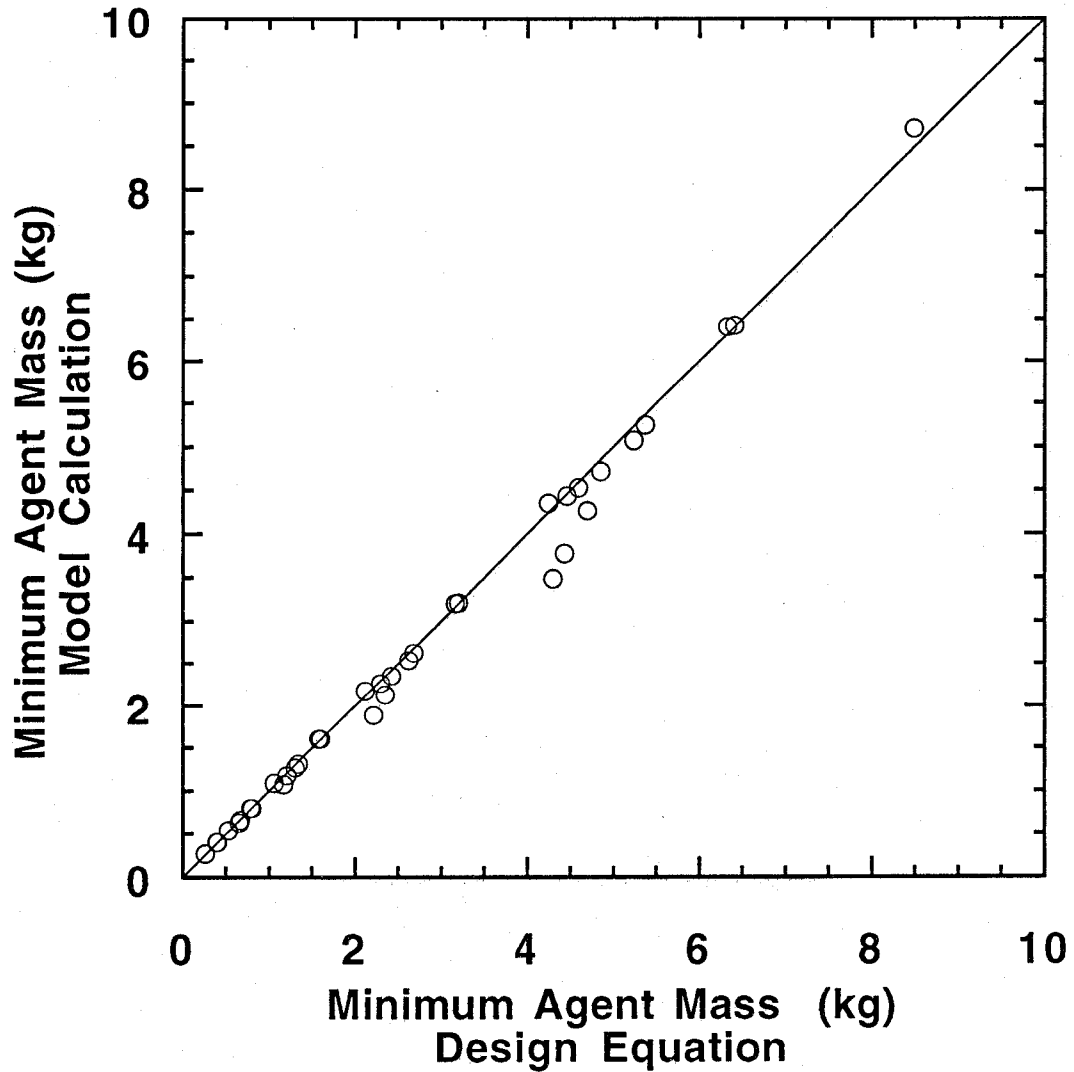


Figure 120. Comparison of the minimum halon 1301 mass from the model calculations and the "design equation" for the pool fire scenario with an agent injection duration of 1.0 s.

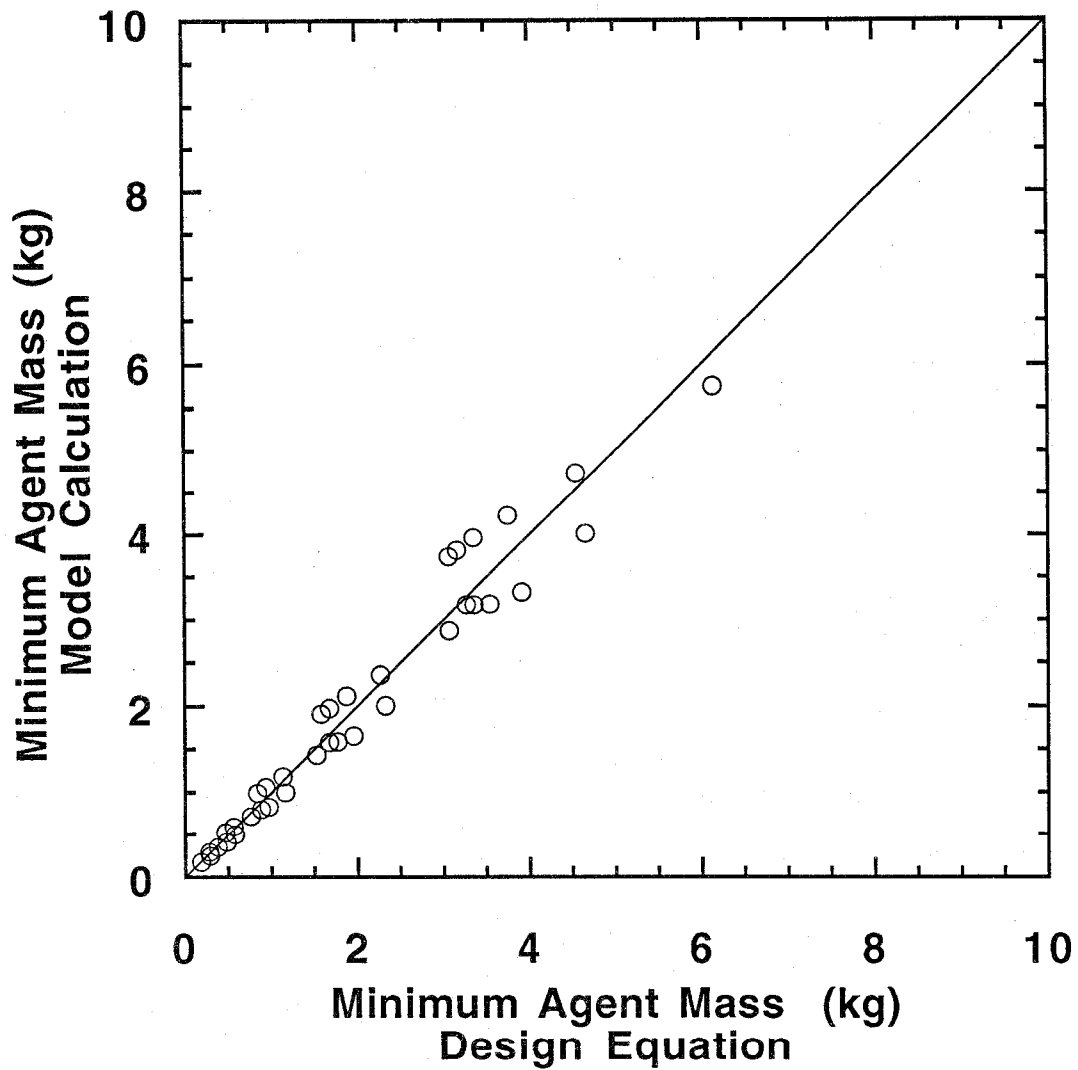


Figure 121. Comparison of the minimum HFC-125 mass from the model calculations and the "design equation" for the spray fire scenario with an agent injection duration of 0.25 s.

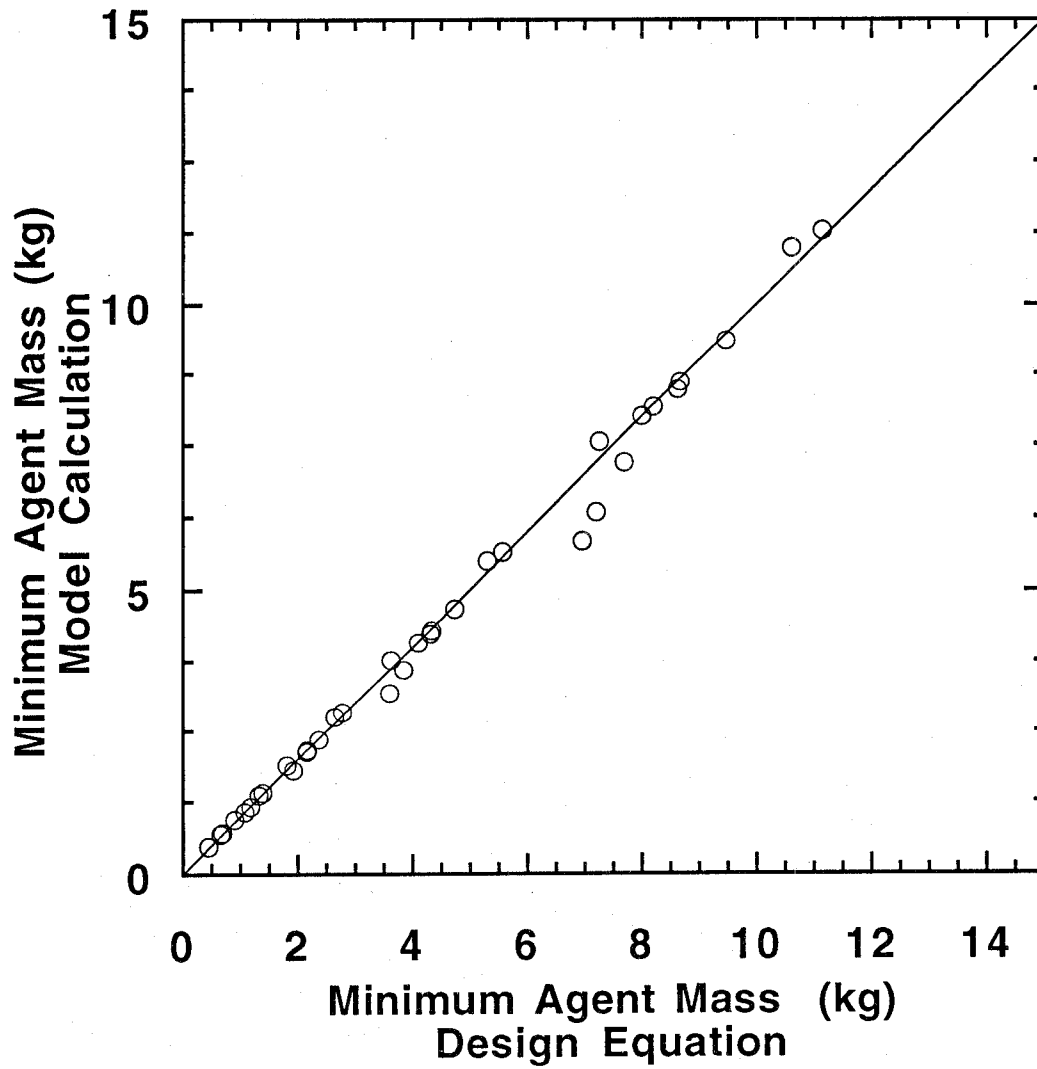


Figure 122. Comparison of the minimum HFC-125 mass from the model calculations and the "design equation" for the spray fire scenario with an agent injection duration of 1.0 s.

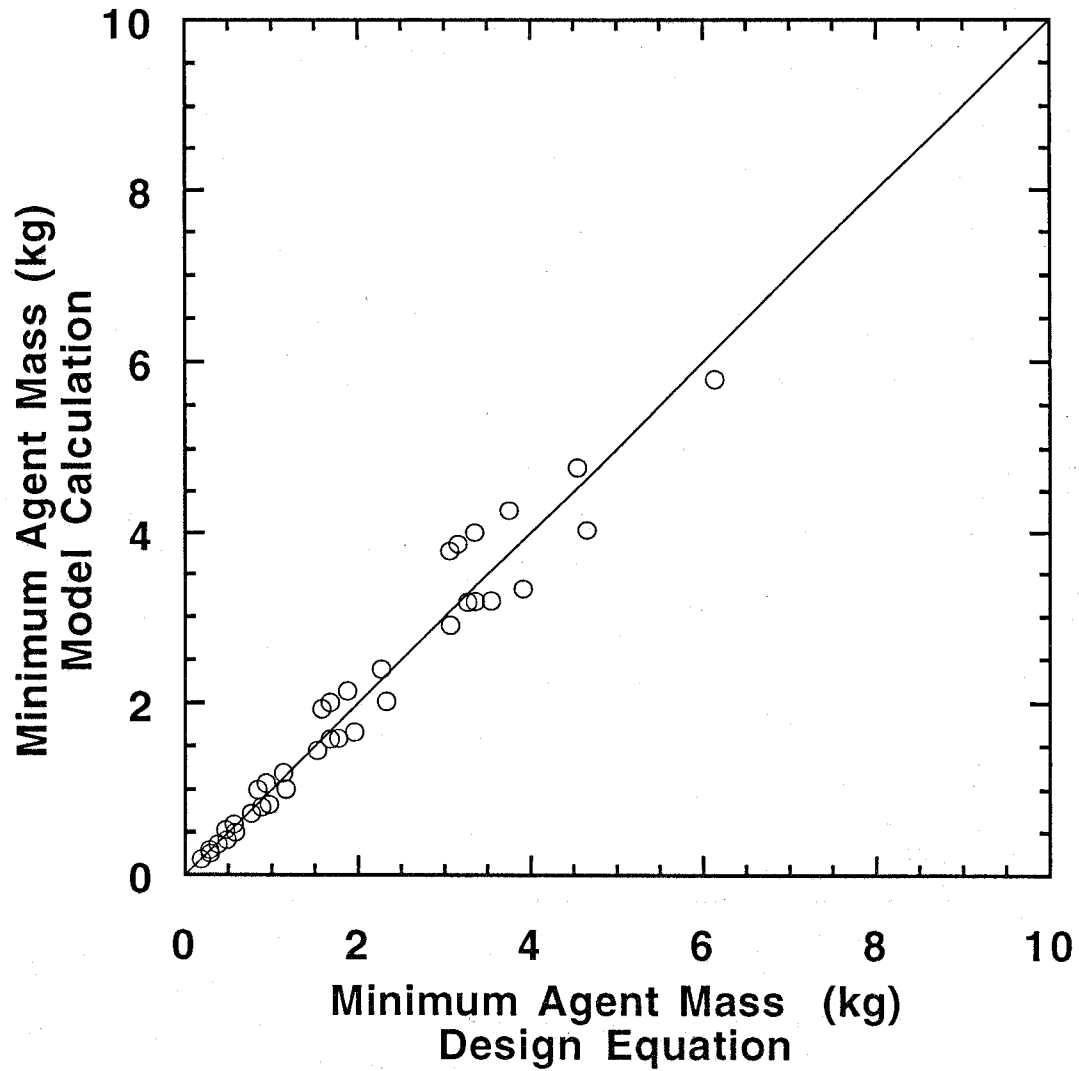


Figure 123. Comparison of the minimum HFC-227 mass from the model calculations and the "design equation" for the spray fire scenario with an agent injection duration of 0.25 s.

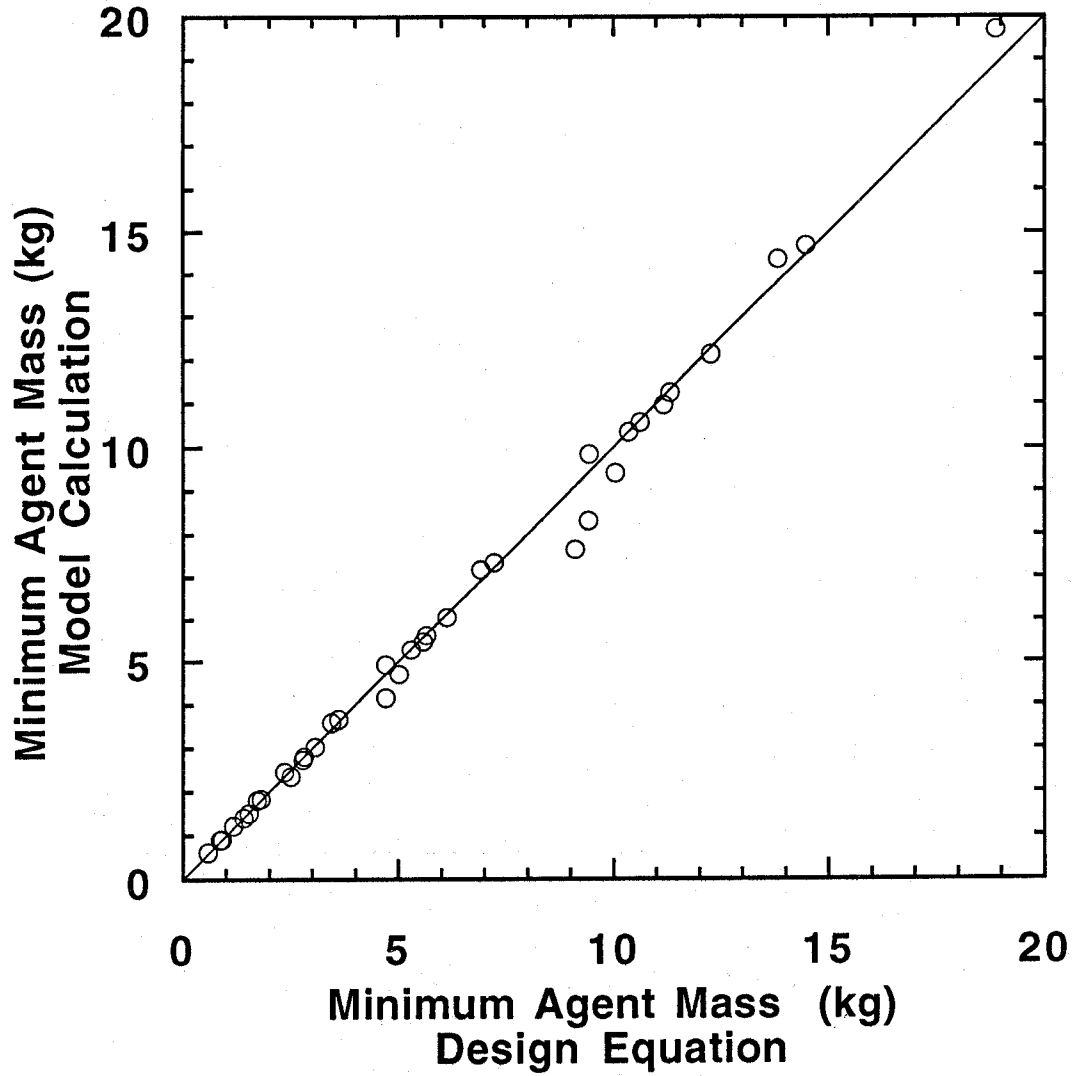


Figure 124. Comparison of the minimum HFC-227 mass from the model calculations and the "design equation" for the spray fire scenario with an agent injection duration of 1.0 s.

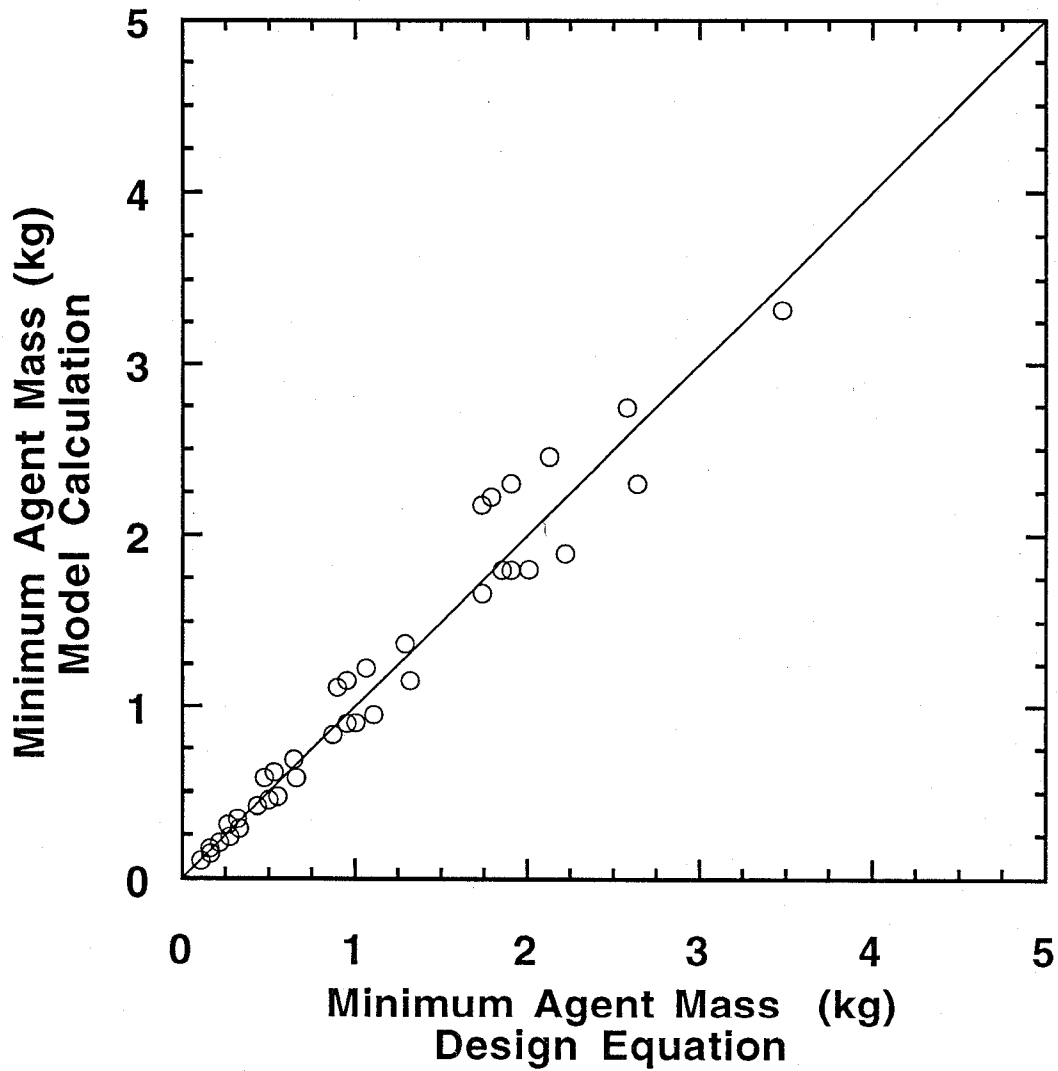


Figure 125. Comparison of the minimum CF_3I mass from the model calculations and the "design equation" for the spray fire scenario with an agent injection duration of 0.25 s.

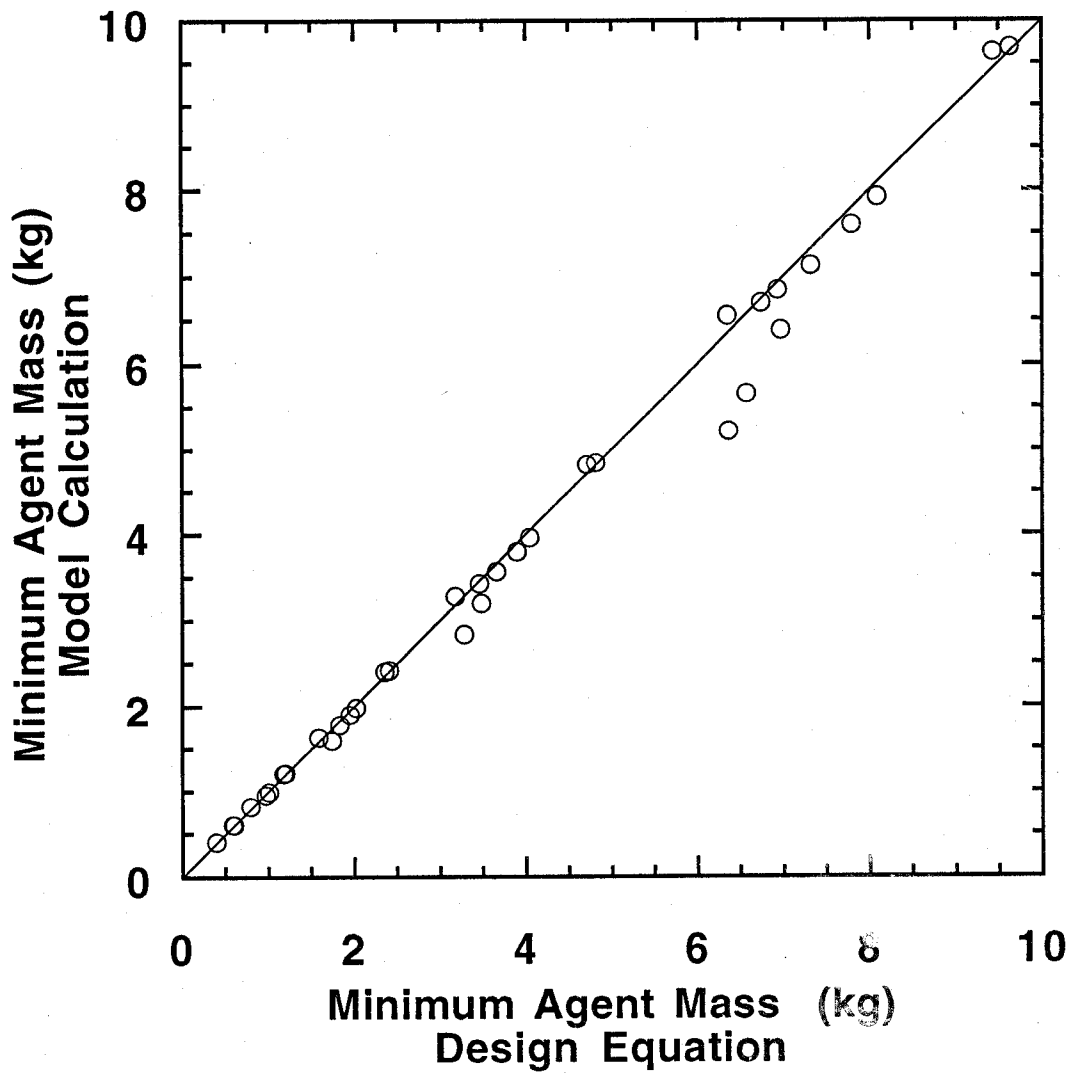


Figure 126. Comparison of the minimum CF_3I mass from the model calculations and the "design equation" for the spray fire scenario with an agent injection duration of 1.0 s.

Table 12. The coefficients in Equation (33) for each agent and fire scenario

Agent	(a) spray fire (kg/m ³)	(b) spray fire (kg/kg _{air} /s)	(a) pool fire (kg/m ³)	(b) pool fire (kg/kg _{air} /s)
halon 1301	0.17	0.165	0.52	0.542
HFC-125	0.37	0.397	0.84	0.974
HFC-227	0.37	0.397	1.1	1.26
CF ₃ I	0.21	0.225	0.77	0.819

obtained given the free stream concentration. For instance, if the free stream concentration is twice X_∞ then $\Delta t = 0.693\tau$. If the free stream concentration chosen is very similar to X_∞ , the duration must be very long ($\Delta t \approx 3\tau$), likewise, if the free stream concentration chosen is very high, then the duration approaches the minimum (Δt_c).

The concentration/duration relationship given above, formally applies to a plug flow only, where the agent free stream concentration takes the form of a step function. It is not applicable when the free stream concentration is not constant which occurs in nacelle model No. 2 (PSR) for example, and more importantly, in real nacelles which are characterized by imperfect mixing. Because of the mixing problem, it is recommended that temporal concentration measurements be conducted in full-scale nacelles to ensure suppression system effectiveness. Following agent discharge, the transient agent concentration should be measured in the free stream near potential fire locations. In addition, temporal agent concentration measurements should be made behind bluff bodies which represent potential fire zones, as is currently the case for halon 1301 certification testing. This is of value because there is no guarantee that the free stream concentration is spatially homogeneous. These measurements made under non-combusting conditions or "cold flow" must be related to an effective free stream concentration to assess suppression system effectiveness. These issues are addressed below, yielding a generalized methodology for the determination of concentration/duration requirements for protection of a particular nacelle, fire scenario, and agent.

Real dispersion effects lead to spatial and temporal variations in the agent concentration. Fire suppression is directly related to the agent concentration in the fire zone, thus adequate free stream temporal concentrations are required at all potential fire locations. The time dependent agent concentration, initially zero in the fire zone or behind a bluff body is given by:

$$X(t) = e^{-t/\tau} \frac{1}{\tau} \int_0^t e^{t'/\tau} X_f(t') dt' \quad (34)$$

which is the solution to the non-homogeneous, linear first-order differential equation describing the local mixing:

$$X_f(t) = \tau \frac{dX(t)}{dt} + X(t) \quad (35)$$

where $X(t)$ is the agent concentration in the recirculation zone, $X_f(t)$ is the free stream concentration, and τ is the appropriate characteristic mixing time for combusting or non-combusting conditions. To

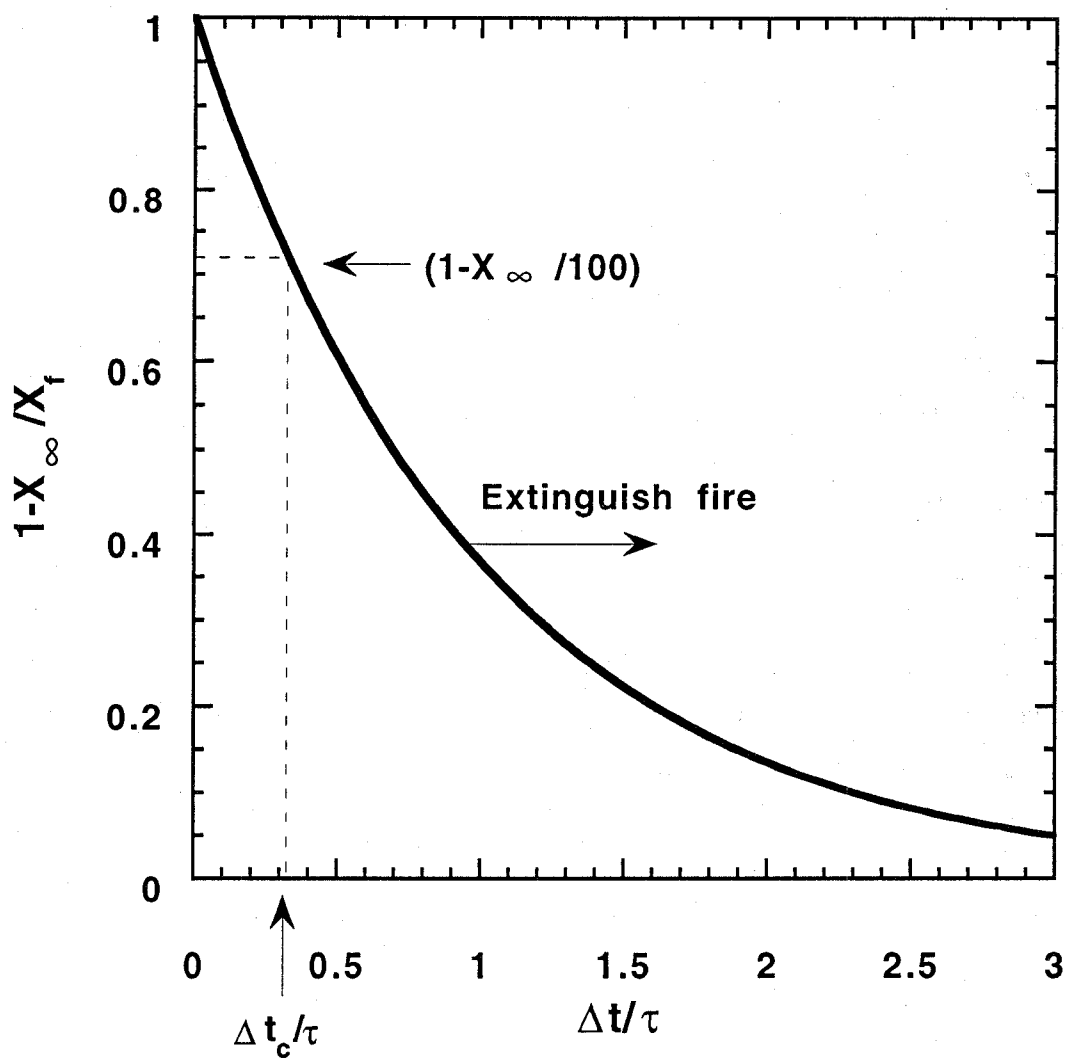


Figure 127. Concentration/duration relation for flame extinguishment assuming a steady agent plug flow.

assess whether the free stream agent concentration is sufficient to extinguish the fire, the integral in Equation (34) must be evaluated. The fire is considered extinguished if $X(t)$ is greater than X_∞ for any discrete time interval. The relative value of $X_f(t)$ to X_∞ is irrelevant. The criteria for extinction is based on the agent concentration in the fire zone only.

The integral in Equation (34) can be evaluated either analytically or numerically. $X_f(t)$ can take any functional form, but in practice, discrete data is recorded from a concentration measuring device. If $X_f(t)$ is well represented by a facile functional form, then the integral can be evaluated and $X(t)$ determined. If not, $X(t)$ can be determined by piecewise integration of Equation (34) using the discrete data. For piecewise integration, given that the discrete data were collected at a regular time interval (δt), and that the curve between two data points is represented by a straight line, the concentration at time t_i is:

$$X(t_i) = \sum_{j=1}^i e^{-\delta t/\tau} (a - b\tau + X(t_{j-1})) + (a + b\delta t - b\tau) \quad (36)$$

where $a = X_f(j-1)$ and $b = (X_f(j) - X_f(j-1))/\delta t$. As an illustration, Figure 128 shows simulated discrete agent concentration data for the free stream (with $\delta t = 0.1$ s) and the predicted concentration in the fire zone using Equation (36) for two different values of τ . At $t = 0$, the agent arrives just upstream of the fire zone. Notice that for the smaller value of τ ($= 0.1$ s), the agent concentration in the fire zone closely follows the concentration in the free stream, whereas there is a significant lag in the fire zone agent concentration for the larger value of τ ($= 1$ s). If the long injection concentration limit (X_∞) for these fire scenarios is taken as 12 %, then it is obvious that there is a large excess of agent for the fire zone characterized by the smaller value of τ , whereas there is just barely sufficient agent for the fire zone characterized by the larger value of τ . This example is intended to emphasize the importance of the order of magnitude difference between the values of τ measured in the baffle stabilized pool fire and in the spray flame.

Winterfeld (1965) found that the characteristic entrainment or mixing time into a baffle stabilized premixed flame is twice as long as the characteristic mixing time in an isothermal flow for the same geometry and velocities. Winterfeld's research was for obstacles in the center of the flow field. In lieu of other data, that observation could be applied to relate combusting to non-combusting characteristic mixing times. Since measurement of the characteristic mixing times (τ) in the combusting and non-combusting cases are different, the results from "cold flow" certification testing is not directly applicable to forecasting fire suppression. Given the temporal concentration in the recirculation zone, however, the free stream concentration can be deduced and then used in Equations (34) or (36) with an appropriate value of τ to assess fire suppression effectiveness. The free stream concentration, $X_f(t)$, could be calculated from solving Equation (35), where τ is the non-combusting characteristic mixing time.

For a particular nacelle, transient agent concentration measurements should be made at many possible fire locations. The performance criterion adopted above evaluates the fire suppression effectiveness at each location independently. Other performance criteria could be added to that criterion, for example requiring that all locations must be at a given concentration for a given duration simultaneously as is the case in the current halon 1301 specifications.

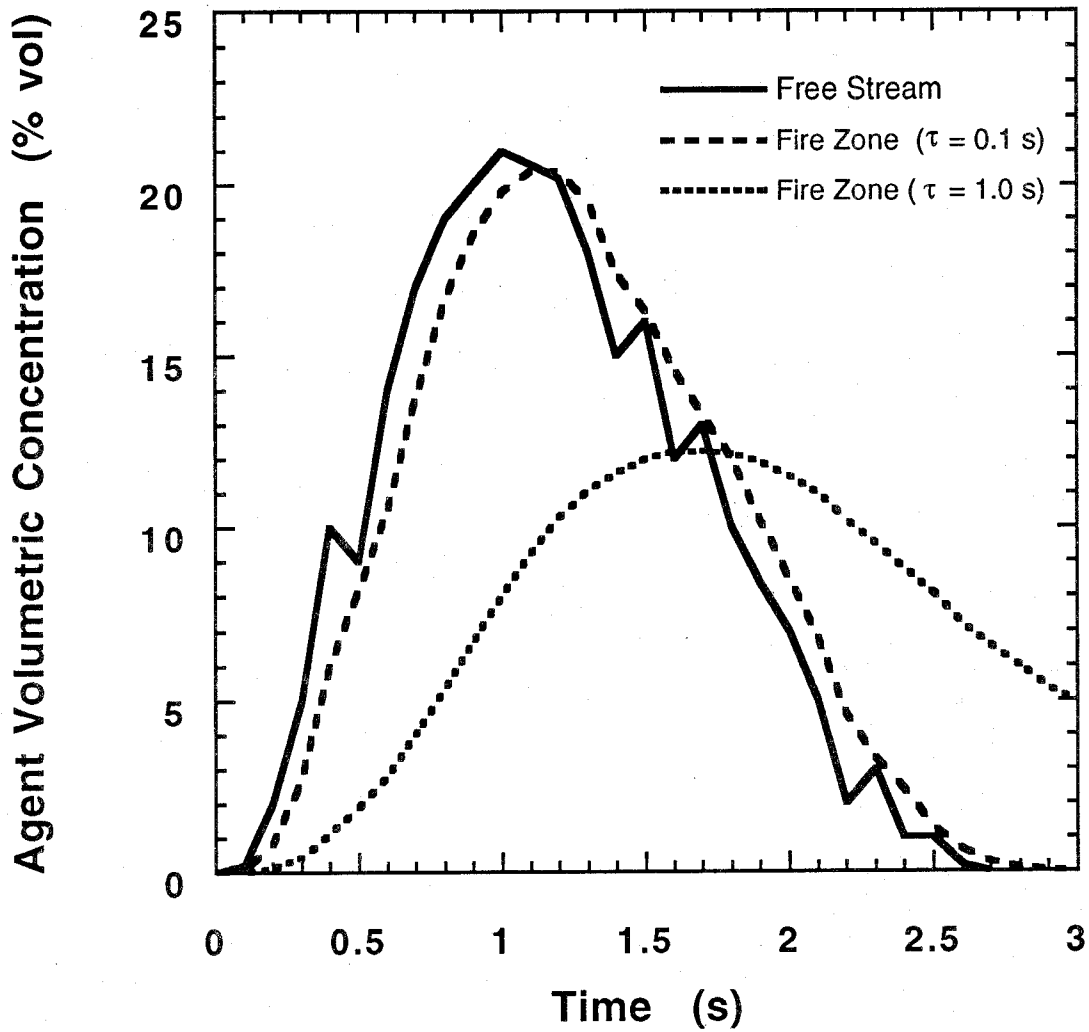


Figure 128. Simulated agent concentration data with predicted concentration build-up in specific fire zones characterized by $\tau = 0.1$ s and 1.0 s.

9.5.10 Procedure for Determination and Validation of Nacelle Fire Suppression Requirements.

The following procedure outlines a methodology to determine agent requirements for fire protection and validate suppression system performance for real engine nacelles.

Step 1. Collect information regarding the nacelle volume, configuration (*e.g.*, rib sizes; locations of other obstacles), air flow, and the environment (operational temperatures and pressures). Available information regarding the nacelle air flow including measurements and/or computations would be useful in determining the type of agent mixing that would likely occur, if zones of low agent concentration ("dead zones") occur and where agent injection location(s) should be to mitigate potential problems.

Step 2. Deduce the worst-case probable fire scenarios which are inferred from the information collected in step 1. Estimate the characteristic mixing time (τ) and critical extinction concentration (X_{∞}) for the fire scenarios.

Two fire scenarios have been considered in the model calculations, namely baffle stabilized pool fires and spray flames. Given the configuration (the location of fuel lines, baffle sizes, geometric blockage, etc.), air flow, and environment, estimate the characteristic mixing time, τ , and the critical agent concentration, X_{∞} (see Section 9.3.2.3.4). More confidence is placed on the estimates for the spray fire scenario due to the extensive testing, while much less confidence is placed on the estimates for the baffle stabilized pool fire scenario. Extrapolations to other conditions should be made conservatively until more data is gathered. Other fire scenarios have not been explicitly addressed in the modeling, most notably re-ignition of fuel from hot surfaces. The re-ignition scenario adds another dimension to the suppression system requirements.

Step 3. Calculate the minimum agent mass for a specified injection duration.

Using the appropriate design equation (Equation (32) for plug flow or Equation (33) otherwise), calculate the minimum agent mass required for fire suppression. Equation (33) should be used in concert with appropriate coefficients as described in Section 9.5.8. It is useful to check the effect of the injection duration on the minimum agent mass to determine if the injection time can be increased without a large agent mass penalty.

Step 4. Add additional mass to the agent quantity obtained in step 3 as a "safety factor." Decide whether to increase the discharge rate or injection time.

The decision to increase the discharge rate or injection time involves trade-offs (see Section 9.5.7). The decision will probably be dictated by experience after full-scale experimentation and successful system design.

Step 5. Calculate the discharge time given the agent mass, storage conditions and piping configuration.

It is prudent to integrate the discharge characteristics into this design guideline. Given the hardware requirements, assess whether the discharge of the required agent amount can be achieved in the specified injection duration (see Section 8.6 of this report). The discharge time of an agent stored at cold temperatures could be estimated to assess its impact. If a

relaxation of the discharge time is possible, potential benefits relating to hardware design can be assessed.

Step 6. Perform certification tests with the agent mass and injection rate prescribed from steps 4 and 5. Measure the agent concentration in the free stream and potential fire zones.

Step 7. Compare temporal agent concentration measurements to concentration and duration criteria.

Follow the methodology outlined in Section 9.5.9 to assess the suppression effectiveness at each measurement location. Check any other performance requirements.

Step 8. If the measured concentrations meet the criteria, then the system is properly designed. If the criteria are not met, then decide if the problem is due to inadequate mixing or insufficient agent mass. If the problem is due to inadequate mixing, then tailor the discharge (*i.e.*, by use of nozzles, tees, etc.) to improve mixing. If the problem is due to inadequate agent mass, then increase the agent amount and return to step 5.

9.5.11 Summary of the Model. There is no simple generic solution to the nacelle fire protection problem. The model developed here illustrates the importance of injection duration, air flow, nacelle free volume, fluid mixing, and fire scenario on the minimum agent suppression requirements. A comparison of the results of the model for halon 1301 suppression requirements with the current Military Specifications showed that the trends with air flow and nacelle volume were well predicted, and that the Military Specification requires larger agent mass. Comparison of the alternative agent requirements to those predicted for halon 1301 showed that a constant multiplier between them exists for each fire scenario. Comparison of the model results with full-scale fire test data for the alternative agents showed consistent trends. Preliminary guidelines in the form of simple algebraic equations were proposed for the minimum agent delivery rates. Certification specifications were discussed and the relationship between concentration and duration was given. A step-by-step procedure was proposed as a guideline for system design and certification. Before application, it is strongly advised that the model be adequately validated using full-scale testing.

9.6 Summary and Recommendations

The following conclusions are made regarding flame suppression and agent effectiveness.

1. A simple mixing model was developed that gives guidance in determining agent requirements for nacelle applications. A step-by-step procedure was proposed as a guideline for system design and certification (see Section 9.5.10).
2. In general, baffle stabilized pool fires were more difficult to extinguish than the baffle stabilized spray fires tested in this study. Larger agent concentrations and longer characteristic agent mixing times were required to achieve suppression in the pool fires due to the structure of the recirculation zone.
3. Of the candidate replacement agents evaluated in the turbulent spray burner, CF_3I was the most effective compound. CF_3I required the least amount of gaseous agent to extinguish the flames on

both a mass and volume basis. The other two alternative agents tested, HFC-125 and HFC-227, were measured to have nearly identical suppression effectiveness, and were significantly less efficient than CF_3I in extinguishing the flames. On a mass basis, none of the agents performed as well as halon 1301.

4. Agent performance measured in the turbulent jet spray burner for low air flows was very similar to the performance measured in the cup burner and in the opposed flow diffusion flame under low strain rate conditions, suggesting that a single test apparatus is sufficient for ranking the effectiveness of alternative agents.
5. The agents required more mass to extinguish flames in the turbulent spray burner when the air was heated. This trend was anticipated, since heating the air adds enthalpy to a flame, and a flame with a higher enthalpy is expected to be more stable. However, increasing the air temperature altered the agent ranking. For temperatures below 150 °C, CF_3I was the most effective agent. For temperatures above 150 °C, the three agents, CF_3I , HFC-125 and HFC-227 were approximately equally effective.
6. The system pressure and the fuel flow did not significantly impact the agent concentration required to obtain extinction over the range of conditions tested in the turbulent spray burner.
7. A model was developed that treats the recirculation zone in baffle stabilized flames as a perfectly stirred reactor, facilitating prediction of the agent concentration required for flame extinction as a function of the agent injection duration.
8. Agent type does not significantly impact mixing rates behind an obstacle in combusting or non-combusting conditions.
9. Mixing times for an agent entraining into a recirculation zone behind an obstacle under non-combusting (cold flow) conditions, such as during agent certification, are different than mixing times under combusting (suppression) conditions. In other words, the rate of fluid mixing into the recirculation zone is impacted by combustion. The mixing time also varies with the blockage ratio, the relative geometric relationship between the open and blocked area associated with a flow obstacle.
10. To achieve a target concentration in the recirculation zone behind an obstacle, the free stream concentration must be maintained for approximately three times the value of the characteristic entrainment or mixing time, τ .
11. There are trade-offs in obtaining a target concentration in the recirculation zone behind a baffle (during both flame suppression and non-combusting certification), involving the agent concentration and its duration in the free stream.
12. CF_3I was the most effective agent in suppressing the ignition of reactants flowing over a hot nickel surface. The other two agents tested, HFC-125 and HFC-227, were both measured to have nearly identical ignition suppression effectiveness, and both were significantly less efficient than CF_3I . HFC-125 was observed to marginally promote ignition in stoichiometric methane/air and propane/air mixtures.

13. A reasonable target concentration for an agent in the fire zone (not the free stream or in non-combusting tests) is the concentration which insures that the most flammable fuel/air ratio cannot occur. This agent concentration insures both flame suppression and prevention of re-ignition for a period of time on the order of the agent injection duration. After this period, however, it is likely that re-ignition will still be possible and therefore other fire prevention strategies should be considered.

A number of cautions must be made regarding utilization of the derived results for full-scale application.

1. Geometrical factors are not scaleable in a one-to-one fashion. Whereas mixing times are influenced by the Reynolds number, mixing is also impacted by the blockage ratio.
2. Fluid mixing may be impacted by changes in air flow due to agent injection itself.
3. Flame stabilization may be enhanced by a heated wall or obstacle.
4. All suppression testing was conducted with gas phase agents. Changes in the rate of agent evaporation or flashing as well as agent dispersion could also impact the relative suppression effectiveness of an agent. Therefore, changes in nacelle conditions, involving air temperature or pressure for example, could significantly impact the relative agent effectiveness in suppressing a fire.

A better understanding of a number of issues would facilitate improved design guidelines for nacelle fire protection.

1. The impact of differences in the rate of agent evaporation and agent dispersion on suppression effectiveness should be independently tested. All suppression testing in this report was conducted with gas phase agents only. This could be particularly important for discharge under low temperature conditions where droplet dynamics could impact the required agent amount.
2. The validity of Equations (16) and (17) should be tested for baffle stabilized pool flames. A large number of issues remain unresolved. Although Winterfeld (1965) studied the differences between entrainment into an eddy in isothermal and combusting flows, his study was conducted over a narrow range of Reynolds numbers and for premixed flames only. Other studies of entrainment into baffle stabilized premixed flames (Bovina, 1958; Mestre, 1966) have only considered a baffle in the middle of the flow field. The isothermal flow simulations presented here show that baffles against a wall must also be considered. Understanding agent entrainment is critical for the careful development of revised agent certification requirements.
3. Comprehensive agent dispersion measurements are needed in full-scale systems to determine the transient agent pulse shape at locations upstream and downstream of agent injection. Is the pulse shape significantly impacted by changes in the air flow induced by agent injection?
4. The peak flammability limits are a possible preliminary target for agent requirements in nacelle applications. For this reason, it would be of interest to understand the effects of initial temperature and fuel type on the peak flammability limits of halogenated agents.

5. To gain further understanding about re-ignition, it is important to model the ignition of reactants flowing over a heated plate, similar to the experiments described in Section 9.5.3. A model that considers detailed kinetics and fluid dynamics should be employed, such as that of Sano and Yamashita (1994) or Vlachos *et al.* (1994). A key element in such a model would be the kinetic and thermophysical data associated with the halogenated compounds. Such information is available for many key molecules including CF_3Br , CF_3I , and C_2HF_5 (Babushok *et al.*, 1995c). It would be beneficial to consider a range of reactant residence times, including times on the order of 1 s, where ignition may occur at relatively low temperatures.
6. Suppression testing of a baffle stabilized spray flame, with the baffle against a wall, is needed. This is a possible nacelle fire scenario and may be a more difficult to extinguish than the configurations investigated in this report. Such a study would allow a direct comparison of suppression in pool flames and spray flames.

9.7 Acknowledgments

The authors are grateful to Nelson Bryner and Kermit Smyth for many helpful discussions and use of their hot surface ignition apparatus, Bill Leach of NAVAWCLK for allowing us to view nacelle certification type testing, and to Jim Allen, Valeri Babushok, David Bagdhadi, Brett Breuel, Paula Garrett, Michael Glover, Andrew Hubbard, Darren Lowe, Roy McLane, Takashi Budda Noto, and Isaura Vazquez of NIST and Terrence Simpson and Mark Mitchell of Walter Kidde Aerospace for their technical assistance.

9.8 References

ASTM-E 659-78, "Standard Test Method for Autoignition Temperature of Liquid Chemicals," *American Society for Testing and Materials*, Philadelphia, PA, this procedure replaced the older ASTM D2155 test in 1978.

ASTM-E 681-94, "Standard Test Method for Concentration Limits of Flammability of Chemicals," *American Society for Testing and Materials*, Philadelphia, PA, 681, 1994.

Altman, R.L., Ling, A.C., Mayer, L.A., and Myronuk, D.J., "Development and Testing of Dry Chemicals in Advanced Extinguishing Systems for Jet Engine Nacelles Fires," *NASA Report JTCG/AS-82-T-002*, NASA-AMES Research Center, Mountain View, CA, (1983).

Babushok, V., personal communication, 1995.

Babushok, V., Burgess, D.R.F., Linteris, G., Tsang, W. and Miziolek, A., "Modeling of Hydrogen Fluoride Formation From Flame Suppressants During Combustion," presented at the *Halon Options Technical Working Conference*, Albuquerque, NM, May 9-11, 1995a.

Babushok, V., Noto, T., Burgess, D.R.F., Hamins, A., and Tsang, W., "Inhibitor Influence on the Bistability of a CSTR," in preparation, 1995b.

Babushok, V., Noto, T., Burgess, D.R.F., Hamins, A., and Tsang, W., "Influence of CF_3I , CF_3Br , and CF_3H on the High Temperature Combustion of Methane," submitted to *Comb. Flame*, 1995c.

Bajpai, S.N., "Extinction of Vapor Fed Diffusion Flames by Halons 1301 and 1211-Part I," *Ser. No. 22430*, *Factory Mutual research Corporation*, Norwood, MA, November (1974).

Ballal, D.R. and Lefebvre, A.H., "Some Fundamental Aspects of Flame Stabilization," *Fifth International Airbreathing Engine Symposium*, Bangalore, India, 1981.

Barat, R.B., Sarofim, A.F., Longwell, J.P., and Bozelli, J.W., "Inhibition of a Fuel Lean Ethylene/Air Flame in a Jet Stirred Combustor by Methyl Chloride: Experimental and Mechanistic Analyses," *Combust. Sci. Tech.* **74**, 361, (1990).

Beardsley, G., "Investigation of the Effect of Air Velocity on the Spontaneous Ignition Temperature of Kerosene Sprayed onto a Heated Tunnel Having a Rectangular Obstruction in the Airstream," Rolls Royce Ltd. Aero Engine Division, *Technical Report Rbts/RI. (FEW.10)*, Feb. 1967.

Beér, J.M. and Chigier, N.A., *Combustion Aerodynamics*, Robert Krieger Publishing Co., Malabar, FL, 1983.

Bennett, M., and Caggianelli, G., Personal Communication, 1995.

Blevins, R.D., *Applied Fluid Dynamics Handbook*, Van Nostrand & Reinhold Co., New York, p. 40, 1984.

Botteri, B., Cretcher, R., and Kane, W., "Aircraft Applications of Halogenated Hydrocarbon Fire Extinguishing Agents," *Published Proceedings of the Symposium An Appraisal of Halogenated Fire Extinguishing Agents*, Washington, DC, National Academy of Sciences, (1972).

Bovina, T.A., "Studies of Exchange Between Re-circulation Zone Behind the Flame Holder and Outer Flow," Seventh Sym. (Int.) on Combustion, *The Combustion Institute*, 692, (1958).

Clodfelter, R.G., "Hot Surface Ignition and Aircraft Safety Criteria," Proceedings of the SAE Aerospace Technology Conference and Exposition, *SAE Technical Paper Series*, Long Beach, CA, (1990).

Coward, H.F., and Jones, G.W., "Limits of Flammability of Gases and Vapors," *Bulletin 503*, Bureau of Mines, National Technical Information Service, Springfield, VA, 1939.

Cutler, D.P., "The Ignition of Gases by Rapidly Heated Surfaces," *Combust. Flame*, **22**, 105, (1974).

Demaree, J., and Dierdorf, P., "Aircraft Installation and Operation of an Extinguishing-Agent Concentration Recorder," Technical Development Report No. 403, National Aviation Facilities Experimental Center, Federal Aviation Agency, (1959).

Detz, C.F., "Threshold Conditions for the Ignition of Acetylene Gas by a Heated Wire," *Combust. Flame*, **26**, 45, (1976).

Dyer, J.H., Marjoram, M.J., and Simmons, R.F., "The Extinction of Fires in Aircraft Jet Engines - Part III," *Fire Tech.*, **13**, 126, (1977a).

Dyer, J.H., Marjoram, M.J., and Simmons, R.F., "The Extinction of Fires in Aircraft Jet Engines - Part IV," *Fire Tech.*, **13**, 223, (1977b).

Finnerty, A.E., "Effect of Halons on the Autoignition of Propane," Western States Section Meeting of the Combustion Institute, Palo Alto, CA, *Paper WSS/CI 75-27*, (1975).

Gerstein, M. and Allen, R.D., "Fire Protection Research Program for Supersonic Transport," Wright Patterson AFB, OH, *AFAPL, Report AFAPL-TR-69-66*, (1964).

Glarborg, P., Kee, R.J., Grcar, J.F., Miller, J.A., "PSR: A Fortran Program for Modeling Well-Stirred Reactors," *Sandia National Laboratories*, Report SAND86-8209, Feb. 1986.

Goodall, D.G. and Ingle, R., *Esso Air World*, **19**, 8, (1966).

Grieme, F., "Aviation Fire Protection," *NFPA Quarterly*, **35**, (No. 1), (1941).

Griffiths, J.F. Coppersthaite, D., Phillips, C.H., Westbrook, C.K., and Pitz, W.J., "Auto-ignition Temperatures of Binary Mixtures of Alkanes in a Closed Vessel: Comparisons between Experimental Measurements and Numerical Predictions," Twenty-Third Sym. (Int.) on Combustion, *The Combustion Institute*, 1745, (1990).

Grosshandler, W., Lowe, D., Rinkinen, B., Presser, C., "A Turbulent Spray Burner for Assessing Halon Alternative Fire Suppressants," *ASME Paper No 93-WA/HT-23*, 1993.

Grosshandler, W., Gann, R.G., and Pitts, W.M., eds., "Evaluation of Alternative In-Flight Fire Suppressants for Full-Scale Testing in Simulated Aircraft Engine Nacelles and Dry Bays," *NIST Special Publication Number SP-861*, (1994).

Grosshandler, W., Lowe, D., Rinkinen, B., and Presser, C., "Assessing Halon Alternatives for Aircraft Engine Nacelle Fire Suppression," *J Heat Transfer*, **117**, 489, (1995).

Hamins, A., Trees, D., Seshadri, K., Chelliah, H.K., "Extinction of Nonpremixed Flames with Halogenated Fire Suppressants," *Combust. Flame*, **99**, 221-230 (1994).

Hansberry, H., "CAA Aircraft Fire Test Program," *NFPA Quarterly*, **42**, (No. 1), (1948).

Hansberry, H., "Aircraft Fire Extinguishment, Part V, Preliminary Report on High-Rate-Discharge Fire-Extinguishing Systems for Aircraft Power Plants," *Technical Development Report No. 260*, Civil Aeronautics Administration, (1956).

Hansberry, H., "Halogenated Extinguishing Agents, Part III, Research at the Technical Development and Evaluation Center Civil Aeronautics Administration," *NFPA Quarterly*, **45**, (No. 10), (1954).

Harwell Laboratories, "HARWELL-FLOW3D Release 3.2, User Manual," *C.D. Department, AEA Industrial Technology*, Harwell Laboratory, Oxfordshire, United Kingdom, 1992.

Hirst, R., "Aviation Fire Research," *NFPA Quarterly*, **57** (No. 2), 141, (1963).

Hirst, R. and Sutton, D., "The Effect of Reduced Pressure and Airflow on Liquid Surface Diffusion Flames," *Combust. Flame*, **5**, 319, (1961).

Hirst, R., Farenden, P.J., and Simmons, R.F., "The Extinction of Fires in Aircraft Jet Engines - Part I," *Fire Tech.*, **12**, 266, (1976).

Hirst, R., Farenden, P.J., and Simmons, R.F., "The Extinction of Fires in Aircraft Jet Engines - Part II," *Fire Tech.*, **13**, 59, (1977).

Hughes, C., "Aircraft Fire Extinguishment, Part II, The Effect of Air Flow on Extinguishing Requirements of a Jet Power-Plant Fire Zone," *Technical Development Report No. 205*, Civil Aeronautics Administration, (1953).

Johnson, A.M., and Grenich, A.F., "Vulnerability Methodology and Protective Measures for Aircraft Fire and Explosion Protection," Wright Patterson AFB, OH, *Technical Report AFWAL-TR-85-2060*, (1986).

Johnson, A.M., Roth, A.J., and Moussa, N.A., "Hot Surface Ignition of Aircraft Fluids," Wright Patterson AFB, OH, *Technical Report AFWAL-TR-88-2101*, (1988).

Kinsey, D., Personal Communication, Chief, Applied Computational Fluid Dynamics Division, Wright Patterson AFB, OH, (1994).

Klein, H., "Jet Engine Fire Protection Program," *AF Technical Report No. 5870*, U.S. Air Force Air Material Command, (1950a).

Klein, H., "New Fire Extinguishing Agents for Aircraft", *NFPA Quarterly*, **43**, (No. 4), (1950b).

Klueg, E.P., and Demaree, J.E., "An Investigation of In-Flight Fire Protection with a Turbofan Powerplant Installation," *FAA Report Na-69-26(DS-68-28)*, (1969).

Kolleck, M., Booz-Allen-Hamilton tabulated survey results of present aircraft systems and operating environments, (1993).

Kuchta, J.M., "Summary of Ignition Properties of Jet Fuels and Other Aircraft Combustible Fluids," Bureau of Mines, Pittsburgh, PA, *Report AFAPL-TR-75-70*, (1975).

Kumagai, S. and Kimura, I., "Ignition of Flowing Gases by Heated Wires," Sixth Sym. (Int.) on Combustion, *The Combustion Institute*, p. 554, 1956.

Kumar, R.K., "Ignition of Hydrogen-Oxygen Mixtures Adjacent to a Hot, Nonreactive Surface," *Combust. Flame*, **75**, 197, (1989).

Landesman, H. and Basinski, J.E., "Investigation of Fire Extinguishing Agents for Supersonic Transport," *Tech. Doc. Rept. ASD-TDR-63-804*, (1964).

- Lauder, B.E. and Spalding, D.B., "The Numerical Computation of Turbulent Flows," *Computer Methods in Applied Mechanics and Engineering*, **3**, 269, (1974).
- Laurendeau, N., "Thermal Ignition of Methane-Air Mixtures by Hot Surfaces: A Critical Examination," *Combust. Flame*, **46**, 29, (1982).
- Leach, W., Private communication, (1994).
- Lefebvre, A.H., *Gas Turbine Combustion*, McGraw-Hill Book Co., New York, 1983.
- Lefebvre, A.H. and Halls, G.A., "Some Experience in Combustion Scaling," *AGARD Advanced Aero Engine Testing*, Pergamon, Oxford, 177, (1959).
- Lemon, L.H., Tarpley, W.B. Freeman, M.K., and Tuno, A.L., "Persistent Fire Suppression for Aircraft Engines," Wright Patterson AFB, OH 45433, *Technical Report AFAPL-TR-79-2130*, (1980).
- Lewis, B., and Von Elbe, G., *Combustion, Flame and Explosions of Gases*, Academic Press, New York, 1961.
- Liñan, A., "The Asymptotic Structure of Counterflow Diffusion Flames for Large Activation Energies," *Acta Astronautica*, **1**, 1007 (1974).
- Longwell, J.P., Frost, E.E., and Weiss, M.A., "Flame Stability in Bluff Body Recirculation Zones," *Ind. Eng. Chem.*, **45**, 1629, (1953).
- Macek, A., "Flammability Limits," *Combust. Sci. Tech.*, **21**, 43, (1979).
- Malcolm, J.E., "Vaporizing Fire Extinguishing Agents," Engineer Research and Development Laboratories, Fort Belvoir, VA, *Interim Report 1177*, Project 8-76-04-003, 1950.
- Mapes, D., "Development and Technical Aspects of the Aircraft-Engine Nacelle Fire Extinguishing System," *Published Proceedings Symposium on Fire Extinguishment Research and Engineering*, U.S. Naval Civil Engineering Research and Evaluation Laboratory Port Hueneme, CA, (1954).
- Mestre, A., "Etudes des Limites de Stabilité en Relation avec la résistance des Obstacles à l'Écoulement," *Combustion Researches and Reviews*, 6th and 7th AGARD Meetings, p. 72-85, Butterworths Scientific, London, 1955.
- McClure, J.D., and Springer, R.J., "Environmental and Operating Requirements for Fire Extinguishing Systems on Advanced Aircraft," for Joint Technical Coordinating Group/Aircraft Survivability, Report No. *JTCG/AS-74-T-0024*, (1974).
- McGrattan, K.B., Rehm, R.G., and Baum, H.R., "Fire Driven Flows in Enclosures," *Journal of Computational Physics*, **110** (2), 285, (1994).
- Middlesworth, C., "Aircraft Fire Extinguishment, Part I, A Study of the Factors Influencing Extinguishing System Design," *Technical Development Report No. 184*, Civil Aeronautics Administration, (1952).
- Middlesworth, C., "Determination of Means to Safeguard Aircraft From Power-Plant Fires in Flight, Part VI, The North American Tornado (Air Force XB-45)," *Technical Development Report No. 221*, Civil Aeronautics Administration, (1954).
- Mulholland, J.A., Sarofim, A.F., and Beer, J.M., "Chemical Effects of Fuel Chlorine on the Envelope Flame Ignition of Droplet Streams," *Combust. Sci. Tech.*, **87**, 139, (1992).
- New, J., and Middlesworth, C., "Aircraft Fire Extinguishment, Part III, An Instrument for Evaluating Extinguishing Systems," *Technical Development Report No. 206*, Civil Aeronautics Administration, (1953).
- NFPA Quarterly*, "Chlorobromomethane," **42**, (No. 1), (1948).
- Parts, L., "Assessment of the Flammability of Aircraft Hydraulic Fluids," Wright Patterson AFB, OH, *Technical Report AFAPL-TR-79-2095*, Oct. 1980.
- Perry, R.H., Green, D.W., Maloney, J.O., Eds., *Perry's Chemical Engineers' Handbook*, 6th Edition, McGraw-Hill Inc., New York, 1984.

Picard, B., Hartsig, D., and Levesque, R., "F/A-18 Engine Bay Fire Reduction," *Technical Memorandum TM 92-172 SA*, Naval Air Warfare Center Aircraft Division, Patuxent River, Maryland, (1993).

Pitts, W.M., Nyden, M.R., Gann, R.G., Mallard, W.G. and Tsang, W., "Construction of an Exploratory List of Chemicals to Initiate the Search for Halon Alternatives," *NIST Technical Note 1279*, U.S. Government Printing Office, Washington, DC, 1990.

Sano, T., and Yamashita, A., "Flame Ignition of Premixed Methane Air Mixtures on a High Temperature Plate," *JSME Int. J., Series B*, **37**, 180 (1994).

Sheinson, R.S., Penner-Hahn, J.E., and Indritz, D., "The Physical and Chemical Action of Fire Suppressants," *Fire Safety Journal*, **15**, 43 (1989).

Smyth, K.C., and Bryner, N.P., "Short-Duration Autoignition Temperature Measurements for Hydrocarbon Fuels," *National Institute of Standards and Technology Report Number NISTIR 4469*, (1990).

Snee, T.J., and Griffiths, J.F., "Criteria for Spontaneous Ignition in Exothermic, Autocatalytic Reactions: Chain Branching and Self-Heating in the Oxidation of Cyclohexane in Closed Vessels," *Combust. Flame*, **75**, 381, (1989).

Sommers, D.E., "Fire Protection Tests in a Small Fuselage-Mounted Turbojet Engine and Nacelle Installation," *Federal Aviation Administration Report RD-70-57*, (1970).

Strasser, A., Waters, N.C., Kuchta, J.M., "Ignition of Aircraft Fluids by Hot Surfaces Under Dynamic Conditions," Wright Patterson AFB, OH, *Report AFAPL-TR-71-86*, (1971).

Strehlow, R.A., *Combustion Fundamentals*, McGraw-Hill, New York, 1984.

Tedeschi, M., and Leach, W., "Halon 1301 Fire Suppression System Effectivity Aboard U.S. Naval Aircraft," *Halon Options Technical Working Conference*, pp.128-136, Albuquerque, NM, (1995).

Tucker, D.M., Drysdale, D.D. and Rasbash, D.J., "The Extinction of Diffusion Flames Burning in Various Oxygen Concentrations by Inert Gases and Bromotrifluoromethane," *Combustion and Flame*, **41**, 293 (1981).

Van Wylen, G.J., and Sonntag, R.E., *Fundamentals of Classical Thermodynamics*, Second Edition, John Wiley and Sons, p. 400, 1978.

Vazquez, I., Grosshandler, W., Rinkinen, W., Glover, M., and Presser, C., "Suppression of Elevated Temperature Hydraulic Fluid and JP-8 Spray Flames," *Proceedings of the Fourth International Symposium on Fire Safety Science*, (1994).

Vlachos, D.G., Schmidt, L.D., and Aris, R., "Ignition and Extinction of Flames Near Surfaces: Combustion of CH₄ in Air," *AIChE Journal*, **40**, 1005 (1994).

Williams, F.A., "A Unified View of Fire Suppression," *Journal of Fire and Flammability*, **5**, 54 (1974).

Winterfeld, G., "On Processes of Turbulent Exchange Behind Flame Holders," Tenth Sym. (Int.) on Combustion, *The Combustion Institute*, 1265, (1965).

Womeldorf, C., King, M., and Grosshandler, W., "Lean Flammability Limit as a Fundamental Refrigerant Property," Interim Technical Report-Phase I for the Air-Conditioning and Refrigeration Technology Institute, *ARTI MCLR Project Number DE-FG02-91 CE23810*, 1995.

Yamaoka, I., and Tsuji, H., "An Experimental Study of Flammability Limits Using Counterflow Flames," Seventeenth Sym. (Int.) on Combustion, *The Combustion Institute*, p. 843, 1978.

Zabetakis, M.G., Furno, A.L., and Jones, G.W., "Minimum Spontaneous Ignition Temperatures of Combustibles in Air," *Ind. Eng. Chem.*, **46**, 2173, (1954).

Zukowski, E.E. and Marble, F.E., "The Role of Wake Transition in the Process of Flame Stabilization on Bluff Bodies," *Combustion Researches and Reviews, 6th and 7th AGARD Meetings*, pp. 167-180, Butterworths Scientific, London, 1955.